

농학박사학위논문

대사공학기반 효모의 발효저해제 다중 내성 증대

**Metabolic engineering of *Saccharomyces cerevisiae* for
tolerance improvement against multiple fermentation
inhibitors**

2015 년 8 월

서울대학교 대학원

농생명공학부 식품생명공학전공

김 선 기

A DISSERTATION FOR THE DEGREE OF DOCTOR OF PHILOSOPHY

**Metabolic engineering of *Saccharomyces cerevisiae* for
tolerance improvement against multiple fermentation
inhibitors**

대사공학기반 효모의 발효저해제 다중 내성 증대

August 2015

Sun-Ki Kim

MAJOR IN FOOD BIOTECHNOLOGY

DEPARTMENT OF AGRICULTURAL BIOTECHNOLOGY

GRADUATE SCHOOL

SEOUL NATIONAL UNIVERSITY

**Metabolic engineering of *Saccharomyces cerevisiae* for
tolerance improvement against multiple fermentation
inhibitors**

Advisor: Professor Jin-Ho Seo

A dissertation submitted in partial fulfillment of

The requirements for the degree of

DOCTOR OF PHILOSOPHY

to the Faculty of Department of Agricultural Biotechnology

at

SEOUL NATIONAL UNIVERSITY

by

Sun-Ki Kim

August 2015

농학박사학위논문

**Metabolic engineering of *Saccharomyces cerevisiae* for tolerance
improvement against multiple fermentation inhibitors**

대사공학기반 효모의 발효저해제 다중 내성 증대

지도교수 서진호

이 논문을 농학박사학위논문으로 제출함

2015년 6월

서울대학교 농생명공학부 식품생명공학전공

김선기

김선기의 농학박사학위논문을 인준함

2015년 6월

위원장 유상렬 (인/서명)

부위원장 서진호 (인/서명)

위원 한지숙 (인/서명)

위원 김경현 (인/서명)

위원 박용철 (인/서명)

ABSTRACT

Fermentation inhibitors present in lignocellulose hydrolysates are inevitable obstacles for achieving economic production of biofuels and biochemicals by various microorganisms. In this thesis, it was shown that spermidine (SPD) functions as a chemical elicitor for enhanced tolerance of *Saccharomyces cerevisiae* against fermentation inhibitors. In addition, the feasibility of constructing an engineered *S. cerevisiae* strain capable of tolerating toxic levels of the major inhibitors without exogenous addition of SPD was explored. Specifically, expression levels of the genes in the SPD biosynthetic pathway were altered. Also, *OAZ1* coding for ornithine decarboxylase (ODC) antizyme and *TPO1* coding for a polyamine transport protein were disrupted to increase an intracellular SPD level through alleviation of feedback inhibition on ODC and prevention of SPD excretion, respectively. Especially, the strain with combination of *OAZ1* and *TPO1* double disruption and *SPE3* overexpression not only contained a spermidine content of 1.1 mg SPD/g cell, which was 171% higher than that for the control strain, but also exhibited 60% and 33% shorter lag-phase periods than that of the control strain under the medium containing furan derivatives and acetic acid, respectively. While it was observed that a positive correlation between intracellular SPD contents and tolerance

phenotypes among the engineered strains accumulating different amounts of intracellular SPD, too much SPD accumulation is likely to cause metabolic burden. Therefore, genetic perturbations for intracellular SPD levels should be optimized in terms of metabolic burden and SPD contents to construct inhibitor tolerant yeast strains. It was also found that the genes involved in purine biosynthesis and cell wall and chromatin stability were related to the enhanced tolerance phenotypes to furfural.

In addition, the potential applicability of the *S. cerevisiae* strains with high SPD contents was examined by extending its application to repeated-batch fermentation and xylose utilization in the presence of fermentation inhibitors. In one application, during the sixteen times of repeated-batch fermentations using glucose as a sole carbon source, the *S. cerevisiae* strains with high SPD contents maintained higher cell viability and ethanol productivity than those of the control strain. As another application, *XYL1*, *XYL2*, and *XYL3* genes constituting the xylose-assimilating pathway were introduced to the engineered strains with high SPD contents. These xylose-fermenting engineered *S. cerevisiae* strains with high SPD contents exhibited 38 ~ 46% higher ethanol productivity than that of the control strain in the synthetic hydrolysates. Interestingly, the engineered strain also showed improved xylose fermentation in the absence of fermentation inhibitors. The

robust strains constructed in this study can be applied to producing chemicals and advanced biofuels from cellulosic hydrolysates.

SPD has been used to combat skin ageing, stimulate human hair growth, treat type 2 diabetes, and increase fruit shelf life. Therefore, construction of a SPD production system using *S. cerevisiae* has a potential for economic uses. In order to facilitate the enhanced production of SPD, the endogenous *SPE1*, *SPE2*, and *SPE3* genes involved in the polyamine biosynthetic pathway were overexpressed to increase polyamine contents. Also, the gene involved in feedback inhibition (*OAZ1*) was disrupted to increase SPD titer further. To export intracellular SPD into culture medium, *TPO1* encoding polyamine transporter protein was overexpressed using a multi-copy vector. It was observed that SPD production yield from xylose (4.0 mg SPD/g xylose) was 3.1-fold higher than that from glucose. In a glucose limited fed-batch fermentation, the SR8 OS123/pTPO1 strain consumed 37.4 g/L xylose and produced 224 mg/L spermidine with a yield of 2.2 mg SPD/g sugars.

Key words: biofuels, spermidine, fermentation inhibitors, feedback inhibition, polyamine transport protein, xylose, repeated-batch fermentation

Student ID: 2009-21235

CONTENTS

Chapter 1

Literature review	1
1.1. Introduction.....	2
1.2. Construction of inhibitor tolerant <i>Saccharomyces cerevisiae</i> strains....	7
1.3. Spermidine	16
1.4. Biosynthesis of spermidine in <i>S. cerevisiae</i>	19
1.5. Objectives of the dissertation.....	22

Chapter 2

Effects of spermidine on tolerance of <i>Saccharomyces cerevisiae</i>	32
2.1. Summary.....	33
2.2. Introduction.....	34
2.3. Materials and methods.....	36
2.4. Results	40
2.4.1. Effects of polyamines on tolerance of <i>S. cerevisiae</i> against furan derivatives	40
2.4.2. Effects of spermidine on tolerance of <i>S. cerevisiae</i> to acetic acid and lignocellulose hydrolysates	43
2.5. Discussion.....	45

Chapter 3

Construction of engineered strains with improved tolerance against multiple inhibitors and ethanol56

3.1. Summary.....	57
3.2. Introduction.....	59
3.3. Materials and methods.....	61
3.4. Results	66
3.4.1. Construction of engineered <i>Saccharomyces cerevisiae</i> stains with high spermidine contents.....	66
3.4.2. Effects of disruption of <i>TPO1</i> coding for polyamine excretion protein on tolerance of <i>S. cerevisiae</i>	69
3.4.3. Identification of genes involved in tolerance against furan derivatives	71
3.5. Discussion.....	76

Chapter 4

Application of engineered *Saccharomyces cerevisiae* strains with high spermidine contents to enhancing ethanol fermentation performance 105

4.1. Summary.....	106
4.2. Introduction.....	108
4.3. Materials and methods.....	111
4.4. Results and discussion.....	116
4.4.1. Effects of high spermidine content on repeated-batch fermentation	116
4.4.2. Introduction of xylose assimilation pathway to the engineered strains with high spermidine contents	119

4.4.3. Fermentation of xylose-fermenting <i>S. cerevisiae</i> strains with high spermidine contents in simulated hydrolysates containing furfural, HMF, and acetic acid	122
4.4.4. Fermentation of xylose-fermenting <i>S. cerevisiae</i> strains with high spermidine contents in corn stover hydrolysate.....	124
4.4.5. Improved xylose fermentation of <i>S. cerevisiae</i> by high spermidine contents in the absence of fermentation inhibitors	125

Chapter 5

Production of spermidine in engineered *Saccharomyces cerevisiae*

.....	138
5.1. Summary.....	139
5.2. Introduction.....	140
5.3. Materials and methods.....	142
5.4. Results	147
5.4.1. Construction of engineered <i>S. cerevisiae</i> producing spermidine	147
5.4.2. Optimization of fermentation conditions for improving spermidine production.....	148
5.4.3. Spermidine production from xylose by the SR8 strain with the spermidine overproduction pathway	151
5.5. Discussion.....	153

Chapter 6

Conclusions 168

References 171

Appendix 1

The data from the heat maps presented in Fig. 3.14.....	198
1.1. D452-2 VS SPD	199
1.2. D452-2 VS DT	203
1.3. DT VS SPD	204

Appendix 2

Simple amino acid tags improve both expression and secretion of <i>Candida antarctica</i> lipase B in recombinant <i>Escherichia coli</i>	206
--	------------

Appendix 3

Application of repeated aspartate tags to improving extracellular production of <i>Escherichia coli</i> L-asparaginase isozyme II.....	267
---	------------

국문 초록	303
--------------------	------------

LIST OF TABLES

Table 1.1. Major fermentation inhibitors present in lignocellulosic hydrolysates from spruce, willow, wheat straw, sugar cane bagasse, and corn stover.....	23
Table 2.1. Comparison of fermentation parameters by <i>S. cerevisiae</i> D452-2 with and without supplementation of 1, 2, and 4 mM spermidine (SPD) in yeast synthetic complete (YSC) medium containing 55 g/L glucose, 2 g/L furfural, and 2 g/L HMF.....	47
Table 3.1. <i>S. cerevisiae</i> strains and plasmids used in Chapter 3.....	81
Table 3.2. List of DNA oligomers used in Chapter 3.....	85
Table 4.1. <i>S. cerevisiae</i> strains and plasmids used in Chapter 4.....	127
Table 5.1. <i>S. cerevisiae</i> strains and plasmids used in Chapter 5.....	155

LIST OF FIGURES

Fig. 1.1. Structure of lignocellulosic biomass	24
Fig. 1.2. The process for conversion of lignocellulosic biomass to ethanol ..	25
Fig. 1.3. Schematic diagram for goals of pretreatment on lignocellulosic material.....	26
Fig. 1.4. Average composition of lignocellulosic biomass and fermentation inhibitors	27
Fig. 1.5. Conversion of furfural (a) and HMF (b) to its alcohol forms by <i>S. cerevisiae</i>	28
Fig. 1.6. A schematic diagram showing key genes involved in tolerance and detoxification of furfural and HMF for <i>S. cerevisiae</i>	29
Fig. 1.7. Chemical structure of putrescine, spermidine, and spermine	30
Fig. 1.8. Polyamine metabolism in <i>S. cerevisiae</i>	31
Fig. 2.1. Intracellular levels of polyamines in <i>S. cerevisiae</i> D452-2 with and without supplementation of 2 mM spermidine (SPD), spermine (SPM), or putrescine (PUT) in yeast synthetic complete (YSC) medium.....	48
Fig. 2.2. Batch fermentation of <i>S. cerevisiae</i> D452-2 (a) and D452-2 supplemented with 2 mM SPD (b), SPM (c), or PUT (d) in the presence of 2 g/L furfural and HMF	49
Fig. 2.3. Comparison of fermentation parameters by <i>S. cerevisiae</i> D452-2 and D452-2 supplemented with 2 mM SPD, SPM, or PUT in the presence of 2 g/L furfural and HMF	50

Fig. 2.4. Intracellular levels of polyamines in <i>S. cerevisiae</i> D452-2 with and without supplementation of 1, 2, and 4 mM SPD in YSC medium	51
Fig. 2.5. Batch fermentation of <i>S. cerevisiae</i> D452-2 without (a) and with 1 mM (b), 2 mM (c), and 4 mM (d) SPD supplementation in the presence of 2 g/L furfural and HMF.....	52
Fig. 2.6 Batch fermentation of <i>S. cerevisiae</i> strains in the presence of 2 g/L furfural and HMF.....	53
Fig. 2.7. Cell growth of <i>S. cerevisiae</i> D452-2 without (a) and with (b) 2 mM SPD supplementation in the presence of 0, 1, 2, and 4 g/L acetic acid.....	54
Fig. 2.8. Batch fermentation of <i>S. cerevisiae</i> D452-2/pXYL123 without (a) and with (b) 2 mM SPD supplementation in corn stover hydrolysate	55
Fig. 3.1. Regulation of polyamine biosynthesis in <i>S. cerevisiae</i>	88
Fig. 3.2. Polyamine transport in yeast.....	89
Fig. 3.3. Strategy for constructing engineered <i>S. cerevisiae</i> having high levels of SPD.....	90
Fig. 3.4. Effects of amplification of genes coding for enzymes in the SPD biosynthetic pathway on polyamine contents (a) and cell growth (b).....	91
Fig. 3.5. Effects of alleviation of feedback inhibition on polyamine contents (a), and cell growth (b).....	92
Fig. 3.6. Intracellular levels of polyamines in <i>S. cerevisiae</i> D452-2, DT, DO+S3, and DTO+S3 strains	93
Fig. 3.7. Comparison of fermentation parameters by <i>S. cerevisiae</i> D452-2, DT, DO+S3, and DTO+S3 strains in the presence of 2 g/L furfural and HMF.....	94

Fig. 3.8. Batch fermentation profiles by <i>S. cerevisiae</i> D452-2 (a), DT (b), DO+S3 (c), and DTO+S3 (d) strains in the presence of 2 g/L furfural and HMF.....	95
Fig. 3.9 Cell growth of <i>S. cerevisiae</i> D452-2, DT, DO+S3, and DTO+S3 strains in the presence of 3 (a) and 4 g/L (b) acetic acid.....	96
Fig. 3.10. Batch fermentation of <i>S. cerevisiae</i> D452-2 (a) and <i>ATG7</i> disrupted D452-2 (DA) (b) supplemented with 2 mM SPD in the presence of 2 g/L furfural and HMF.....	97
Fig. 3.11. <i>In vitro</i> assay of reduction activity toward furfural (a) and HMF (b)	98
Fig. 3.12. Batch fermentation of <i>S. cerevisiae</i> D452-2 without (a) and with (b) 2 mM SPD supplementation and the DT strain (c) in the presence of 4 g/L furfural	99
Fig. 3.13. Comparison of furfural conversion patterns by <i>S. cerevisiae</i> D452-2 with and without 2 mM SPD supplementation and the DT strain	100
Fig. 3.14. Differently expressed genes between <i>S. cerevisiae</i> D452-2 without and with 2 mM SPD supplementation (a), D452-2 and the DT strain (b), and the DT strain and D452-2 with 2 mM SPD supplementation (c) in response to furfural	101
Fig. 3.15. Comparison of fermentation parameters by <i>S. cerevisiae</i> D452-2 and engineered strains in the presence of 2 g/L furfural and HMF	102
Fig. 3.16. Cell growth of <i>S. cerevisiae</i> D452-2 and engineered strains (a) and batch fermentation of <i>S. cerevisiae</i> D452-2 (b), DT (c), and RAH (d) strains in the presence of 2 g/L furfural and HMF	103
Fig. 3.17. Cell growth of <i>S. cerevisiae</i> D452-2, DT, DTO+S3, and RAH strains in the presence of 8% (v/v) ethanol	104

Fig. 4.1. Effects of yeast cell viability on fermentation ability during repeated-batch fermentation using glucose as a sole carbon source	129
Fig. 4.2. Comparison of fermentation parameters by <i>S. cerevisiae</i> D452-2, DT, TOS3, Z1, and TZ1 strains in the YSCD (50 g/L glucose) medium containing 2 g/L furfural and HMF.....	130
Fig. 4.3. Comparison of fermentation parameters by <i>S. cerevisiae</i> X, DTX, TOS3X, Z1X, and TZ1X strains in the YSCDX (70 g/L glucose and 40 g/L xylose) medium containing 2 g/L furfural and HMF.....	131
Fig. 4.4. Batch fermentation of <i>S. cerevisiae</i> X (a), DTX (b), TOS3X (c), Z1X (d), and TZ1X (e) strains in the YSCDX (70 g/L glucose and 40 g/L xylose) medium containing 2 g/L furfural and HMF	132
Fig. 4.5. Comparison of fermentation parameters by <i>S. cerevisiae</i> X, DTX, and TOS3X strains in simulated hydrolysates containing high concentration of furan derivatives (1 g/L acetic acid, 2 g/L furfural, and 2 g/L HMF) (a and b) and acetic acid (3 g/L acetic acid, 0.4 g/L furfural and 0.8 g/L HMF) (c and d)	133
Fig. 4.6. Batch fermentation of <i>S. cerevisiae</i> X (a) and TOS3X (b) strains in corn stover hydrolysate	134
Fig. 4.7. Comparison of <i>S. cerevisiae</i> X without (a) and with (b) 2 mM SPD supplementation and the TOS3X strain (c) in the second cycle of the repeated-batch fermentation	135
Fig. 4.8. Comparison of fermentation parameters by <i>S. cerevisiae</i> X strain with and without 2 mM SPD supplementation and the TOS3X strain during the repeated-batch fermentation experiments using the YSCDX (65 g/L glucose and 40 g/L xylose) medium	136

Fig. 4.9. Batch fermentation of <i>S. cerevisiae</i> X (a) and TOS3X (b) strains in the YSCDX (70 g/L glucose and 40 g/L xylose) medium	137
Fig. 5.1. Strategy for production of SPD in culture medium by engineered <i>S. cerevisiae</i>	157
Fig. 5.2. Comparison of SPD production by <i>S. cerevisiae</i> D452-2/p42K, D452-2/pTPO1, OS123/p42K, and OS123/pTPO1 strains	158
Fig. 5.3. Batch fermentation of <i>S. cerevisiae</i> OS123/pTPO1 strain in 50 ml YP medium containing 50 g/L glucose with 200 mg/L G418 at 30°C and 300 rpm under various pH conditions.....	159
Fig. 5.4. Comparison of SPD production by <i>S. cerevisiae</i> OS123/pTPO1 strain under various pH conditions	160
Fig. 5.5. Comparison of SPD production by <i>S. cerevisiae</i> D452-2/p42K, D452-2/pTPO1, OS123/p42K, and OS123/pTPO1 strains at pH 2.4	161
Fig. 5.6. Batch fermentation of <i>S. cerevisiae</i> OS123/pTPO1 strain in 50 ml YP medium (pH 2.4) containing 50 g/L glucose under various fermentation conditions	162
Fig. 5.7. Intracellular levels of polyamines in <i>S. cerevisiae</i> D452-2/p42K, D452-2/pTPO1, OS123/p42K, and OS123/pTPO1 strains at pH 2.4	163
Fig. 5.8. Batch fermentation of <i>S. cerevisiae</i> SR8 OS123/pTPO1 strain in 50 ml YP medium (pH 2.4) containing 50 g/L xylose with 400 mg/L G418....	164
Fig. 5.9. Comparison of maximum putrescine and spermine concentrations obtained from glucose and xylose fermentations.....	165
Fig. 5.10. Glucose limited fed-batch fermentation by the SR8 OS123/pTPO1 strain.....	166

Fig. 5.11. Comparison of SPD production by *S. cerevisiae* OS123/pTPO1 and OS123/pmTPO1 strains 167

Chapter 1

Literature review

1.1. Introduction

Lignocellulosic biomass including corn stover, sugar cane, wood, straw, and waste residues from agriculture and forestry is a promising resource for producing fuels and chemicals. In contrast to sugar or starch-based resources, lignocellulose-derived fuels might be able to replace substantial portions of the transportation fuels produced from petroleum without competition with increasing food demand (Hahn-Hagerdal et al., 2006). Nevertheless, utilization of lignocellulose as feedstock for producing fuels and chemicals has been hampered due to the recalcitrant nature of lignocellulose materials (Lynd et al., 2008) (Fig. 1.1).

The process for production of ethanol from lignocellulosic biomass consists of five unit operations: (1) desizing, (2) pretreatment, (3) enzymatic hydrolysis, (4) fermentation, and (5) ethanol recovery (Fig. 1.2). In the second step of the process, in order to release fermentable sugars from lignocellulosic biomass, pretreatment and hydrolysis of lignocellulose are necessary (Lynd et al., 2005) (Fig. 1.3). To date, various physicochemical pretreatment processes, such as dilute acid, alkali, steam explosion, and hydro-thermal methods (Agbor et al., 2011; Mosier et al., 2005) have been developed. The dilute acid pretreatment is considered as the most simple and economical process and has often

been employed for large scale operation (Jung et al., 2013). However, this process generates substantial amounts of fermentation inhibitors at toxic levels in lignocellulose hydrolysates (Fig. 1.4 and Table 1.1). Furan derivatives (2-furaldehyde (furfural) and 5-hydroxymethyl-2-furfural (HMF)), carboxylic acids (acetic acid and formic acid), and phenolic compounds (Almeida et al., 2007) are major inhibitors and aggravate both growth and fermentation capabilities of fermenting microorganisms. Furfural and HMF are formed by dehydration of pentose and hexose sugars, respectively, and phenolic compounds are formed by degradation of lignin and carbohydrates during pretreatment (Dunlop, 1948; Popoff and Theander, 1976; Ulbricht et al., 1984). While acetic acid is generated by de-acetylation of hemicelluloses, formic acid is a degradation product of furfural and HMF (Dunlop, 1948; Ulbricht et al., 1984).

Furan derivatives not only inhibit the growth of yeast and prolong lag-phase period but also decrease ethanol yield and productivity. When the toxicity was compared, although HMF required longer time to be converted by yeast, furfural had a more severe inhibitory effect than HMF (Liu et al., 2004). This was confirmed by the observation showing that exit times from lag-phases coincided with complete conversion of furfural into furfuryl alcohol even though HMF remained in the culture medium at the exit times (Kim et al., 2015). The toxic

effects of furan derivatives could be explained several mechanisms. Furfural and HMF has been reported to directly inhibit several oxidoreductases including alcohol dehydrogenase (ADH), aldehyde dehydrogenase (ALDH), and pyruvate dehydrogenase (PDH) (Modig et al., 2002). Furfural also decreased activity of the glycolytic enzymes including hexokinase and glycerol aldehyde-3-phosphate dehydrogenase (Banerjee et al., 1981). The addition of furfural and HMF also decreased intracellular levels of NADH, NADPH, and ATP in a xylose-fermenting *S. cerevisiae* strain by 58%, 85%, and 42%, respectively (Ask et al., 2013). These result might be caused by the fact that *S. cerevisiae* converts furan derivatives using NAD(P)H as cofactors and repair damages caused by diverse stress conditions through ATP dependent pathways (Lans et al., 2012). Moreover, thiol reactivity of furfural and HMF induces oxidative stress in *S. cerevisiae*, leading to damage in mitochondria and vacuole membranes, the actin cytoskeleton, and nuclear chromatin (Allen et al., 2010; Kim and Hahn, 2013).

The pKa value of acetic acid is 4.76, and the toxic effect on *S. cerevisiae* is attributed to the undissociated form. The undissociated form of acetic acid can penetrate into the plasma membrane from the medium and then dissociates due to high intracellular pH. The dissociation of acetic acid decreases the intracellular pH, and *S.*

cerevisiae consumes ATP to pump protons out of the cells (Pampulha and Loureiro-dias, 1989). Consequently, undissociated form of acetic acid causes ATP depletion and growth inhibition. For example, yeast cells cannot grow at pH 4.6 in batch fermentation with spruce hydrolysate (Palmqvist et al., 1998). As pH adjusted from 4.6 to 5.0, *S. cerevisiae* started to grow. This pH dependent growth in lignocellulose hydrolysates was resulted from high concentration of the undissociated form of acetic acid at low pH. Moreover, metabolomics data revealed that the addition of acetic acid induced substantially accumulation of metabolites involved in the non-oxidative pentose phosphate pathway (PPP) including sedoheptulose-7-phosphate, ribulose-5-phosphate, and ribose-5-phosphate and erythrose-4-phosphate (Sanda et al., 2011). Also, acetic acid has been proven to cause chronological ageing by inducing an apoptosis-like response (Burtner et al., 2009; Fabrizio and Longo, 2008; Herker et al., 2004; Ludovico et al., 2001).

While ethanol yield and productivity decrease at high concentrations of furan derivatives and acetic acid, low concentrations of these inhibitors rather increase ethanol yield. *Saccharomyces cerevisiae* can convert furfural and HMF to less toxic alcohols, furfuryl alcohol and furan dimethanol, respectively, by an oxygen independent manner (Liu et al., 2008; Taherzadeh et al., 1999a; Taherzadeh et al., 2000a) (Fig. 1.5). Because these conversions require NAD(P)H as cofactors, *S. cerevisiae*

has additional option for maintaining redox balance and thus can minimize carbon flux toward glycerol and xylitol (Wahlbom and Hahn-Hagerdal, 2002). When 0.5 g/L furfural was added to the medium, glycerol concentration decreased from 4.66 g/L to 3.66 g/L and ethanol yield increased from 0.450 g ethanol/g sugars to 0.487 g ethanol/g sugars in *S. cerevisiae* (Avanasi et al., 2013). In the background *S. cerevisiae* strains overexpressing *ADHI* encoding alcohol dehydrogenase or *ADHI* mutant derived from TMB3000 (Laadan et al., 2008), addition of 40 mM (3.84 g/L) furfural or 40 mM (5.04 g/L) HMF also increase ethanol production and yield, compared with the absence of furan derivatives (Ishii et al., 2013). In addition, presence of 20 mM (1.2 g/L) acetic acid improves ethanol yield by stimulating ATP production (Greetham, 2014).

1.2. Construction of inhibitor tolerant *Saccharomyces cerevisiae* strains

Because the toxic nature of the fermentation inhibitors is one of the roadblocks toward large-scale production of lignocellulosic bioethanol (Almeida et al., 2009; Almeida et al., 2007; Park et al., 2011), various physical and chemical methods and fermentation strategies have been developed to remove or reduce these inhibitory compounds in lignocellulose hydrolysate (Yang and Wyman, 2008).

In fermentation strategies for efficient fermentation of lignocelluloses hydrolysates, large inoculum size was used to decrease inhibition problems (Chung and Lee, 1985; Palmqvist and Hahn-Hagerdal, 2000a; Pienkos and Zhang, 2009). For example, using an initial cell density of 10 g/L, a ethanol productivity of 3.0 g/L·h with final yield of 0.44 g ethanol/g sugars have been obtained when spruce hydrolysate was fermented without pH adjustment (pH 4.8) (Stenberg et al., 1998). Second, cell immobilization and recirculation for retaining stability of cell activities have been explored (Kirdponpattara and Phisalaphong, 2013; Palmqvist and Hahn-Hagerdal, 2000b). Immobilization of yeast cells reduces contamination risk (Sembiring et al., 2013) and fermentation time (Karagoz and Ozkan, 2014), makes the separation of cells easy (Sembiring et al., 2013), and protects the cells from

fermentation inhibitors (Kirdponpattara and Phisalaphong, 2013). Therefore, immobilized *S. cerevisiae* by several immobilizing agents produced ethanol at high yield and productivity compared to free cells (Behera et al., 2011; Nikolic et al., 2010; Razmovski and Vucurovic, 2011). Recently, lignocellulose based immobilizing materials were developed to replace classical immobilizing agents for cheap and easy production of ethanol (Singh et al., 2013). In addition, cell recirculation can be used to recycle biocatalysts. In a related study recycling both hydrolysis enzymes and yeast cells, enzymatic hydrolysis and fermentation time was reduced to a total of 48 h (Sarks et al., 2014). Third, fed-batch fermentation designed to feed the substrate at a low rate has been reported to be advantageous (Rudolf et al., 2005). Since the concentration of inhibitors can be kept low in a fed-batch mode, the inhibition effects decrease. The optimized feeding rate is equal to the *in vivo* detoxification rate of yeast cells. For example, while batch fermentation of spruce hydrolysate was strongly inhibited by the presence of the inhibitors, efficient production of ethanol was fulfilled in fed-batch fermentation without any detoxification methods (Taherzadeh et al., 1999b). However, it is difficult to determine the optimal feeding rate based on the compositions and concentrations of inhibitors present in the hydrolyaste because synergistic and antagonistic effects among the fermentation inhibitors cannot be

exactly calculated. To solve this problem, on-line measurement of CO₂ evolution rate reflecting growth rate was coupled to determine feeding rate (Nilsson et al., 2001; Taherzadeh et al., 2000b). Using this feeding strategy, fed-batch fermentation of the hydrolysates containing 1.4 ~ 5 g/L furfural and 2.4 ~ 6.5 g/L HMF was successfully achieved (Taherzadeh et al., 2000b).

Still, these detoxification methods usually require additional steps and equipments and hence are not economical for practical use (Mussatto and Roberto, 2004). Therefore, development of inhibitor-tolerant microorganisms is imperative for cost-effective bioethanol production. There are three strategies to construct inhibitor tolerant yeast strains: (1) improving *in vivo* conversion capacity of yeast cells toward furan derivatives. (2) enhancing genetic background and reprogramming pathways to overcome toxic effects caused by fermentation inhibitors. (3) an evolutionary engineering approach.

The toxic effects of furfural and HMF are resulted from the attached aldehyde functional group, and *S. cerevisiae* cells convert the aldehyde group into less toxic alcohols. The reduction of furan derivatives by *S. cerevisiae* has been shown to be coupled with both NADH and NADPH, and the ratio of the activities was strain dependant (Nilsson et al., 2005). Overexpression of oxidoreductases, such as alcohol dehydrogenases

(*ADH1*, *ADH6*, and *ADH7*) (Almeida et al., 2008; Liu et al., 2008; Petersson et al., 2006), aldo-keto reductase (*GRE2*) (Moon and Liu, 2012), and aldehyde dehydrogenase (*ALD6*) (Park et al., 2011) from *S. cerevisiae*, or xylose reductase (*XYL1*) from *Scheffersomyces stipitis* (Almeida et al., 2009) has been shown to increase the specific furfural and HMF conversion rates and hence decreases the lag-phase of the cell growth in the presence of furfural and HMF. This strategy was well reviewed by Liu (Liu, 2011), and therefore will not be discussed in detail in this thesis.

Additionally, the NADPH-producing pentose phosphate pathway (PPP) and oxidative stress response pathways are critical factors for tolerance against furan derivatives (Gorsich et al., 2006; Kim and Hahn, 2013) (Fig. 1.6). While the control *S. cerevisiae* strain was able to grow after 24 h in the lag phase, single gene deletion mutants of the PPP genes (*ZWF1*, *GND1*, *TKL1*, and *RPE1*) are unable to grow in the medium containing 25 mM (2.4 g/L) furfural (Gorsich et al., 2006). Especially, the *ZWF1* encoding glucose-6-phosphate dehydrogenase deficient mutant exhibited the highest growth defect, confirming that this enzyme catalyzes the rate-limiting step of the PPP. On the other hand, overexpression of *ZWF1* enabled yeast cells to grow in the medium containing 50 mM (4.8 g/L) furfural where the control strain cannot grow. This result is probably not due to the enhanced reduction of

furfural into furfuryl alcohol because furfural is mainly converted by using NADH in *S. cerevisiae*. PPP may function by maintaining NADPH pool required for activity of many stress responsive proteins (Carmel-Harel and Storz, 2000). Meanwhile, furfural and HMF cause damage in mitochondria and vacuole membranes, the actin cytoskeleton, and nuclear chromatin by inducing oxidative stress (Allen et al., 2010). Recently, the underlying mechanisms involved in induction of oxidative stress by furfural and HMF were investigated (Kim and Hahn, 2013). Both furfural and HMF activate the YAP1 transcriptional factor, a major oxidative stress regulator (Ma and Liu, 2010a), via the H₂O₂-independent pathway and deplete cellular glutathione (GSH) levels by acting as thiol-reactive electrophiles. The *in vitro* and *in vivo* thiol reactivity of furfural toward GSH was higher than that of HMF. Therefore, overexpression of an active *YAP1* mutant (C620F) and *YAP1* target genes (*CTA1* and *CTT1*) coding for catalases enhanced tolerance of *S. cerevisiae* to furan derivatives. Also, addition of GSH to culture medium and overexpression of the genes involved in the GSH biosynthetic pathway (*GSH1* and *GLR1*) improved tolerance to furfural but not to HMF. In another study, *SSK2* encoding a mitogen-activated protein (MAP) kinase kinase kinase of the high osmolarity glycerol (HOG) signaling pathway was founded as a novel gene target in coping with furfural stress (Kim et al., 2012a). The transposon

mutant strain (Tn 2) having a transcriptionally downregulated *SSK2* level displayed enhanced furfural tolerance. The Tn 2 showed a substantial decrease of intracellular levels of reactive oxygen species (ROS) and activation of HOG1. Such a decrease in ROS might be ascribed to the increased transcriptional levels of *CTTI* and *GLR1* genes, which are the HOG1 downstream target genes involved in ROS reduction.

Complex gene interactions and regulator networks for adaptation of *S. cerevisiae* to furan derivatives have been comprehensively investigated (Li and Yuan, 2010; Liu et al., 2004; Ma and Liu, 2010a). In an adaptation process to HMF, seven transcription factor genes (*YAP1*, *YAP5*, *YAP6*, *PDR1*, *PDR3*, *RPN4*, and *HSF1*) were identified as key regulators for the induced expression response. *YAP1* encoding a b-ZIP (basic region leucine zipper) transcription factor plays an important role in the multidrug resistance and oxidative stress response of *S. cerevisiae* by recognizing the YAP1 response elements (TRE) in the promoter region (Fernandes et al., 1997; Harbison et al., 2004; Wiatrowski and Carlson, 2003). It was found that many genes were regulated directly by *YAP1* or indirectly by *YAP5* and *YAP6* (Ma and Liu, 2010a). The PDR gene family encoding plasma membrane proteins functions as transporters of ATP-binding cassette (ABC) proteins. These proteins not only mediate transportation of a wide range

of substrates but also exhibit multiple functions in response to a variety of unrelated chemical stresses (Jungwirth and Kuchler, 2006; Mamnun et al., 2002). For cell survival and adaptation in the presence of furan derivatives, HMF-induced transcriptional factors (*PDR1* and *PDR3*) regulating numerous members of the PDR genes has been shown to be imperative (MacPherson et al., 2006; Moye-Rowley, 2003). Also, *ATRI* and *FLRI* genes encoding multidrug-resistance (MDR) proteins are involved in coping with various chemical stresses (Alarco et al., 1997; Jungwirth et al., 2000; Kanazawa et al., 1988). Another necessary component of HMF tolerance involves genes functioning in protein folding, modification, and destination, which is essential to alleviate toxicity caused by degraded proteins and to restore protein functions. These genes are regulated by *RPN4*, *HSF1*, and other co-regulators (Lee et al., 2002; Mannhaupt et al., 1999). Based on these fundamental findings, inhibitor tolerant *S. cerevisiae* strains were constructed by overexpressing genes encoding MDR proteins (*ATRI* and *FLRI*) and a transcriptional factor (*YAPI*) (Alriksson et al., 2010). Among them, ethanol productivity of 0.17 g/L·h was obtained for the *YAPI* overexpressing strain in fermentation with spruce hydrolysate, which was 240% higher than the control strain.

While tolerance or detoxifying mechanisms of furfural and HMF have been intensively studied, metabolic engineering strategies for

constructing tolerant strains to carboxylic acids, such as acetic acid and formic acid have been rare (van Maris et al., 2006). Unlike furfural and HMF, generation of acetic acid is inevitable regardless of pretreatment methods as it is formed by the hydrolysis of acetylxytan in hemicelluloses (Fig. 1.4). Moreover, concentrations of acetic acid in cellulosic hydrolysates are higher than furfural and HMF (Table 1.1). Therefore, identification of environmental and genetic perturbations eliciting enhanced tolerance of fermenting microorganisms to acetic acid has been anticipated.

While previous studies have focused on iterative identification and engineering of cellular pathways responsible for enhanced tolerance to specific inhibitors (Alriksson et al., 2010; Gorsich et al., 2006; Kim and Hahn, 2013; Park et al., 2011; Sanda et al., 2011; Sundstrom et al., 2010), these incremental improvements based on combinations of the identified target pathways might not yield optimal strains tolerant to multiple inhibitors. Moreover, accumulated ethanol by yeast and other minor fermentation inhibitors may exert additional stresses to yeast cells especially when combined with the major fermentation inhibitors (Ma and Liu, 2010b). Therefore, it is necessary to construct engineered *S. cerevisiae* strains exhibiting tolerance to multiple inhibitors (furfural, HMF, and acetic acid) and ethanol for efficient production of cellulosic ethanol. Instead of chasing individual cellular pathways related with

enhanced tolerance to each components of fermentation inhibitors, an approach to identify and exploit a global mediator eliciting the enhanced tolerance to multiple inhibitors simultaneously was undertaken.

1.3. Spermidine

Polyamines including putrescine, spermidine, and spermine are low molecular weight aliphatic nitrogen compounds that are found ubiquitously in microorganisms, plants, and animals (Hamana and Matsuzaki, 1992) (Fig. 1.7). The original discovery of the polyamines dates back to 1678 when Antonie van Leeuwenhoek observed that the seminal fluid contains a slowly crystallizing substance (van Leeuwenhoek, 1678). However, the tools necessary to study molecular function of the polyamines have only recently become available. The intracellular concentrations of the polyamines are in the millimolar range. Although free polyamine concentrations are low, they are mostly ionically bound to DNA, RNA, proteins, and phospholipids. Many studies have reported the role of spermidine in stabilizing chromatin, as well as in processes ranging from DNA replication, transcription and translation, to the regulation of cell growth and apoptosis (Childs et al., 2003; Oredsson, 2003; Wallace et al., 2003). The effects of the spermidine are, however, far from simple, with both induction and inhibition of biosynthetic and catabolic enzyme activities being associated with increased and decreased apoptosis (Schipper et al., 2000). On the other side, abnormal levels of spermidine are also associated with cancer and other hyperproliferative diseases, thus

making spermidine function and metabolism attractive targets for therapeutic intervention (Casero and Marton, 2007).

Spermidine interacts with acidic phospholipids in membranes as well as DNA and RNA (Schuber, 1989). In general, spermidine increases the rigidity of the membrane by forming complexes with phospholipids and proteins. In addition, spermidine is associated with rare physiological process. In hypusination, spermidine functions as a substrate for the hypusine modification of the putative eukaryotic translation initiation factor 5A (eIF5A) (Chattopadhyay et al., 2008) (Fig. 1.8). eIF5A is a highly conserved and essential protein present in all organisms from archaeobacteria to mammals (Schnier et al., 1991), and the hypusine/deoxyhypusine modification of eIF5A is essential in all eukaryotic cells (Kang and Hershey, 1994). Therefore, when a polyamine auxotroph is grown in the presence of very limiting concentrations of spermidine, most of the spermidine is used for the modification of eIF5A.

In plants, these amines are associated with defense to diverse environmental stresses (Bouchereau et al., 1999). Polyamine-deficient yeast cells are much more sensitive to elevated temperature (Balasundaram et al., 1996), paromomycin (Balasundaram et al., 1999), and incubation in oxygen (Balasundaram et al., 1993). Furthermore, it

was reported that spermidine (SPD) extends lifespan of *S. cerevisiae* through induction of autophagy (Eisenberg et al., 2009). These observations suggest that adequate modulation of polyamine contents in *S. cerevisiae* might improve tolerance to fermentation inhibitors and ethanol.

1.4. Biosynthesis of spermidine in *S. cerevisiae*

The rate-limiting step in SPD biosynthesis is the production of putrescine ornithine decarboxylase (ODC) which is encoded by the *SPE1* gene (Wallace et al., 2003) (Fig. 1.8). ODC has a short half-life and is destroyed by the 26S proteasome (Elias et al., 1995). However, unlike most proteins, ODC is not ubiquitinated, instead a specialized regulatory protein, ODC antizyme (OAZ1), binds to the carboxylic end of the monomeric form of ODC and presents the ODC to the 26S proteasome for degradation (Palanimurugan et al., 2004). OAZ1 itself is subject to ubiquitin-mediated proteolysis by the proteasome. However, degradation of OAZ1 is efficiently inhibited by polyamines (Palanimurugan et al., 2004). Another precursor for SPD biosynthesis, decarboxylated S-adenosyl-methionine, is produced by S-adenosylmethionine decarboxylase (AdoMetDC) which is encoded by the *SPE2* gene. Unlike ODC, AdoMetDC is ubiquitinated before degradation by the 26S proteasome. By addition of an aminopropyl group, putrescine is subsequently converted to SPD by spermidine synthase which is encoded by the *SPE3* gene. Spermidine synthase is constitutively expressed and are primarily regulated by the availability of their substrates.

SPD levels are furthermore controlled by their uptake or excretion into

the environment. SPD uptake is mainly catalyzed by DUR3 and SAM3 (Uemura et al., 2007), and SPD excretion is mainly catalyzed by TPO5 on Golgi or post-Golgi secretory vesicles (Tachihara et al., 2005) and TPO1 on the plasma membrane (Uemura et al., 2005). Therefore, when both the *DUR3* and *SAM3* genes were disrupted, a half of the SPD uptake activity decreased compared with the parent strain (Uemura et al., 2007). On the other hand, polyamine transport by TPO1 was dependent on pH. SPD uptake occurred at alkaline pH (pH 8.0), whereas inhibition of SPD uptake was observed at acidic pH (pH 5.0). Specifically, When TPO1 was expressed with the single-copy plasmid in the *TPO1* gene-disrupted mutant, low but significant uptake at pH 8.0 and excretion of SPD at pH 5.0 were observed (Uemura et al., 2005). These results indicated that TPO1 catalyzes SPD excretion at acidic pH.

Therefore, in this study, in order to facilitate the enhanced tolerance without exogenous addition of SPD, genetic perturbations eliciting higher SPD levels in *S. cerevisiae* were identified. The endogenous *SPE1*, *SPE2*, and *SPE3* genes involved in the polyamine biosynthetic pathway were overexpressed to increase polyamine contents (Fig. 1.8). As polyamine synthesis is controlled by feedback regulation on ODC, high levels of SPD might increase OAZ1 which mediates ubiquitin-independent degradation of ODC by the proteasome (Palanimurugan et

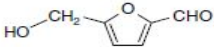
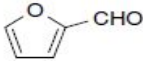
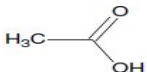
al., 2004). Therefore, the *OAZ1* gene was disrupted for alleviating the feedback regulation of ODC by accumulated SPD in yeast. In order to further increase SPD levels in yeast, the *TPO1* gene coding for polyamine transport protein which mainly excretes polyamines to the medium (Uemura et al., 2007) was also disrupted.

1.5. Objectives of the dissertation

This dissertation has focused on enhancing tolerance of *S. cerevisiae* to multiple lignocellulose-derived fermentation inhibitors through modulation of spermidine contents. The specific objectives of this research are listed:

- 1) Improvement of tolerance of *S. cerevisiae* against major fermentation inhibitors (furfural, HMF, and acetic acid) by using spermidine (SPD) as a chemical elicitor,
- 2) Construction of inhibitor tolerant *S. cerevisiae* strains by combining the amplification of the genes coding for enzymes in the SPD biosynthetic pathway along with disruption of the genes involved in feedback inhibition (*OAZ1*) and SPD excretion (*TPO1*),
- 3) Improvement of ethanol production in cell recycling repeated-batch fermentation and xylose utilization in the presence of fermentation inhibitors through modulation of SPD contents,
- 4) Production of SPD by overexpressing the endogenous *TPO1* gene coding for polyamine transporter protein in the engineered *S. cerevisiae* strain accumulating high concentration of SPD.

Table 1.1. Major fermentation inhibitors present in lignocellulosic hydrolysates from spruce, willow, wheat straw, sugar cane bagasse, and corn stover (Almeida et al., 2007)

Group of Compounds	Concentrations (g/L)				
	Spruce	Willow	Wheat	Sugar cane	Corn stover
Furan derivatives					
 5-Hydroxymethyl-2-furaldehyde (HMF)	2.0	n.q.	n.i.	0.6	0.06
 2-Furaldehyde	0.5	n.q.	n.i.	1.9	11
Aliphatic acids					
 Acetic acid	2.4	n.q.	1.6	4.4	1.6
 Formic acid	1.6	n.q.	1.4	1.4	
Total phenolics	3.1	2.5	0.7	4.5	

n.q. not quantified; n.i. not identified.

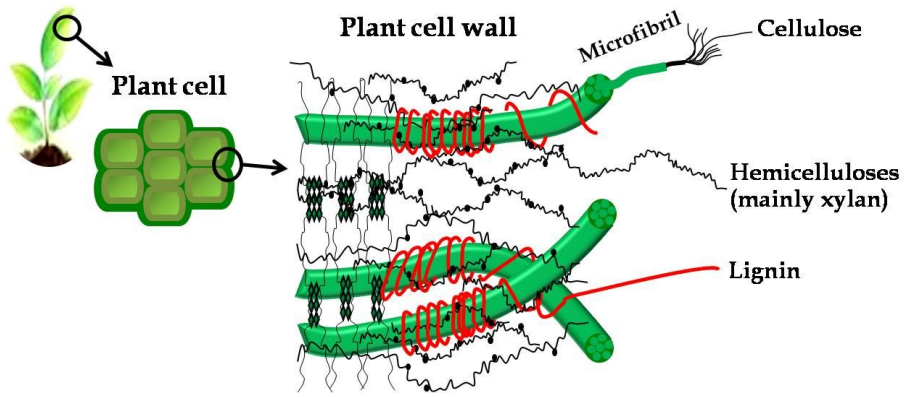


Fig. 1.1. Structure of lignocellulosic biomass.

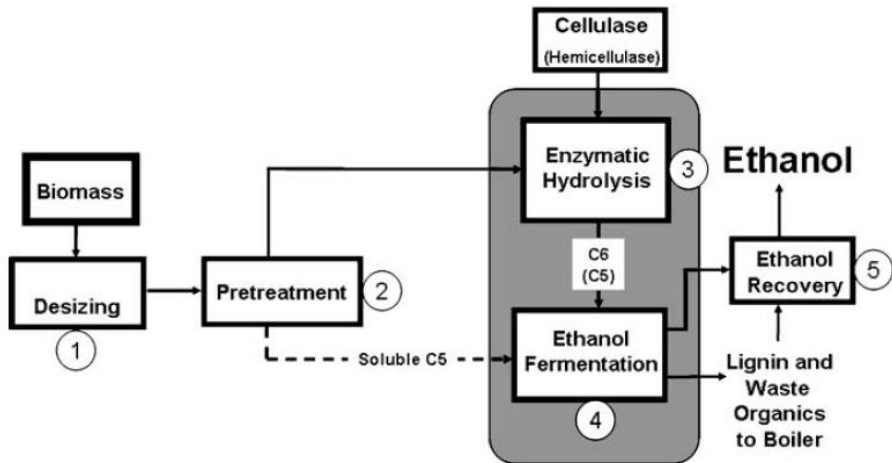


Fig. 1.2. The process for conversion of lignocellulosic biomass to ethanol (Merino and Cherry, 2007). *Step 1* The biomass is physically reduced in size to increase surface area. *Step 2* pretreatment consisting of exposure to high pressure, temperature and extremes of pH is conducted to destroy the plant cell wall and expose the sugar polymers to the liquid phase. *Step 3* Enzymatic hydrolysis using a complex mix of glycosyl hydrolases to convert sugar polymers to monomeric sugars. *Step 4* Fermentation of the monomeric sugars to ethanol by microorganism. *Step 5* Ethanol recovery from the fermentation using distillation or some other separation technology. *C6* and *C5* refer to glucose derived from cellulose hydrolysis and pentose sugars (mainly xylose) derived from hemicelluloses, respectively.

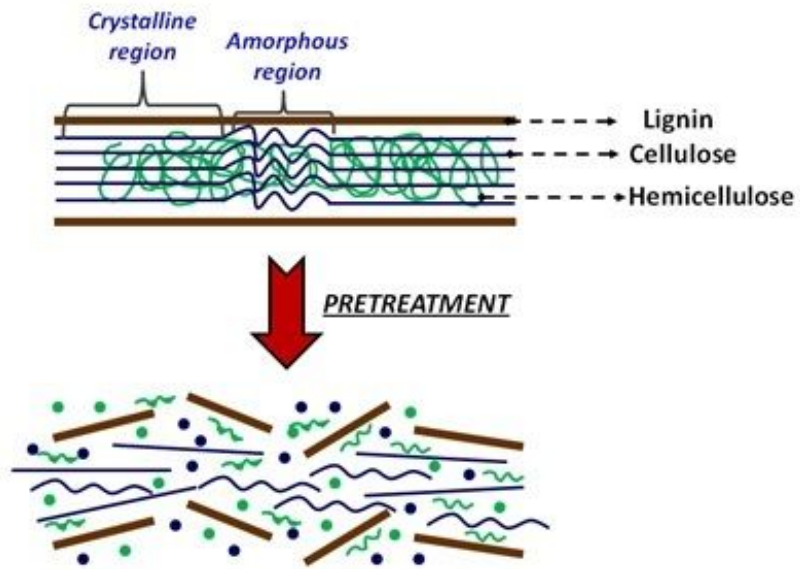


Fig. 1.3. Schematic diagram for goals of pretreatment on lignocellulosic material (Hsu et al., 1980).

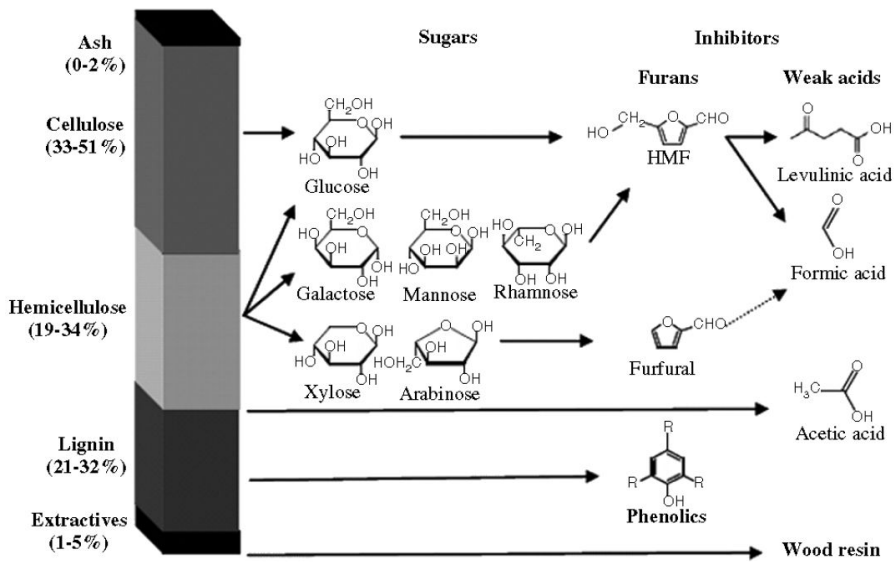


Fig. 1.4. Average composition of lignocellulosic biomass and fermentation inhibitors (Almeida et al., 2007).

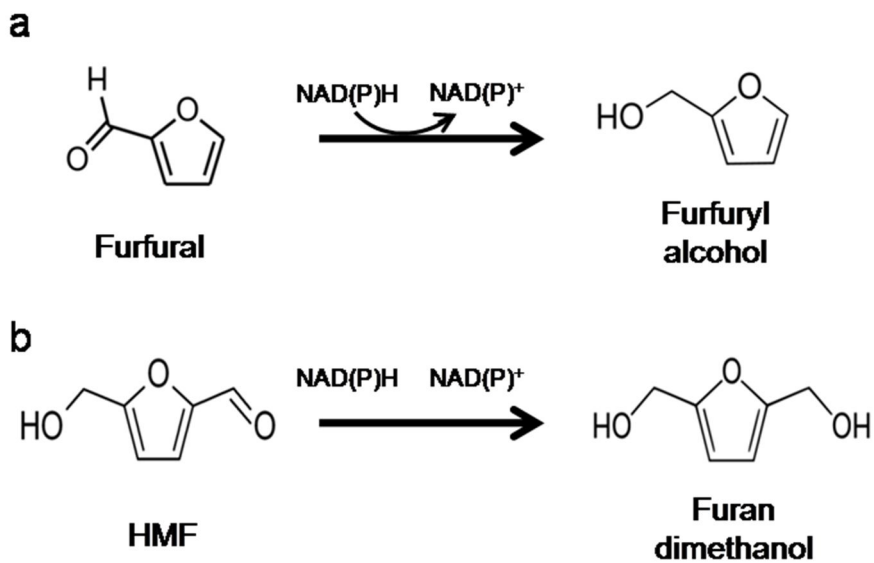


Fig. 1.5. Conversion of furfural (a) and HMF (b) to its alcohol forms by *S. cerevisiae*.

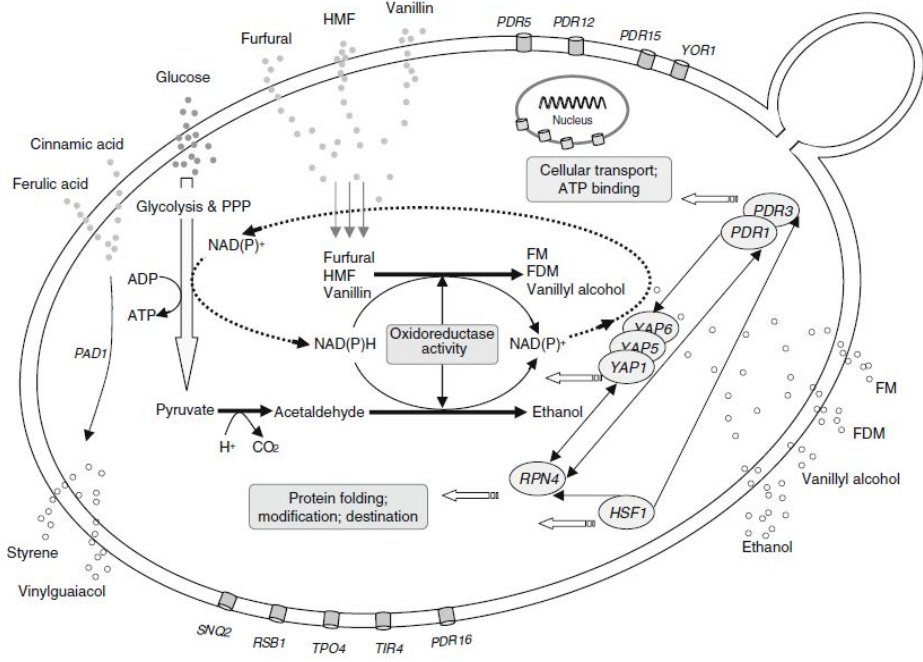
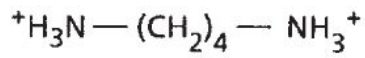
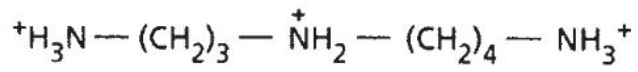


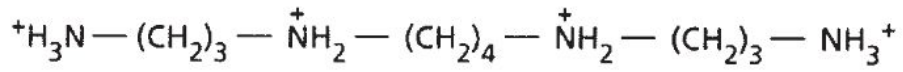
Fig. 1.6. A schematic diagram showing key genes involved in tolerance and detoxification of furfural and HMF for *S. cerevisiae* (Liu, 2011).



Putrescine



Spermidine



Spermine

Fig. 1.7. Chemical structure of putrescine, spermidine, and spermine.

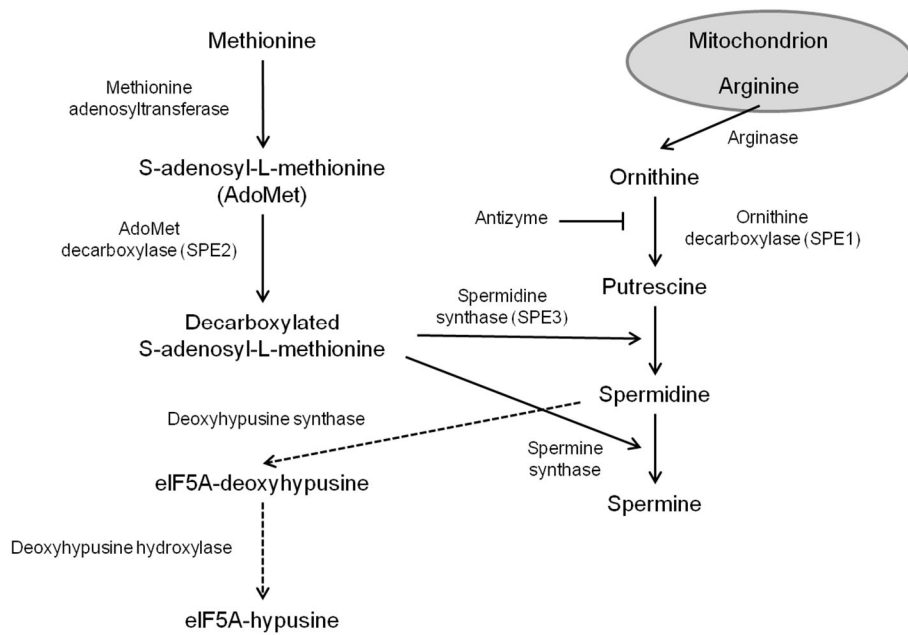


Fig. 1.8. Polyamine metabolism in *S. cerevisiae* (Minois et al., 2011).

Chapter 2

Effects of spermidine on tolerance of *Saccharomyces cerevisiae*

2.1. Summary

Formation of fermentation inhibitors (furfural, HMF, and acetic acid) during the pretreatment of lignocellulose hydrolyzates is an unavoidable obstacle for achieving economic production of biofuels and chemicals. These inhibitors aggravate both growth and fermentation capabilities of fermenting microorganisms. In order to construct engineered strains exhibiting enhanced tolerance to multiple inhibitors simultaneously, a strategy to identify and exploit a global mediator that is capable of enhancing tolerance to multiple inhibitors was undertaken. It was shown that both spermidine and spermine function as chemical elicitor for enhanced tolerance of *S. cerevisiae* against furan derivatives. Especially, the addition of 2 mM spermidine into culture medium was an optimal concentration to improve tolerance of *S. cerevisiae* D452-2 against furan derivatives and acetic acid. In addition, the effects of spermidine supplementation on tolerance of the yeast were also confirmed in corn stover hydrolysate that contains numerous fermentation inhibitors such as furfural, HMF and acetic acid.

2.2. Introduction

Fermentation inhibitors present in lignocellulose hydrolysates are among major hindrances for the commercialization of biofuel production. Among them, furfural, HMF, and acetic acid are major inhibitors which negatively affect microbial growth, metabolism, and ethanol production. As such, metabolic engineering strategies for constructing tolerant strains against the inhibitors have been actively attempted.

In this study, instead of chasing individual cellular pathways related with enhanced tolerance to each component of fermentation inhibitors, a strategy to identify and exploit a global mediator that is capable of enhancing tolerance to multiple inhibitors was undertaken. As target molecules, polyamines including putrescine, spermidine, and spermine are evaluated because polyamines are found ubiquitously in both eukaryotes and prokaryotes and associated with defense to diverse environmental stresses (Bouchereau et al., 1999). In plants, the transgenic plants with high spermidine contents by overexpressing the spermidine synthase gene exhibited enhanced tolerance to various stresses including chilling, freezing, salinity, hyperosmosis, drought, and paraquat toxicity (Kasukabe et al., 2004). Also, it was reported that cellular polyamines provide protection from H₂O₂ damage that is

distinct from the protective role of glutathione, strongly supporting a unique role for polyamines in protection from oxidative stress (Rider et al., 2007).

In this chapter, to investigate effects of polyamines on tolerance phenotypes of yeast against fermentation inhibitors, it was examined whether exogenously added spermidine (SPD), spermine (SPM), or putrescine (PUT) can alter tolerance of *S. cerevisiae* to multiple inhibitors including furan derivatives and acetic acid.

2.3. Materials and methods

2.3.1. *S. cerevisiae* strains

S. cerevisiae D452-2 (*MAT α* , *leu2*, *his3*, *ura3*, and *can1*), L2612 (*MAT α* , *leu2-3,112*, *ura3-52*, *trp1-298*, *can1*, *cyn1*, and *gal⁺*), and CEN.PK2-1D (*MAT α* , *leu2-3,112*, *ura3-52*, *trp1-289*, and *his3 Δ MAL2-8c SUC2*) were used to evaluate effects of polyamine addition on tolerance to fermentation inhibitors including furan derivatives and acetic acid.

2.3.2. Culture conditions and fermentation experiments

Yeast strains were pre-cultured at 30°C and 250 rpm for 48 h in YP medium (10 g/L yeast extract, 20 g/L bacto peptone) with 20 g/L glucose. A defined yeast synthetic complete (YSC) medium (6.7 g/L yeast nitrogen without amino acids and 2.0 g/L synthetic complete supplement mixture) containing appropriate amounts of sugars was used for fermentation experiments.

For the tolerance test experiments, pre-cultured cells from YP medium with 20 g/L glucose were harvested and inoculated into main cultures with initial optical density (OD₆₀₀) of 0.5~1.0. Flask fermentation experiments were performed at 30°C and 80 rpm in 50 ml YSC

medium containing 48~60 g/L glucose with 2 g/L furfural and HMF or 1, 2, or 4 g/L of acetate. For the fermentation with lignocellulose hydrolysate, corn stover hydrolysate was prepared by National Renewable Energy Laboratory (<http://www.nrel.gov/biomass/pdfs/47764.pdf>). Briefly, dilute sulfuric acid and heat from steam were used in a two stage pretreatment process. After the pretreatment reaction, a lot of water along with some extents of the acetic acid and furfural were vaporized. The leftover hydrolysate slurry was cooled by dilution water, and its pH was adjusted from 1 to 5-6 by using ammonia. The hydrolysate was mixed with 50 mM sodium citrate buffer (pH 4.8) at 20% (w/v). For enzymatic hydrolysis, 0.1 ml of 2:1 mixture of cellulase (Celluclast 1.5 L, Sigma, USA) and cellobiase (Novozyme 188, Sigma, USA) was added per gram of dry sample weight. The reaction using a 500 mL-scale baffled flask (Nalgene, Rochester, NY, USA) was carried out at 50°C and 150 rpm for 48 h. After enzymatic hydrolysis, the samples were centrifuged at 13,000 rpm for 10 min. The supernatant was collected and supplemented with concentrated autoclaved YSC medium to result in a hydrolysate mixture with 6.7 g/L yeast nitrogen without amino acids and 2.0 g/L synthetic complete supplement mixture. Initial cell densities were adjusted to OD₆₀₀ of 0.8 and fermentations were performed at 30°C and 80 rpm in 50 ml working volume.

2.3.3. Analytical Methods

Optical density was measured with a spectrophotometer (RF5301, Shimadzu, Kyoto, Japan) at 600 nm. Glucose, xylose, ethanol, furfural, and HMF concentrations were determined by high performance liquid chromatography (HPLC, Agilent Technologies 1200 Series) using a REZEX ROA organic acid column (Phenomenex, Torrance, USA). The column was eluted with 5 mM H₂SO₄ at a flow rate of 0.6 ml/min at 60°C, and detection was made with a reflective index detector. Furfuryl alcohol and furan dimethanol concentrations were determined by a UV detect at 215 nm using a BIO-RAD Aminex HPX-87H ion exclusion column. The column was eluted with 84% (v/v) 5 mM H₂SO₄ and 16% (v/v) acetonitrile at a flow rate of 0.4 ml/min at 25°C. In order to measure intracellular concentrations of polyamines, 10 ml of cell cultures were washed two times with sterilized water. After collected cells were resuspended in 1.6 ml of cold 5% TCA solution and incubated on ice for 1 h with vortexing every 15 min, supernatants were neutralized with 100 µl of 2 M K₂HPO₄. 1,7-diaminopentane was used as the internal standard (IS). For the derivatization, 1 ml of dansyl chloride reagent (5 mg/ml) dissolved in acetone and 0.5 ml of saturated NaHCO₃ solution were added to 1 ml of sample solution containing IS. After the reaction mixture was incubated at 40°C for 1 h with

occasional shaking, the solution was dried under vacuum and 1 ml of acetonitrile was added. The concentrations of polyamines were determined using an HPLC system equipped with a CAPCELL PAK C18 MG column (Shiseido, Tokyo, Japan) according to the method described previously (Innocente et al., 2007; Moret and Conte, 1996).

2.4. Results

2.4.1. Effects of polyamines on tolerance of *S. cerevisiae* against furan derivatives

While addition of three polyamines into culture media generally increased corresponding polyamine content in *S. cerevisiae* D452-2 (Fig. 2.1), the addition of 2 mM SPD increased intracellular SPD contents substantially whereas the addition of 2 mM of SPM and PUT did not increase corresponding polyamines contents as much as SPD. The highest polyamine content of 2.5 mg SPD/g cell was obtained from the strain supplemented with 2 mM SPD, which was six-fold higher than that of a control strain without polyamine supplementation (Fig. 2.1).

Microaerobic batch fermentations of *S. cerevisiae* D452-2 with and without 2 mM polyamines (SPD, SPM, and PUT) supplementation were carried out using yeast synthetic complete (YSC) medium containing 2 g/L of furfural and 2 g/L of HMF. Addition of both 2 g/L of furfural and 2 g/L of HMF substantially inhibited cell growth (Fig. 2.2a). Under the furfural and HMF challenge, the addition of 2 mM SPD or SPM shortened the lag-phase period from 62 h to 25 h (Fig. 2.2 and Fig. 2.3a). However, the addition of PUT to culture medium did not shorten the lag-phase. In all cases with polyamine supplementation, exit

times from lag-phases coincided with complete conversion of furfural into furfuryl alcohol even though HMF remained in the culture medium at the exit times. These results confirmed that furfural is a major inhibitor of glucose consumption and ethanol production by yeast (Liu et al., 2008; Park et al., 2011). Because of the shortened lag period with the addition of SPD and SPM, volumetric ethanol productivities in both cases were 88% higher than the culture without SPD and SPM (Fig. 2.3b). The reason for this improvement by SPD and SPM supplementation is ascribed to the faster detoxification of furfural than the control culture without supplementation. Although both of SPD and SPM function as a chemical elicitor for enhanced tolerance of *S. cerevisiae* against furan derivatives, SPD was chosen as a target molecular because the SPM biosynthetic pathway requires an additional enzyme (SPE4) compared to that of SPD. In order to determine an optimum concentration of SPD for eliciting tolerance against furan derivatives, various concentrations (0, 1, 2, and 4 mM) of SPD were applied into the culture medium containing 2 g/L of furfural and 2 g/L of HMF. Intracellular levels of SPD were proportional to the amounts of SPD supplemented (Fig. 2.4). Of four tested conditions, supplementation of 1 and 2 mM SPD improved tolerance whereas 4 mM SPD addition aggravated tolerance against furan derivatives (Fig. 2.5). Because the growth pattern of the strain supplemented with 4 mM

SPD was similar to that of the control strain in the YSC medium without furan derivatives, it was postulated that an excess amount of SPD (4 mM) might cause detrimental phenotypes against furan derivatives. The addition of 2 mM SPD into culture medium resulted in 19% higher ethanol productivity than the addition of 1 mM SPD (Table 2.1), suggesting that 2 mM SPD seemed to be an optimal concentration to improve tolerance of *S. cerevisiae* D452-2 against furan derivatives. In all cases, specific rates of glucose consumption and ethanol production were almost identical. The positive effects of SPD supplementation on tolerance against furfural and HMF in yeast were also confirmed for other *S. cerevisiae* strains (L2612 and CEN.PK2-1D) (Fig. 2.6).

2.4.2. Effects of spermidine on tolerance of *S. cerevisiae* to acetic acid and lignocelluloses hydrolysates

The concentrations of acetic acid in lignocellulose hydrolysates are often higher than the furan derivatives (Almeida et al., 2007). Acetic acid is toxic to *S. cerevisiae* and strongly inhibits cell growth and fermentation of yeast. Especially, the fermentation of xylose that is the second most abundant sugar in lignocellulose hydrolysates is known to be highly inhibited by acetic acid (Lee et al., 2012; Wei et al., 2013). Therefore, the effects of SPD addition on tolerance of yeast against acetic acid were investigated. While lag-phase periods increased with increasing acetic acid concentrations (Fig. 2.7), addition of 2 mM SPD shortened the lag-phase periods from 12 h to 4 h at 2 g/L of acetate, and 73 h to 36 h at 4 g/L of acetate (Fig. 2.7). The initial pH values of culture media were 3.6 for with SPD supplementation and 3.2 for without SPD supplementation when acetate concentration was 4 g/L. Because low pH increases toxicity of acetic acid by increasing the undissociated form of acetic acid, it was investigated if SPD supplementation can improve tolerance of *S. cerevisiae* to acetic acid under identical pH conditions. With 4 g/L acetic acid concentration and the pH value of medium with SPD supplementation adjusted to 3.2, the lag-phase period was 48 h, which was still 34% shorter than that of the control strain (Fig. 2.7b). At the end of fermentation, the pH values of

the control strain and 2 mM SPD addition with pH adjustment to 3.2 were identical (pH 2.8). These results indicated that SPD basicity was not a major factor for improved tolerance of *S. cerevisiae* to acetic acid. In addition, it was examined that the effects of SPD supplementation on tolerance of yeast against corn stover hydrolysate that contains numerous fermentation inhibitors in addition to 0.4 g/L furfural, 0.8 g/L HMF, and 3.3 g/L acetic acid. Interestingly, it was consistently observed that the beneficial effects of SPD supplementation on tolerance of yeast even when using corn stover hydrolysate (Fig. 2.8). Because of the shortened lag period with the addition of SPD (59 h vs. 48 h), the volumetric ethanol productivity was 55% higher than the culture without SPD supplementation.

2.5. Discussion

Previous studies have reported that *S. cerevisiae* mutants incapable of synthesizing SPD require supplementation of SPD for optimal growth (Balasundaram et al., 1991; Cohn et al., 1978; Hamasaki-Katagiri et al., 1998) and that one of the important roles for SPD is to activate the eukaryotic translation initiation factor 5A (eIF5A) through hypusine biosynthesis (Chattopadhyay et al., 2008). However, there remains the unanswered question why *S. cerevisiae* cells have a large excess of intracellular SPD and hypusinated eIF5A, because wild-type *S. cerevisiae* cells have 1,000-fold and 20-fold higher intracellular SPD and hypusinated eIF5A than those needed for optimal growth (Chattopadhyay et al., 2008). One possible explanation could be that high levels of SPD in baker's yeast might be important for adaptation and survival in diverse environmental stresses.

In this chapter, a unique strategy has been demonstrated to shorten the extended lag-phase period caused by lignocellulose-derived inhibitors. It was found that the chemical perturbation eliciting higher SPD levels improved tolerance of *S. cerevisiae* to furan derivatives and acetic acid. A previous showed that several genes were abundantly transcribed in the transgenic plants with high SPD contents that in the wild type under stress condition (Kasukabe et al., 2004). These genes include those for

stress-responsive transcription factors such as dehydration responsive element-binding and stress-protective proteins. Therefore, it was postulated that supplementation of SPD might induce different gene expression pattern and hence improve tolerance of *S. cerevisiae* to fermentation inhibitors. This hypothesis was examined in the next chapter. Nevertheless, this chemical perturbation is not desirable for large-scale fermentations because of additional costs. Therefore, metabolic engineering approach for high levels of SPD without extracellular addition of SPD is necessary for economic production of biofuels.

Table 2.1. Comparison of fermentation parameters by *S. cerevisiae* D452-2 with and without supplementation of 1, 2, and 4 mM spermidine (SPD) in yeast synthetic complete (YSC) medium containing 55 g/L glucose, 2 g/L furfural, and 2 g/L HMF

Polyamine	Maximum specific growth rate (1/h)	Ethanol concentration (g/L)	Ethanol productivity (g/L·h)	Furfural conversion rate (mg/L·h)	HMF conversion rate (mg/L·h)
None	0.087	18.34	0.17	31	23
1 mM SPD	0.082	19.16	0.27	54	32
2 mM SPD	0.090	19.87	0.32	53	33
4 mM SPD	-	0.18	0.01	-	-

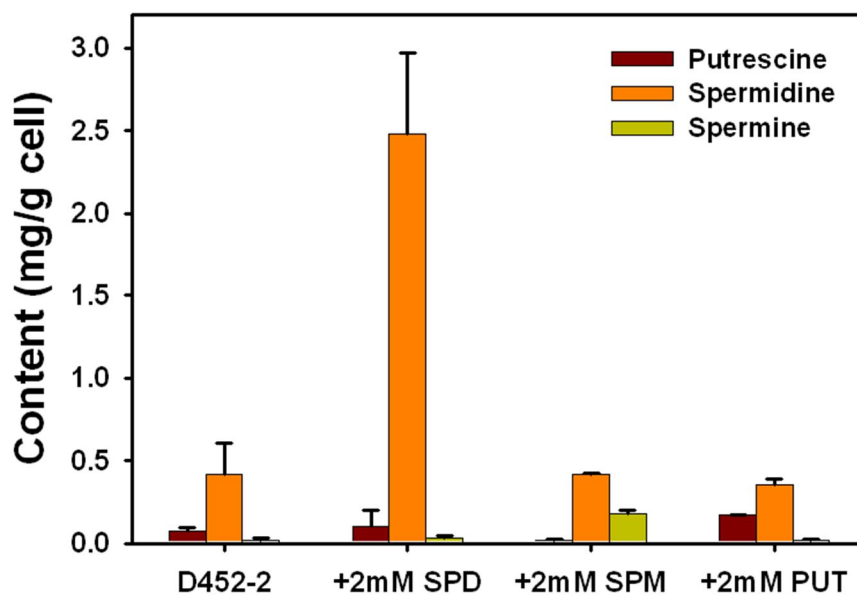


Fig. 2.1. Intracellular levels of polyamines in *S. cerevisiae* D452-2 with and without supplementation of 2 mM spermidine (SPD), spermine (SPM), or putrescine (PUT) in yeast synthetic complete (YSC) medium. Results are the mean of duplicate experiments and error bars indicate s.d..

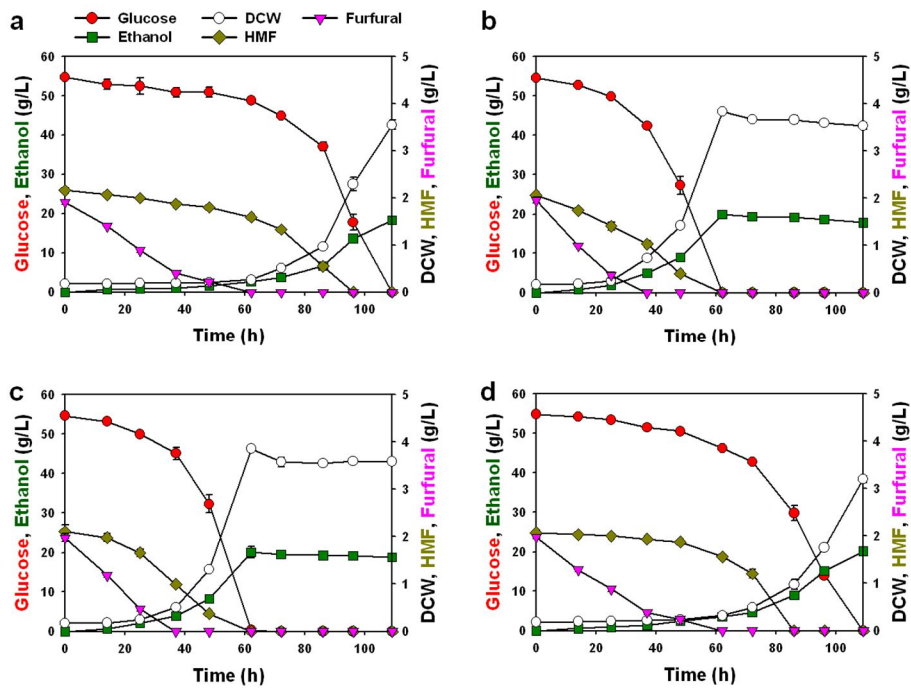


Fig. 2.2. Batch fermentation of *S. cerevisiae* D452-2 (a) and D452-2 supplemented with 2 mM SPD (b), SPM (c), or PUT (d) in the presence of 2 g/L furfural and HMF. Results are the mean of triplicate experiments and error bars indicate s.d..

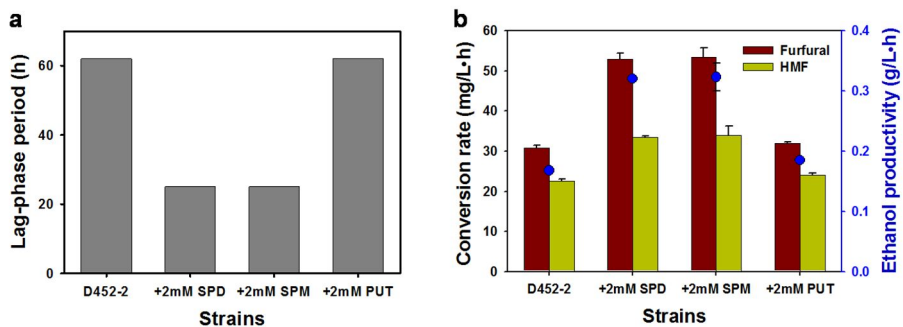


Fig. 2.3. Comparison of fermentation parameters by *S. cerevisiae* D452-2 and D452-2 supplemented with 2 mM SPD, SPM, or PUT in the presence of 2 g/L furfural and HMF. (a) Lag-phase periods. (b) Furfural and HMF conversion rates and ethanol productivities. Results are the mean of duplicate experiments and error bars indicate s.d..

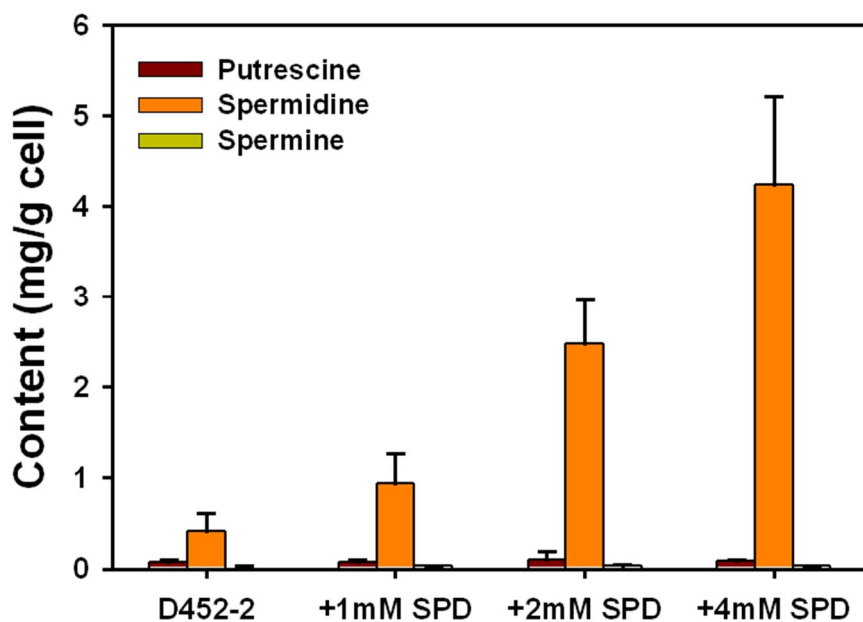


Fig. 2.4. Intracellular levels of polyamines in *S. cerevisiae* D452-2 with and without supplementation of 1, 2, and 4 mM SPD in YSC medium. Results are the mean of duplicate experiments and error bars indicate s.d..

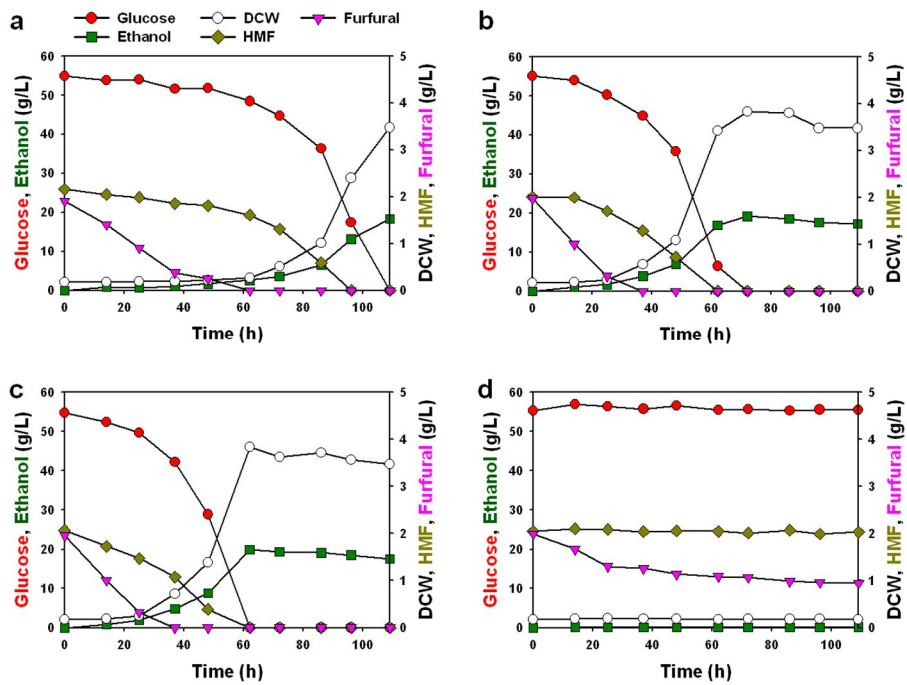


Fig. 2.5. Batch fermentation of *S. cerevisiae* D452-2 without (a) and with 1 mM (b), 2 mM (c), and 4 mM (d) SPD supplementation in the presence of 2 g/L furfural and HMF.

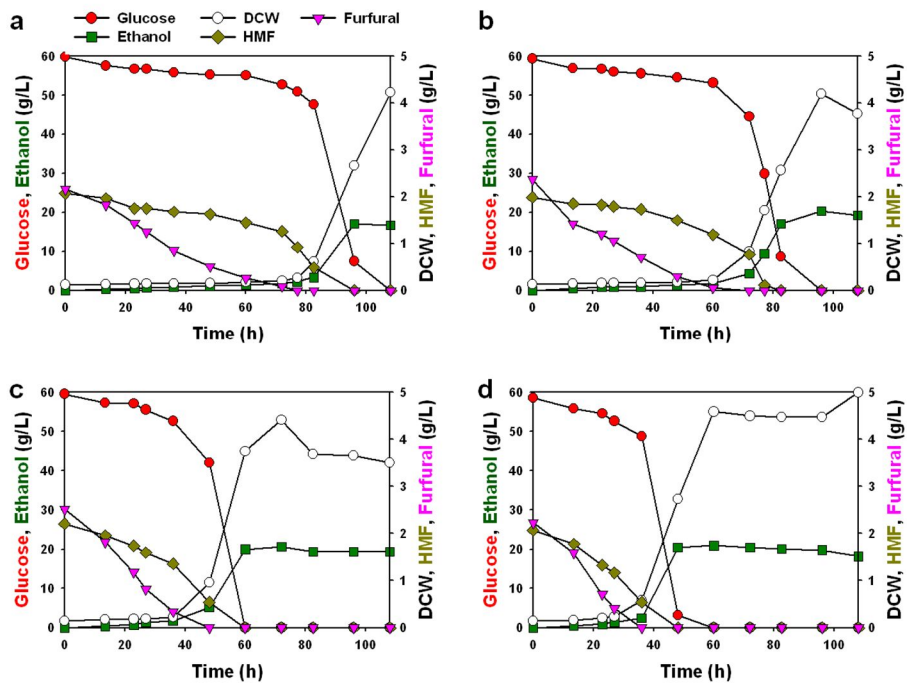


Fig. 2.6. Batch fermentation of *S. cerevisiae* strains in the presence of 2 g/L furfural and HMF. (a) *S. cerevisiae* L2612, (b) *S. cerevisiae* L2612 + 2 mM SPD (c) *S. cerevisiae* CEN.PK2-1D, (d) *S. cerevisiae* CEN.PK2-1D + 2 mM SPD.

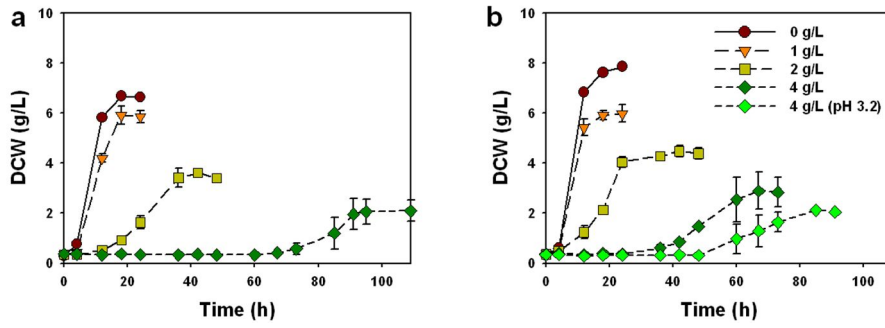


Fig. 2.7. Cell growth of *S. cerevisiae* D452-2 without (a) and with (b) 2 mM SPD supplementation in the presence of 0, 1, 2, and 4 g/L acetic acid. Results are the mean of duplicate experiments and error bars indicate s.d..

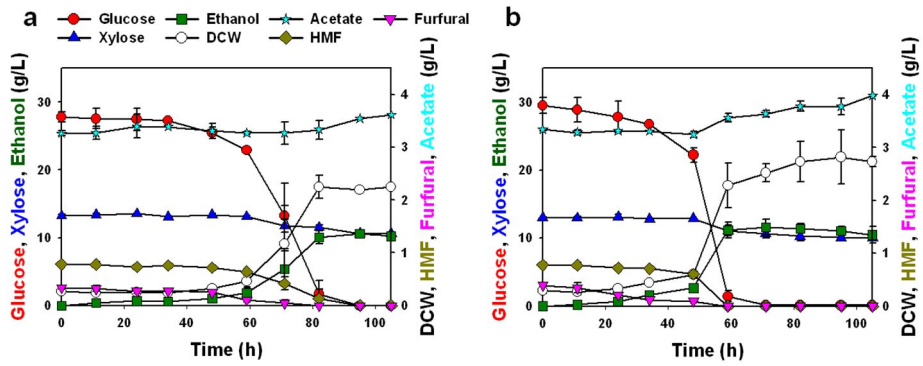


Fig. 2.8. Batch fermentation of *S. cerevisiae* D452-2/pXYL123 without (a) and with (b) 2 mM SPD supplementation in corn stover hydrolysate. Results are the mean of duplicate experiments and error bars indicate s.d..

Chapter 3

Construction of engineered strains with improved tolerance against multiple inhibitors and ethanol

3.1. Summary

It was shown that spermidine functions as a chemical elicitor for enhanced tolerance of *S. cerevisiae* against major fermentation inhibitors. In this chapter, the feasibility of constructing an engineered *S. cerevisiae* strain capable of tolerating toxic levels of the major inhibitors without exogenous addition of spermidine was explored. Firstly, expression levels of the genes in the spermidine biosynthetic pathway were amplified. Also, *OAZ1* coding for ornithine decarboxylase (ODC) antizyme and *TPO1* coding for the polyamine transport protein were disrupted to increase intracellular spermidine levels through alleviation of feedback inhibition on ODC and prevention of spermidine excretion. By combining the amplification of genes coding for enzymes in the spermidine biosynthetic pathway with disruption of the genes involved in feedback inhibition (*OAZ1*) and spermidine excretion (*TPO1*), engineered strains with improved tolerance against multiple inhibitors (furfural, HMF, and acetic acid) and ethanol were constructed. Especially, the strain with combination of *OAZ1* and *TPO1* double disruption and overexpression of *SPE3* not only contained spermidine content of 1.1 mg spermidine/g cell, which was 171% higher than that of the control strain, but also exhibited 60% and 33% shorter lag-phase periods than that of the control strain under

the medium containing furan derivatives and acetic acid. While it was observed that a positive correlation between intracellular spermidine contents and tolerance phenotypes among the engineered strains accumulating different amounts of intracellular spermidine, too much spermidine accumulation is likely to cause metabolic burden. Therefore, intracellular spermidine contents should be well balanced with metabolic burden caused by genetic perturbations to construct optimal inhibitor tolerant *S. cerevisiae* strains. It was also found that the genes involved in purine biosynthesis and cell wall and chromatin stability were related to the enhanced tolerance phenotypes to furfural. The strains developed in this study can have broad applications not only to produce ethanol but also many other biochemicals and biofuels from lignocellulosic biomass.

3.2. Introduction

It was observed that a chemical perturbation (addition of 2 mM spermidine (SPD) into culture media) enhanced tolerance of yeast against major inhibitory compounds (furan derivatives and acetic acid) present in lignocellulose hydrolysates. Therefore, a genetic engineering strategy for high SPD contents without extracellular addition of SPD is required for economic production of ethanol.

Polyamine synthesis is mainly controlled by feedback inhibition on ornithine decarboxylase (ODC), which is the rate-limiting enzyme in polyamine production. High levels of SPD might increase ODC antizyme (Oaz1p) which mediates ubiquitin-independent degradation of ODC by the proteasome (Palanimurugan et al., 2004) (Fig. 3.1). Intracellular polyamine levels are furthermore controlled by their uptake or excretion into the culture medium. While polyamine transport protein (TPO1) uptakes spermidine at alkaline pH (pH 8.0), TPO1 excretes spermidine into the medium at acidic pH (pH 5.0) (Uemura et al., 2005) (Fig. 3.2). Therefore, TPO1 is expected to excrete spermidine because pH of medium gradually decreases as microorganisms grow.

In order to increase intracellular SPD contents without exogenous addition of it, the endogenous *SPE1*, *SPE2*, and *SPE3* genes involved in the polyamine biosynthetic pathway were overexpressed (Fig. 3.3).

Also, the *OAZ1* gene was disrupted for alleviating the feedback regulation of ODC by accumulated SPD in yeast. In order to further increase SPD levels, the *TPO1* gene coding for the polyamine transport which mainly excretes polyamines to the medium (Uemura et al., 2007) was also disrupted (Fig. 3.3).

In addition, genes differentially expressed by chemical and genetic perturbations under furfural conditions were captured by using RNA sequencing (RNA-seq) method. Specifically, the transcriptional changes caused by the addition of furfural were measured. Also, the transcriptional responses of the control strain (*S. cerevisiae* D452-2), the SPD supplemented control strain (+ 2 mM SPD), and DT strain against furfural were compared. Overexpression of the genes downregulated under furfural conditions and upregulated in + 2 mM SPD and DT strains can lead to improved tolerance to furfural. These results suggest that enhanced tolerance to multiple lignocellulose-derived inhibitors and ethanol can be implemented through chemical and genetic perturbations that have not been considered previously.

3.3. Materials and methods

3.3.1. Strains and plasmids

Escherichia coli TOP10 (Invitrogen, Carlsbad, CA, USA) was used for gene cloning and genetic manipulation. *S. cerevisiae* D452-2 (*MAT α* , *leu2*, *his3*, *ura3*, and *can1*) was used for constructing the recombinant strains with high levels of SPD contents and tolerance against inhibitors. Strains and plasmids used in this work are described in Table 3.1. The primers used for disruption of the chromosomal *OAZ1*, *TPO1*, and *ATG7* and cloning of the genes involved in the SPD biosynthetic pathway (*SPE1*, *SPE2*, and *SPE3*) and the target genes identified by RNA sequencing (*ADE17*, *PIR3*, and *HTA2*) are listed in Table 3.2.

3.3.2. Yeast transformation

Transformation of the cassettes for overexpressing enzymes in the SPD biosynthetic pathway (*SPE1*, *SPE2*, and *SPE3*), *ADE17*, *PIR3*, and *HTA2* genes was performed using the yeast EZ-Transformation kit (BIO 101, Vista, CA). Transformation of the cassettes for disrupting *OAZ1*, *TPO1*, and *ATG7* was also performed using the yeast EZ-Transformation kit. pRS403_SPE2, pRS405_SPE1, pRS406_SPE3, pRS403_PIR3, pRS405_ADE17, pRS406_HTA2, pAUR_d_OAZ1, pRS405_d_TPO1, and pAUR_d_ATG7 plasmids were cut with *MscI*,

AflIII, *NcoI*, *NdeI*, *EcoRI*, *NcoI*, *BlnI*, *NcoI*, and *XbaI*, respectively, and transformed. Transformants were selected on YSC medium containing 20 g/L glucose. Amino acids (histidine and leucine) and uracil were added as necessary. For the selection of *OAZ1* or *ATG7* disrupted strain, YP medium containing 20 g/L glucose and 0.4 mg/L aureobasidin was used.

3.3.3. Culture conditions and fermentation experiments

LB medium with 50 µg/ml of ampicillin when required was used for *E. coli* culture. Yeast strains were pre-cultured at 30°C and 250 rpm for 48 h in YP medium (10 g/L yeast extract, 20 g/L bacto peptone) with 20 g/L glucose. A defined YSC medium (6.7 g/L yeast nitrogen without amino acids and 2.0 g/L synthetic complete supplement mixture) containing appropriate amounts of sugars was used for fermentation experiments.

For the tolerance test experiments, pre-cultured cells from YP medium with 20 g/L glucose were harvested and inoculated into main cultures with initial optical density (OD₆₀₀) of 0.5~1.0. Flask fermentation experiments were performed at 30°C and 80 rpm in 50 ml YSC medium containing 48~60 g/L glucose with 2 g/L furfural and HMF, 4 g/L furfural, 1, 2, or 4 g/L of acetate, or 8% (v/v) ethanol.

3.3.4. Analytical Methods

The same as in chapter 2.

3.3.5. Reduction activity assays toward HMF and furfural

The crude protein extracts were prepared as described previously (Park et al., 2011). To determine reduction activity toward HMF and furfural, the reaction solution was formulated with 100 μ l of 100 mM potassium phosphate buffer (pH 7.2), 60 μ l of 33 mM furfural or HMF, and 20 μ l of the crude enzyme solution. The absorbance change at 30°C and 340 nm of wavelength was monitored by a 96-well microplate reader (Molecular Devices, Sunnyvale, CA, USA) after addition of 20 μ l of 1 mM NAD(P)H. One unit of reduction activity was defined as the amount of enzyme oxidizing 1 μ mol NAD(P)H per minute under the reaction conditions. Protein concentration was determined by the protein assay kit (Bio-Rad, Richmond, USA).

3.3.6. RNA-seq analysis by next generation sequencing (NGS)

For the RNA-seq experiment, initial OD₆₀₀ values were adjusted to 1.3, and flask fermentation experiments were performed at 30°C and 80 rpm in 50 ml YSC medium containing 50 g/L glucose with 4 g/L furfural. The RNA-seq was carried out in the Illumina MiSeq platform. In order

to make a messenger RNA (mRNA) library for the NGS, total RNA was extracted by the Qiagen RNA extraction kit (Qiagen, Germany). mRNAs were retrieved by magnetic oligo-dT beads (Illumina, San Diego, CA, US) and constructed a cDNA library for next generation sequencing by the TruSeq RNA sample preparation kit (Illumina, San Diego, CA, US). Sequencing of the cDNA library was carried out in the MiSeq machine with the paired-end sequencing reagent kit (version 2.0, 2 x 250 cycles). The number of total reads for 12 libraries (4 samples x 3 replicates) with quality over Q30 was 25,847,149 from the sequencing. The quality of raw reads was inspected by the FastQC program (<http://www.bioinformatics.bbsrc.ac.uk/projects/fastqc>) and low-quality reads were filtered using the Bioconductor/R package (Gentleman et al., 2004). The 5' and 3' ends of reads were trimmed by the Phred quality score (threshold < Q20) using the ShortRead package in the Bioconductor/R package (Morgan et al., 2009). We used the sequences of *S. cerevisiae* strain S288c as a reference genome for read alignment by the Bowtie2 program (Langmead and Salzberg, 2012) and used the transcript database (TxDb.Scerevisiae.UCSC.sacCer2.sgdGene) in the Annotation package in Bioconductor/R package. Counting reads mapped on coding regions were the Rsamtools package (Gentleman et al., 2004). Differentially expressed genes (DEGs) among different conditions were examined by the edgeR package (Robinson et

al., 2010).

3.4. Results

3.4.1. Construction of engineered *Saccharomyces cerevisiae* strains with high spermidine contents

It was hypothesized that spermidine (SPD) might be overproduced in *S. cerevisiae* through altering expression levels of the enzymes involved in the SPD biosynthesis pathway. To this end, the following genes were selected as genetic perturbation targets. The key enzymes involved in the SPD biosynthesis include ornithine decarboxylase (ODC), *S*-adenosylmethionine decarboxylase (SAMDC), and spermidine synthase (SPDS), which are encoded by *SPE1*, *SPE2*, and *SPE3*, respectively (Fig. 3.3). We constructed expression cassettes consisting of *SPE1*, *SPE2*, and *SPE3* genes under the control of a strong and constitutive promoter (*GPD_P*) and integrated these cassettes into the *S. cerevisiae* genome. A set of seven strains overexpressing three genes combinatorially was constructed (Table 3.1) and intracellular levels of SPD, spermine (SPM), and putrescine (PUT) in each strain were measured. Among the strains tested, single or double overexpressing strains did not show SPD levels as high as the levels of intracellular SPD in yeast when 2 mM SPD was supplemented (Fig. 3.4a). When three genes were overexpressed simultaneously (S123), intracellular SPD levels were almost identical to the case of 2 mM SPD

supplementation. Growth patterns of the engineered strains were almost identical to that of the control D452-2 strain in the YSC medium without fermentation inhibitors. However, in YSC medium containing 2 g/L furfural and 2 g/L HMF, the engineered *S. cerevisiae* strains (S2, S12, S13, S23, and S123) failed to grow, or showed prolonged lag-phase periods (S1 and S3) compared with the control strain (Fig. 3.4b). A previous study reported that when furan derivatives were added, the intracellular ATP concentration was 19% lower than that of the control strain (Ask et al., 2013). Because ODC antizyme is also known to cause continuous consumption of ATP when it mediates the degradation of overproduced ODC (Porat et al., 2008), it was reasoned that *SPE1* overexpression in the presence of furfural might cause detrimental effects to yeast cells due to ATP depletion. Therefore, to relieve the ATP depletion and improve tolerance, *OAZ1* coding for ODC antizyme was additionally disrupted in the engineered strains. The effects of the *OAZ1* disruption on SPD contents were similar to the *SPE1* overexpression, and a combination of *OAZ1* disruption and *SPE1* overexpression elevated SPD contents further. The highest SPD content of 6.5 mg/g cell was obtained when *OAZ1* disruption and overexpression of *SPE1*, *SPE2*, and *SPE3* were combined (DO+S123). As a result, the intracellular SPD level of the OS123 strain was 15.5-fold higher than that of the control strain (Fig. 3.5a).

Fermentation experiments were also performed to investigate if the disruption of *OAZ1* and overexpression of three *SPE* genes improves tolerance of yeast in the presence of 2 g/L furfural and 2 g/L HMF. Although the disruption of *OAZ1* in the engineered strains overexpressing two or three *SPE* genes (DO+S12, DO+S13, and DO+S123) resulted in poor growth, the disruption of *OAZ1* in an engineered strain overexpressing *SPE1* only (DO+S1) led to better growth than the control D452-2 strain under 2 g/L of furfural and 2 g/L of HMF (Fig. 3.5b). Among these engineered strains, the DO+S3 strain expressing *SPE3* showed the shortest lag-phase period of 72 h, which was 33% shorter than that of the control strain. These results indicate that double or triple overexpression of three *SPE* genes might cause metabolic burden and hence result in a prolonged lag-phase period. In conclusion, genetic perturbations for higher SPD levels should be optimized in terms of metabolic burden and SPD contents to construct inhibitor tolerant yeast strains.

3.4.2. Effects of disruption of *TPO1* coding for polyamine excretion protein on tolerance of *S. cerevisiae*

In addition to the metabolic fluxes toward the synthesis of SPD, intracellular concentrations of SPD can change by polyamine excretion. It was hypothesized that the strategy of blocking the excretion of SPD would be more effective than that of expanding metabolic fluxes toward the synthesis of SPD in terms of metabolic burden and SPD contents. Therefore, the excretion of SPD was blocked by disrupting *TPO1* coding for polyamine transport protein (Uemura et al., 2007) in order to increase intracellular polyamine contents and inhibitor tolerance. Disruption of the *TPO1* gene in the D452-2 strain and the engineered strain overexpressing *SPE3* resulted in spermidine content of 0.79 mg SPD/g cell (the DT strain) and 1.1 mg SPD/g cell (the DTO+S3 strain), which were 90% and 171% higher than that of the control strain (Fig. 3.6).

Batch fermentations were performed with three engineered *S. cerevisiae* strains (DT, DO+S3, and DTO+S3) exhibiting higher SPD levels and the parental strain (D452-2) in YSC medium containing 2 g/L furfural and 2 g/L HMF. As expected, all three engineered strains (DT, DO+S3, and DTO+S3) exhibited much shorter lag-phase periods (48 ~ 60 h vs. 120 h) as compared to the control D452-2 strain (Fig.

3.7a and Fig. 3.8). Among them, the highest ethanol productivity of 0.24 g/L·h was obtained for the DT strain, which was 85% higher than the control strain (Fig. 3.7b). The reason for this improvement was ascribed to the faster conversion rate of furfural than the control strain. Interestingly, among the engineered strains capable of accumulating higher levels of SPD, only the DTO+S3 strain showed higher tolerance to acetate. The DT strain showed a prolonged lag-phase period compared with the control strain, suggesting that *TPO1* is involved in coping with acetate stress. *TPO1* which functions as a drug/toxin transporter and multidrug efflux pump was demonstrated to improve resistance to a wide range of chemicals (Sa-Correia and Tenreiro, 2002). However, when genetic perturbations of the DT and DO+S3 strains were combined (DTO+S3), detrimental effects of *TPO1* disruption were compensated. The maximum specific growth rates (μ_{MAX}) of the DTO+S3 strain were 16% and 96% higher than the control strain when acetate concentrations were 3 and 4 g/L, respectively. In addition, the DTO+S3 strain showed a shorter lag-phase period (72 h vs. 107 h) than the control strain when acetate concentration was 4 g/L (Fig. 3.9).

3.4.3. Identification of genes involved in tolerance against furan derivatives

The previous study reported that SPD supplementation upregulated several autophagy related genes (most significantly *ATG7*) and extended lifespan of *S. cerevisiae* through induction of autophagy (Eisenberg et al., 2009). Atg7p is an autophagy related protein which is required for autophagosome formation (Klionsky et al., 2003). The deletion of *ATG7* diminished the lifespan-extending effects of SPD supplementation in yeast (Eisenberg et al., 2009), suggesting that Atg7p might play a pivotal role in extending life-span via autophagy. As such, it was hypothesized that the supplementation of SPD might improve tolerance against fermentation inhibitors via autophagy. However, it was observed that disruption of *ATG7* did not influence the beneficial effects of SPD supplementation on tolerance against furan derivatives (Fig. 3.10). These results suggest that the SPD supplementation might elicit the improved tolerance independent of autophagy. Therefore, to investigate putative mechanisms involved in the beneficial effects of SPD on detoxification of furan derivatives, it was examined if NADH- and NADPH-dependent activities of furfural and HMF reductions can be enhanced by SPD supplementation or overproduction. Crude extracts of *S. cerevisiae* D452-2 with 2 mM

SPD supplementation (+ 2 mM SPD), the DT strain capable of accumulating higher SPD without SPD supplementation, and the control strain were prepared and *in vitro* reduction activities of the crude extracts with furfural and HMF were measured. While specific activity of the crude extract of the + 2 mM SPD toward furfural was slightly higher than that of the control and DT strains, specific activities toward HMF were almost identical (Fig. 3.11). These results indicate that the mechanism involved in improved detoxification rates of furan derivatives by high levels of intracellular SPD might not be directly related to the change of NAD(P)H pools and the reduction activities of oxidoreductases toward furfural and HMF.

In all fermentation experiments, exit times from lag-phases coincided with complete conversion of furfural into furfuryl alcohol even though HMF remained in the culture medium at the exit times. These results confirmed that furfural is a major inhibitor in lignocellulose hydrolysates. Therefore, the RNA seq experiment was conducted in the medium containing furfural to obtain more concise data. While the control strain failed to grow in the presence of 4 g/L furfural, the + 2 mM SPD and DT strain were able to grow after 62 ~ 77 h in the lag phase (Fig. 3.12). To identify the genes involved in tolerance against furfural, the transcriptional responses of the control strain (*S. cerevisiae*

D452-2), the SPD supplemented control strain (+ 2 mM SPD), and DT strain against furfural were measured at 15 h after inoculation using RNA sequencing (RNA-Seq) (Fig. 3.13). The transcript levels of 94 and 14 genes changed more than a four-fold in the + 2 mM SPD and DT strains, respectively, as compared to the control strain ($P \leq 0.01$) (Fig. 3.14a,b). Identification of the genes contributing to the tolerance phenotypes from these enormous transcriptional changes, either individually or in combination, is unfeasible. Among several solutions have been proposed to simplify the detection of biologically relevant changes, the approach using independent parallel lines and selecting target genes occurring among the parallel lines was adopted (de Kok et al., 2012; Hong et al., 2011). Therefore, it was hypothesized that the genes contributing to the tolerance phenotypes of yeast would be differentially expressed genes both in + 2 mM SPD and DT strains. These genes were *ADE17* coding for a bifunctional purine biosynthesis protein and *PIR3* for O-glycosylated covalently-bound cell wall protein. Both *ADE17* and *PIR3* were upregulated by 18.0 folds in the + 2 mM SPD, and 5.3 and 6.2 folds in the DT strain as compared to the control strain. As a target for tolerance improvement against furfural, the genes upregulated in the + 2 mM SPD relative to the DT strain were also selected. *HTA2* coding for a histone H2A protein and *YDR034C-A* were

upregulated by 6.9 and 45.0 folds in the + 2 mM SPD as compared to the DT strain (Fig. 3.14c). Because only *HTA2* was also upregulated in the + 2 mM SPD as compared to the control strain, *HTA2* was selected as a target gene. The three genes, *ADE17*, *PIR3*, and *HTA2*, were downregulated to 40.7, 6.1, and 25.9 folds in response to furfural in the control strain, suggesting that furfural might cause lower expression of those genes. Therefore, it was hypothesized that overexpression of these genes in *S. cerevisiae* D452-2 might improve tolerance to furfural.

Overexpression cassettes containing *ADE17*, *PIR3*, and *HTA2* genes controlled by the *tHXT7* promoter (Hauf et al., 2000) were constructed and integrated to the *S. cerevisiae* genome. Engineered strains overexpressing one of the three genes (*ADE17*, *PIR3*, and *HTA2*) indeed exhibited shorter lag-phase periods than that of the control strain (Fig. 3.15a and Fig. 3.16). Among them, the highest ethanol productivity of 0.21 g/L·h was obtained for the D452-2 strain overexpressing *ADE17* and *HTA2* (RAH). The ethanol productivity and conversion rates of furan derivatives by the RAH strain were comparable to those by the DT strain under the same conditions (Fig. 3.15b). It was also investigated if the engineered strains showed an improvement in tolerance to ethanol. The lag-phase periods and maximum specific growth rates of the engineered strains were identical

to those of the control D452-2 strain in the YSC medium containing 8% (v/v) ethanol. However, the DTO+S3 and RAH strains increased maximum dry cell weight (DCW) under the ethanol stress condition (Fig. 3.17). Especially, the maximum DCW of the DTO+S3 strain was 26% higher than that of the control strain (Fig. 3.17).

In this chapter, yeast strains exhibiting improved tolerance without chemical perturbations were constructed. Moreover, differentially expressed genes by chemical and genetic perturbations under furfural conditions were captured, and it was demonstrated that overexpression of the downregulated genes under furfural conditions can lead to improved tolerance to furfural. This study not only identified new gene targets for understanding endogenous tolerance mechanisms against fermentation inhibitors, but also constructed numerous engineered strains showing various tolerance phenotypes.

3.5. Discussion

The engineered strains exhibiting improved phenotypes against fermentation inhibitors can be served as customized host strains for fermenting cellulosic hydrolysates containing different amounts of fermentation inhibitors. In the case of utilizing lignocellulose hydrolysates containing high levels of furfural, for example, the DT strain exhibiting the highest tolerance against furfural could be used. *Tpo1p* which functions as a drug/toxin transporter and multidrug efflux pump is one of the significant elements for yeast survival and adaptation under inhibitory HMF concentrations (Ma and Liu, 2010a). However, disruption of *TPO1* improved tolerance against furfural without affecting tolerance against HMF. On the other hand, for lignocellulose hydrolysates containing high levels of acetic acid, the DTO+S3 strain showing improved tolerance to both furan derivatives and acetic acid could be applicable. In conclusion, this study successfully constructed not only the DT strain exhibiting substantial tolerance to furfural but also the DTO+S3 strain exhibiting tolerance to multiple inhibitors including furan derivatives and acetic acid.

Three genes (*ADE17*, *PIR3*, and *HTA2*) involved in tolerance against furfural in yeast were identified through comparing the transcriptomes of the D452-2 strain with and without chemical and genetic

perturbations eliciting improved tolerance to furfural. Furfural decreased transcript levels of several genes including *ADE17*, *PIR3*, and *HTA2*. However, *S. cerevisiae* strains with improved tolerance to furfural (the + 2 mM SPD and DT strains) exhibited higher transcript levels of *ADH17*, *PIR3*, and *HTA2* as compared to the control strain. Under zinc starvation and oxidative stress, a bifunctional purine biosynthesis protein encoded by *ADE17* has been reported to be upregulated for adaptation in yeast cells (Grossklaus et al., 2013; Parente et al., 2013). These results are in agreement with our results showing that overexpression of *ADE17* improved tolerance of *S. cerevisiae* against furfural. A previous study reported that damage to the cell wall caused by furfural was undetected by the current scanning electron microscope (SEM) analysis (Allen et al., 2010). However, the results presented in this study indicated that cell wall stability is one of the important factors affecting tolerance of *S. cerevisiae* to furfural because yeast cells overexpressing *PIR3*, which is known to be upregulated in case of cell wall stress (Jung and Levin, 1999; Terashima et al., 2000) and required for cell wall stability (Klis et al., 2002), exhibited improved tolerance to furfural. In addition, a histone H2A protein encoded by *HTA2* required for chromatin assembly and efficient DNA double-strand break repair (Downs et al., 2000) was identified as an overexpression target in this study. Because furfural

causes accumulation of reactive oxygen species (ROS) and damage to nuclear chromatin (Allen et al., 2010), it is likely that overexpression of *HTA2* alleviated damage to chromatin caused by furfural. Interestingly, although the engineered strains (DT, DO+S3, and DTO+S3) showed increased tolerance to furan derivatives, only the DTO+S3 strain also exhibited faster recovery of growth than the control strain under acetate stress conditions. Finally, an engineered strain with inhibitor tolerance identical to the case of SPD supplementation without extracellular addition was pursued through optimization of expression levels of the identified genes. It was observed that genetic perturbations for higher SPD levels need to be optimized in terms of metabolic burden and SPD contents. These results are consistent with the previous study, which presented that tolerance phenotypes of *E. coli* against furfural were affected by both specific activity of FucO, an NADH dependent propanediol (and furfural) oxidoreductase, and metabolic burden caused by target protein overexpression (Wang et al., 2013a). Therefore, future optimization of expression levels of the enzymes involved in SPD biosynthesis might further improve tolerance against inhibitors. Also, modulation of SPD contents can be coupled with other strategies including overexpression of oxidoreductases (Almeida et al., 2008; Petersson et al., 2006) and *ZWF1* gene (Gorsich et al., 2006) to improve tolerance further.

The undissociated form of acetic acid can penetrate into the plasma membrane from the fermentation medium and then dissociates due to high intracellular pH. The dissociation of acetic acid decreases the intracellular pH, and the cells consume ATP to neutralize pH by pumping protons out of the cells (Pampulha and Loureirodias, 1989). This ATP deficiency causes inhibition of cell growth. Moreover, the presence of acetic acid slows down the flux of the non-oxidative pentose phosphate pathway (PPP) and hence overexpression of a gene encoding a PPP-related enzyme, transaldolase or transketolase, improved the tolerance of *S. cerevisiae* to acetic acid (Hasunuma et al., 2011). Additional experiments are necessary to elucidate the key genes involved in tolerance of *S. cerevisiae* to acetic acid including genes coding for proton pumps and PPP-related enzymes.

In addition, the effects of SPD on tolerance of *S. cerevisiae* to coniferyl aldehyde, isobutanol, lactic acid, succinic acid, 3-hydroxypropionic acid, malic acid, and heat shock were investigated. Coniferyl aldehyde is one of the major phenolic inhibitors. *S. cerevisiae* strains with high SPD contents exhibited a higher maximum DCW than that of the control strain in a medium containing lactic acid, succinic acid, or malic acid. However, growth patterns of these strains were similar to that of the control strain under heat shock condition (42°C) or in a

medium containing isobutanol, coniferyl aldehyde, or 3-hydroxypropionic acid.

Table 3.1. *S. cerevisiae* strains and plasmids used in Chapter 3

Name	Description	Reference
Strains		
D452-2	<i>MATα, leu2, his3, ura3, and can1</i>	(Hosaka et al., 1992)
DO	D452-2 Δ <i>OAZ1</i>	This study
DT	D452-2 Δ <i>TPO1</i>	This study
DTO	D452-2 Δ <i>TPO1</i> Δ <i>OAZ1</i>	This study
DA	D452-2 Δ <i>ATG7</i>	This study
S1	D452-2 overexpressing <i>SPE1</i>	This study
S2	D452-2 overexpressing <i>SPE2</i>	This study
S3	D452-2 overexpressing <i>SPE3</i>	This study
S12	D452-2 overexpressing <i>SPE1,2</i>	This study
S13	D452-2 overexpressing <i>SPE1,3</i>	This study
S23	D452-2 overexpressing <i>SPE2,3</i>	This study

(be continued)

Name	Description	Reference
S123	D452-2 overexpressing <i>SPE1,2,3</i>	This study
DO+S1	DO overexpressing <i>SPE1</i>	This study
DO+S2	DO overexpressing <i>SPE2</i>	This study
DO+S3	DO overexpressing <i>SPE3</i>	This study
DO+S12	DO overexpressing <i>SPE1,2</i>	This study
DO+S13	DO overexpressing <i>SPE1,3</i>	This study
DO+S23	DO overexpressing <i>SPE2,3</i>	This study
DO+S123	DO overexpressing <i>SPE1,2,3</i>	This study
DTO+S3	DTO overexpressing <i>SPE3</i>	This study
RA	D452-2 overexpressing <i>ADE17</i>	This study
RP	D452-2 overexpressing <i>PIR3</i>	This study
RH	D452-2 overexpressing <i>HTA2</i>	This study
RAP	D452-2 overexpressing <i>ADE17</i> and <i>PIR3</i>	This study

(be continued)

Name	Description	Reference
RAH	D452-2 overexpressing <i>ADE17</i> and <i>HTA2</i>	This study
RPH	D452-2 overexpressing <i>PIR3</i> and <i>HTA2</i>	This study
RAPH	D452-2 overexpressing <i>ADE17</i> , <i>PIR3</i> , and <i>HTA2</i>	This study
Plasmids		
pRS403	<i>HIS3</i> , an integrative plasmid	(Sikorski and Hieter, 1989)
pRS405	<i>LEU2</i> , an integrative plasmid	(Sikorski and Hieter, 1989)
pRS406	<i>URA3</i> , an integrative plasmid	(Sikorski and Hieter, 1989)
pRS423GPD	<i>HIS3</i> , <i>GPD</i> promoter, <i>CYCI</i> terminator, a multicopy plasmid	(Christianson et al., 1992)
pRS426HXT	<i>URA3</i> , <i>tHXT7</i> promoter, <i>CYCI</i> terminator, a multicopy plasmid	(Park et al., 2011)
pRS403HXT	<i>HIS3</i> , <i>tHXT7</i> promoter, <i>CYCI</i> terminator, an integrative plasmid	This study
pRS405HXT	<i>LEU2</i> , <i>tHXT7</i> promoter, <i>CYCI</i> terminator, an integrative plasmid	This study
pRS406HXT	<i>URA3</i> , <i>tHXT7</i> promoter, <i>CYCI</i> terminator, an integrative plasmid	This study
pAUR101	Aureobasidin resistance	TAKARA Co.

(be continued)

Name	Description	Reference
pXYL123	<i>TDH3_P-XYL1-TDH3_T, PGK1_P-XYL2-PGK1_T, TDH3_P-XYL3-TDH3_T</i> in pRS306	(Kim et al., 2012b)
pRS403_SPE2	<i>SPE2</i> under the control of <i>GPD</i> promoter in pRS403	This study
pRS405_SPE1	<i>SPE1</i> under the control of <i>GPD</i> promoter in pRS405	This study
pRS406_SPE3	<i>SPE3</i> under the control of <i>GPD</i> promoter in pRS406	This study
pRS403_PIR3	<i>PIR3</i> under the control of <i>tHXT7</i> promoter in pRS403HXT	This study
pRS405_ADE17	<i>ADE17</i> under the control of <i>tHXT7</i> promoter in pRS405HXT	This study
pRS406_HTA2	<i>HTA2</i> under the control of <i>tHXT7</i> promoter in pRS406HXT	This study
pAUR_d_OAZ1	pAUR101 with 180 bp of the truncated <i>S. cerevisiae OAZ1</i> gene	This study
pRS405_d_TPO1	pRS405 with 400 bp of the truncated <i>S. cerevisiae TPO1</i> gene	This study
pAUR_d_ATG7	pAUR101 with 600 bp of the truncated <i>S. cerevisiae ATG7</i> gene	This study

Table 3.2. List of DNA oligomers used in Chapter 3. The italicized sequences indicate the recognition sites of the corresponding restriction enzymes. [F] and [R] mean the forward and reverse primers, respectively

Name	Sequence (5' → 3')	Restriction enzyme	Amplified gene
SPE1[F]	<i>GGACTAGTATGTCTAGTACTCAAGTAGGAAATGCTCT</i>	<i>SpeI</i>	<i>SPE1</i>
SPE1[R]	<i>CCGCTCGAGTCAATCGAGTTCAGAGTCTATGTATACTATAT</i>	<i>XhoI</i>	
SPE2[F]	<i>GGACTAGTATGACTGTCACCATAAAAGAATTGACTAACC</i>	<i>SpeI</i>	<i>SPE2</i>
SPE2[R]	<i>CCGCTCGAGTCATATTTTCTTCTGCAATTCATATAGAAAAGGTG</i>	<i>XhoI</i>	
SPE3[F]	<i>GGACTAGTATGGCACAAGAAATCACTCACCCAAC</i>	<i>SpeI</i>	<i>SPE3</i>
SPE3[R]	<i>CCGCTCGAGCTAATTTAATTCCTTGGCTGCCAG</i>	<i>XhoI</i>	
GPDp[F]	<i>CGCGGATCCACCCTCACTAAAGGGAACAAAAGC</i>	<i>BamHI</i>	<i>GPDp-SPE1-CYC1t</i> <i>GPDp-SPE2-CYC1t</i> <i>GPDp-SPE3-CYC1t</i>
CYC1t_1[R]	<i>ATAAGAATGCGGCCGCGTAATACGACTCACTATAGGG</i>	<i>NotI</i>	
HXTp_1[F] ^a	<i>GGGGCGCCGGCTCGGGCCCCTGCTTCTGAG</i>	<i>NaeI</i>	
HXTp_2[F]	<i>CCAATGCATTCGGGCCCTGCTTCTGAG</i>	<i>NsiI</i>	<i>tHXT7p-MCS-CYC1t^c</i>
CYC1t_2[R]	<i>CGAGCTCCGTAATACGACTCACTATAGGGC</i>	<i>SacI</i>	
ADE17[F]	<i>AAAAC TGCAGATGGCCAATTACACAAAACCGCAAT</i>	<i>PstI</i>	<i>ADE17</i>
ADE17[R]	<i>ACGCGTCGACCTAATGGTGGAAACAAACGGATTGG</i>	<i>SalI</i>	

(be continued)

Name	Sequence (5' → 3')	Restriction enzyme	Amplified gene
PIR3[F]	CGCGGATCCATGCAATATAAAAAGCCATTAGTCGTCTC	<i>Bam</i> HI	<i>PIR3</i>
PIR3[R]	CCGGAATTCTCAACAGTCAATTAATCTATAGCTTGCAAATAAA	<i>Eco</i> RI	
HTA2[F]	CCGGAATTCATGTCCGGTGGTAAAGGTGGTAAA	<i>Eco</i> RI	<i>HTA2</i>
HTA2[R]	ACGCGTCGACTTACAGTTCTTGAGAAGCTTTGGCAG	<i>Sal</i> I	
d_OAZ1[F]	ACATGCATGCATCTCAATTCATATTAGATTACAATGTTCCGTC	<i>Sph</i> I	Truncated <i>OAZ1</i>
d_OAZ1[R]	GGGGTACCCCAATTGTAACCATCGTGGCTATTATTATTTTA	<i>Kpn</i> I	
Check_OAZ1[F]	CTTTCTACGTATAGTTTGGCTAGTGGGG		Check for disruption of <i>OAZ1</i>
Check_pAUR[R]	AAATACCGCATCAGGCGCCATTCG		
d_TPO1[F]	ATAAGAATGCGGCCGCGCCATTTTGGGTATCACGCTTTTTGTTC	<i>Not</i> I	Truncated <i>TPO1</i>
d_TPO1[R]	CGCGGATCCGCAACGAAAAGTGGGAAGCGAAA	<i>Bam</i> HI	
Check_TPO1[F]	CGTTGCCGAGCAGAGACCTGTAC		Check for disruption of <i>TPO1</i>
Check_pRS405[R]	CATTCAGGCTGCGCAACTGTTG		
d_ATG7[F]	ACATGCATGCCTCTAACCAAAAATTTTCTCAGCGTGTTG	<i>Sph</i> I	Truncated <i>ATG7</i>
d_ATG7[R]	GGGGTACCTGCTGAGCCTCCTCGTTTACTAATTTAT	<i>Kpn</i> I	
Check_ATG7[F] ^d	AACAGTTTTACATGTGCGGCCAGAGCC		Check for disruption of <i>ATG7</i>

^aCYC1t_1[R] was used as the reverse primer.

^bAmplified gene was ligated to the pRS403 and pRS405 to construct the pRS403HXT and pRS405HXT, respectively.

^cAmplified gene was ligated to the pRS406 to construct the pRS406HXT.

^dCheck_pAUR[R] was used as the reverse primer.

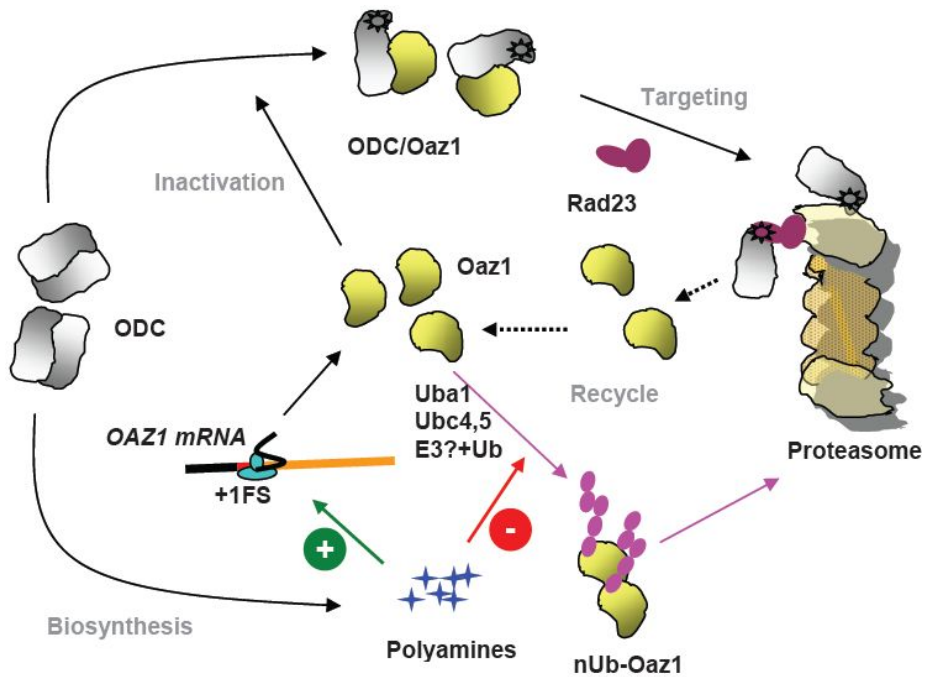


Fig. 3.1. Regulation of polyamine biosynthesis in *S. cerevisiae* (Palanimurugan et al., 2004). Polyamines regulate their biosynthesis by inducing ornithine decarboxylase (ODC) degradation. Excess amounts of polyamines induce +1 ribosomal frameshifting and hence increase OAZ1 protein levels. OAZ1 degrades ODC by forming ODC/OAZ1 heterodimer. This conformational change induces exposure of ODC degradation signal, which targets ODC for ubiquitin independent proteasomal degradation. Meanwhile, OAZ1 itself is also degraded by the proteasome. Excess amounts of polyamines inhibit the ubiquitylation of OAZ1 and hence block OAZ1 degradation.

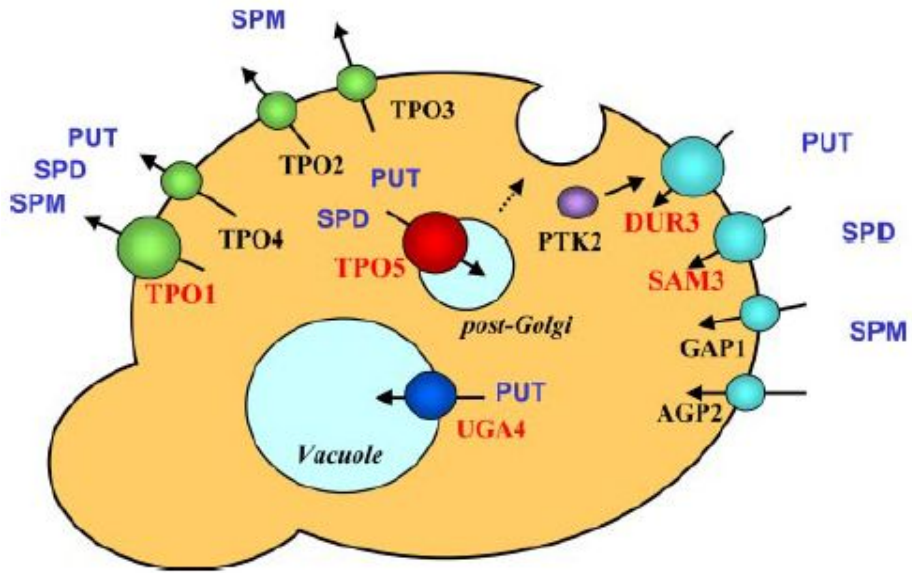


Fig. 3.2. Polyamine transport in yeast (Uemura et al., 2007). Polyamine uptake is mainly catalyzed by DUR3 and SAM3. Polyamine excretion is catalyzed by TPO1–5, located on either the plasma membrane or post-Golgi secretory vesicles. Proteins shown in *red characters* are more strongly involved in polyamine transport than those shown in *black*.

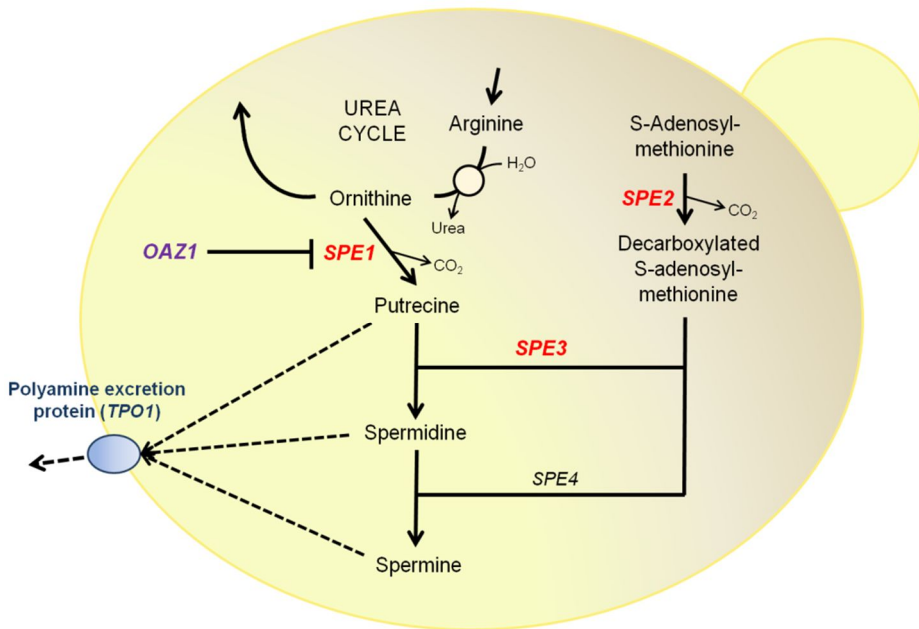


Fig. 3.3. Strategy for constructing engineered *S. cerevisiae* having high levels of SPD (Kim et al., 2015). Fluxes in the SPD biosynthetic pathway were amplified by overexpressing ornithine decarboxylase (ODC, *SPE1*), *S*-adenosylmethionine decarboxylase (*SPE2*), and spermidine synthase (*SPE3*). High levels of spermidine upregulate ODC antizyme (*OAZ1*) expression and Oaz1p mediates degradation of ODC. For alleviation of the feedback inhibition on ODC, *OAZ1* coding for ODC antizyme was disrupted. As a polyamine transporter (Tpo1p) located in *S. cerevisiae* plasma membrane excretes intracellular SPD to the medium, *TPO1* was also disrupted in order to minimize the loss of intracellular SPD.

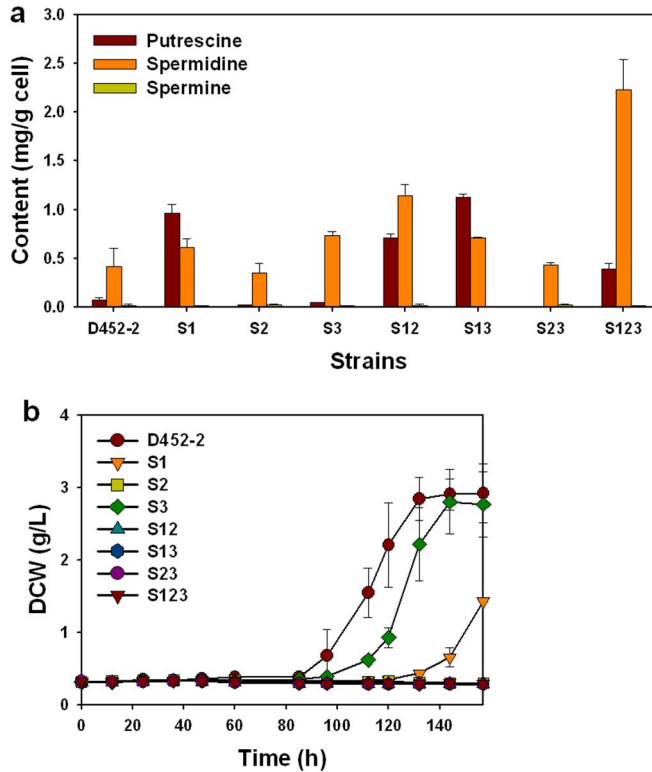


Fig. 3.4. Effects of amplification of genes coding for enzymes in the SPD biosynthetic pathway on polyamine contents (a) and cell growth (b). (a) Intracellular levels of polyamines in engineered strains. Abbreviations: S1, D452-2 overexpressing *SPE1*; S2, D452-2 overexpressing *SPE2*; S3, D452-2 overexpressing *SPE3*; S12, D452-2 overexpressing *SPE1,2*; S13, D452-2 overexpressing *SPE1,3*; S23, D452-2 overexpressing *SPE2,3*; S123, D452-2 overexpressing *SPE1,2,3*. (b) Cell growth of S1, S2, S3, S12, S13, S23, S123, and control D452-2 strain on a defined synthetic medium in the presence of 2 g/L furfural and HMF. Results are the mean of duplicate experiments and error bars indicate s.d..

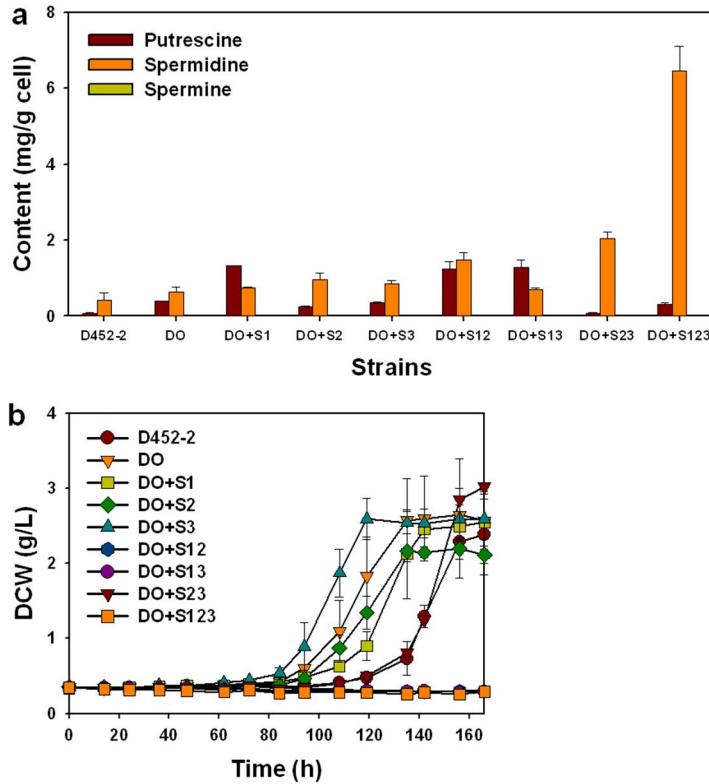


Fig. 3.5. Effects of alleviation of feedback inhibition on polyamine contents (a), and cell growth (b). (a) Intracellular levels of polyamines in engineered strains. Abbreviations: DO, D452-2 $\Delta OAZI$; DO+S1, DO overexpressing *SPE1*; DO+S2, DO overexpressing *SPE2*; DO+S3, DO overexpressing *SPE3*; DO+S12, DO overexpressing *SPE1,2*; DO+S13, DO overexpressing *SPE1,3*; DO+S23, DO overexpressing *SPE2,3*; DO+S123, DO overexpressing *SPE1,2,3*. (b) Cell growth of DO, DO+S1, DO+S2, DO+S3, DO+S12, DO+S13, DO+S23, DO+S123, and control D452-2 strain on a defined synthetic medium in the presence of 2 g/L furfural and HMF. Results are the mean of duplicate experiments and error bars indicate s.d..

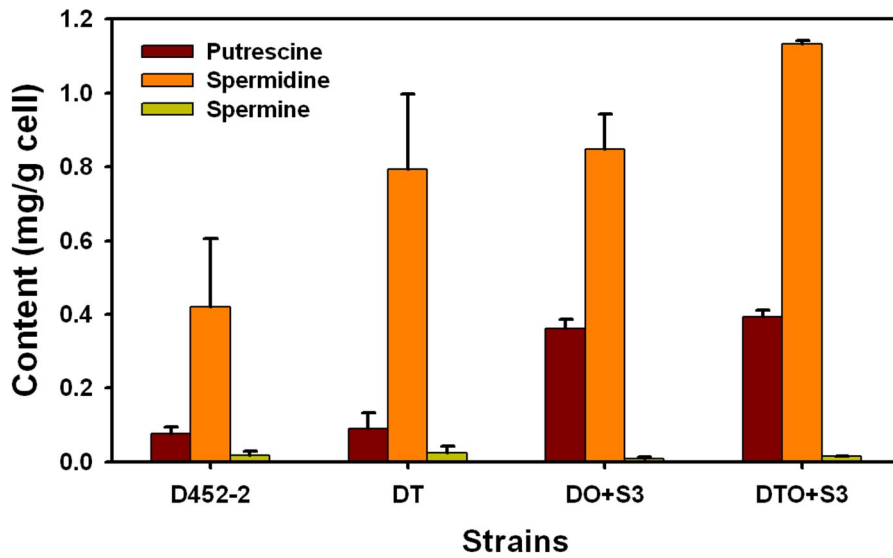


Fig. 3.6. Intracellular levels of polyamines in *S. cerevisiae* D452-2, DT, DO+S3, and DTO+S3 strains. Results are the mean of duplicate experiments and error bars indicate s.d..

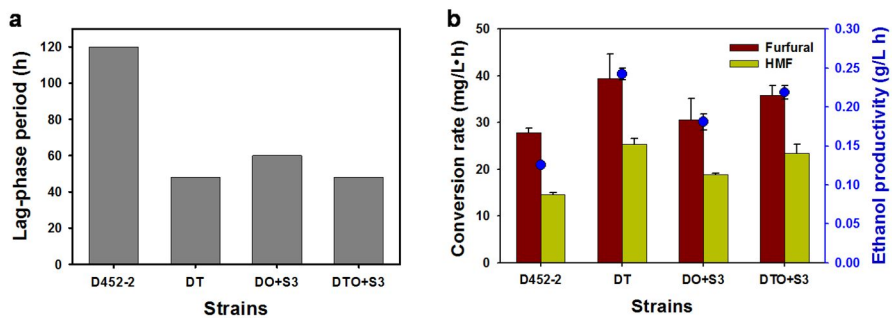


Fig. 3.7. Comparison of fermentation parameters by *S. cerevisiae* D452-2, DT, DO+S3, and DTO+S3 strains in the presence of 2 g/L furfural and HMF. (a) Lag-phase periods. (b) Furfural and HMF conversion rates and ethanol productivities. Results are the mean of duplicate experiments and error bars indicate s.d..

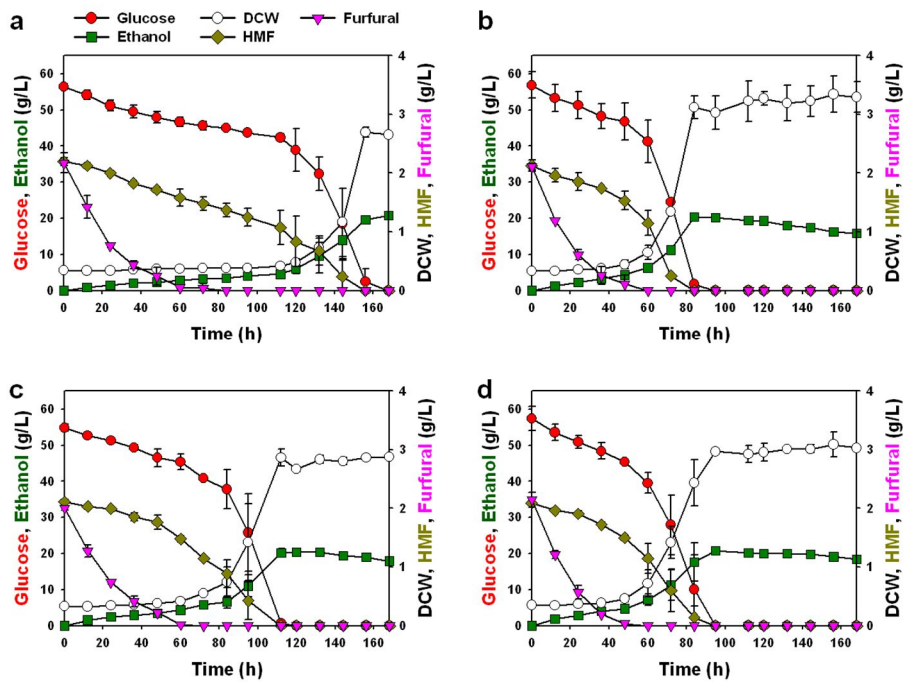


Fig. 3.8. Batch fermentation profiles by *S. cerevisiae* D452-2 (a), DT (b), DO+S3 (c), and DTO+S3 (d) strains in the presence of 2 g/L furfural and HMF. Results are the mean of duplicate experiments and error bars indicate s.d..

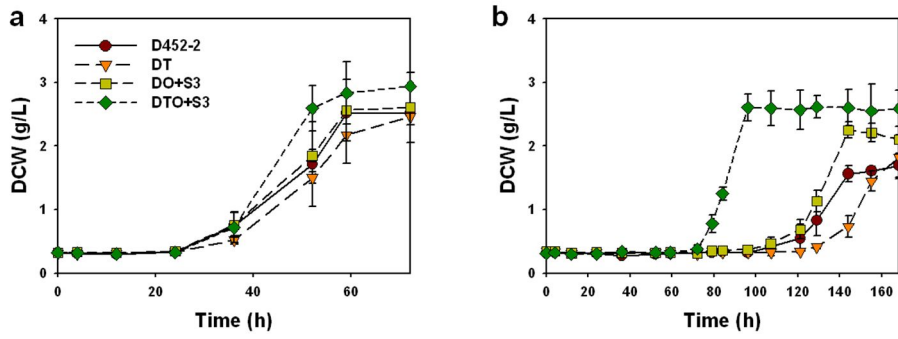


Fig. 3.9. Cell growth of *S. cerevisiae* D452-2, DT, DO+S3, and DTO+S3 strains in the presence of 3 (a) and 4 g/L (b) acetic acid. Results are the mean of duplicate experiments and error bars indicate s.d..

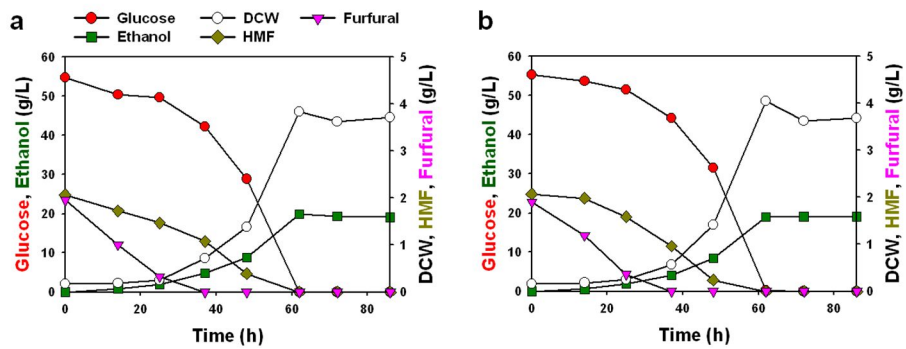


Fig. 3.10. Batch fermentation of *S. cerevisiae* D452-2 (a) and *ATG7* disrupted D452-2 (DA) (b) supplemented with 2 mM SPD in the presence of 2 g/L furfural and HMF.

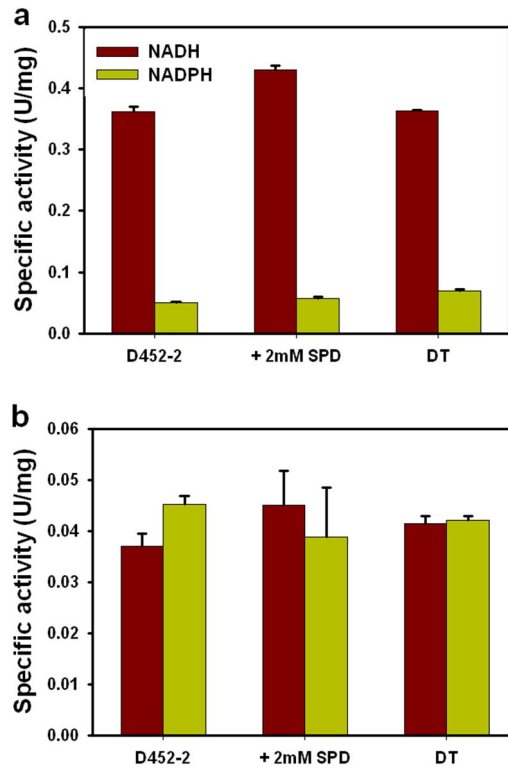


Fig. 3.11. *In vitro* assay of reduction activity toward furfural (a) and HMF (b). The crude protein extracts of *S. cerevisiae* D452-2 with and without 2 mM SPD supplementation and the DT strain were subjected to reduction activity using NAD(P)H as cofactor. Results are the mean of duplicate experiments and error bars indicate s.d..

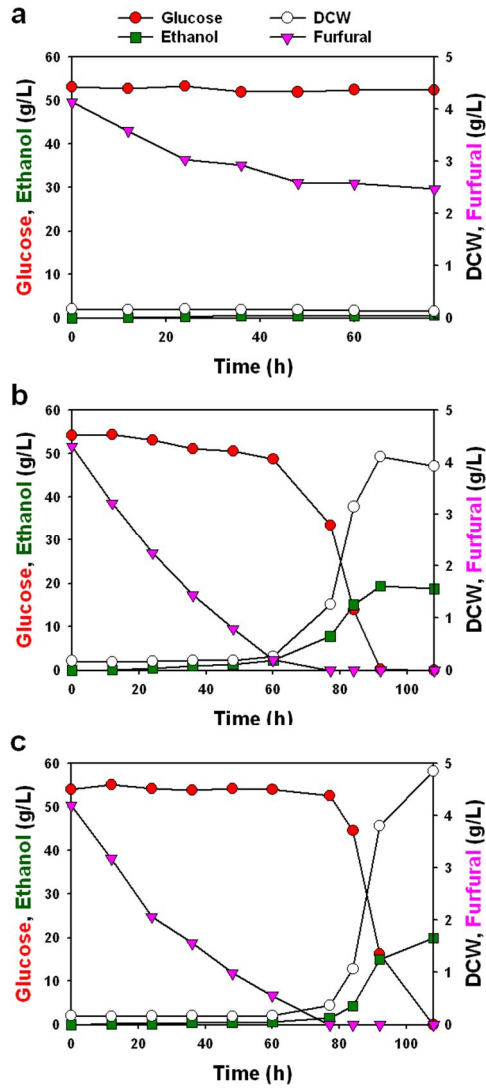


Fig. 3.12. Batch fermentation of *S. cerevisiae* D452-2 without (a) and with (b) 2 mM SPD supplementation and the DT strain (c) in the presence of 4 g/L furfural.

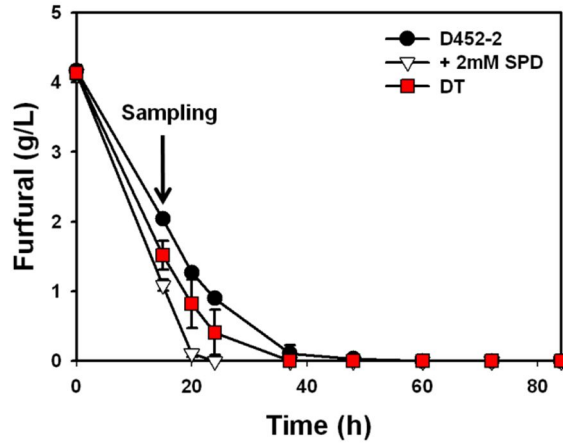


Fig. 3.13. Comparison of furfural conversion patterns by *S. cerevisiae* D452-2 with and without 2 mM SPD supplementation and the DT strain. The arrow points the sampling time for RNA sequencing experiment. Results are the mean of triplicate experiments and error bars indicate s.d..

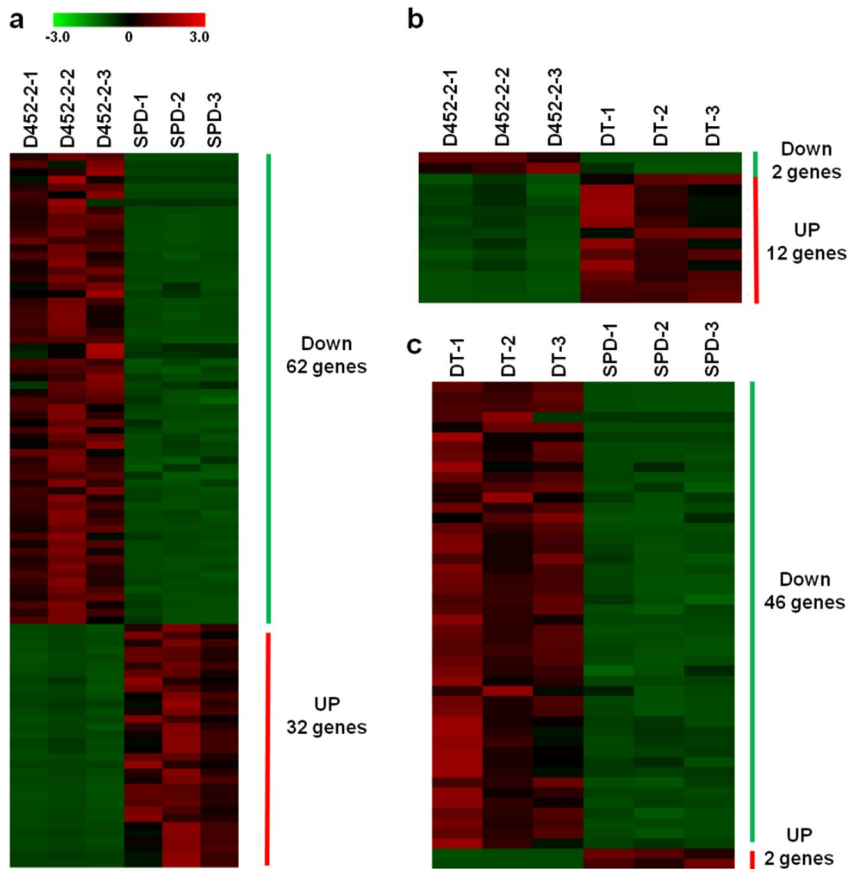


Fig. 3.14. Differently expressed genes between *S. cerevisiae* D452-2 without and with 2 mM SPD supplementation (a), D452-2 and the DT strain (b), and the DT strain and D452-2 with 2 mM SPD supplementation (c) in response to furfural. D452-2-1, D452-2-2, and D452-2-3 were the triplicates of control experiment; SPD-1, SPD-2, and SPD-3 mean the triplicates of supplementation of 2 mM SPD experiment; DT-1, DT-2, and DT-3 mean the triplicates of the DT strain experiment. The detailed data were listed in Appendix.

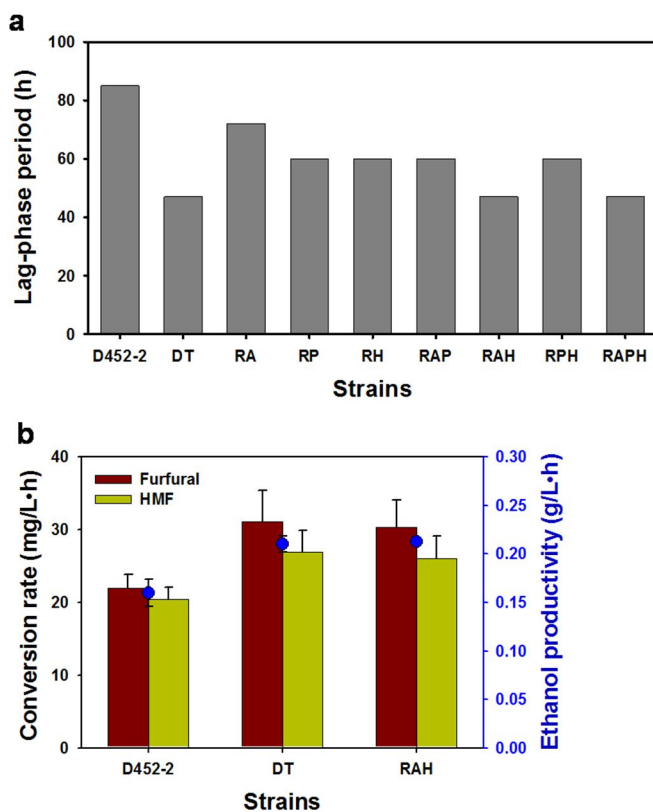


Fig. 3.15. Comparison of fermentation parameters by *S. cerevisiae* D452-2 and engineered strains in the presence of 2 g/L furfural and HMF. (a) Lag-phase period. Abbreviations: DT, D452-2 $\Delta TPO1$; RA, D452-2 overexpressing *ADE17*; RP, D452-2 overexpressing *PIR3*; RH, D452-2 overexpressing *HTA2*; RAP, D452-2 overexpressing *ADE17* and *PIR3*; RAH, D452-2 overexpressing *ADE17* and *HTA2*; RPH, D452-2 overexpressing *PIR3* and *HTA2*; RAPH, D452-2 overexpressing *ADE17*, *PIR3*, and *HTA2*. (b) Higher furfural and HMF conversion rates and ethanol productivities of the engineered strains (DT and RHA). Results are the mean of duplicate experiments and error bars indicate s.d..

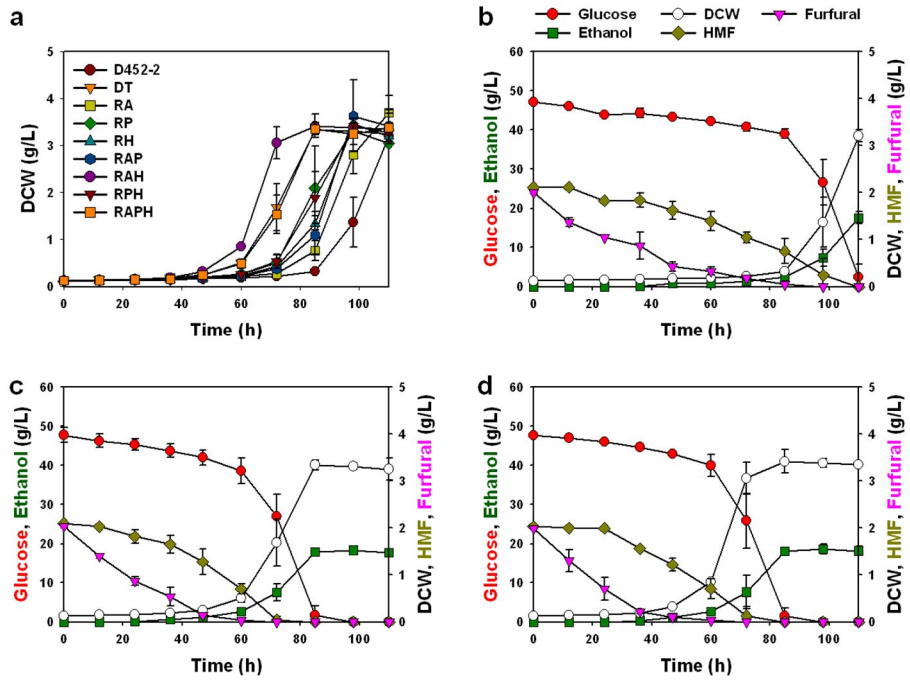


Fig. 3.16. Cell growth of *S. cerevisiae* D452-2 and engineered strains (a) and batch fermentation of *S. cerevisiae* D452-2 (b), DT (c), and RAH (d) strains in the presence of 2 g/L furfural and HMF. Results are the mean of duplicate experiments and error bars indicate s.d..

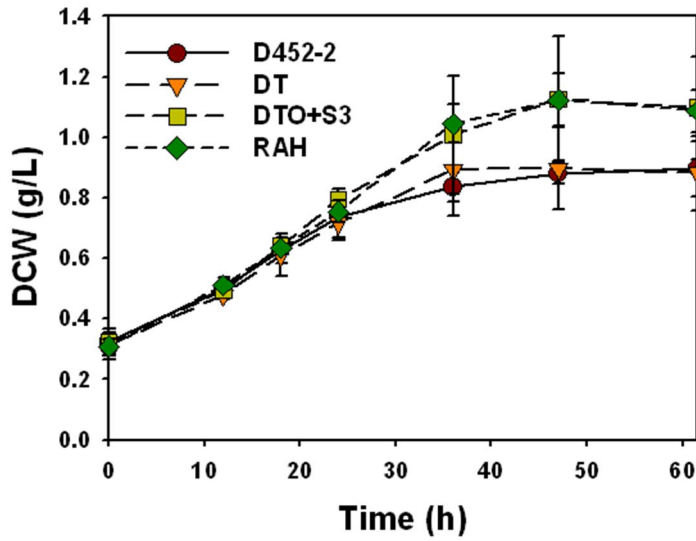


Fig. 3.17. Cell growth of *S. cerevisiae* D452-2, DT, DTO+S3, and RAH strains in the presence of 8% (v/v) ethanol. Results are the mean of duplicate experiments and error bars indicate s.d..

Chapter 4

Application of engineered *Saccharomyces cerevisiae* strains with high spermidine contents to enhancing ethanol fermentation performance

4.1. Summary

Efforts to construct robust *S. cerevisiae* strains suitable for various fermentation conditions including repeated-batch fermentation and xylose utilization in the presence of fermentation inhibitors have mainly focused on iterative identification and pathway engineering responsible for specific fermentation condition. Instead of pursuing specific genetic perturbations, it was sought to construct general purpose *S. cerevisiae* strains exhibiting improved sugar fermentation under various fermentation conditions. To this end, the engineered strains with high spermidine contents were used as host cells because high intracellular spermidine contents are associated with tolerance to diverse stresses. As examples of application, it was evaluated that its fermentation ability in repeated-batch fermentation and xylose fermentation in the presence of inhibitors (fufural, HMF, and acetic acid). First, the engineered strains exhibited improved glucose fermentation during the sixteen times of repeated-batch fermentations. At the sixteenth fermentation, ethanol productivities of the DT and TOS3 strains were 19% and 31% higher than that of the control strain, respectively. Second, xylose-fermenting *S. cerevisiae* strains with high spermidine contents exhibited approximately 40% higher ethanol productivity than that of the control strain in the minimal medium

containing furfural, HMF, and acetic acid. Third, in the medium containing glucose and xylose mixture without fermentation inhibitors, the engineered strain also showed improved xylose fermentation. The engineered strains constructed in this study can be applied to production of other biofuels and biochemicals. In all the fermentation experiments, *S. cerevisiae* strains with high SPD contents produced almost identical concentrations of xylitol, glycerol, and acetic acid.

4.2. Introduction

Plant biomass has received considerable attention as a renewable energy source, which could help to reduce both the world's dependence on fossil fuels and greenhouse gas emissions (Farrell et al., 2006; Naik et al., 2010). However, economic production of bioethanol and biochemicals are still pursued from corn and starch based biomass (Huang et al., 2014; Wang et al., 2013b; Yangcheng et al., 2013). In the corn and starch based ethanol industries, high ethanol titer in a short fermentation time is obtained by a high-gravity fermentation, and yeast cells at the end of each batch fermentation are reused as inoculum for the next fermentation (Bai et al., 2008; Verbelen et al., 2009). This repeated-batch fermentation system reduces the costs related with fresh yeast biomass propagation. For economic production of biofuels, the utilization of all sugars and maintenance of viable yeast cells throughout the fermentation cycles are prerequisites (Bai et al., 2008; Pereira et al., 2012). Therefore, *S. cerevisiae* strains with high viability were evolved and isolated from sugarcane distilleries and used by the industry (Argueso et al., 2009; Maristela Freitas and Laluce, 1998; Pereira et al., 2010). In addition, optimization of inoculum refreshing step, medium composition, and temperature has been designed to prevent decrease in yeast cell viability (Laluce et al., 2009; Pereira et al., 2012; Thomas et al., 1998).

It was recently presented that adequate modulation of spermidine (SPD) contents in *S. cerevisiae* improved ethanol fermentation in minimal media containing fermentation inhibitors and ethanol (Kim et al., 2015). Furthermore, it was reported that SPD extends lifespan of *S. cerevisiae* (Eisenberg et al., 2009). These observations suggest that the engineered strains with high SPD contents might exhibit high viability and ethanol production rate in the repeated-batch fermentation scheme. Based on this hypothesis, it was examined if these previously constructed engineered strains exhibited improved ethanol production rate in the repeated-batch fermentation.

In contrary to corn and starch based biomass, lignocellulosic biomass can provide an abundant renewable resource for production of biofuels and chemicals as alternative to the oil refineries without competition with food production. However, unlike sugar-containing and starchy biomass, the lignocellulosic hydrolysates contain glucose and xylose as major carbon sources, and hence economic conversion of xylose into biofuels through xylose utilization is essential. Moreover, development of an inhibitor tolerant *S. cerevisiae* strain is one of the major research challenges because lignocellulosic hydrolysates contain fermentation inhibitors including 2-furaldehyde (furfural), 5-hydroxymethyl-2-furfural (HMF), and acetic acid (Almeida et al., 2007; Hahn-Hagerdal

et al., 2006). While a xylose-fermenting *S. cerevisiae* strain with tolerance to acetic acid was constructed (Hasunuma et al., 2011), any attempts to construct xylose-fermenting *S. cerevisiae* strains exhibiting tolerance to furfural, HMF, and acetic acid simultaneously have not been considered previously. In this study, xylose-fermenting *S. cerevisiae* strains exhibiting tolerance to furfural, HMF, and acetic acid simultaneously were successfully constructed by introducing the xylose assimilation pathway to the previously constructed engineered strains with high SPD contents.

It was also investigated whether the engineered strains showed improved xylose fermentation in the absence of fermentation inhibitors. Interestingly, the xylose-fermenting engineered *S. cerevisiae* strain with high SPD content showed improved xylose consumption rates throughout the repeated-batch fermentation cycles in the absence of fermentation inhibitors.

4.3. Materials and methods

4.3.1. Strains, plasmids, and media

Escherichia coli TOP10 (Invitrogen, Carlsbad, CA, USA) was used for plasmid construction. *S. cerevisiae* D452-2 (*MAT α* , *leu2*, *his3*, *ura3*, and *can1*), DT, and TOS3 stains (Kim et al., 2015) were used for constructing xylose-fermenting strains with improved tolerance to fermentation inhibitors. Plasmid pSR6-X123 expressing *XYL1*, *XYL2*, and *XYL3* from *Scheffersomyces stipitis* (Kim et al., 2012b) was used for xylose assimilation. Strains and plasmids used in this work are described in Table 4.1.

E. coli was grown in LB medium (5 g/L yeast extract, 10 g/L bacto tryptone, and 10 g/L NaCl) with 50 μ g/ml of ampicillin for genetic manipulation. *S. cerevisiae* strains were pre-cultured at 30°C and 250 rpm for 48 h in YP medium (10 g/L yeast extract and 20 g/L bacto peptone) with 20 g/L glucose. A defined YSC medium (6.7 g/L yeast nitrogen without amino acids and 2.0 g/L synthetic complete supplement mixture) containing appropriate amounts of sugars was used for fermentation experiments.

4.3.2. Genetic manipulation

The gene encoding glucose-6-phosphate dehydrogenase (ZWF1) was PCR-amplified from the genomic DNA of *S. cerevisiae* D452-2 using ZWF1[F] (5'-CGCGGATCCATGAGTGAAGGCCCGTCAAATT-3') and ZWF1[R] (5'-CCCAAGCTTCTAATTATCCTTCGTATCTTCTGGCTTAG-3') primers. After digestion of the PCR product with *Bam*HI and *Hind*III restriction enzymes, the nucleotides were ligated with plasmid pRS403HXT (Kim et al., 2015), resulting in the construction of plasmid pZWF1.

Transformation of the cassettes for overexpressing the enzymes in the xylose assimilation pathway (*XYL1*, *XYL2*, and *XYL3*) and glucose-6-phosphate dehydrogenase (*ZWF1*) was performed using the yeast EZ-Transformation kit (BIO 101, Vista, CA). Transformants were selected on YSC medium containing 20 g/L glucose. Amino acids and nucleotides were added as necessary.

4.3.3. Yeast viability test

Yeast survival plating of *S. cerevisiae* D452-2 with and without 2 mM SPD supplementation, DT, and TOS3 strains followed the previous report with minor modification (Fabrizio and Longo, 2003). Briefly, 50 mL cultures were inoculated with 1% (v/v) of a fresh overnight culture and incubated at 30°C and 80 rpm in YSC medium containing 50 g/L

glucose and supplemented with a 4-fold excess of tryptophan, leucine, uracil, and histidine. For *S. cerevisiae* with 2 mM SPD supplementation, 2 mM SPD was added to stationary culture at day 3. Yeast cell viability was monitored in YSC medium by measuring colony-forming units (CFUs) in every 48 h. The number of CFUs at day 3 was set to be the initial survival (100%) and was used to determine the time-dependent viability.

4.3.4. Repeated-batch fermentation

For repeated-batch fermentation experiments, the first fermentation cycle was initiated with initial optical density (OD₆₀₀) of 140. To maintain microaerobic condition and maximize ethanol productivity, flask fermentation experiments were performed at 30°C and 80 rpm in 50 ml YSC medium containing 100 g/L glucose or a mixture of 65 g/L glucose and 40 g/L xylose. At the end of each cycle, the culture broth was centrifuged at 13,000 rpm for 10 min, and the *S. cerevisiae* cells were entirely recycled to inoculate for the next cycle. This procedure was repeated for 15 times in the YSC medium containing only glucose and for 4 times a mixture of glucose and xylose.

4.3.5. Fermentation in medium containing fermentation inhibitors

To test tolerance of *S.cerevisiae* strains to furan derivatives, pre-cultured cells from YP medium with 20 g/L glucose were harvested and inoculated into main cultures with initial optical density (OD₆₀₀) of 0.4 for glucose fermentations and 0.6 for fermentations of a mixture of glucose and xylose. Flask fermentation experiments were performed at 30°C and 80 rpm in 50 ml YSC medium containing 50 g/L glucose or a mixture of 70 g/L glucose and 40 g/L xylose with 2 g/L furfural and HMF.

For the fermentation with simulated hydrolysates, initial OD₆₀₀ values were adjusted to 0.8, and flask fermentation experiments were performed at 30°C and 80 rpm in 50 ml YSC medium containing 70 g/L glucose and 40 g/L xylose with 1 g/L acetic acid, 2 g/L furfural, and 2 g/L HMF or 3 g/L acetic acid, 0.4 g/L furfural, and 0.8 g/L HMF.

For the fermentation of lignocelluloses hydrolysate, enzymatic hydrolysis of corn stover hydrolysate from National Renewable Energy Laboratory was conducted as the same as chapter 2. After enzymatic hydrolysis, the samples were centrifuged at 13,000 rpm for 10 min. The supernatant was collected and supplemented with concentrated autoclaved YSC medium to obtain a hydrolysate mixture with 6.7 g/L yeast nitrogen without amino acids and 2.0 g/L synthetic complete supplement mixture. Initial cell densities were adjusted to OD₆₀₀ of 0.9

and fermentations were performed at 30°C and 80 rpm in 50 ml working volume.

4.3.6. Determination of cell and metabolite concentrations

Optical density (OD) of the cells was measured with a spectrophotometer (RF5301, Shimadzu, Kyoto, Japan) at 600 nm. Dry cell mass was obtained by multiplication of OD with a pre-determined conversion factor, 0.30 g/L/OD.

Concentrations of glucose, xylose, xylitol, glycerol, acetic acid, ethanol, furfural, and HMF were determined by high performance liquid chromatography (HPLC, Agilent Technologies 1200 Series) equipped with a REZEX ROA organic acid column (Phenomenex, Torrance, USA). The column was eluted with 5 mM H₂SO₄ at a flow rate of 0.6 ml/min at 60°C. Furfuryl alcohol and furan dimethanol, conversion products of furfural and HMF, concentrations were determined by UV detection at 215 nm using a BIO-RAD Aminex HPX-87H ion exclusion column. The column was eluted with 84% (v/v) 5 mM H₂SO₄ and 16% (v/v) acetonitrile at a flow rate of 0.4 ml/min at 25°C.

4.4. Results and discussion

4.4.1. Effects of high spermidine content on repeated-batch fermentation

Among the engineered strains with high spermidine (SPD) contents constructed as described previously, the DT (D452-2 $\Delta TPO1$) and TOS3 (D452-2 $\Delta TPO1 \Delta OAZ1$ overexpressing *SPE3*) strains (Table 4.1) showed the highest furfural and acetic acid tolerance, respectively (Kim et al., 2015). Therefore, in this chapter, these strains were used as host cells to improve ethanol fermentation performance. First, it was examined whether the DT and TOS3 strains exhibit high viability as the same as the addition of 2 mM SPD because SPD is known to extend lifespan of *S. cerevisiae* (Eisenberg et al., 2009). As shown in Fig. 4.1a, the fraction of viable *S. cerevisiae* D452-2 cells substantially decreased over time and was 1.4% at day 9. However, when 2 mM SPD was supplied to ageing D452-2 cells (at day 3), the viable fraction of D452-2 cells increased and was more than half at day 9. While the DT and TOS3 strains maintained higher viability than the control strain at day 5, the extents were much lower than the case of 2 mM SPD addition.

It was expected that viability of yeast cells might be proportionally related to the fermentation performance. To this end, fermentation

activities during repeated-batch fermentation were investigated. Microaerobic batch fermentations of *S. cerevisiae* D452-2 with and without 2 mM SPD supplementation, DT, and TOS3 strains were carried out using yeast synthetic complete (YSC) medium containing 100 g/L glucose. During the sixteen times of repeated-batch fermentations by recycling cells from the previous fermentation, ethanol productivity of the control D452-2 strain gradually decreased from 6.6 g/L·h to 3.9 g/L·h (Fig. 4.1b). On the other hand, ethanol productivity of the D452-2 strain with 2 mM SPD supplementation was maintained until twelfth fermentation and then decreased from 6.7 g/L·h to 5.0 g/L·h at the thirteenth fermentation. While ethanol productivity profiles of the DT and TOS3 strains were almost identical to that of the control strain until ninth fermentation, the DT and TOS3 strains maintained its fermentation activities during the last eight fermentations (from ninth to sixteenth) whereas the D452-2 control strain continuously decreased its fermentation ability. At the sixteenth fermentation, ethanol productivities of the DT and TOS3 strains were 19% and 31% higher than that of the control strain, respectively. In conclusion, when using glucose as a carbon source, fermentation ability of *S. cerevisiae* is proportionally associated with its viability during the cell recycling repeated-batch fermentation, and robust *S. crevisiae* strains suitable for maintaining high ethanol productivity in repeated-

batch fermentation were successfully constructed.

4.4.2. Introduction of xylose assimilation pathway to the engineered strains with high spermidine contents

As another application of *S. cerevisiae* strains with high SPD contents, it was examined if tolerance phenotypes of the DT and TOS3 strains were maintained after introduction of the xylose assimilation pathway. Also, *S. cerevisiae* D452-2 and DT strains overexpressing *ZWF1* (Z1 and TZ1) were used as the control (Table 4.1) because overexpression of *ZWF1* is one of the most effective strategies for relieving the toxic effects of furan derivatives (Almeida et al., 2008; Gorsich et al., 2006; Kim and Hahn, 2013; Liu et al., 2008; Moon and Liu, 2012; Park et al., 2011; Petersson et al., 2006). As expected, all of the engineered strains (DT, TOS3, Z1, and TZ1) showed the shorter lag-phase period and higher ethanol productivity than those of the control strain under the medium containing 2 g/L of furfural and 2 g/L of HMF (Fig. 4.2). However, when the xylose assimilation pathway was introduced to the Z1 strain (Z1X), this strain did not grow at all in a mixture of glucose and xylose containing furan derivatives (Fig. 4.3a and Fig. 4.4). Xylose reductase (XYL1) from *S. stipitis* is a NADPH preferred aldose reductase, acting with various aldose substrates (Nogae and Johnston, 1990). Therefore, when paired with *ZWF1* overexpression, known to increase cytoplasmic NADPH levels, this non-specific xylose reductase

might generate a futile cycle by reducing various aldose substrates (Verduyn et al., 1985), resulting in metabolic burden. On the other hand, introduction of the xylose assimilation pathway to the DT and TOS3 strains (DTX and TOS3X) (Table 4.1) did not alter tolerance phenotypes of the strains. Both of engineered strains exhibited shorter lag-phase periods (47 h vs. 73 h) as compared to the control X strain (Fig. 4.3a). Among them, the highest ethanol productivity of 0.31 g/L·h was obtained for the DTX strain, which was 32% higher than the control X strain (Fig. 4.3b). The reason for this improvement was ascribed to the faster conversion rate of furfural than the control strain. The furfural and HMF added were converted to furfuryl alcohol and furan dimethanol, respectively (data not shown). When genetic perturbations of the DTX and Z1X strains were combined (TZ1X), combination of *TPO1* disruption with *ZWF1* overexpression in the xylose-fermenting *S. cerevisiae* strain, detrimental effects of *ZWF1* overexpression were partially compensated by *TPO1* disruption. However, the TZ1X strain still exhibited a prolonged lag-phase period of 108 h as compared to the control X strain. These results indicated that introduction of the xylose assimilation pathway to the inhibitor tolerant *S. cerevisiae* strain alone does not ensure its tolerance phenotypes. In conclusion, by introducing the xylose assimilation pathway to the engineered strains with high SPD contents, xylose-

fermenting *S. cereviale* strain with tolerance to furan derivatives was successfully constructed.

4.4.3. Fermentation of xylose-fermenting *S. cerevisiae* strains with high spermidine contents in simulated hydrolysates containing furfural, HMF, and acetic acid

While HMF and furfural are formed by dehydration of hexoses and pentoses, respectively, acetic acid is formed by de-acetylation of hemicelluloses. Synergistic effects of combinations of acetic acid and furan derivatives severely aggravate both growth and fermentation ability of yeast strains (Palmqvist et al., 1999). Therefore, construction of xylose-fermenting *S. cerevisiae* strains exhibiting tolerance to furfural, HMF and acetic acid simultaneously is mandatory for economic production of cellulosic biofuels.

Batch fermentations were performed with *S. cerevisiae* X, DTX, and TOS3X strains in simulated hydrolysates containing high concentrations of furan derivatives (1 g/L acetic acid, 2 g/L furfural, and 2 g/L HMF) and acetic acid (3 g/L acetic acid, 0.4 g/L furfural, and 0.8 g/L HMF) according to the inhibitor compositions in lignocellulose hydrolysates (Almeida et al., 2007). These two representative compositions were chosen because different pretreatment conditions resulted in lignocellulose hydrolysates with high concentration of furan derivatives or acetic acid (Aguilar et al., 2002). In the artificial hydrolysate with high furfural concentration, the DTX and TOS3X

strains exhibited shorter lag-phase periods than that of the control X strain (Fig. 4.5a). The profiles of ethanol productivity and conversion rates of furan derivatives by the X, DTX, and TOS3X strains were similar to those in the case of fermentation in the medium containing furan derivatives only (2 g/L of furfural and 2 g/L of HMF) (Fig. 4.3b and Fig. 4.5b). Among them, the highest ethanol productivity of 0.34 g/L·h was obtained for the DTX strain, which was 46% higher than the control strain. These results indicated that the tolerance phenotypes of the DTX and TOS3X strains to furan derivatives were maintained under multi-stress conditions including furan derivatives and acetic acid.

On the other hand, batch fermentations were performed with *S. cerevisiae* X, DTX and TOS3X strains in the simulated hydrolysate containing high concentration of acetic acid. In this fermentation condition, DTX and TOS3X strains also exhibited shorter lag-phase periods (48~60 h vs. 85 h) as compared to the control X strain (Fig. 4.5c). Among them, the highest ethanol productivity of 0.31 g/L·h was obtained for the TOS3X strain, which was 38% higher than the control strain (Fig. 4.5d). These results are consistent with our previous study, which presented that among the engineered strains with high SPD contents, only the TOS3 strain exhibited tolerance phenotype to acetic acid (Kim et al., 2015).

4.4.4. Fermentation of xylose-fermenting *S. cerevisiae* strains with high spermidine contents in corn stover hydrolysate

It was examined whether the engineered strain exhibited an enhanced fermentation ability in corn stover hydrolysate that contains numerous fermentation inhibitors in addition to furfural, HMF and acetic acid. After enzymatic hydrolysis and supplementation with concentrated YSC medium, concentrations of acetic acid, HMF and furfural in corn stover hydrolysate mixture were 3.3 g/L, 0.8 g/L and 0.4 g/L, respectively. Therefore, fermentation experiment was designed to perform with X (control) and TOS3X strains because the TOS3X strain showed the most improved tolerance phenotype in the fermentation of simulated hydrolysate containing high concentration of acetic acid. As expected, the ethanol productivity of the TOS3X strain was 14% higher than that of the control strain (Fig. 4.6). However, the extent was much lower than the case of the fermentation of simulated hydrolysates (0.4 g/L furfural, 0.8 g/L HMF and 3 g/L acetic acid). These different extents of improvement might be caused by other inhibitors (formic acid and phenolic compounds) present in corn stover hydrolysate in addition to furfural, HMF and acetic acid.

4.4.5. Improved xylose fermentation of *S. cerevisiae* by high spermidine contents in the absence of fermentation inhibitors

Finally, it was investigated whether the engineered strains exhibited improved xylose fermentation in the absence of fermentation inhibitors because high concentrations (>10 g/L) of xylose itself is toxic to the *S. cerevisiae* cells, causing delayed cell growth (Kim et al., 2013). During the four times of repeated-batch fermentations by the X strain with and without 2 mM SPD supplementation and the TOS3X strain, initially added 62 ~ 65 g/L glucose was completely consumed in every 4 h (Fig. 4.7). While xylose consumption rates of the all three strains decreased over batches, the TOS3X strain represented 23 ~ 47% higher xylose consumption rate and 6 ~ 16% higher ethanol productivity than those of the control X strain throughout the fermentation cycles without any change of byproduct (xylitol, glycerol and acetic acid) accumulation (Fig. 4.7 and Fig. 4.8). The TOS3X strain also showed high xylose consumption rate and ethanol productivity in a batch fermentation with the low initial OD₆₀₀ value (OD₆₀₀ = 1.0) (Fig. 4.9). In contrary to the case of glucose fermentation, the beneficial effects of 2 mM SPD addition on ethanol productivity were not realized in glucose and xylose mixture fermentation. It was previously presented that transcriptional responses between *S. cerevisiae* D452-2 strain with 2

mM SPD supplementation and the engineered strain with high SPD contents were much different (Kim et al., 2015). Therefore, it was speculated that enhanced xylose fermentation of the TOS3X strain might be resulted from different gene expression levels, and additional experiments are necessary to elucidate the key genes involved in this phenotype. When combined with previous iterative metabolic and evolutionary engineering approach for efficient xylose metabolism by engineered *S. cerevisiae* (Kim et al., 2013; Lee et al., 2012; Matsushika et al., 2012; Watanabe et al., 2007; Young et al., 2012; Zhou et al., 2012), introduction of genetic perturbations present in TOS3 (*TPO1* and *OAZ1* double-disruption with *SPE3* overexpression) might further improve xylose fermentation by *S. cerevisiae*.

Table 4.1. *S. cerevisiae* strains and plasmids used in Chapter 4

Name	Description	Reference
Strains		
D452-2	<i>MATα</i> , <i>leu2</i> , <i>his3</i> , <i>ura3</i> , and <i>can1</i>	(Hosaka et al., 1992)
DT	D452-2 Δ <i>TPO1</i>	(Kim et al., 2015)
TOS3	D452-2 Δ <i>TPO1</i> Δ <i>OAZ1</i> overexpressing <i>SPE3</i>	(Kim et al., 2015)
Z1	D452-2 overexpressing <i>ZWF1</i>	This study
TZ1	D452-2 Δ <i>TPO1</i> overexpressing <i>ZWF1</i>	This study
X	D452-2 overexpressing <i>XYL1,2,3</i>	This study
DTX	D452-2 Δ <i>TPO1</i> overexpressing <i>XYL1,2,3</i>	This study
TOS3X	D452-2 Δ <i>TPO1</i> Δ <i>OAZ1</i> overexpressing <i>SPE3</i> and <i>XYL1,2,3</i>	This study
Z1X	D452-2 overexpressing <i>ZWF1</i> and <i>XYL1,2,3</i>	This study
TZ1X	D452-2 Δ <i>TPO1</i> overexpressing <i>ZWF1</i> and <i>XYL1,2,3</i>	This study

(be continued)

Name	Description	Reference
Plasmids		
pRS403HXT	<i>HIS3</i> , <i>tHXT7</i> promoter, <i>CYC1</i> terminator, an integrative plasmid	(Kim et al., 2015)
pZWF1	<i>ZWF1</i> under the control of <i>tHXT7</i> promoter in pRS403HXT	This study
pSR6-X123	<i>TDH3_P-XYL1-TDH3_T</i> , <i>PGK1_P-XYL2-PGK1_T</i> , <i>TDH3_P-XYL3-TDH3_T</i> in pRS306	(Kim et al., 2012b)

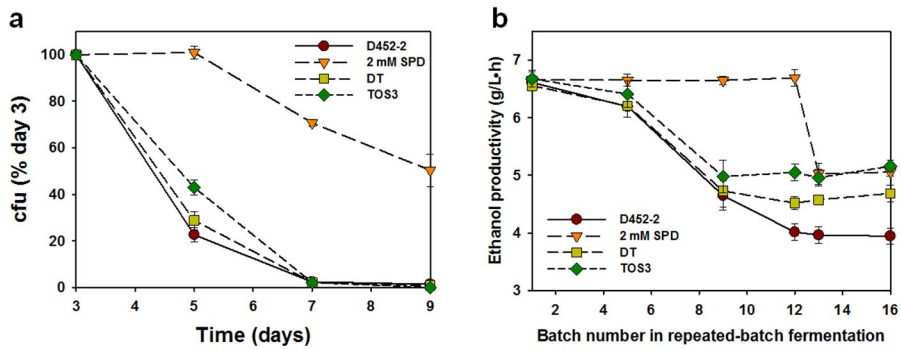


Fig. 4.1. Effects of yeast cell viability on fermentation ability during repeated-batch fermentation using glucose as a sole carbon source. (a) Survival determined during chronological ageing of *S. cerevisiae* cells. 2 mM SPD was added to medium at day 3, and the number of colony-forming units (CFUs) at day 3 was set to be 100%. Abbreviations: DT, D452-2 $\Delta TPO1$; TOS3, D452-2 $\Delta TPO1 \Delta OAZ1$ overexpressing *SPE3*. (b) Profiles of ethanol productivities during the repeated-batch fermentation experiments using the YSCD (100 g/L glucose) media. Ethanol productivity was calculated when more than 93% of glucose was consumed at each condition. Results are the mean of duplicate experiments and error bars indicate s.d..

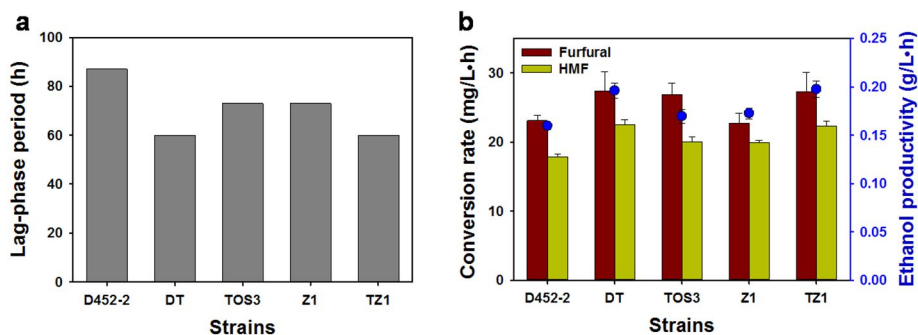


Fig. 4.2. Comparison of fermentation parameters by *S. cerevisiae* D452-2, DT, TOS3, Z1, and TZ1 strains in the YSCD (50 g/L glucose) medium containing 2 g/L furfural and HMF. (a) Lag-phase periods. (b) Furfural and HMF conversion rates and ethanol productivities. Results are the mean of duplicate experiments and error bars indicate s.d..

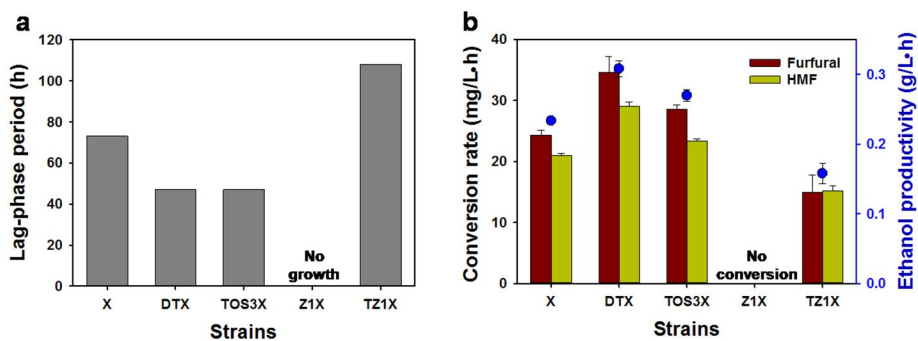


Fig. 4.3. Comparison of fermentation parameters by *S. cerevisiae* X, DTX, TOS3X, Z1X, and TZ1X strains in the YSCDX (70 g/L glucose and 40 g/L xylose) medium containing 2 g/L furfural and HMF. (a) Lag-phase periods. (b) Furfural and HMF conversion rates and ethanol productivities. Results are the mean of duplicate experiments and error bars indicate s.d..

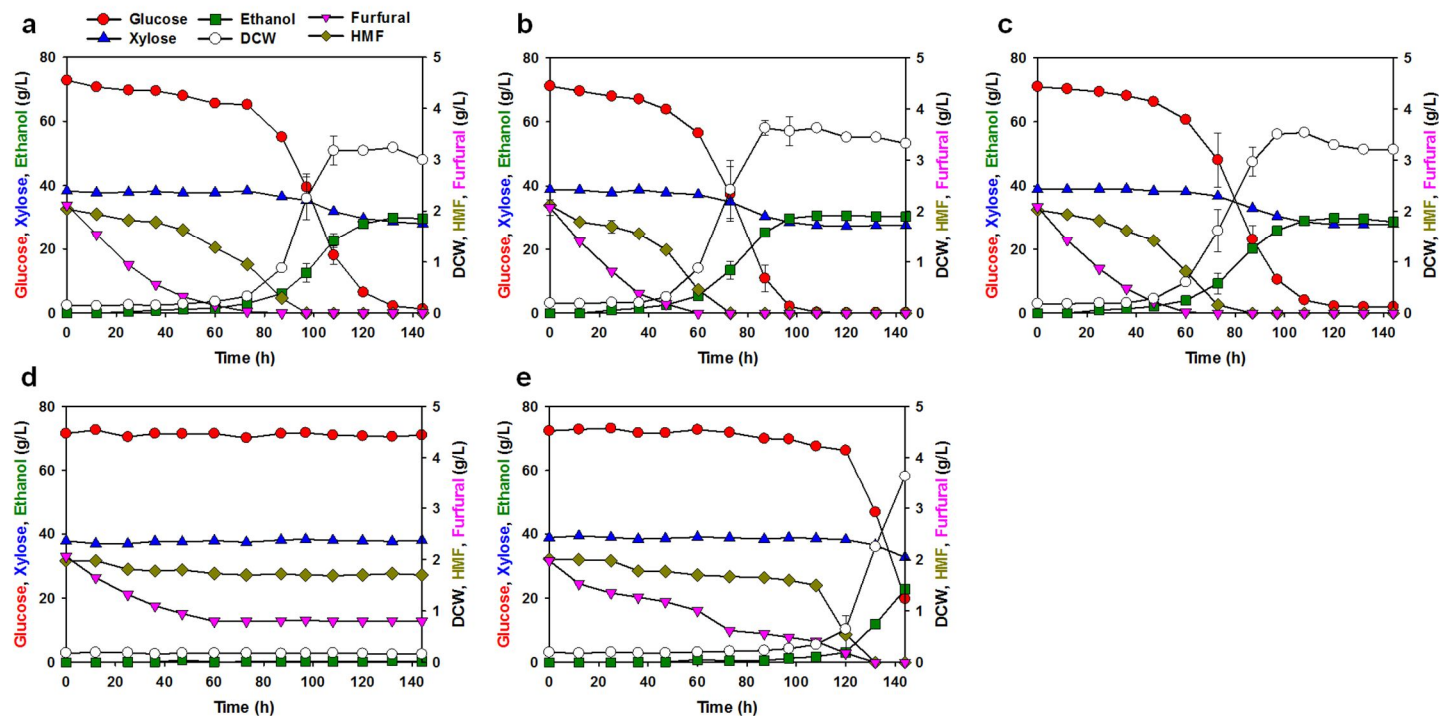


Fig. 4.4. Batch fermentation of *S. cerevisiae* X (a), DTX (b), TOS3X (c), Z1X (d), and TZ1X (e) strains in the YSCDX (70 g/L glucose and 40 g/L xylose) medium containing 2 g/L furfural and HMF. Results are the mean of duplicate experiments and error bars indicate s.d..

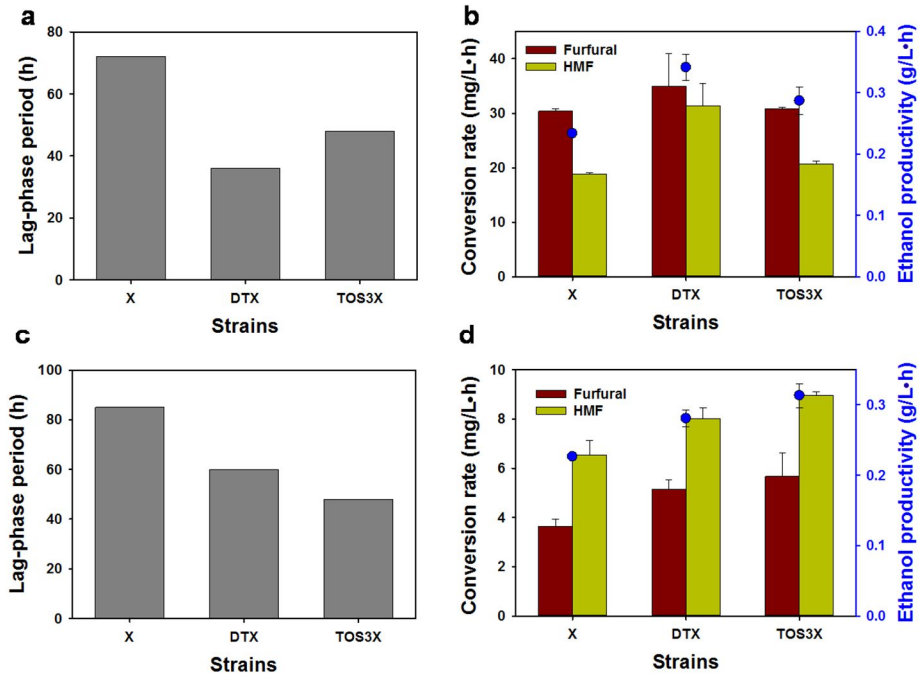


Fig. 4.5. Comparison of fermentation parameters by *S. cerevisiae* X, DTX, and TOS3X strains in simulated hydrolysates containing high concentration of furan derivatives (1 g/L acetic acid, 2 g/L furfural, and 2 g/L HMF) (a and b) and acetic acid (3 g/L acetic acid, 0.4 g/L furfural and 0.8 g/L HMF) (c and d). (a and c) Lag-phase periods. (b and d) Furfural and HMF conversion rates and ethanol productivities. Results are the mean of duplicate experiments and error bars indicate s.d..

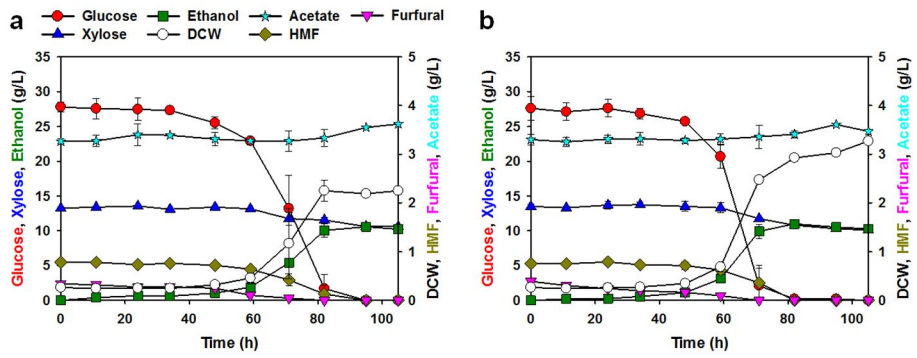


Fig. 4.6. Batch fermentation of *S. cerevisiae* X (a) and TOS3X (b) strains in corn stover hydrolysate. Results are the mean of duplicate experiments and error bars indicate s.d..

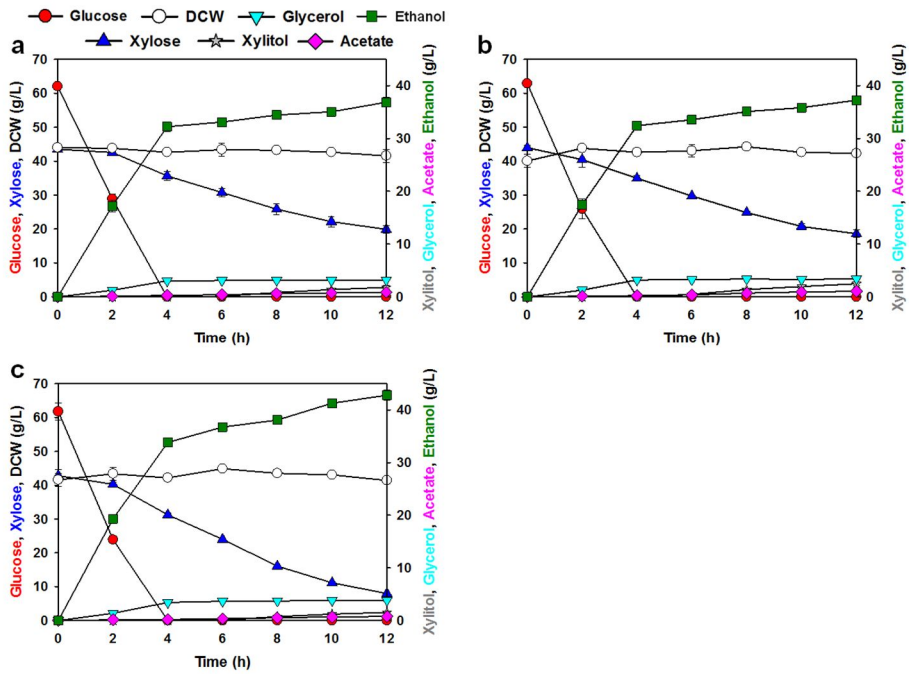


Fig. 4.7. Comparison of *S. cerevisiae* X without (a) and with (b) 2 mM SPD supplementation and the TOS3X strain (c) in the second cycle of the repeated-batch fermentation. Results are the mean of duplicate experiments and error bars indicate s.d..

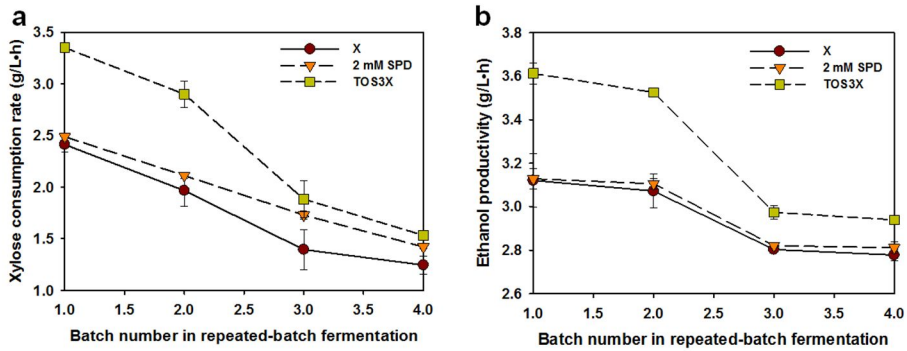


Fig. 4.8. Comparison of fermentation parameters by *S. cerevisiae* X strain with and without 2 mM SPD supplementation and the TOS3X strain during the repeated-batch fermentation experiments using the YSCDX (65 g/L glucose and 40 g/L xylose) media. (a) Xylose consumption rates. Abbreviations: X, D452-2 overexpressing *XYL1,2,3*; TOS3X, D452-2 $\Delta TPO1\Delta OAZ1$ overexpressing *XYL1,2,3*. (b) Ethanol productivities. All parameters were calculated at 12 h. Results are the mean of duplicate experiments and error bars indicate s.d..

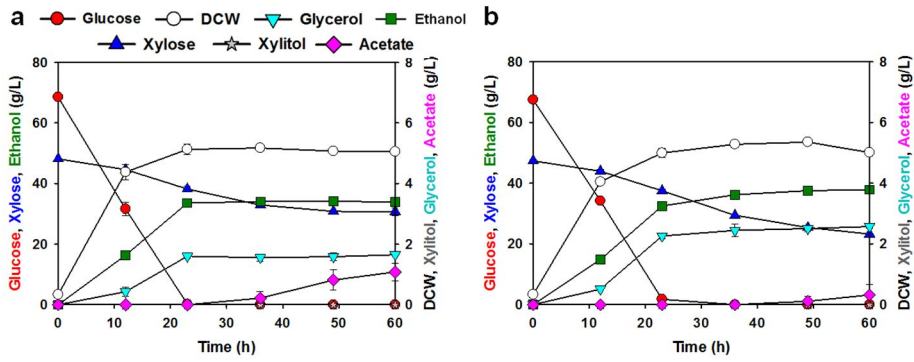


Fig. 4.9. Batch fermentation of *S. cerevisiae* X (a) and TOS3X (b) strains in the YSCDX (70 g/L glucose and 40 g/L xylose) medium. An initial cell density was adjusted to 0.3 g/l. Results are the mean of duplicate experiments and error bars indicate s.d..

Chapter 5

Production of spermidine in engineered

Saccharomyces cerevisiae

5.1. Summary

Spermidine has been known to promote human hair growth. In addition, spermidine may be helpful for treating type 2 diabetes and preventing skin aging. Therefore, construction of a spermidine production system using *S. cerevisiae* has a potential for economic applications. The endogenous *SPE1*, *SPE2*, and *SPE3* genes involved in the polyamine biosynthetic pathway were overexpressed to produce spermidine in *S. cerevisiae*. Also, *OAZ1* encoding ornithine decarboxylase (ODC) antizyme was disrupted to increase spermidine production further through alleviation of feedback inhibition on ODC. To export intracellular spermidine into culture medium, *TPO1* encoding the polyamine transporter protein was overexpressed using a multi-copy vector. As a result, the resulting strain (OS123/pTPO1) produced 63.6 mg/L spermidine with a yield of 1.3 mg spermidine/g glucose. In addition, genetic perturbations for spermidine overproduction were introduced into xylose-fermenting SR8 strain. In a glucose limited fed-batch fermentation, the resulting strain (SR8 OS123/pTPO1) consumed 37.4 g/L xylose and produced 224 mg/L spermidine with a yield of 2.2 mg spermidine/g sugars.

5.2. Introduction

Spermidine (SPD) has been considered as a mediator of key cellular functions including proliferation and differentiation (Pegg and Mccann, 1982; Vuohelainen et al., 2010). SPD also stabilizes DNA, RNA, and various kinds of proteins (Ballas et al., 1983; Oredsson, 2003). In recent years, SPD has been used to combat skin ageing, stimulate human hair growth, treat type 2 diabetes, and increase fruit shelf life (Nambeesan et al., 2010; Pichiah et al., 2011; Ramot et al., 2011; Rinaldi et al., 2005). Regarding the safety and sustainability issue, biological production of SPD has gained an interest from academia and industries. While biological production of putrescine, a precursor of SPD, was investigated using recombinant *Escherichia coli*, any attempts for microbial production of SPD has not been reported yet (Qian et al., 2009). In the chapter 2, the concentration of SPD in *Saccharomyces cerevisiae* was 5.5-fold higher than that of putrescine. Therefore, construction of a SPD production system using *S. cerevisiae*, a GRAS (Generally Recognized as Safe) microorganism, has a potential for economic uses. In order to facilitate the enhanced production of SPD, the endogenous *SPE1*, *SPE2*, and *SPE3* genes involved in the polyamine biosynthetic pathway were overexpressed to increase polyamine contents (Fig. 5.1). Also, the gene involved in feedback inhibition (*OAZI*) was disrupted to increase SPD titer further.

To export intracellular spermidine into culture medium, *TPO1* encoding polyamine transporter protein was overexpressed using a multi-copy vector. The activity of H⁺ antiporter is dependent on the presence of H⁺ gradient across the plasma membrane (Papouskova and Sychrova, 2007). Therefore, pH of culture medium was optimized in terms of TPO1 activity and cell growth. However, it was found that SPD production was repressed by the presence of glucose. To circumvent this problem, the feasibility of efficient SPD production from xylose was explored.

5.3. Materials and methods

5.3.1. Strains and plasmids

Escherichia coli TOP10 (Invitrogen, Carlsbad, CA, USA) was used for plasmid construction. *S. cerevisiae* D452-2 (*MAT α* , *leu2*, *his3*, *ura3*, and *can1*), OS123 (Kim et al., 2015), and SR8 (Kim et al., 2013) strains were used for constructing spermidine overproducing strains. Strains and plasmids used in this work are described in Table 5.1.

5.3.2. Genetic manipulation

The gene encoding polyamine transporter protein (TPO1) was PCR-amplified from genomic DNA of *S. cerevisiae* D452-2 using TPO1[F] (5'-GGACTAGTAAAATGTCGGATCATTCTCCCATTTC-3') and TPO1[R] (5'-CCGCTCGAGTTAAGCGGCGTAAGCATACTTG-3') primers. After digestion of the PCR product with *SpeI* and *XhoI* restriction enzymes, the nucleotides were ligated with plasmid p423GPD (Christianson et al., 1992), resulting in the construction of plasmid p423GPD-TPO1. The *TPO1* expression cassette consisting of *GPD_P-TPO1-CYC1_T* was PCR-amplified from p423GPD-TPO1 plasmid using GPDp[F] and CYC1t_1[R] primers from the previous study (Kim et al., 2015). After digestion of the PCR product with

*Bam*HI and *Not*I restriction enzymes, the *TPO1* expression cassette was ligated with plasmid p42K (Christianson et al., 1992), resulting in the construction of plasmid pTPO1. The gene encoding T52E mutant of TPO1 (mTPO1) was synthesized from IDT Inc. and then cloned into plasmid p42K as described above.

The truncated *OAZ1* gene was obtained by PCR-amplified from genomic DNA of *S. cerevisiae* D452-2 using d_OAZ1[F] (5'-ATAAG-AATGCGGCCGCATCTCAATTCATATTAGATTACAATGTTC-3') and d_OAZ1[R] (5'-CGCGGATCCCCTACTATTCAGTAAAGATGG-TAATAC-3') primers. The 300 bp-size DNA fragment was cut with *Not*I and *Bam*HI, and combined with pRS404 plasmid, resulting in plasmid p404_d_OAZ1 construction. The *OAZ1* disruption was confirmed by the PCR using two primers of ch_OAZ1[F] (5'-CTTTCTACGTATAGTTTGGCTAGTGGGG-3') and ch_pRS404[R] (5'-CATTTCAGGCTG-CGCAACTGTTG-3').

Transformation of cassettes for overexpressing *TPO1*, *mTPO1*, *SPE1*, *SPE2*, and *SPE3* and disrupting *OAZ1* was performed using the yeast EZ-Transformation kit (BIO 101, Vista, CA). Transformants were selected on YSC medium (6.7 g/L yeast nitrogen without amino acids and 2.0 g/L synthetic complete supplement mixture)

Transformants were selected on YP medium containing 20 g/L glucose

with 200 mg/L G418.

5.3.3. Culture conditions and fermentation experiments

E. coli was grown in LB medium (5 g/L yeast extract, 10 g/L bacto tryptone, and 10 g/L NaCl) with 50 µg/ml of ampicillin for genetic manipulation. *S. cerevisiae* strains were pre-cultured at 30°C and 250 rpm for 24 h in YPD medium (10 g/L yeast extract, 20 g/L bacto peptone, and 20 g/L glucose) containing 200 mg/L G418. YP medium containing appropriate amount of sugars with 200 or 400 mg/L G418 was used for fermentation experiments, and medium pH was adjusted by 5 N HCl and 2 N NaOH.

For SPD production, pre-cultured cells from YP medium with 20 g/L glucose were harvested and inoculated into main cultures with initial optical density (OD₆₀₀) of 1.0. Fermentation experiments in a test tube scale were performed at 30°C and 300 rpm in 5 ml YP medium containing 50 g/L glucose with 200 mg/L G418. Flask fermentation experiments were performed at 30°C and 300 or 80 rpm in 50 ml YP medium containing 50 g/L glucose or xylose with 200 or 400 mg/L G418.

A fed-batch fermentation was carried out in a bench-top fermentor (Bioengineering AG, Wald, Switzerland) with 1 L of YP medium

containing 85 g/L xylose and 20 g/L glucose. Initial cell density was adjusted to OD₆₀₀ of 10.0, and fermentation was performed at 200 rpm, and 0.2 vvm of air supply. After the depletion of glucose added initially, 600 g/L glucose solution was fed at a rate from 1.8 g/h to 0.3 g/h. Medium acidity and temperature were maintained at pH 2.4 and 30°C.

5.3.4. Analytical Methods

Optical density was measured with a spectrophotometer (RF5301, Shimadzu, Kyoto, Japan) at 600 nm. Glucose, xylose, and ethanol concentrations were determined by high performance liquid chromatography (HPLC, Agilent Technologies 1200 Series) using a REZEX ROA organic acid column (Phenomenex, Torrance, USA). The column was eluted with 5 mM H₂SO₄ at a flow rate of 0.6 ml/min at 60°C, and detection was made with a reflective index detector. In order to measure concentrations of polyamines (SPD, putrescien, and spermine), the culture broth was centrifuged at 13,000 rpm for 10 min, and then 190 µl of the supernatant was mixed with 10 µl of 1,7-diaminopentane as the internal standard (IS). For the derivatization, 200 µl of dansyl chloride reagent (5 mg/ml) dissolved in acetone and 100 µl of saturated NaHCO₃ solution were added to a 200 µl of sample solution containing IS. After the reaction mixture was incubated at 40°C for 1 h with occasional shaking, the sample was extracted with 1

ml of diethyl ether. The extract was dried under nitrogen flow and the residue was re-dissolved in 200 μ l of acetonitrile. The concentrations of polyamines were determined using an HPLC system equipped with a CAPCELL PAK C18 MG column (Shiseido, Tokyo, Japan) according to the method described previously (Innocente et al., 2007; Moret and Conte, 1996). The intracellular concentrations of polyamines were determined as described in the previous report (Kim et al., 2015).

5.4. Results

5.4.1. Construction of engineered *S. cerevisiae* producing spermidine

In the Chapter 3, among the engineered *S. cerevisiae* strains, the OS123 strain (Table 5.1) showed the highest intracellular spermidine (SPD) content of 6.46 mg SPD/g cell, which was 15.5-fold higher than that of the control strain. Therefore, the OS123 strain was used to efficiently produce SPD extracellularly. While production of SPD was not detected in the control D452-2 strain, the OS123 strain produced 0.61 mg/L SPD in culture medium (Fig. 5.2). Overexpression of *TPO1* encoding the polyamine transporter protein could improve SPD production further. Therefore, the *TPO1* expression cassette was constructed under the control of a strong and constitutive promoter (*GPD_p*) and cloned into p42K multi-copy plasmid. The resulting vector (pTPO1) was transformed to *S. cerevisiae* D452-2 and OS123 strains. As expected, overexpression of the *TPO1* gene in the OS123 strain (OS123/pTPO1) resulted in 191% higher SPD titer than that of the control strain (OS123/p42K) (Fig. 5.2). However, when *TPO1* was overexpressed in *S. cerevisiae* D452-2, the resulting strain (D452-2/pTPO1) could not excrete SPD at all into culture medium.

5.4.2. Optimization of fermentation conditions for improving spermidine production

It was observed that the function of TPO1 in the OS123 strain plays an important role in producing SPD. Nevertheless, SPD titer is not high enough for economic uses. Therefore, optimization of fermentation conditions including medium pH, aeration, and G418 concentration was done. It was speculated that activity of TPO1 protein might be dependent on the medium pH as reported as another H⁺ antiporter (Papouskova and Sychrova, 2007). To this end, fermentations were performed at various pH conditions (pH 2.4, 3.4, 4.4, 5.7, and 6.5). While growth patterns of the OS123/pTPO1 strain under pH 3.4 ~ 6.5 were similar, cell growth was somewhat inhibited at pH 2.4 (Fig. 5.3). However, SPD production increased as medium pH decreased, and the highest SPD concentration of 20.2 mg/L was observed at pH 2.4 (Fig. 5.4). To confirm that the activity of TPO1 protein is responsible for pH dependent SPD production, fermentations of D452-2/p42K, D452-2/pTPO1, OS123/p42K, and OS123/pTPO1 strains were performed at pH 2.4. At this fermentation condition, introduction of a multi-copy plasmid for *TPO1* overexpression enabled the D452-2 control strain to produce SPD in culture medium (Fig. 5.5). Overexpression of the *TPO1* gene in the OS123 strain (OS123/pTPO1) also resulted in

20.2 mg/L SPD titer, which was 122% higher than that of the control strain (OS123/p42K). These results indicated that the activity of TPO1 is dependent on H⁺ gradient across the plasma membrane, and hence an acidic pH condition is favorable for SPD production.

As a preliminary experiment, batch fermentations were performed under 80 rpm and 300 rpm conditions with initial pH of 2.4. Interestingly, while accumulation patterns of ethanol, glycerol, and acetate were almost identical, the OS123/pTPO1 strain produced 37.1 mg/L SPD under 80 rpm condition, which was 84% higher than that of the strain under 300 rpm condition (Fig. 5.6). A quantitative relationship between the oxygen supply and SPD production will be determined in a bioreactor scale.

However, produced SPD was taken up by *S. cerevisiae* cells after 24 h. A previous study showed that *S. cerevisiae* takes up SPD by using several polyamine transporters including DUR3 and SAM3 (Uemura et al., 2007). In order to overcome this problem, 400 mg/L G418 was supplemented to YP medium instead of 200 mg/L. It was hypothesized that high G418 concentration might increase pTPO1 stability and hence enable the OS123/pTPO1 strain to excrete SPD into culture medium continuously. As expected, the OS123 strain produced 63.6 mg/L SPD in YP medium containing 400 mg/L G418, which was 71% higher than

that of the strain in 200 mg/L G418 (Fig. 5.6). Also, produced SPD maintained until end of the fermentation. In conclusion, maximum SPD titer increased from 20.2 mg/L to 63.6 mg/L through optimization of fermentation condition including medium pH, aeration, and G418 concentration.

In the optimized fermentation condition for SPD production (pH 2.4, 90 rpm, and 400 mg/L G418), intracellular levels of SPD, spermine, and putrescine in D452-2/p42K, D452-2/pTPO1, OS123/p42K, and OS123/pTPO1 strains were measured. While an intracellular SPD level of the D452-2/p42K strain was 60% higher than that of the D452-2/pTPO1 strain, OS123/p42K and OS123/pTPO1 strains showed almost identical SPD contents (Fig. 5.7). These results indicated that the TPO1 activity was not high enough to excrete all of the intracellular SPD in the OS123 strain because this strain highly accumulated SPD in the cells. Nevertheless, overexpression of the *TPO1* gene in the OS123 strain improved SPD production, confirming that the rate-limiting step in SPD production was SPD excretion by TPO1.

5.4.3. Spermidine production from xylose by the SR8 strain with the spermidine overproduction pathway

When glucose was used as a carbon source for SPD production, it was consistently observed that SPD production occurred after glucose depletion (Fig. 5.3 and Fig. 5.6). To solve this problem, it was sought to use xylose as another carbon source. The xylose-fermenting SR8 strain was constructed previously by rational and evolutionary approaches (Kim et al., 2013). A quadruple auxotrophic mutant of the SR8 strain (SR8 -4) was kindly donated by Prof. Yong-Su Jin at University of Illinois at Urbana-Champaign. Using the SR8 -4 strain as a host cell, the SR8 OS123 strain (*OAZI* disrupted SR8 strain overexpressing *SPE1*, *SPE2*, and *SPE3* genes) was constructed. Also, multi-copy plasmid for *TPO1* overexpression was introduced to the SR8 OS123 strain (SR8 OS123/pTPO1). To compare SPD production between glucose and xylose, fermentation of SR8 OS123/pTPO1 strain was performed in the optimized fermentation condition (pH 2.4, 90 rpm, and 400 mg/L G418) using 50 g/L xylose as a carbon source. Although the SR8 OS123/pTPO1 strain only consumed 14.2 g/L xylose in 72 h because xylose assimilation enzymes severely affected by pH (Webb and Lee, 1992), the SR8 OS123/pTPO1 strain produced 56.4 mg/L SPD (Fig. 5.8). Therefore, SPD production yield from xylose

(4.0 mg SPD/g xylose) was 3.1-fold higher than that from glucose obtained in Fig. 5.6c. In addition to SPD, production of other polyamines (putrescine and spermine) by OS123/pTPO1 and SR8 OS123/pTPO1 strains were measured. While these strains excreted putrescine into culture medium approximately at a half of the amount of SPD, spermine was not detected at all in the medium (Fig. 5.9).

Low concentrations of glucose are known to improve xylose fermentation by regenerating NAD(P)H and enhancing xylose uptake (Krahulec et al., 2010; Lee et al., 2000). Therefore, in order to maximize SPD production from xylose, a glucose limited fed-batch fermentation using the SR8 OS123/pTPO1 strain was designed. Glucose was constantly fed at the rate from 1.8 g/h to 0.3 g/h after depletion of glucose initially added. The fed-batch fermentation resulted in consumption of 37.4 g/L xylose and production of 224 mg/L SPD in 61 h with a yield of 2.2 mg spermidine/g sugars (Fig. 5.10). In this fermentation condition, while the SR8 OS123/pTPO1 strain produced 37.0 mg/L putrescine, spermine was also not detected at all.

5.5. Discussion

In this chapter, SPD successfully produced by overexpressing the *TPO1* gene in the OS123 strain (OS123/pTPO1). Also, optimization of fermentation conditions was conducted to improve SPD titer further. It was clearly shown that SPD production was strongly dependent on TPO1 activity. TPO1 is known to take up SPD at alkaline pH and catalyze SPD excretion at acidic pH. However, it was observed that TPO1 activity was still not high enough to excrete all of the intracellular SPD in the OS123 strain (Fig. 5.7). Therefore, to achieve higher TPO1 activity, the T52E mutant of TPO1 (mTPO1) was introduced to the OS123 strain (OS123/pmTPO1). It was reported that mTPO1 exhibited approximately 60% higher SPD uptake activity than that of the wild type TPO1 at alkaline pH (Uemura et al., 2005). However, this strain rather produced 50% lower SPD than that of the OS123/pTPO1 strain (Fig. 5.11), possibly because higher activity of mTPO1 was only proven at alkaline pH. Thus substitution of TPO1 was not pursued further.

A previous study has shown that intracellular levels of putrescine in D452-2 and OS123 strains were 4.2-fold and 17.1-fold higher than that of the spermine in minimal medium. In contrast to this result, while intracellular contents of putrescine were not detected at all in these

strains (Fig. 5.7), high amount of putrescine (~ 30 mg/L) was excreted into culture medium (Fig. 5.9). Therefore, it was speculated that *S. cerevisiae* strains excreted intracellular putrescine into culture medium at acidic pH condition (pH 2.4).

Also, a previous study reported that enzymes involved in the arginine and methionine biosynthetic pathways, which are the precursors for SPD production, were expressed at higher levels in anaerobic condition (de Groot et al., 2007). These results are in agreement with the results showing that the OS123/pTPO1 strain produced 37.1 mg/L SPD under 80 rpm condition, which was 84% higher than that of the strains under 300 rpm condition.

In batch fermentations for SPD production from glucose, it was consistently observed that SPD production increased at low concentration of glucose or after glucose depletion. *FMS1* encoding one of the SPD metabolic enzymes has been reported to be completely repressed by the presence of glucose (White et al., 2001). Therefore, it was postulated that SPD related genes coding for enzymes involved in the SPD biosynthetic pathway were also repressed by the presence of glucose. To circumvent this problem, xylose was used as a carbon source to achieve high yield of SPD production.

Table 5.1. *S. cerevisiae* strains and plasmids used in Chapter 5

Name	Description	Reference
Strains		
D452-2	<i>MATα</i> , <i>leu2</i> , <i>his3</i> , <i>ura3</i> , and <i>can1</i>	(Hosaka et al., 1992)
OS123	D452-2 Δ <i>OAZ1</i> overexpressing <i>SPE1,2,3</i>	(Kim et al., 2015)
D452-2/p42K	D452-2 transformed with pRS42K	This study
D452-2/pTPO1	D452-2 transformed with pTPO1	This study
OS123/p42K	OS123 transformed with pRS42K	This study
OS123/pTPO1	OS123 transformed with pTPO1	This study
SR8	D452-2 Δ <i>ALD6</i> overexpressing multicopy <i>XYL1,2,3</i> evolved on xylose	(Kim et al., 2013)
SR8 -4	SR8 <i>ura3</i> , <i>trp1</i> , <i>leu2</i> , and <i>his3</i>	Prof. Yong-Su Jin
SR8 OS123	SR8 Δ <i>OAZ1</i> overexpressing <i>SPE1,2,3</i>	This study
SR8 OS123/pTPO1	SR8 OS123 transformed with pTPO1	This study

(be continued)

Name	Description	Reference
Plasmids		
p423GPD	<i>HIS3</i> , <i>GPD</i> promoter, <i>CYCI</i> terminator, a multicopy plasmid	(Christianson et al., 1992)
p42K	<i>KanMX</i> resistance, a multicopy plasmid	(Christianson et al., 1992)
pRS404	<i>TRP1</i> , an integrative plasmid	(Sikorski and Hieter, 1989)
pTPO1	<i>TPO1</i> under the control of <i>GPD</i> promoter in pRS42K	This study
pmTPO1	<i>mTPO1</i> (T52E) under the control of <i>GPD</i> promoter in pRS42K	This study
p404_d_OAZ1	pRS404 with 300 bp of the truncated <i>S. cerevisiae OAZ1</i> gene	This study

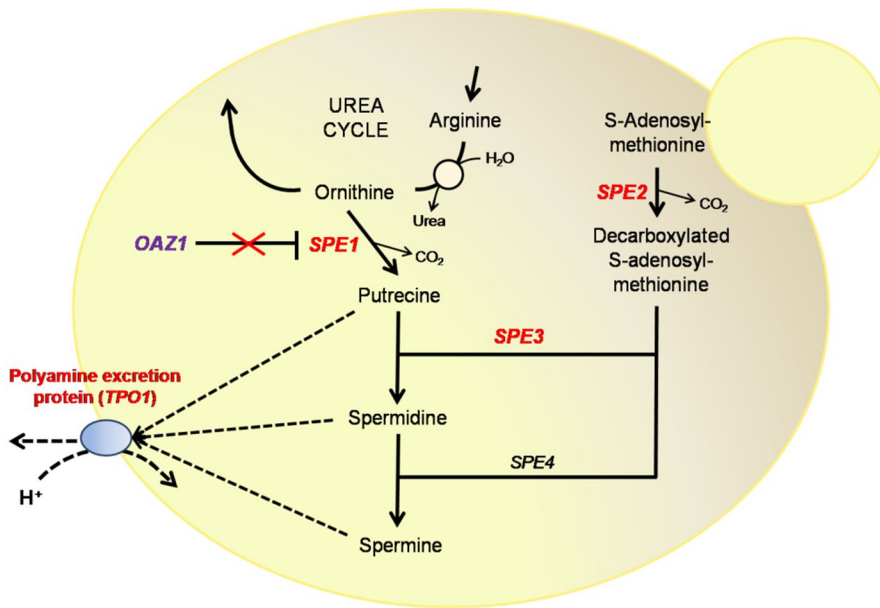


Fig. 5.1. Strategy for production of SPD in culture medium by engineered *S. cerevisiae*. Fluxes in the SPD biosynthetic pathway were amplified by overexpressing ornithine decarboxylase (ODC, *SPE1*), *S*-adenosylmethionine decarboxylase (*SPE2*), and spermidine synthase (*SPE3*). For alleviation of the feedback inhibition on ODC, *OAZ1* coding for ODC antizyme was disrupted. As a polyamine transporter (Tpo1p) located in *S. cerevisiae* plasma membrane was overexpressed in order to excrete intracellular SPD to the medium.

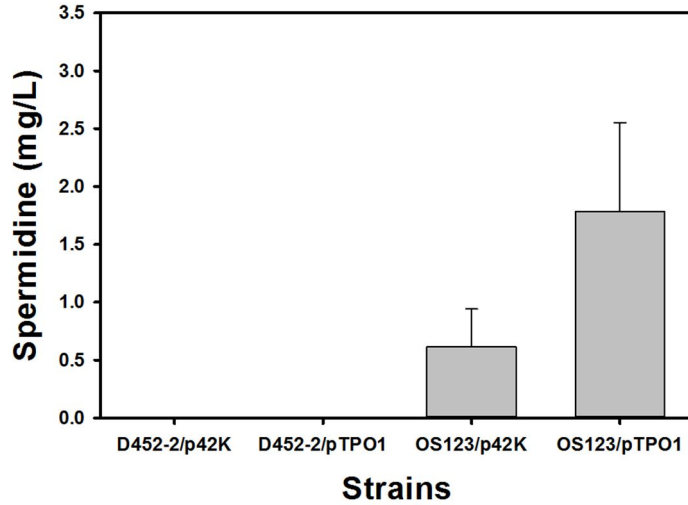


Fig. 5.2. Comparison of SPD production by *S. cerevisiae* D452-2/p42K, D452-2/pTPO1, OS123/p42K, and OS123/pTPO1 strains. SPD concentrations were measured after 24 h cultivation at 30°C and 300 rpm in 5 ml YP medium containing 50 g/L glucose with 200 mg/L G418. Abbreviations: OS123, D452-2 $\Delta OAZ1$ overexpressing *SPE1,2,3*; pTPO1, a vector for overexpressing *TPO1* under the control of *GPD* promoter in p42K. Results are the mean of triplicate experiments and error bars indicate s.d..

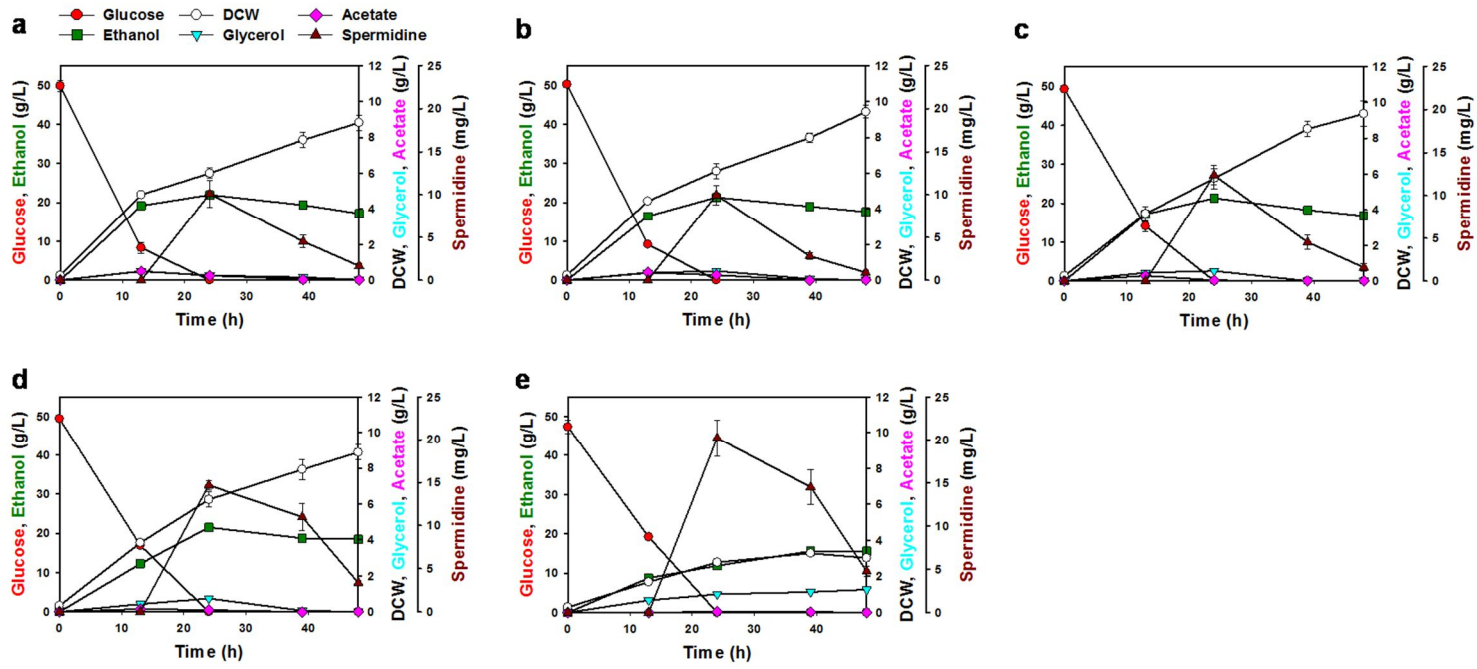


Fig. 5.3. Batch fermentation of *S. cerevisiae* OS123/pTPO1 strain in 50 ml YP medium containing 50 g/L glucose with 200 mg/L G418 at 30°C and 300 rpm under various pH conditions. (a) pH 6.5, (b) pH 5.7, (c) pH 4.4, (d) pH 3.4, (e) pH 2.4. Results are the mean of duplicate experiments and error bars indicate s.d..

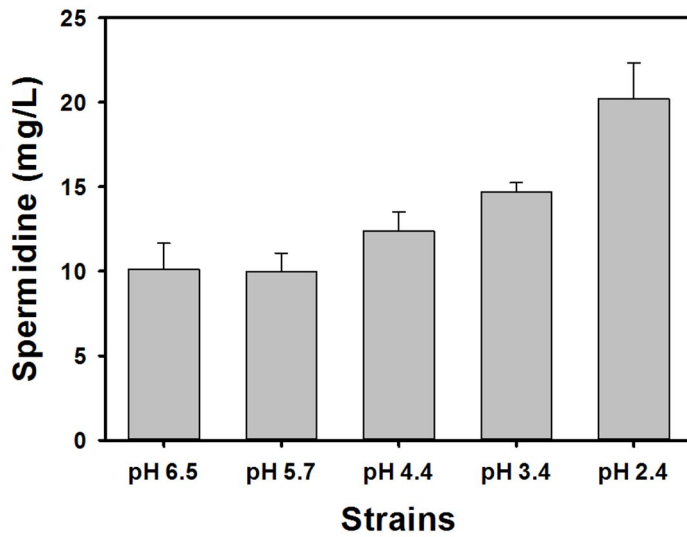


Fig. 5.4. Comparison of SPD production by *S. cerevisiae* OS123/pTPO1 strain under various pH conditions. SPD concentrations were measured after 24 h cultivation at 30°C and 300 rpm in 50 ml YP medium containing 50 g/L glucose with 200 mg/L G418. (a) pH 6.5, (b) pH 5.7, (c) pH 4.4, (d) pH 3.4, (e) pH 2.4. Results are the mean of duplicate experiments and error bars indicate s.d..

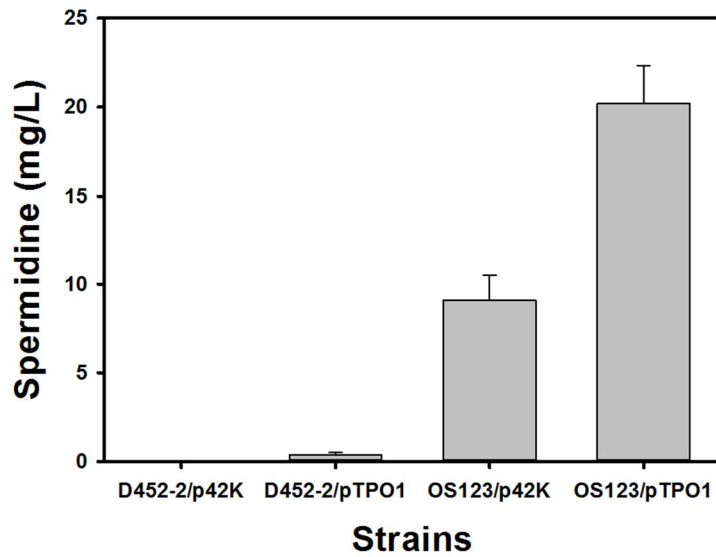


Fig. 5.5. Comparison of SPD production by *S. cerevisiae* D452-2/p42K, D452-2/pTPO1, OS123/p42K, and OS123/pTPO1 strains at pH 2.4. SPD concentrations were measured after 24 h cultivation at 30°C and 300 rpm in 50 ml YP medium containing 50 g/L glucose with 200 mg/L G418. Results are the mean of triplicate experiments and error bars indicate s.d..

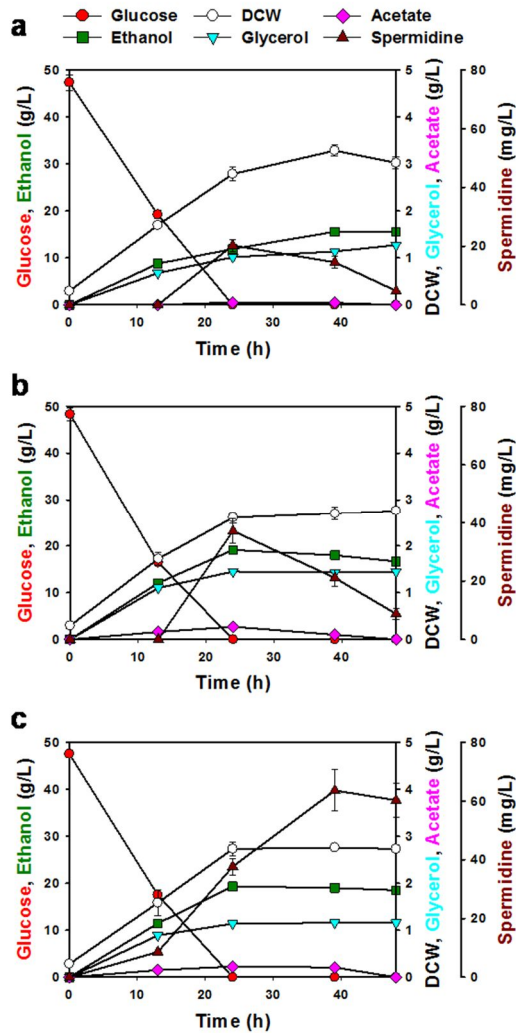


Fig. 5.6. Batch fermentation of *S. cerevisiae* OS123/pTPO1 strain in 50 ml YP medium (pH 2.4) containing 50 g/L glucose under various fermentation conditions. (a) 300 rpm + 200 mg/L G418, (b) 90 rpm + 200 mg/L G418, (c) 90 rpm + 400 mg/L G418. Results are the mean of duplicate experiments and error bars indicate s.d..

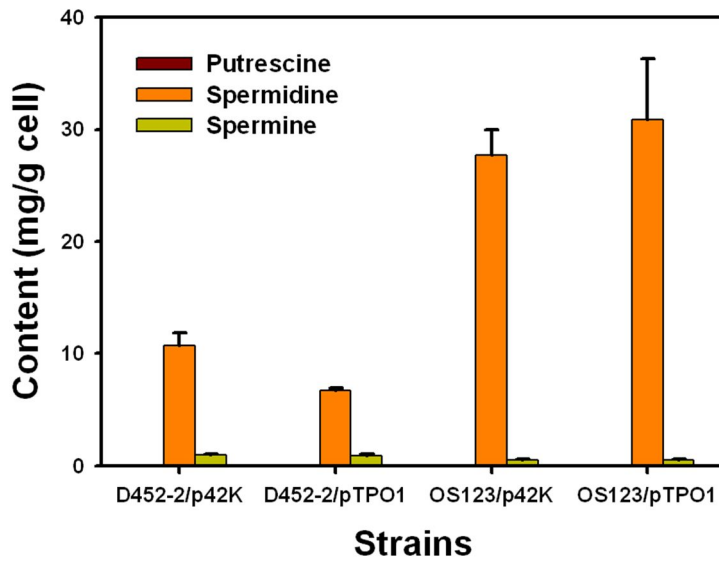


Fig. 5.7. Intracellular levels of polyamines in *S. cerevisiae* D452-2/p42K, D452-2/pTPO1, OS123/p42K, and OS123/pTPO1 strains at pH 2.4. Cells were harvested after 24 h cultivation at 30°C and 90 rpm in 50 ml YP medium (pH 2.4) containing 50 g/L glucose with 400 mg/L G418. Results are the mean of triplicate experiments and error bars indicate s.d..

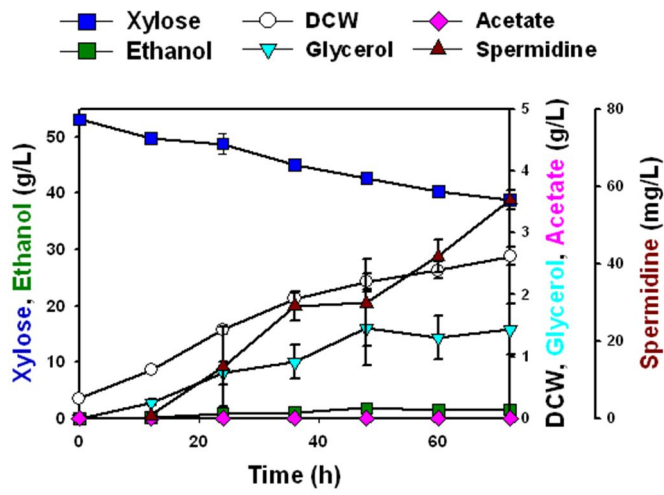


Fig. 5.8. Batch fermentation of *S. cerevisiae* SR8 OS123/pTPO1 strain in 50 ml YP medium (pH 2.4) containing 50 g/L xylose with 400 mg/L G418. Results are the mean of triplicate experiments and error bars indicate s.d..

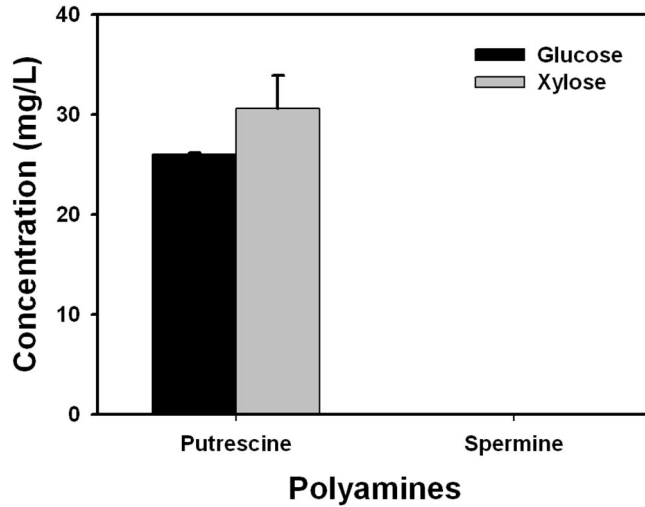


Fig. 5.9. Comparison of maximum putrescine and spermine concentrations obtained from glucose and xylose fermentations. Maximum putrescine and spermine concentrations were calculated from the glucose fermentation by *S. cerevisiae* OS123/pTPO1 strain and xylose fermentation by SR8 OS123/pTPO1 strain in 50 ml YP medium (pH 2.4) containing 50 g/L glucose or xylose with 400 mg/L G418. Results are the mean of duplicate experiments and error bars indicate s.d..

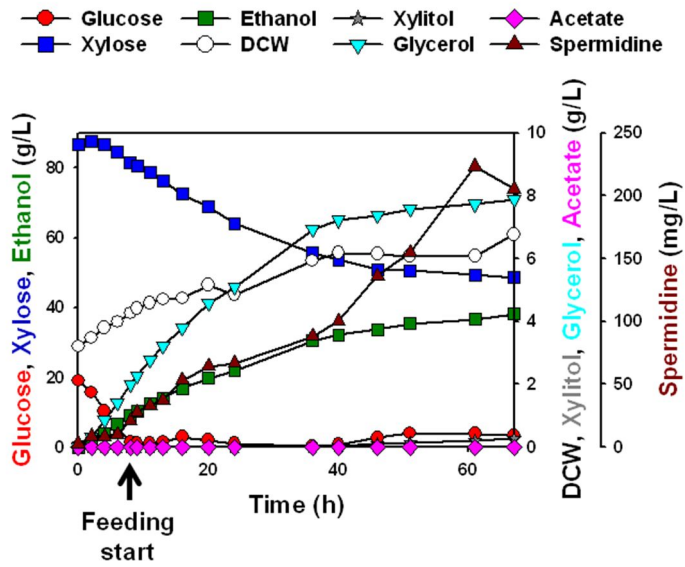


Fig. 5.10. Glucose limited fed-batch fermentation by the SR8 OS123/pTPO1 strain. After depletion of 20 g/L initial glucose, 600 g/L glucose solution was fed into the bioreactor. Medium acidity and temperature were maintained at pH 2.4 and 30°C throughout the cultivation.

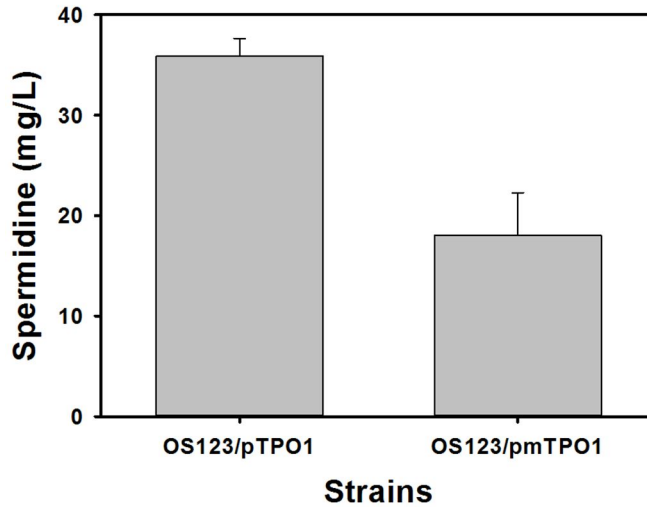


Fig. 5.11. Comparison of SPD production by *S. cerevisiae* OS123/pTPO1 and OS123/pmTPO1 strains. SPD concentrations were measured after 24 h cultivation at 30°C and 90 rpm in 50 ml YP medium (pH 2.4) containing 50 g/L glucose with 200 mg/L G418. Abbreviations: OS123, D452-2 Δ OAZI overexpressing *SPE1,2,3*; pTPO1, a vector for overexpressing *TPO1* under the control of *GPD* promoter in p42K; pmTPO1, a vector for overexpressing *TPO1* mutant (T52E) under the control of *GPD* promoter in p42K. Results are the mean of triplicate experiments and error bars indicate s.d..

Chapter 6

Conclusions

The main objective of this dissertation is construction of robust yeast strains for efficient utilization of lignocellulose hydrolysates. For this purpose, it was shown that spermidine (SPD) functions as a chemical elicitor for enhanced tolerance of *S. cerevisiae* against major fermentation inhibitors. Metabolic engineering for construction of an engineered *S. cerevisiae* strain capable of tolerating toxic levels of the major inhibitors without exogenous addition of SPD was attempted. The endogenous *SPE1*, *SPE2*, and *SPE3* genes involved in the polyamine biosynthetic pathway were overexpressed to produce spermidine in *S. cerevisiae*. Also, *OAZ1* coding for ornithine decarboxylase (ODC) antizyme and *TPO1* coding for the polyamine transport protein were disrupted to increase intracellular SPD levels through alleviation of feedback inhibition on ODC and prevention of SPD excretion, respectively. The constructed engineered yeast strains exhibiting improved tolerance against the major inhibitors including furfural, HMF, and acetic acid. Moreover, differentially expressed genes by chemical and genetic perturbations under furfural conditions were captured, and overexpression of the downregulated genes under furfural conditions can lead to improved tolerance to furfural.

The potential applicability of the *S. cerevisiae* strains with high SPD contents was examined by successfully extending its application to repeated-batch fermentation and xylose utilization in the presence of

fermentation inhibitors. Also, construction of SPD production system using *S. cerevisiae* has huge potential for economic use. It was observed that SPD production yield from xylose (4.0 mg SPD/g xylose) was 3.1-fold higher than that from glucose. In a glucose limited fed-batch fermentation, the SR8 OS123/pTPO1 strain consumed 37.4 g/L xylose and produced 224 mg/L spermidine with a yield of 2.2 mg SPD/g sugars.

References

Agbor, V. B., Cicek, N., Sparling, R., Berlin, A., Levin, D. B., 2011. Biomass pretreatment: fundamentals toward application. *Biotechnol Adv.* 29, 675-685.

Aguilar, R., Ramirez, J. A., Garrote, G., Vazquez, M., 2002. Kinetic study of the acid hydrolysis of sugar cane bagasse. *J Food Eng.* 55, 309-318.

Alarco, A. M., Balan, I., Talibi, D., Mainville, N., Raymond, M., 1997. AP1-mediated multidrug resistance in *Saccharomyces cerevisiae* requires *FLR1* encoding a transporter of the major facilitator superfamily. *J Biol Chem.* 272, 19304-19313.

Allen, S. A., Clark, W., McCaffery, J. M., Cai, Z., Lanctot, A., Slininger, P. J., Liu, Z. L., Gorsich, S. W., 2010. Furfural induces reactive oxygen species accumulation and cellular damage in *Saccharomyces cerevisiae*. *Biotechnol Biofuels.* 3.

Almeida, J. R., Bertilsson, M., Gorwa-Grauslund, M. F., Gorsich, S., Liden, G., 2009. Metabolic effects of furaldehydes and impacts on biotechnological processes. *Appl Microbiol Biotechnol.* 82, 625-638.

Almeida, J. R. M., Modig, T., Petersson, A., Hähn-Hägerdal, B., Lidén, G., Gorwa-Grauslund, M. F., 2007. Increased tolerance and conversion of inhibitors in lignocellulosic hydrolysates by *Saccharomyces cerevisiae*. *J Chem Technol Biotechnol.* 82, 340-349.

Almeida, J. R. M., Roder, A., Modig, T., Laadan, B., Liden, G., Gorwa-Grauslund, M. F., 2008. NADH- vs NADPH-coupled reduction of 5-hydroxymethyl furfural (HMF) and its implications on product distribution in *Saccharomyces cerevisiae*. *Appl Microbiol Biotechnol.* 78, 939-945.

Alriksson, B., Horvath, I. S., Jonsson, L. J., 2010. Overexpression of *Saccharomyces cerevisiae* transcription factor and multidrug resistance genes conveys enhanced resistance to lignocellulose-derived fermentation inhibitors. *Process Biochem.* 45, 264-271.

Argueso, J. L., Carazzolle, M. F., Mieczkowski, P. A., Duarte, F. M., Netto, O. V. C., Missawa, S. K., Galzerani, F., Costa, G. G. L., Vidal, R. O., Noronha, M. F., Dominska, M., Andrietta, M. G. S., Andrietta, S. R., Cunha, A. F., Gomes, L. H., Tavares, F. C. A., Alcarde, A. R., Dietrich, F. S., McCusker, J. H., Petes, T. D., Pereira, G. A. G., 2009. Genome structure of a *Saccharomyces cerevisiae* strain widely used in bioethanol production. *Genome Res.* 19, 2258-2270.

Ask, M., Bettiga, M., Mapelli, V., Olsson, L., 2013. The influence of HMF and furfural on redox-balance and energy-state of xylose-utilizing *Saccharomyces cerevisiae*. *Biotechnol Biofuels.* 6.

Avanasi, R. N., Murthy, G. S., Chaplen, F. W. R., Beatty, C., 2013. Fermentation of glucose/xylose/xylulose in the presence of furfural by yeast for ethanol production. *Biol Eng Trans.* 6, 157-172.

Bai, F. W., Anderson, W. A., Moo-Young, M., 2008. Ethanol fermentation technologies from sugar and starch feedstocks. *Biotechnol*

Adv. 26, 89-105.

Balasundaram, D., Tabor, C. W., Tabor, H., 1991. Spermidine or spermine is essential for the aerobic growth of *Saccharomyces cerevisiae*. Proc Natl Acad Sci USA. 88, 5872-5876.

Balasundaram, D., Tabor, C. W., Tabor, H., 1993. Oxygen toxicity in a polyamine-depleted *spe2*Δ mutant of *Saccharomyces cerevisiae*. Proc Natl Acad Sci USA. 90, 4693-4697.

Balasundaram, D., Tabor, C. W., Tabor, H., 1996. Sensitivity of polyamine-deficient *Saccharomyces cerevisiae* to elevated temperatures. J Bacteriol. 178, 2721-2724.

Balasundaram, D., Tabor, C. W., Tabor, H., 1999. Sensitivity of spermidine-deficient *Saccharomyces cerevisiae* to paromomycin. Antimicrob Agents Ch. 43, 1314-1316.

Ballas, S. K., Mohandas, N., Marton, L. J., Shohet, S. B., 1983. Stabilization of Erythrocyte Membranes by Polyamines. Proc Natl Acad Sci USA. 80, 1942-1946.

Banerjee, N., Bhatnagar, R., Viswanathan, L., 1981. Inhibition of glycolysis by furfural in *Saccharomyces cerevisiae*. European J Appl Microbiol Biotechnol. 11, 226-228.

Behera, S., Mohanty, R. C., Ray, R. C., 2011. Ethanol production from mahula (*Madhuca latifolia* L.) flowers with immobilized cells of *Saccharomyces cerevisiae* in *Luffa cylindrica* L. sponge discs. Appl Energ. 88, 212-215.

Bouchereau, A., Aziz, A., Larher, F., Martin-Tanguy, J., 1999. Polyamines and environmental challenges: recent development. *Plant Sci.* 140, 103-125.

Burtner, C. R., Murakami, C. J., Kennedy, B. K., Kaeberlein, M., 2009. A molecular mechanism of chronological aging in yeast. *Cell Cycle.* 8, 1256-1270.

Carmel-Harel, O., Storz, G., 2000. Roles of the glutathione- and thioredoxin-dependent reduction systems in the *Escherichia coli* and *Saccharomyces cerevisiae* responses to oxidative stress. *Annu Rev Microbiol.* 54, 439-461.

Casero, R. A., Marton, L. J., 2007. Targeting polyamine metabolism and function in cancer and other hyperproliferative diseases. *Nat Rev Drug Discov.* 6, 373-390.

Chattopadhyay, M. K., Park, M. H., Tabor, H., 2008. Hypusine modification for growth is the major function of spermidine in *Saccharomyces cerevisiae* polyamine auxotrophs grown in limiting spermidine. *Proc Natl Acad Sci USA.* 105, 6554-6559.

Childs, A. C., Mehta, D. J., Gerner, E. W., 2003. Polyamine-dependent gene expression. *Cell Mol Life Sci.* 60, 1394-1406.

Christianson, T. W., Sikorski, R. S., Dante, M., Shero, J. H., Hieter, P., 1992. Multifunctional yeast high-copy-number shuttle vectors. *Gene.* 110, 119-122.

Chung, I. S., Lee, Y. Y., 1985. Ethanol fermentation of crude acid

hydrolyzate of cellulose using high-level yeast inocula. *Biotechnol Bioeng.* 27, 308-315.

Cohn, M. S., Tabor, C. W., Tabor, H., 1978. Isolation and characterization of *Saccharomyces cerevisiae* mutants deficient in S-adenosylmethionine decarboxylase, spermidine, and spermine. *J Bacteriol.* 134, 208-213.

de Groot, M. J. L., Daran-Lapujade, P., van Breukelen, B., Knijnenburg, T. A., de Hulster, E. A. F., Reinders, M. J. T., Pronk, J. T., Heck, A. J. R., Slijper, M., 2007. Quantitative proteomics and transcriptomics of anaerobic and aerobic yeast cultures reveals post-transcriptional regulation of key cellular processes. *Microbiol.* 153, 3864-3878.

de Kok, S., Nijkamp, J. F., Oud, B., Roque, F. C., de Ridder, D., Daran, J. M., Pronk, J. T., van Maris, A. J. A., 2012. Laboratory evolution of new lactate transporter genes in a *jen1Δ* mutant of *Saccharomyces cerevisiae* and their identification as *ADY2* alleles by whole-genome resequencing and transcriptome analysis. *FEMS Yeast Res.* 12, 359-374.

Downs, J. A., Lowndes, N. F., Jackson, S. P., 2000. A role for *Saccharomyces cerevisiae* histone H2A in DNA repair. *Nature.* 408, 1001-1004.

Dunlop, A. P., 1948. Furfural formation and behavior. *Ind Eng Chem.* 40, 204-209.

Eisenberg, T., Knauer, H., Schauer, A., Buttner, S., Ruckstuhl, C., Carmona-Gutierrez, D., Ring, J., Schroeder, S., Magnes, C., Antonacci, L., Fussi, H., Deszcz, L., Hartl, R., Schraml, E., Criollo, A., Megalou,

E., Weiskopf, D., Laun, P., Heeren, G., Breitenbach, M., Grubeck-Loebenstein, B., Herker, E., Fahrenkrog, B., Frohlich, K. U., Sinner, F., Tavernarakis, N., Minois, N., Kroemer, G., Madeo, F., 2009. Induction of autophagy by spermidine promotes longevity. *Nat Cell Biol.* 11, 1305-1314.

Elias, S., Bercovich, B., Kahana, C., Coffino, P., Fischer, M., Hilt, W., Wolf, D. H., Ciechanover, A., 1995. Degradation of ornithine decarboxylase by the mammalian and yeast 26s proteasome complexes requires all the components of the protease. *Eur J Biochem.* 229, 276-283.

Fabrizio, P., Longo, V. D., 2003. The chronological life span of *Saccharomyces cerevisiae*. *Aging Cell.* 2, 73-81.

Fabrizio, P., Longo, V. D., 2008. Chronological aging-induced apoptosis in yeast. *BBA-Mol Cell Res.* 1783, 1280-1285.

Farrell, A. E., Plevin, R. J., Turner, B. T., Jones, A. D., O'Hare, M., Kammen, D. M., 2006. Ethanol can contribute to energy and environmental goals. *Science.* 311, 506-508.

Fernandes, L., RodriguesPousada, C., Struhl, K., 1997. Yap, a novel family of eight bZIP proteins in *Saccharomyces cerevisiae* with distinct biological functions. *Mol Cell Biol.* 17, 6982-6993.

Gentleman, R. C., Carey, V. J., Bates, D. M., Bolstad, B., Dettling, M., Dudoit, S., Ellis, B., Gautier, L., Ge, Y., Gentry, J., Hornik, K., Hothorn, T., Huber, W., Iacus, S., Irizarry, R., Leisch, F., Li, C., Maechler, M., Rossini, A. J., Sawitzki, G., Smith, C., Smyth, G.,

Tierney, L., Yang, J. Y., Zhang, J., 2004. Bioconductor: open software development for computational biology and bioinformatics. *Genome Biol.* 5, R80.

Gorsich, S. W., Dien, B. S., Nichols, N. N., Slininger, P. J., Liu, Z. L., Skory, C. D., 2006. Tolerance to furfural-induced stress is associated with pentose phosphate pathway genes *ZWF1*, *GND1*, *RPE1*, and *TKL1* in *Saccharomyces cerevisiae*. *Appl Microbiol Biotechnol.* 71, 339-349.

Greetham, D., 2014. Presence of low concentrations of acetic acid improves fermentations using *Saccharomyces cerevisiae*. *J Bioprocess Biotech.* 5.

Grossklaus, D. D., Bailao, A. M., Rezende, T. C. V., Borges, C. L., de Oliveira, M. A. P., Parente, J. A., Soares, C. M. D., 2013. Response to oxidative stress in *Paracoccidioides* yeast cells as determined by proteomic analysis. *Microbes Infect.* 15, 347-364.

Hahn-Hagerdal, B., Galbe, M., Gorwa-Grauslund, M. F., Liden, G., Zacchi, G., 2006. Bio-ethanol - the fuel of tomorrow from the residues of today. *Trends Biotechnol.* 24, 549-556.

Hamana, K., Matsuzaki, S., 1992. Polyamines as a Chemotaxonomic Marker in Bacterial Systematics. *Crit Rev Microbiol.* 18, 261-283.

Hamasaki-Katagiri, N., Katagiri, Y., Tabor, C. W., Tabor, H., 1998. Spermine is not essential for growth of *Saccharomyces cerevisiae*: identification of the *SPE4* gene (spermine synthase) and characterization of a *spe4* deletion mutant. *Gene.* 210, 195-201.

Harbison, C. T., Gordon, D. B., Lee, T. I., Rinaldi, N. J., Macisaac, K. D., Danford, T. W., Hannett, N. M., Tagne, J. B., Reynolds, D. B., Yoo, J., Jennings, E. G., Zeitlinger, J., Pokholok, D. K., Kellis, M., Rolfe, P. A., Takusagawa, K. T., Lander, E. S., Gifford, D. K., Fraenkel, E., Young, R. A., 2004. Transcriptional regulatory code of a eukaryotic genome. *Nature*. 431, 99-104.

Hasunuma, T., Sanda, T., Yamada, R., Yoshimura, K., Ishii, J., Kondo, A., 2011. Metabolic pathway engineering based on metabolomics confers acetic and formic acid tolerance to a recombinant xylose-fermenting strain of *Saccharomyces cerevisiae*. *Microb Cell Fact*. 10.

Hauf, J., Zimmermann, F. K., Muller, S., 2000. Simultaneous genomic overexpression of seven glycolytic enzymes in the yeast *Saccharomyces cerevisiae*. *Enzyme Microb Technol*. 26, 688-698.

Herker, E., Jungwirth, H., Lehmann, K. A., Maldener, C., Frohlich, K. U., Wissing, S., Buttner, S., Fehr, M., Sigrist, S., Madeo, F., 2004. Chronological aging leads to apoptosis in yeast. *J Cell Biol*. 164, 501-507.

Hong, K. K., Vongsangnak, W., Vemuri, G. N., Nielsen, J., 2011. Unravelling evolutionary strategies of yeast for improving galactose utilization through integrated systems level analysis. *Proc Natl Acad Sci USA*. 108, 12179-12184.

Hosaka, K., Nikawa, J., Kodaki, T., Yamashita, S., 1992. A dominant mutation that alters the regulation of *INO1* expression in *Saccharomyces cerevisiae*. *J Biochem*. 111, 352-358.

Hsu, T. A., Ladisch, M. R., Tsao, G. T., 1980. Alcohol from cellulose. *Chemtech*. 10, 315-319.

Huang, X. N., Chen, M., Lu, X. F., Li, Y. M., Li, X., Li, J. J., 2014. Direct production of itaconic acid from liquefied corn starch by genetically engineered *Aspergillus terreus*. *Microb Cell Fact*. 13.

Innocente, N., Biasutti, A., Padovese, A., Moret, S., 2007. Determination of biogenic amines in cheese using HPLC technique and direct derivatization of acid extract. *Food Chem*. 101, 1285-1289.

Ishii, J., Yoshimura, K., Hasunuma, T., Kondo, A., 2013. Reduction of furan derivatives by overexpressing NADH-dependent Adh1 improves ethanol fermentation using xylose as sole carbon source with *Saccharomyces cerevisiae* harboring XR-XDH pathway. *Appl Microbiol Biotechnol*. 97, 2597-2607.

Jung, U. S., Levin, D. E., 1999. Genome-wide analysis of gene expression regulated by the yeast cell wall integrity signalling pathway. *Mol Microbiol*. 34, 1049-1057.

Jung, Y. H., Kim, I. J., Kim, H. K., Kim, K. H., 2013. Dilute acid pretreatment of lignocellulose for whole slurry ethanol fermentation. *Bioresour Technol*. 132, 109-114.

Jungwirth, H., Kuchler, K., 2006. Yeast ABC transporters - a tale of sex, stress, drugs, and aging. *FEBS Lett*. 580, 1131-1138.

Jungwirth, H., Wendler, F., Platzer, B., Bergler, H., Hogenauer, G., 2000. Diazaborine resistance in yeast involves the efflux pumps Ycflp

and Flr1p and is enhanced by a gain-of-function allele of gene *YAP1*. Eur J Biochem. 267, 4809-4816.

Kanazawa, S., Driscoll, M., Struhl, K., 1988. *ATRI*, a *Saccharomyces cerevisiae* gene encoding a transmembrane protein required for aminotriazole resistance. Mol Cell Biol. 8, 664-673.

Kang, H. A., Hershey, J. W. B., 1994. Effect of initiation factor eIF-5A depletion on protein synthesis and proliferation of *Saccharomyces cerevisiae*. J Biol Chem. 269, 3934-3940.

Karagoz, P., Ozkan, M., 2014. Ethanol production from wheat straw by *Saccharomyces cerevisiae* and *Scheffersomyces stipitis* co-culture in batch and continuous system. Bioresour Technol. 158, 286-293.

Kasukabe, Y., He, L. X., Nada, K., Misawa, S., Ihara, I., Tachibana, S., 2004. Overexpression of spermidine synthase enhances tolerance to multiple environmental stresses and up-regulates the expression of various stress regulated genes in transgenic *Arabidopsis thaliana*. Plant Cell Physiol. 45, 712-722.

Kim, D., Hahn, J. S., 2013. Roles of the Yap1 transcription factor and antioxidants in *Saccharomyces cerevisiae*'s tolerance to furfural and 5-hydroxymethylfurfural, which function as thiol-reactive electrophiles generating oxidative stress. Appl Environ Microbiol. 79, 5069-5077.

Kim, H. S., Kim, N. R., Kim, W., Choi, W., 2012a. Insertion of transposon in the vicinity of *SSK2* confers enhanced tolerance to furfural in *Saccharomyces cerevisiae*. Appl Microbiol Biotechnol. 95, 531-540.

Kim, S. K., Jin, Y. S., Choi, I. G., Park, Y. C., Seo, J. H., 2015. Enhanced tolerance of *Saccharomyces cerevisiae* to multiple lignocellulose-derived inhibitors through modulation of spermidine contents. *Metab Eng.* 29, 46-55.

Kim, S. R., Ha, S. J., Kong, I. I., Jin, Y. S., 2012b. High expression of *XYL2* coding for xylitol dehydrogenase is necessary for efficient xylose fermentation by engineered *Saccharomyces cerevisiae*. *Metab Eng.* 14, 336-343.

Kim, S. R., Skerker, J. M., Kang, W., Lesmana, A., Wei, N., Arkin, A. P., Jin, Y. S., 2013. Rational and evolutionary engineering approaches uncover a small set of genetic changes efficient for rapid xylose fermentation in *Saccharomyces cerevisiae*. *Plos One.* 8.

Kirdponpattara, S., Phisalaphong, M., 2013. Bacterial cellulose-alginate composite sponge as a yeast cell carrier for ethanol production. *Biochem Eng J.* 77, 103-109.

Klionsky, D. J., Cregg, J. M., Dunn, W. A., Emr, S. D., Sakai, Y., Sandoval, I. V., Sibirny, A., Subramani, S., Thumm, M., Veenhuis, M., Ohsumi, Y., 2003. A unified nomenclature for yeast autophagy-related genes. *Dev Cell.* 5, 539-545.

Klis, F. M., Mol, P., Hellingwerf, K., Brul, S., 2002. Dynamics of cell wall structure in *Saccharomyces cerevisiae*. *Fems Microbiol Rev.* 26, 239-256.

Krahulec, S., Petschacher, B., Wallner, M., Longus, K., Klimacek, M., Nidetzky, B., 2010. Fermentation of mixed glucose-xylose substrates

by engineered strains of *Saccharomyces cerevisiae*: role of the coenzyme specificity of xylose reductase, and effect of glucose on xylose utilization. *Microb Cell Fact.* 9.

Laadan, B., Almeida, J. R. M., Radstrom, P., Hahn-Hagerdal, B., Gorwa-Grauslund, M., 2008. Identification of an NADH-dependent 5-hydroxymethylfurfural-reducing alcohol dehydrogenase in *Saccharomyces cerevisiae*. *Yeast.* 25, 191-198.

Laluce, C., Tognolli, J. O., de Oliveira, K. F., Souza, C. S., Morais, M. R., 2009. Optimization of temperature, sugar concentration, and inoculum size to maximize ethanol production without significant decrease in yeast cell viability. *Appl Microbiol Biotechnol.* 83, 627-637.

Langmead, B., Salzberg, S. L., 2012. Fast gapped-read alignment with Bowtie 2. *Nat Methods.* 9, 357-359.

Lans, H., Marteijn, J. A., Vermeulen, W., 2012. ATP-dependent chromatin remodeling in the DNA-damage response. *Epigenet Chromatin.* 5.

Lee, S. H., Kodaki, T., Park, Y. C., Seo, J. H., 2012. Effects of NADH-preferring xylose reductase expression on ethanol production from xylose in xylose-metabolizing recombinant *Saccharomyces cerevisiae*. *J Biotechnol.* 158, 184-191.

Lee, T. I., Rinaldi, N. J., Robert, F., Odom, D. T., Bar-Joseph, Z., Gerber, G. K., Hannett, N. M., Harbison, C. T., Thompson, C. M., Simon, I., Zeitlinger, J., Jennings, E. G., Murray, H. L., Gordon, D. B., Ren, B., Wyrick, J. J., Tagne, J. B., Volkert, T. L., Fraenkel, E., Gifford,

D. K., Young, R. A., 2002. Transcriptional regulatory networks in *Saccharomyces cerevisiae*. *Science*. 298, 799-804.

Lee, W. J., Ryu, Y. W., Seo, J. H., 2000. Characterization of two-substrate fermentation processes for xylitol production using recombinant *Saccharomyces cerevisiae* containing xylose reductase gene. *Process Biochem*. 35, 1199-1203.

Li, B. Z., Yuan, Y. J., 2010. Transcriptome shifts in response to furfural and acetic acid in *Saccharomyces cerevisiae*. *Appl Microbiol Biotechnol*. 86, 1915-1924.

Liu, Z. L., 2011. Molecular mechanisms of yeast tolerance and in situ detoxification of lignocellulose hydrolysates. *Appl Microbiol Biotechnol*. 90, 809-825.

Liu, Z. L., Moon, J., Andersh, B. J., Slininger, P. J., Weber, S., 2008. Multiple gene-mediated NAD(P)H-dependent aldehyde reduction is a mechanism of in situ detoxification of furfural and 5-hydroxymethylfurfural by *Saccharomyces cerevisiae*. *Appl Microbiol Biotechnol*. 81, 743-753.

Liu, Z. L., Slininger, P. J., Dien, B. S., Berhow, M. A., Kurtzman, C. P., Gorsich, S. W., 2004. Adaptive response of yeasts to furfural and 5-hydroxymethylfurfural and new chemical evidence for HMF conversion to 2,5-bis-hydroxymethylfuran. *J Ind Microbiol Biotechnol*. 31, 345-352.

Ludovico, P., Sousa, M. J., Silva, M. T., Leao, C., Corte-Real, M., 2001. *Saccharomyces cerevisiae* commits to a programmed cell death process

in response to acetic acid. *Microbiology*. 147, 2409-2415.

Lynd, L. R., Laser, M. S., Brandsby, D., Dale, B. E., Davison, B., Hamilton, R., Himmel, M., Keller, M., McMillan, J. D., Sheehan, J., Wyman, C. E., 2008. How biotech can transform biofuels. *Nat Biotechnol*. 26, 169-172.

Lynd, L. R., van Zyl, W. H., McBride, J. E., Laser, M., 2005. Consolidated bioprocessing of cellulosic biomass: an update. *Curr Opin Biotechnol*. 16, 577-583.

Ma, M. G., Liu, Z. L., 2010a. Comparative transcriptome profiling analyses during the lag phase uncover *YAP1*, *PDR1*, *PDR3*, *RPN4*, and *HSF1* as key regulatory genes in genomic adaptation to the lignocellulose derived inhibitor HMF for *Saccharomyces cerevisiae*. *BMC Genomics*. 11.

Ma, M. G., Liu, Z. L., 2010b. Mechanisms of ethanol tolerance in *Saccharomyces cerevisiae*. *Appl Microbiol Biotechnol*. 87, 829-845.

MacPherson, S., Larochelle, M., Turcotte, B., 2006. A fungal family of transcriptional regulators: the zinc cluster proteins. *Microbiol Mol Biol Rev*. 70, 583-604.

Mamnun, Y. M., Pandjaitan, R., Mahe, Y., Delahodde, A., Kuchler, K., 2002. The yeast zinc finger regulators Pdr1p and Pdr3p control pleiotropic drug resistance (PDR) as homo- and heterodimers in vivo. *Mol Microbiol*. 46, 1429-1440.

Mannhaupt, G., Schnall, R., Karpov, V., Vetter, I., Feldmann, H., 1999.

Rpn4p acts as a transcription factor by binding to PACE, a nonamer box found upstream of 26S proteasomal and other genes in yeast. *FEBS Lett.* 450, 27-34.

Maristela Freitas, S. P., Laluce, C., 1998. Ethanol tolerance of thermotolerant yeasts cultivated on mixtures of sucrose and ethanol. *J Ferment Bioeng.* 85, 388-397.

Matsushika, A., Goshima, T., Fujii, T., Inoue, H., Sawayama, S., Yano, S., 2012. Characterization of non-oxidative transaldolase and transketolase enzymes in the pentose phosphate pathway with regard to xylose utilization by recombinant *Saccharomyces cerevisiae*. *Enzyme Microb Technol.* 51, 16-25.

Merino, S. T., Cherry, J., 2007. Progress and challenges in enzyme development for biomass utilization. *Adv Biochem Eng Biotechnol.* 108, 95-120.

Minois, N., Carmona-Gutierrez, D., Madeo, F., 2011. Polyamines in aging and disease. *Aging.* 3, 716-732.

Modig, T., Liden, G., Taherzadeh, M. J., 2002. Inhibition effects of furfural on alcohol dehydrogenase, aldehyde dehydrogenase and pyruvate dehydrogenase. *Biochem J.* 363, 769-776.

Moon, J., Liu, Z. L., 2012. Engineered NADH-dependent GRE2 from *Saccharomyces cerevisiae* by directed enzyme evolution enhances HMF reduction using additional cofactor NADPH. *Enzyme Microb Technol.* 50, 115-120.

Moret, S., Conte, L. S., 1996. High-performance liquid chromatographic evaluation of biogenic amines in foods - An analysis of different methods of sample preparation in relation to food characteristics. *J Chromatogr A*. 729, 363-369.

Morgan, M., Anders, S., Lawrence, M., Aboyoun, P., Pages, H., Gentleman, R., 2009. ShortRead: a bioconductor package for input, quality assessment and exploration of high-throughput sequence data. *Bioinformatics*. 25, 2607-2608.

Mosier, N., Wyman, C., Dale, B., Elander, R., Lee, Y. Y., Holtzapple, M., Ladisch, M., 2005. Features of promising technologies for pretreatment of lignocellulosic biomass. *Bioresour Technol*. 96, 673-686.

Moye-Rowley, W. S., 2003. Transcriptional control of multidrug resistance in the yeast *Saccharomyces*. *Prog Nucleic Acid Res Mol Biol*. 73, 251-279.

Mussatto, S. I., Roberto, I. C., 2004. Alternatives for detoxification of diluted-acid lignocellulosic hydrolyzates for use in fermentative processes: a review. *Bioresour Technol*. 93, 1-10.

Naik, S. N., Goud, V. V., Rout, P. K., Dalai, A. K., 2010. Production of first and second generation biofuels: A comprehensive review. *Renew Sust Energ Rev*. 14, 578-597.

Nambeesan, S., Datsenka, T., Ferruzzi, M. G., Malladi, A., Mattoo, A. K., Handa, A. K., 2010. Overexpression of yeast spermidine synthase impacts ripening, senescence and decay symptoms in tomato. *Plant J*.

63, 836-847.

Nikolic, S., Mojovic, L., Pejin, D., Rakin, M., Vukasinovic, M., 2010. Production of bioethanol from corn meal hydrolyzates by free and immobilized cells of *Saccharomyces cerevisiae* var. *ellipsoideus*. *Biomass Bioenerg.* 34, 1449-1456.

Nilsson, A., Gorwa-Grauslund, M. F., Hahn-Hagerdal, B., Liden, G., 2005. Cofactor dependence in furan reduction by *Saccharomyces cerevisiae* in fermentation of acid-hydrolyzed lignocellulose. *Appl Environ Microbiol.* 71, 7866-7871.

Nilsson, A., Taherzadeh, M. J., Liden, G., 2001. Use of dynamic step response for control of fed-batch conversion of lignocellulosic hydrolyzates to ethanol. *J Biotechnol.* 89, 41-53.

Nogae, I., Johnston, M., 1990. Isolation and characterization of the *ZWF1* gene of *Saccharomyces cerevisiae*, encoding glucose-6-phosphate dehydrogenase. *Gene.* 96, 161-169.

Oredsson, S. M., 2003. Polyamine dependence of normal cell-cycle progression. *Biochem Soc T.* 31, 366-370.

Palanimurugan, R., Scheel, H., Hofmann, K., Dohmen, R. J., 2004. Polyamines regulate their synthesis by inducing expression and blocking degradation of ODC antizyme. *Embo J.* 23, 4857-4867.

Palmqvist, E., Galbe, M., Hahn-Hagerdal, B., 1998. Evaluation of cell recycling in continuous fermentation of enzymatic hydrolysates of spruce with *Saccharomyces cerevisiae* and on-line monitoring of

glucose and ethanol. *Appl Microbiol Biotechnol.* 50, 545-551.

Palmqvist, E., Grage, H., Meinander, N. Q., Hahn-Hagerdal, B., 1999. Main and interaction effects of acetic acid, furfural, and *p*-hydroxybenzoic acid on growth and ethanol productivity of yeasts. *Biotechnol Bioeng.* 63, 46-55.

Palmqvist, E., Hahn-Hagerdal, B., 2000a. Fermentation of lignocellulosic hydrolysates. I: inhibition and detoxification. *Bioresour Technol.* 74, 17-24.

Palmqvist, E., Hahn-Hagerdal, B., 2000b. Fermentation of lignocellulosic hydrolysates. II: inhibitors and mechanisms of inhibition. *Bioresour Technol.* 74, 25-33.

Pampulha, M. E., Loureirodias, M. C., 1989. Combined effect of acetic acid, pH and ethanol on intracellular pH of fermenting yeast. *Appl Microbiol Biotechnol.* 31, 547-550.

Papouskova, K., Sychrova, H., 2007. Production of *Yarrowia lipolytica* Nha2 Na⁺/H⁺ antiporter improves the salt tolerance of *Saccharomyces cerevisiae*. *Folia Microbiol.* 52, 600-602.

Parente, A. F. A., De Rezende, T. C. V., De Castro, K. P., Bailao, A. M., Parente, J. A., Borges, C. L., Silva, L. P., Soares, C. M. D., 2013. A proteomic view of the response of *Paracoccidioides* yeast cells to zinc deprivation. *Fungal Biol.* 117, 399-410.

Park, S. E., Koo, H. M., Park, Y. K., Park, S. M., Park, J. C., Lee, O. K., Park, Y. C., Seo, J. H., 2011. Expression of aldehyde dehydrogenase 6

reduces inhibitory effect of furan derivatives on cell growth and ethanol production in *Saccharomyces cerevisiae*. *Bioresour Technol.* 102, 6033-6038.

Pegg, A. E., Mccann, P. P., 1982. Polyamine metabolism and function. *Am J Physiol.* 243, 212-221.

Pereira, F. B., Gomes, D. G., Guimares, P. M. R., Teixeira, J. A., Domingues, L., 2012. Cell recycling during repeated very high gravity bio-ethanol fermentations using the industrial *Saccharomyces cerevisiae* strain PE-2. *Biotechnol Lett.* 34, 45-53.

Pereira, F. B., Guimaraes, P. M. R., Teixeira, J. A., Domingues, L., 2010. Selection of *Saccharomyces cerevisiae* strains for efficient very high gravity bio-ethanol fermentation processes. *Biotechnol Lett.* 32, 1655-1661.

Petersson, A., Almeida, J. R. M., Modig, T., Karhumaa, K., Hahn-Hagerdal, B., Gorwa-Grauslund, M. F., Liden, G., 2006. A 5-hydroxymethyl furfural reducing enzyme encoded by the *Saccharomyces cerevisiae ADH6* gene conveys HMF tolerance. *Yeast.* 23, 455-464.

Pichiah, P. B. T., Suriyakalaa, U., Kamalakkannan, S., Kokilavani, P., Kalaiselvi, S., SankarGanesh, D., Gowri, J., Archunan, G., Cha, Y. S., Achiraman, S., 2011. Spermidine may decrease ER stress in pancreatic beta cells and may reduce apoptosis via activating AMPK dependent autophagy pathway. *Med Hypotheses.* 77, 677-679.

Pienkos, P. T., Zhang, M., 2009. Role of pretreatment and conditioning

processes on toxicity of lignocellulosic biomass hydrolysates. *Cellulose*. 16, 743-762.

Popoff, T., Theander, O., 1976. Formation of aromatic compounds from carbohydrates: Part III. Reaction of D-glucose and D-fructose in slightly acidic, aqueous solution. *Acta Chem Scand B*. 30, 397-402.

Porat, Z., Landau, G., Bercovich, Z., Krutauz, D., Glickman, M., Kahana, C., 2008. Yeast antizyme mediates degradation of yeast ornithine decarboxylase by yeast but not by mammalian proteasome - New insights on yeast antizyme. *J Biol Chem*. 283, 4528-4534.

Qian, Z. G., Xia, X. X., Lee, S. Y., 2009. Metabolic engineering of *Escherichia coli* for the production of putrescine: a four carbon diamine. *Biotechnol Bioeng*. 104, 651-662.

Ramot, Y., Tiede, S., Biro, T., Abu Bakar, M. H., Sugawara, K., Philpott, M. P., Harrison, W., Pietila, M., Paus, R., 2011. Spermidine promotes human hair growth and is a novel modulator of human epithelial stem cell functions. *Plos One*. 6.

Razmovski, V., Vucurovic, V., 2011. Ethanol production from sugar beet molasses by *S. cerevisiae* entrapped in an alginate-maize stem ground tissue matrix. *Enzyme Microb Technol*. 48, 378-385.

Rider, J. E., Hacker, A., Mackintosh, C. A., Pegg, A. E., Woster, P. M., Casero, R. A., 2007. Spermine and spermidine mediate protection against oxidative damage caused by hydrogen peroxide. *Amino Acids*. 33, 231-240.

Rinaldi, F., Sorbellini, E., Baroni, S., Benedusi, A., 2005. Use of spermine and/or spermidine against skin ageing in dietary, pharmaceutical or cosmetic compositions. Patent PCT/EP2004/008572.

Robinson, M. D., McCarthy, D. J., Smyth, G. K., 2010. edgeR: a Bioconductor package for differential expression analysis of digital gene expression data. *Bioinformatics*. 26, 139-140.

Rudolf, A., Alkasrawi, M., Zacchi, G., Liden, G., 2005. A comparison between batch and fed-batch simultaneous saccharification and fermentation of steam pretreated spruce. *Enzyme Microb Technol*. 37, 195-204.

Sa-Correia, I., Tenreiro, S., 2002. The multidrug resistance transporters of the major facilitator superfamily, 6 years after disclosure of *Saccharomyces cerevisiae* genome sequence. *J Biotechnol*. 98, 215-226.

Sanda, T., Hasunuma, T., Matsuda, F., Kondo, A., 2011. Repeated-batch fermentation of lignocellulosic hydrolysate to ethanol using a hybrid *Saccharomyces cerevisiae* strain metabolically engineered for tolerance to acetic and formic acids. *Bioresour Technol*. 102, 7917-7924.

Sarks, C., Jin, M. J., Sato, T. K., Balan, V., Dale, B. E., 2014. Studying the rapid bioconversion of lignocellulosic sugars into ethanol using high cell density fermentations with cell recycle. *Biotechnol Biofuels*. 7.

Schipper, R. G., Penning, L. C., Verhofstad, A. A. J., 2000. Involvement of polyamines in apoptosis. Facts and controversies: effectors or protectors? *Semin Cancer Biol*. 10, 55-68.

Schnier, J., Schwelberger, H. G., Smitmcbride, Z., Kang, H. A., Hershey, J. W. B., 1991. Translation initiation factor 5A and its hypusine modification are essential for cell viability in the yeast *Saccharomyces cerevisiae*. *Mol Cell Biol.* 11, 3105-3114.

Schuber, F., 1989. Influence of polyamines on membrane functions. *Biochem J.* 260, 1-10.

Sembiring, K. C., Mulyani, H., A, I. F., Dahnum, D., Sudiyani, Y., 2013. Rice flour and white glutinous rice flour for use on immobilization of yeast cell in ethanol production. *Energy Procedia.* 32, 99-104.

Sikorski, R. S., Hieter, P., 1989. A system of shuttle vectors and yeast host strains designed for efficient manipulation of DNA in *Saccharomyces cerevisiae*. *Genetics.* 122, 19-27.

Singh, A., Sharma, P., Saran, A. K., Singh, N., Bishnoi, N. R., 2013. Comparative study on ethanol production from pretreated sugarcane bagasse using immobilized *Saccharomyces cerevisiae* on various matrices. *Renew Energ.* 50, 488-493.

Stenberg, K., Tengborg, C., Galbe, M., Zacchi, G., Palmqvist, E., Hahn-Hagerdal, B., 1998. Recycling of process streams in ethanol production from softwoods based on enzymatic hydrolysis. *Appl Biochem Biotechnol.* 70-2, 697-708.

Sundstrom, L., Larsson, S., Jonsson, L. J., 2010. Identification of *Saccharomyces cerevisiae* genes involved in the resistance to phenolic fermentation inhibitors. *Appl Biochem Biotechnol.* 161, 106-115.

Tachihara, K., Uemura, T., Kashiwagi, K., Igarashi, K., 2005. Excretion of putrescine and spermidine by the protein encoded by *YKL174c* (*TPO5*) in *Saccharomyces cerevisiae*. *J Biol Chem.* 280, 12637-12642.

Taherzadeh, M. J., Gustafsson, L., Niklasson, C., Liden, G., 1999a. Conversion of furfural in aerobic and anaerobic batch fermentation of glucose by *Saccharomyces cerevisiae*. *J Biosci Bioeng.* 87, 169-174.

Taherzadeh, M. J., Gustafsson, L., Niklasson, C., Liden, G., 2000a. Physiological effects of 5-hydroxymethylfurfural on *Saccharomyces cerevisiae*. *Appl Microbiol Biotechnol.* 53, 701-708.

Taherzadeh, M. J., Niklasson, C., Liden, G., 1999b. Conversion of dilute-acid hydrolyzates of spruce and birch to ethanol by fed-batch fermentation. *Bioresour Technol.* 69, 59-66.

Taherzadeh, M. J., Niklasson, C., Liden, G., 2000b. On-line control of fed-batch fermentation of dilute-acid hydrolyzates. *Biotechnol Bioeng.* 69, 330-338.

Terashima, H., Yabuki, N., Arisawa, M., Hamada, K., Kitada, K., 2000. Up-regulation of genes encoding glycosylphosphatidylinositol (GPI)-attached proteins in response to cell wall damage caused by disruption of *FKSI* in *Saccharomyces cerevisiae*. *Mol Gen Genet.* 264, 64-74.

Thomas, K. C., Hynes, S. H., Ingledew, W. M., 1998. Initiation of anaerobic growth of *Saccharomyces cerevisiae* by amino acids or nucleic acid bases: ergosterol and unsaturated fatty acids cannot replace oxygen in minimal media. *J Ind Microbiol Biotechnol.* 21, 247-253.

Uemura, T., Kashiwagi, K., Igarashi, K., 2007. Polyamine uptake by DUR3 and SAM3 in *Saccharomyces cerevisiae*. J Biol Chem. 282, 7733-7741.

Uemura, T., Tachihara, K., Tomitori, H., Kashiwagi, K., Igarashi, K., 2005. Characteristics of the polyamine transporter TPO1 and regulation of its activity and cellular localization by phosphorylation. J Biol Chem. 280, 9646-9652.

Ulbricht, R. J., Northup, S. J., Thomas, J. A., 1984. A review of 5-hydroxymethylfurfural (HMF) in parenteral solutions. Fund Appl Toxicol. 4, 843-853.

van Leeuwenhoek, A., 1678. Observationes D. Anthonii Leeuwenhoek, de Natis e'semine genitali Animalculis. Phil Trans. 12, 1040-1046.

van Maris, A. J. A., Abbott, D. A., Bellissimi, E., van den Brink, J., Kuyper, M., Luttik, M. A. H., Wisselink, H. W., Scheffers, W. A., van Dijken, J. P., Pronk, J. T., 2006. Alcoholic fermentation of carbon sources in biomass hydrolysates by *Saccharomyces cerevisiae*: current status. Anton Leeuw Int J G. 90, 391-418.

Verbelen, P. J., Saerens, S. M. G., Van Mulders, S. E., Delvaux, F., Delvaux, F. R., 2009. The role of oxygen in yeast metabolism during high cell density brewery fermentations. Appl Microbiol Biotechnol. 82, 1143-1156.

Verduyn, C., Vankleef, R., Frank, J., Schreuder, H., Vandijken, J. P., Scheffers, W. A., 1985. Properties of the NAD(P)H-dependent xylose reductase from the xylose-fermenting yeast *Pichia stipitis*. Biochem J.

226, 669-677.

Vuohelainen, S., Pirinen, E., Cerrada-Gimenez, M., Keinanen, T. A., Uimari, A., Pietila, M., Khomutov, A. R., Janne, J., Alhonen, L., 2010. Spermidine is indispensable in differentiation of 3T3-L1 fibroblasts to adipocytes. *J Cell Mol Med.* 14, 1683-1692.

Wahlbom, C. F., Hahn-Hagerdal, B., 2002. Furfural, 5-hydroxymethyl furfural, and acetoin act as external electron acceptors during anaerobic fermentation of xylose in recombinant *Saccharomyces cerevisiae*. *Biotechnol Bioeng.* 78, 172-178.

Wallace, H. M., Fraser, A. V., Hughes, A., 2003. A perspective of polyamine metabolism. *Biochem J.* 376, 1-14.

Wang, X., Yomano, L. P., Lee, J. Y., York, S. W., Zheng, H. B., Mullinnix, M. T., Shanmugam, K. T., Ingram, L. O., 2013a. Engineering furfural tolerance in *Escherichia coli* improves the fermentation of lignocellulosic sugars into renewable chemicals. *Proc Natl Acad Sci USA.* 110, 4021-4026.

Wang, Y. Z., Li, K. P., Huang, F., Wang, J. H., Zhao, J. F., Zhao, X., Garza, E., Manow, R., Grayburn, S., Zhou, S. D., 2013. Engineering and adaptive evolution of *Escherichia coli* W for L-lactic acid fermentation from molasses and corn steep liquor without additional nutrients. *Bioresour Technol.* 148, 394-400.

Watanabe, S., Abu Saleh, A., Pack, S. P., Annaluru, N., Kodaki, T., Makino, K., 2007. Ethanol production from xylose by recombinant *Saccharomyces cerevisiae* expressing protein-engineered NADH-

preferring xylose reductase from *Pichia stipitis*. Microbiology. 153, 3044-3054.

Webb, S. R., Lee, H., 1992. Characterization of xylose reductase from the yeast *Pichia stipitis* - evidence for functional thiol and histidyl groups. J Gen Microbiol. 138, 1857-1863.

Wei, N., Quarterman, J., Kim, S. R., Cate, J. H. D., Jin, Y. S., 2013. Enhanced biofuel production through coupled acetic acid and xylose consumption by engineered yeast. Nat Commun. 4.

White, W. H., Gunyuzlu, P. L., Toyn, J. H., 2001. *Saccharomyces cerevisiae* is capable of *de novo* pantothenic acid biosynthesis involving a novel pathway of β -alanine production from spermine. J Biol Chem. 276, 10794-10800.

Wiatrowski, H. A., Carlson, M., 2003. Yap1 accumulates in the nucleus in response to carbon stress in *Saccharomyces cerevisiae*. Eukaryot Cell. 2, 19-26.

Yang, B., Wyman, C. E., 2008. Pretreatment: the key to unlocking low-cost cellulosic ethanol. Biofuels, Bioprod and Biorefin. 2, 26-40.

Yangcheng, H. Y., Jiang, H. X., Blanco, M., Jane, J. L., 2013. Characterization of normal and waxy corn starch for bioethanol production. J Agr Food Chem. 61, 379-386.

Young, E. M., Comer, A. D., Huang, H., Alper, H. S., 2012. A molecular transporter engineering approach to improving xylose catabolism in *Saccharomyces cerevisiae*. Metab Eng. 14, 401-411.

Zhou, H., Cheng, J. S., Wang, B. L., Fink, G. R., Stephanopoulos, G., 2012. Xylose isomerase overexpression along with engineering of the pentose phosphate pathway and evolutionary engineering enable rapid xylose utilization and ethanol production by *Saccharomyces cerevisiae*. *Metab Eng.* 14, 611-622.

Appendix 1

The data from the heat maps presented in Fig.

3.14

Appendix 1.1. D452-2 VS SPD

Gene	D452-2				SPD				pValue	log2 Fold Change
	RPKM-1	RPKM-2	RPKM-3	Means	RPKM-1	RPKM-2	RPKM-3	Means		
YCR021C	639	1052	1245	978.7	12	22	21	18.3	0.0000004	-5.7
YBL108W	10	1	12	7.7	0	0	0	0.0	0.0023398	-5.5
YLR307C-A	249	297	518	354.7	7	8	11	8.7	0.0000025	-5.4
YLL030C	1	9	4	4.7	0	0	0	0.0	0.0045057	-5.2
YHR185C	2	2	3	2.3	0	0	0	0.0	0.0054950	-5.1
YPL038W-A	8	2	11	7.0	0	0	0	0.0	0.0113190	-4.8
YAR035C-A	18	29	0	15.7	0	0	0	0.0	0.0135865	-4.6
YJR005C-A	255	322	275	284.0	14	14	8	12.0	0.0000343	-4.5
YLL055W	89	147	227	154.3	7	5	13	8.3	0.0000779	-4.2
YLR134W	7953	8291	6865	7703.0	492	406	466	454.7	0.0000921	-4.1
YDL243C	9127	9689	5490	8102.0	452	426	543	473.7	0.0001105	-4.0
YOL165C	87	69	105	87.0	4	4	9	5.7	0.0002293	-4.0
YFL055W	209	246	271	242.0	11	17	22	16.7	0.0001837	-3.9
YHL046C	19	16	12	15.7	1	0	2	1.0	0.0038245	-3.6
YNL277W-A	25	50	45	40.0	2	3	4	3.0	0.0024629	-3.6
YLL057C	134	226	345	235.0	13	24	23	20.0	0.0005015	-3.6
YGR142W	809	915	925	883.0	88	66	80	78.0	0.0005482	-3.5
YBL008W-A	6	11	12	9.7	0	3	0	1.0	0.0128930	-3.5
YDR374C	11	6	32	16.3	1	2	1	1.3	0.0017769	-3.4
YCL026C-A	839	574	845	752.7	73	47	94	71.3	0.0007129	-3.4
YLL056C	4781	6743	5218	5580.7	405	479	845	576.3	0.0009150	-3.3
YCR102W-A	82	78	55	71.7	8	3	12	7.7	0.0031061	-3.2
YFL057C	10352	6438	6159	7649.7	866	510	1177	851.0	0.0013204	-3.2
YFL056C	5120	3234	4516	4290.0	380	341	680	467.0	0.0013698	-3.2
YOR388C	27	20	26	24.3	3	2	3	2.7	0.0026603	-3.1
YGL138C	1	1	9	3.7	0	1	1	0.7	0.0133982	-3.1
YLR012C	3	14	57	24.7	1	2	5	2.7	0.0069386	-3.1
YDR278C	18	20	22	20.0	1	4	2	2.3	0.0079673	-3.1

(be continued)

Gene	D452-2				SPD				pValue	log2 Fold Change
	RPKM-1	RPKM-2	RPKM-3	Means	RPKM-1	RPKM-2	RPKM-3	Means		
YPL021W	13	14	23	16.7	1	1	4	2.0	0.0071232	-3.0
YLR346C	2679	1833	5671	3394.3	552	252	508	437.3	0.0028306	-3.0
YAL018C	0	1	1	0.7	1	6	7	4.7	0.0136502	-3.0
YKL068W-A	1946	2121	3283	2450.0	367	308	295	323.3	0.0031323	-2.9
YEL045C	48	33	49	43.3	9	6	2	5.7	0.0064592	-2.9
YKR076W	1391	914	860	1055.0	147	98	214	153.0	0.0038633	-2.8
YPL240C	606	985	962	851.0	67	140	166	124.3	0.0040553	-2.8
YHR126C	34	68	93	65.0	11	8	6	8.3	0.0061053	-2.8
YBR008C	2064	2016	1262	1780.7	275	204	342	273.7	0.0057001	-2.7
YNL129W	177	132	258	189.0	24	31	29	28.0	0.0067521	-2.7
YNL130C-A	124	115	329	189.3	19	30	36	28.3	0.0086335	-2.7
YLR461W	75	82	53	70.0	5	16	15	12.0	0.0087948	-2.7
YBL100W-C	93	67	88	82.7	8	3	31	14.0	0.0138911	-2.6
YDL114W	11	16	18	15.0	1	5	3	3.0	0.0124273	-2.6
YJR047C	60	48	46	51.3	13	7	5	8.3	0.0100865	-2.6
YGL007W	73	96	57	75.3	9	11	15	11.7	0.0099967	-2.6
YER106W	29	18	25	24.0	5	5	3	4.3	0.0106542	-2.6
YCL026C-B	3690	2553	2671	2971.3	612	316	656	528.0	0.0088030	-2.6
YPL171C	1937	2640	3279	2618.7	243	416	764	474.3	0.0090239	-2.5
YGL183C	47	54	44	48.3	7	11	7	8.3	0.0110512	-2.5
YER103W	195	334	351	293.3	31	61	63	51.7	0.0094326	-2.5
YML131W	2816	3242	4216	3424.7	472	598	758	609.3	0.0099144	-2.5
YPL058C	181	180	90	150.3	29	26	26	27.0	0.0101793	-2.5
YDL059C	221	274	322	272.3	37	59	52	49.3	0.0110883	-2.5
YMR244W	87	119	97	101.0	10	23	25	19.3	0.0117788	-2.5
YDR111C	72	48	86	68.7	13	9	15	12.3	0.0118230	-2.5
YLR460C	659	1044	1040	914.3	101	154	268	174.3	0.0115577	-2.4
YBL065W	184	152	98	144.7	27	34	19	26.7	0.0139916	-2.4
YPR093C	506	347	399	417.3	89	54	99	80.7	0.0127877	-2.4
YJL045W	23	35	42	33.3	3	7	10	6.7	0.0142828	-2.4
YNL133C	152	236	355	247.7	36	42	60	46.0	0.0137356	-2.4
YMR265C	368	215	226	269.7	66	37	53	52.0	0.0133787	-2.4

(be continued)

Gene	D452-2				SPD				pValue	log2 Fold Change
	RPKM-1	RPKM-2	RPKM-3	Means	RPKM-1	RPKM-2	RPKM-3	Means		
YOR058C	307	328	351	328.7	61	55	73	63.0	0.0133919	-2.4
YKL070W	670	634	273	525.7	125	101	72	99.3	0.0147420	-2.4
YHR030C	84	49	62	65.0	238	339	404	327.0	0.0146423	2.4
YBL002W	88	53	80	73.7	483	321	336	380.0	0.0147273	2.4
YGR189C	99	106	123	109.3	369	802	673	614.7	0.0108457	2.5
YPL028W	129	74	85	96.0	571	456	555	527.3	0.0107621	2.5
YBL003C	57	41	85	61.0	355	290	361	335.3	0.0111530	2.5
YDR077W	946	575	785	768.7	3495	4029	5248	4257.3	0.0098395	2.5
YOL058W	180	183	93	152.0	877	1202	604	894.3	0.0087498	2.6
YGR176W	15	18	4	12.3	101	70	45	72.0	0.0113183	2.6
YLR110C	2435	2254	943	1877.3	12005	13260	7557	10940.7	0.0083031	2.6
YGR061C	32	27	13	24.0	70	223	122	138.3	0.0078649	2.6
YDR019C	17	10	15	14.0	38	105	97	80.0	0.0074738	2.6
YJL159W	645	597	426	556.0	1962	4582	3955	3499.7	0.0067043	2.6
YJR048W	172	165	153	163.3	1325	1246	684	1085.0	0.0066635	2.7
YMR122W-A	783	423	416	540.7	2766	3492	3628	3295.3	0.0063054	2.7
YIL117C	23	37	49	36.3	91	339	306	245.3	0.0061948	2.7
YKL096W	39	41	19	33.0	85	325	248	219.3	0.0060226	2.7
YOR128C	29	55	43	42.3	92	425	379	298.7	0.0055228	2.7
YPL163C	30	29	18	25.7	167	233	116	172.0	0.0057790	2.7
YNL289W	11	10	16	12.3	89	86	81	85.3	0.0049730	2.8
YLR194C	118	89	104	103.7	560	819	812	730.3	0.0037490	2.9
YKR091W	15	15	14	14.7	52	181	185	139.3	0.0021226	3.1
YPL231W	62	57	38	52.3	407	506	460	457.7	0.0018246	3.1
YGL055W	55	53	33	47.0	436	534	308	426.0	0.0015124	3.2
YKL096W-A	616	353	388	452.3	4112	3650	4389	4050.3	0.0014370	3.2
YPL187W	122	135	74	110.3	1181	1283	643	1035.7	0.0013878	3.2
YLR413W	14	18	15	15.7	127	148	177	150.7	0.0013095	3.2
YLR359W	31	44	49	41.3	143	644	569	452.0	0.0009093	3.3
YLR058C	35	55	51	47.0	122	782	693	532.3	0.0008194	3.4
YAR015W	58	61	23	47.3	262	792	412	488.7	0.0007654	3.4
YKR080W	24	37	37	32.7	99	571	489	386.3	0.0006726	3.5

(be continued)

Gene	D452-2				SPD				pValue	log2 Fold Change
	RPKM-1	RPKM-2	RPKM-3	Means	RPKM-1	RPKM-2	RPKM-3	Means		
YMR120C	17	25	13	18.3	100	629	284	337.7	0.0000706	4.2
YKL163W	29	20	12	20.3	109	656	318	361.0	0.0000732	4.2

Appendix 1.2. D452-2 VS DT

Gene	D452-2				DT				pValue	log2 Fold Change
	RPKM-1	RPKM-2	RPKM-3	Means	RPKM-1	RPKM-2	RPKM-3	Means		
YBL107W-A	21	16	9	15.3	0	0	0	0.0	0.010133	-4.9
YHR145C	18	24	46	29.3	7	2	2	3.7	0.014432	-2.7
YMR120C	17	25	13	18.3	67	144	83	98.0	0.013032	2.4
YIL160C	12	9	3	8.0	74	38	31	47.7	0.012897	2.5
YOL084W	11	9	8	9.3	92	42	27	53.7	0.011570	2.5
YDR536W	12	12	15	13.0	90	81	42	71.0	0.009183	2.6
YDL222C	24	27	19	23.3	186	161	68	138.3	0.008690	2.6
YKL163W	29	20	12	20.3	58	195	111	121.3	0.007598	2.6
YDL023C	36	63	26	41.7	307	368	154	276.3	0.005290	2.8
YKL005C	52	63	32	49.0	362	378	264	334.7	0.004493	2.8
YDL022W	50	91	50	63.7	482	530	264	425.3	0.004237	2.8
YKL004W	167	161	101	143.0	1392	1332	881	1201.7	0.001955	3.1
YLL028W	147	99	131	125.7	1298	1069	1471	1279.3	0.000843	3.4
YKL003C	152	134	149	145.0	4250	5025	5600	4958.3	0.000003	5.1

Appendix 1.3. DT VS SPD

Gene	DT				SPD				pValue	log2 Fold Change
	RPKM-1	RPKM-2	RPKM-3	Means	RPKM-1	RPKM-2	RPKM-3	Means		
YCR021C	590	765	826	727.0	12	22	21	18.3	0.000002	-5.3
YKL003C	4250	5025	5600	4958.3	164	147	122	144.3	0.000003	-5.1
YLL028W	1298	1069	1471	1279.3	60	33	43	45.3	0.000008	-4.8
YHR185C	2	4	0	2.0	0	0	0	0.0	0.013128	-4.6
YAR035C-A	8	23	12	14.3	0	0	0	0.0	0.013394	-4.6
YLR013W	5	2	2	3.0	0	0	0	0.0	0.014134	-4.6
YLR307C-A	261	192	189	214.0	7	8	11	8.7	0.000041	-4.5
YJR005C-A	317	223	284	274.7	14	14	8	12.0	0.000042	-4.5
YHL045W	10	5	6	7.0	0	2	0	0.7	0.010833	-3.6
YKL004W	1392	1332	881	1201.7	132	99	75	102.0	0.000475	-3.6
YGR139W	11	25	26	20.7	1	4	0	1.7	0.003103	-3.5
YHL046C	10	25	9	14.7	1	0	2	1.0	0.005970	-3.5
YDL243C	6501	5815	4214	5510.0	452	426	543	473.7	0.000611	-3.5
YFL015W-A	3	11	13	9.0	0	0	3	1.0	0.013943	-3.5
YMR244W	161	208	248	205.7	10	23	25	19.3	0.000691	-3.5
YOL165C	56	53	69	59.3	4	4	9	5.7	0.001292	-3.4
YLL055W	81	75	95	83.7	7	5	13	8.3	0.000963	-3.4
YHR126C	67	84	125	92.0	11	8	6	8.3	0.001337	-3.3
YLR134W	6204	4176	3368	4582.7	492	406	466	454.7	0.001090	-3.3
YOR388C	28	25	23	25.3	3	2	3	2.7	0.002154	-3.2
YGR142W	738	689	684	703.7	88	66	80	78.0	0.001518	-3.2
YEL045C	48	52	57	52.3	9	6	2	5.7	0.003113	-3.1
YPL021W	13	18	23	18.0	1	1	4	2.0	0.005323	-3.1
YNL277W-A	26	27	21	24.7	2	3	4	3.0	0.011665	-3.0
YFL056C	4697	2623	4115	3811.7	380	341	680	467.0	0.002437	-3.0
YKL005C	362	378	264	334.7	41	53	32	42.0	0.002545	-3.0
YPL058C	203	222	215	213.3	29	26	26	27.0	0.002594	-3.0
YFL057C	7991	4642	7038	6557.0	866	510	1177	851.0	0.002771	-3.0

(be continued)

Gene	DT				SPD				pValue	log2 Fold Change
	RPKM-1	RPKM-2	RPKM-3	Means	RPKM-1	RPKM-2	RPKM-3	Means		
YIR013C	21	18	11	16.7	0	2	4	2.0	0.013769	-2.9
YFL055W	160	95	99	118.0	11	17	22	16.7	0.004248	-2.8
YDR535C	21	42	12	25.0	6	1	3	3.3	0.009177	-2.8
YCL026C-A	632	315	515	487.3	73	47	94	71.3	0.005055	-2.8
YLL056C	3074	3280	3850	3401.3	405	479	845	576.3	0.007396	-2.6
YHR139C	37	22	11	23.3	3	6	2	3.7	0.010395	-2.6
YDR536W	90	81	42	71.0	5	18	17	13.3	0.008385	-2.6
YNL194C	121	105	29	85.0	8	20	13	13.7	0.009566	-2.6
YNL195C	141	98	45	94.7	10	18	17	15.0	0.009862	-2.5
YJR095W	37	22	15	24.7	3	7	2	4.0	0.012361	-2.5
YIL057C	85	33	25	47.7	7	5	12	8.0	0.012535	-2.5
YGL007W	71	80	62	71.0	9	11	15	11.7	0.012166	-2.5
YLL057C	115	103	107	108.3	13	24	23	20.0	0.009950	-2.5
YLR142W	249	275	199	241.0	21	56	63	46.7	0.010311	-2.5
YBR008C	1565	1455	1505	1508.3	275	204	342	273.7	0.011155	-2.5
YPL240C	545	629	725	633.0	67	140	166	124.3	0.012424	-2.4
YKR076W	902	578	910	796.7	147	98	214	153.0	0.013088	-2.4
YOL084W	92	42	27	53.7	8	10	11	9.7	0.014110	-2.4
YBL003C	41	49	53	47.7	355	290	361	335.3	0.005081	2.8
YDR034C-A	0	0	0	0.0	7	10	23	13.3	0.003537	5.5

Appendix 2

**Simple amino acid tags improve both expression
and secretion of *Candida antarctica* lipase B in
recombinant *Escherichia coli***

Abstract

Escherichia coli is the best-established microbial host strain for production of proteins and chemicals, but has a weakness for not secreting high amounts of active heterologous proteins to the extracellular culture medium, of which origins belong to whether prokaryotes or eukaryotes. In this study, *Candida antarctica* lipase B (CalB), a popular eukaryotic enzyme which catalyzes a number of biochemical reactions and barely secreted extracellularly, was expressed functionally at a gram scale in culture medium by using a simple amino acid-tag system of *E. coli*. New fusion tag systems consisting of a pelB signal sequence and various anion amino acid tags facilitated both intracellular expression and extracellular secretion of CalB. Among them, the N-terminal five aspartate tag changed the quaternary structure of the dimeric CalB and allowed production of 1.9 g/L active CalB with 65 U/ml activity in culture medium, which exhibited the same enzymatic properties as the commercial CalB. This PelB-anion amino acid tag-based expression system for CalB can be extended to production of other industrial proteins hardly expressed and exported from *E. coli*, thereby increasing target protein concentrations and minimizing purification steps.

Keywords: *Candida antarctica* lipase B/ *Escherichia coli*/ extracellular secretion/ polyanionic amino acid tag/ quaternary structure change

Introduction

Escherichia coli is one of the first choices for production of various proteins and chemicals. To meet these demands and to produce foreign proteins massively, enormous genetic tools and microbial variants have been developed. Although the *E. coli* systems have been used for commercialization of therapeutic or industrial proteins, some drawbacks limit their expansion to various applications: formation of insoluble protein aggregates, protein mis-folding, lack of post-translational modification machineries and poor ability of protein secretion (Choi and Lee, 2004; Mergulhao et al., 2005). Although technologies have been developed to overcome those hurdles, extracellular secretion of proteins is still limited. *E. coli* has the endogenous protein excretion systems. Development of many signal peptides guiding the target proteins to the periplasmic space, and overexpression of periplasmic machineries for correct folding and secretion increased the possibility of extracellular protein production. In most Gram-negative bacteria, the SecB-dependent pathway which allows proteins to cross the inner membrane is extended by terminal branches of the general secretion pathway (GSP) that permit extracellular secretion (Pugsley, 1993a). A periplasmic protein adopts tertiary and even quaternary structures in order to be recognized by the

secretion machinery, but no signal for extracellular secretion has been verified (Sandkvist, 2001). Yet *E. coli* can produce a milligram scale of target proteins in the periplasmic space or in culture medium. Two or three cases reported a gram scale production, however, of which proteins were originated from prokaryotes (Choi and Lee, 2004; Mergulhao et al., 2005).

The lipase B from a yeast *Candida antarctica* (CalB) is a representative eukaryotic lipase studied in over 450 research papers currently listed on the PubMed and catalyzes a surprising diversity of chemical reactions including many different regio- and enantio-selective syntheses (Anderson et al., 1998). CalB has three disulfide bonds and a homodimeric structure. To express CalB actively and massively in *E. coli*, various genetic and microbial techniques have been attempted such as its binding to various signal sequences, amino acid tags and expression-boosting domains, co-expression of helper proteins for easy protein folding and deletion of the related chromosomal genes (Sorensen and Mortensen, 2005). In spite of enormous efforts, however, recombinant CalBs were accumulated in the *E. coli* cytoplasm mostly as a form of insoluble inclusion body, or were secreted at a milligram scale in a few cases (Blank et al., 2006). It has been presented that polycationic amino acid tags fused at the C-terminal of CalB dramatically increased the

soluble amount of CalB in the cytoplasm (Jung et al., 2011). However, such an enhancement of CalB solubility was not proportional to an increase in CalB specific activity, which is similar to that of other studies because of an inherent protein folding problem in *E. coli*. To date, affinity tags with polycationic amino acids such as histidines, arginines or lysines have been developed only for easy purification of the target protein among crude protein solution (Kweon et al., 2005; Lee et al., 2009).

Meanwhile, the signal peptide is necessary for the protein export and the mature part of the exported protein also plays an important role in its translocation. An attaching the signal sequence to a cytoplasmic protein alone does not ensure its translocation through an inner membrane (Tomassen et al., 1985). There are some reports that an alteration in the N-terminal end of an exported protein exerts a dramatic effect on the protein transport (Le Loir et al., 1998; Li et al., 1988). The exported proteins commonly have a negative charge in the first 5 amino acid residues (MacIntyre et al., 1990), whereas CalB has only one at position +6. This fact suggests that an adequate alteration of the N-terminal end of CalB could improve transport efficiency across the inner membrane.

Based on this hypothesis, in this study, novel amino acid tag systems

were developed to increase an expression level and extracellular transport efficiency of CalB in *E. coli*.

Materials and Methods

Bacterial strains and plasmids

E. coli TOP10 and BL21 star (DE3) (Invitrogen, Grand Island, NY, USA) strains were used for genetic manipulation and CalB production, respectively. The CalB gene and its recombinant genes were located behind the *T7* promoter in derivatives of plasmid pET-26b(+) (EMD Millipore, Darmstadt, Germany) and their transcription was induced by adding isopropyl- β -D-thiogalactopyranoside (IPTG). Plasmid pColdIII-CalB containing the open reading frame of the CalB gene from *Candida antarctica* ATCC32657 (Jung et al., 2011) was used as the source of the CalB gene. Plasmids pKD46, pKD13 and pCP20 for *E. coli* chromosomal gene deletion (Datsenko and Wanner, 2000) were provided by the *E. coli* Genetic Resource Center (Yale University, USA).

Genetic manipulation

The CalB genes were amplified by the polymerase chain reaction (PCR) using plasmid pColdIII-CalB as the PCR template. PCR DNA primers used for CalB amplification were designed to be specific for the 5'-, 3'-end or a mutation site of the CalB gene and contain the recognition site

of DNA digestion enzyme as shown in Table S1. To amplify the CalB genes, the DNA primers were formulated with a forward oligomer and CalB[R]. For example, CalB[F] or D5-CalB[F] and CalB[R] were used to express the gene coding for the authentic CalB without any tags or recombinant CalB with the N-terminal 5-aspartate tag, respectively. To combine each recombinant CalB gene with the gene coding for the N-terminal pelB leader sequence in plasmid pET-26B(+), the forward primers were designed to remove the transcriptional initiation codon (ATG) of the CalB gene and locate the CalB gene behind the leader sequence in frame. The DNA sequence coding for each amino acid tag was designed as described in the previous report (Jung et al., 2011). After gene amplification, all the PCR products were cut with appropriate restriction enzymes (Table S1) and ligated with plasmid pET-26b(+) digested with the same enzymes. Naming of the resulting plasmids followed such type: pET-26b(+)-the name of the expressed CalB, for example, pET-26b(+)-P-D5-CalB for P-D5-CalB expression. The nucleotide sequence of the recombinant CalB genes was verified by DNA sequencing. Their names and schematic structure are shown in Fig. 1.

To construct five variants of P-D5-CalB (L169R, V174R, V246R, P285R and A308R), overlap extension PCR was performed with site-

specific PCR primers (Table S1). For example, two DNA fragments were amplified with two PCR primer sets of P-D5-CalB[F] and L169R[R], and L169R[F] and CalB[R]. Using the two DNA fragments as PCR templates and primers of P-D5-CalB[F] and CalB[R], the recombinant CalB L169R gene was obtained and then cloned into plasmid pET-26b(+) as described above.

For the His-tag mediated purification of CalB and D5-CalB, the CalB genes were amplified with the forward primers, P-CalB[F] or P-D5-CalB[F], and the reverse primer, CalBXaHis[R] (Table S1), using pColdIII-CalB plasmid as the template. The PCR products were ligated with plasmid pET-26b(+) as described above. These new constructs contained the Factor Xa recognition sequence and the His-tag sequence in a row at each C-terminus.

Deletion of chromosomal genes in *E. coli* BL21 star (DE3)

As the previous report (Datsenko and Wanner, 2000), plasmid pKD13 containing the kanamycin resistance gene was used as a template for the construction of the *gspDE* deletion cassette. Two PCR primers of d_gspDE[F] and d_gspDE[R] were designed to contain 40 nucleotides of the 5'- and 3'-end sequences of the chromosomal *gspDE* gene and the kanamycin resistance gene fragments (Table S1). After

transformation of plasmid pKD46 into *E. coli* BL21 star (DE3), a 1.4 kb PCR product containing the *gspDE* gene and kanamycin resistance gene was introduced into *E. coli* BL21 star (DE3)/pKD46 by electroporation. The clones resistant on kanamycin were selected and transformed with plasmid pCP20 containing the FLP recombinase gene for removal of the kanamycin resistance gene. After heat treatment at 42°C, the transformants deficient in the *gspDE* gene and without the kanamycin resistance gene and plasmid pCP20 were collected. The *gspDE* deletion was confirmed by the PCR using two PCR primers of ch_gspDE[F] and ch_gspDE[R] (Table S1).

Culture conditions

The recombinant *E. coli* BL21 star (DE3) cells harboring each CalB expression vector were pre-cultured in LB medium (5 g/L yeast extract and 10 g/L bacto-trypton) at 37°C and 230 rpm for 12 h. After harvesting the cells, the cell pellets were used for inoculation. A batch culture using a 500 mL-scale baffled flask (Nalgene, Rochester, NY, USA) was carried out at 37°C and 230 rpm in 100 ml of a defined medium (pH 6.8) containing (per liter) 20 g glucose, 4 g (NH₄)₂HPO₄, 13.5 g KH₂PO₄, 1.7 g citric acid, 1.4 g MgSO₄·7H₂O and 10 ml trace metal solution. The trace metal solution was composed of per liter of 5 mol HCl, 10 g FeSO₄·7H₂O, 2.25 g ZnSO₄·7H₂O, 1 g CuSO₄·5H₂O,

0.5 g $\text{MnSO}_4 \cdot 4\text{H}_2\text{O}$, 0.23 g $\text{Na}_2\text{B}_4\text{O}_7 \cdot 10\text{H}_2\text{O}$, 2 g CaCl_2 , 0.1 g $(\text{NH}_4)_6\text{Mo}_7\text{O}_{24}$. At the logarithmic phase of growth (optical density at 600 nm (OD_{600}) $\approx 0.8 \sim 1.2$), expression of recombinant CalBs was induced by adding IPTG at a final concentration of 0.2 mM. The induced cells were cultivated at 20°C and 200 rpm for additional 20 h.

A fed-batch cultivation was carried out in a 2.5 L-scale bioreactor (Kobiotech Co., Incheon, Korea) containing 1 L of the same defined medium and at 37°C, 1,200 rpm and 1 vvm of air supply. After depletion of 20 g/L initial glucose, a feeding solution containing 800 g/L glucose and 20 g/L $\text{MgSO}_4 \cdot 7\text{H}_2\text{O}$ was automatically added by a feeding strategy of the pH-stat operation mode (Park et al., 2005). At the $\text{OD}_{600\text{nm}}$ reached around 120, IPTG was added at the same manner of the batch culture and temperature was shifted to 20°C.

Protein fractionation

To collect the CalBs secreted from the recombinant cells, the culture broth was centrifuged at 15,000 rpm for 10 min and its supernatant was named the medium fraction. To obtain the intracellular protein fractions, the collected culture broth was concentrated or diluted to adjust its OD_{600} to be 10. This broth was centrifuged at 13,000 rpm and 4°C for 10 min. The cell pellets were resuspended in 50 mM Tris-Cl buffer (pH

9.0) and disrupted by an ultrasonic machine (Cole-Parmer, USA) on ice. The total, soluble and insoluble fractions of intracellular proteins were prepared as described in the previous report (Jung et al., 2011).

Proteins in the periplasm were isolated by an osmotic shock method as previously described (Neu and Heppel, 1965) with some modifications. The cell pellets were resuspended in an ice-cold Tris-HCl buffer (33 mM, pH 8.0) containing 20% (w/v) sucrose and 0.5 mM Na₂EDTA. After shaking for 10 min at room temperature, the cells were harvested by centrifugation at 13,000 rpm and 4°C for 10 min. The supernatant was removed and the cell pellets were suspended in 0.5 ml of ice-cold water. After shaking for 10 min, the cell suspension was centrifuged at 13,000 rpm and 4°C for 10 min. The pellets and supernatant were called the cytoplasm and periplasmic fractions, respectively, and stored at -20°C until assay.

Protein purification

For enzymatic characterization of recombinant CalBs, *E. coli* BL21 star (DE3) harboring plasmid pET-26b(+)-P-CalB or pET-26b(+)-P-D5-CalB was cultured by the fed-batch fermentation strategy. Recombinant CalBs presented in the culture medium were collected and purified with the His-tag mediated purification procedure. After the culture broth was

centrifuged at 13,000 rpm and 4°C for 10 min, 500 ml of the supernatant was mixed with 500 ml of a His-tag binding buffer containing 20 mM NaH₂PO₄ (pH 7.4), 0.5 M NaCl and 30 mM imidazole. The prepared samples were loaded into a HisTrap FF column (1 mL) packed with the Ni Sepharose Fast Flow (GE Healthcare, Buckinghamshire, UK), followed by washing with 10 ml of the His-tag binding buffer at a flow rate of 1.0 ml/min. An ÄCTA FPLC (GE Healthcare) was used to monitor the protein elution. The His-tag binding buffer with a linear gradient of imidazole from 30 to 500 mM was continuously flowed into the column. The proteins eluted from the column were collected.

To remove the His-tag at the C-terminus of the purified CalBXaHis and D5-CalBXaHis, the eluents were treated with Factor Xa protease in accordance with the manufacturer's protocol (New England Biolabs, Ipswich, UK), followed by loading into a HiLoad XK-16 Superdex 200 prep-grade column (GE Healthcare), which was previously equilibrated with 20 mM Tris-HCl (pH 8.0) and 200 mM NaCl. The collected eluents with the purified CalB or D5-CalB were used for enzyme analysis.

Enzyme assays

To visualize recombinant CalBs, the protein samples were fractionated by sodium dodecyl sulfate–polyacrylamide gel electrophoresis (SDS-PAGE) with 12% acrylamide. The protein bands on SDS-PAGE gels were stained with Coomassie brilliant blue R-250 and quantitatively analyzed by a densitometer.

To determine CalB activity, the reaction solution was formulated with 175 μ l of 50 mM Tris-HCl buffer (pH 9.0), 5 μ l of 20% (w/w) Triton X-100 and 10 μ l of 10 mM *p*-nitrophenyl butyrate (*p*-NPB, Sigma, USA) dissolved in absolute iso-propanol. The absorbance change at 30°C and 400 nm of wavelength was monitored by a 96-well microplate reader (Molecular Devices, Sunnyvale, CA, USA) after addition of 10 μ l enzyme solution. One unit (U) of CalB activity was defined as the amount of CalB able to release 1 μ mol *p*-NP (*p*-nitrophenol) from *p*-NPB per minute. Specific CalB activity was calculated by the division of CalB activity by dry cell weight.

To determine alkaline phosphatase (PhoA) activity, 10 μ l of the crude enzyme solution was added to 190 μ l reaction buffer containing 0.1 M Tris-HCl buffer (pH 8.0), 1 mM MgCl₂ and 1 mM *p*-nitrophenyl phosphate (*p*-NPP, Sigma, USA). The absorbance change at 37°C and 400 nm of wavelength was monitored by a 96-well microplate reader (Molecular Devices, Sunnyvale, CA, USA). One unit (U) of PhoA

activity was defined as the amount of PhoA able to release 1 μmol *p*-NP (*p*-nitrophenol) from *p*-NPP per minute. Specific PhoA activity was calculated by the division of PhoA activity by dry cell weight.

To characterize the enzymatic properties of D5-CalB, a standard CalB (Sigma Cat No. 62288), recombinant CalB and D5-CalB purified as described above were used. Using initial *p*-NPB concentrations of 125, 250, 500, 1000 and 1500 μM , kinetic constants of k_{cat} , K_m and k_{cat}/K_m were obtained from each Lineweaver–Burk plot. The optimal activities for CalB were determined with various buffers: pH 6.0 and 7.0, 50 mM sodium phosphate buffer; pH 8.0, 9.0 and 10.0, 50 mM Tris-HCl buffer; pH 11.0, 50 mM borate buffer. The optimal reaction temperatures were decided in a temperature range of 10°C to 60°C. To assess the enzyme stability, the standard and recombinant CalBs were incubated in 50 mM Tris-HCl buffer (pH 9.0) for 15 days at 4°C or 24 hours at 30°C.

Crystallization and X-ray data collection

Crystals of D5-CalB were grown by the sitting-drop vapor diffusion method at 24°C. A purified D5-CalB solution of 9 mg/mL in 20 mM Tris-HCl (pH 8.0) and 200 mM NaCl was mixed with an equal volume (1 μl each) of the reservoir solution consisting of 100 mM phosphate-citrate (pH 4.2) and 40% (v/v) polyethylene glycol (PEG) 600. The

crystals of D5-CalB with approximate dimensions of 0.1 mm x 0.1 mm x 0.2 mm were obtained within a few days. The crystals were frozen without any cryoprotectant solution.

X-ray diffraction data of the D5-CalB crystal was collected at 100 K on an ADSC Quantum 270 CCD detector system (Area Detector Systems Corporation, Poway, CA, USA) located at the experimental station BL-5C of the Pohang Light Source, Korea. For each image, the crystal was rotated by 1°. The raw data were processed and scaled using the *HKL-2000* program suite (Otwinowski and Minor, 1997). The statistics of data collection were summarized in Table S2. The D5-CalB crystal belongs to the space group $P6_5$, with unit cell parameters of $a = 123.66$ Å, $b = 123.66$ Å, and $c = 191.85$ Å (Table S2). Four monomers of D5-CalB are present in the asymmetric unit, giving a crystal volume per protein mass (V_M) of 3.10 Å³ Da⁻¹ and a solvent content of 60%, respectively.

Structure determination and refinement

The structure of D5-CalB was solved by the molecular replacement method using the monomer model of *Candida antarctica* lipase B (PDB ID: 1TCA). A cross-rotational search followed by a translational search was performed using the *Phaser* program (McCoy et al., 2005).

Subsequent manual model building and restrained refinement were carried out using the *COOT* program (Emsley and Cowtan, 2004) and *REFMAC5* program (Murshudov et al., 1997), respectively. Several rounds of model building, simulated annealing, positional refinement, and individual *B*-factor refinement were performed. The refinement statistics were listed in Table S2. The atomic coordinates and structure factors (PDB ID codes 3W9B for D5-CalB) were deposited in the Protein Data Bank.

Results and Discussion

Design of amino acid tag systems for extracellular production of CalB

Among the 20 standard amino acids, two acidic (negative-charged) amino acids (aspartate (D) and glutamate (E)) and their amides with polar uncharged side chains (asparagine (N) and glutamine (Q)), and one basic (positive-charged) amino acid (lysine (K)) were chosen as the N-terminal tag partners. To express and secrete recombinant CalBs in *E. coli*, the 5'-end of the CalB gene without its own translational initiation codon was combined with the genes coding for the pelB signal sequence and five-repeated amino acids in a row. Schematic diagrams for the CalB expression cassettes in pET-26b(+) plasmid derivatives and their names are displayed in Fig. 1A.

Effects of amino acid tags on CalB expression patterns

To investigate the effect of five types of the amino acid tags on CalB expression, recombinant *E. coli* BL21 star (DE3) strains overexpressing each recombinant CalB gene were cultured batch-wise and crude CalB enzymes present in the intracellular and extracellular fractions were subjected to lipase activity (Fig. 1B) and SDS-PAGE (Fig. S1) analyses.

The controls of CalB and D5-CalB without the signal sequence showed a basal level of lipase activity in both fractions. Combination of the pelB signal sequence facilitated intracellular and extracellular expression of CalB. Moreover, four types of the amino acid tags except for the basic lysine tag increased an average intracellular lipase activity to 0.24 ± 0.06 U/mg cell, which was 2.4 times higher than that of the P-CalB. Among them, the negative-charged tags composed of 5 aspartates (P-D5-CalB) and glutamates (P-E5-CalB) dramatically triggered CalB expression in culture medium. The neutral tags for P-N5-CalB and P-Q5-CalB also improved the extracellular production of CalB, but their extents were lower than the negative-charged tags. The basic lysine tag prevented CalB expression in both the intracellular and extracellular spaces, of which reason was probably that poly lysine segments inhibited protein transport through the SecYEG protein translocation channel by electrostatic interaction (Liang et al., 2012). The highest specific lipase activities of 2.2 ± 0.7 U/mg cell in the culture broth and 0.3 ± 0.08 U/mg cell in the intracellular fraction were obtained for recombinant *E. coli* BL21 star (DE3) overexpressing P-D5-CalB, which were 8.4- and 3.0-times higher than the corresponding values of the case of CalB alone. As well as the enzyme activity assay, SDS-PAGE analysis also showed the high secretion of recombinant CalB in the culture medium (Fig. S1). The protein band of the secreted

CalB for the case of P-D5-CalB (Lane E) was much thicker than other cases. It was located at a slightly higher position in the gel than the theoretical molecular weight (33 kDa) because the amino acid tag still remained at the N-terminus and the pelB signal sequence was cut off by a signal peptidase, which was verified by the N-terminal amino acid sequencing of recombinant CalBs present in the intracellular and extracellular spaces (data not shown). Meanwhile, it was doubtful that the amino acid tags could disorder the outer membrane and hence increase the recombinant CalB secretion. The enzyme activity of a periplasmic enzyme, alkaline phosphatase, was assayed in the intracellular protein fraction and culture medium of BL21 star (DE3) strains expressing P-CalB and P-D5-CalB. As shown in Fig. S2, the alkaline phosphatase activity was not detectable in the culture medium, confirming the exact secretion of recombinant CalBs without outer membrane leakage.

To investigate the effect of negative charge distribution at the N-terminus on CalB expression and secretion, a series of amino acid tags consisting of 1-9 aspartates was fused with the N-terminal of CalB as shown in Fig. 1A. More than one aspartate tag increased intracellular production of recombinant CalBs to an average specific lipase activity of 0.22 ± 0.12 U/mg cell, which was 2.2 times higher than 0.10 ± 0.01

U/mg cell for P-CalB (Fig. 1C). Other than the enhancement of intracellular expression, more repetition of aspartate in the N-terminus dramatically increased extracellular secretion of CalB, of which extents depended on its length. Interestingly, more than six aspartates inhibited or did not affect CalB expression both intracellularly and extracellularly, indicating that five aspartates is the optimum amino acid tag for CalB expression. According to our hypothesis, modulation of negative charge around the N-terminal of CalB not only increased intracellular production but also facilitated the extracellular secretion of active CalB with the aid of the pelB signal sequence. To apply this strategy to other proteins, a target protein should first be translocated to the periplasmic space by the SecB secretion machinery and adopt its proper tertiary and quaternary structures in the periplasmic space as the same as recombinant CalBs.

Batch and fed-batch production of recombinant CalB

Actually, the pelB signal sequence is known to deliver the target protein from the cytoplasm to the periplasm (Mergulhao et al., 2005). Considering the above results, the five aspartate tag is supposed to play a role of protein transport across the outer membrane. To investigate the role of the five aspartates tag, batch cultures of the recombinant *E. coli* strain overexpressing P-CalB or P-D5-CalB were carried out and

lipase activities of recombinant CalBs collected over time in the cytoplasmic and periplasmic spaces of the cells, and in the culture medium were analyzed. As shown in Figs. 2 A and B, the growth patterns of the two recombinant *E. coli* strains were almost identical. For lipase localization, the specific lipase activity of D5-CalB (a processed form of P-D5-CalB) in the culture medium was about 6.1 times higher than that of CalB (a processed form of P-CalB) in the broth whereas D5 combination only increased the specific activity of the periplasmic D5-CalB by a two-fold, relative to that of CalB. (Table S3). Although the relative amount of both extracellular CalB and D5-CalB increased over time, D5-CalB had much higher tendency of extracellular secretion than CalB. These results indicated that the recombinant D5-CalB in the periplasm has higher efficiency of transport across the outer membrane than the authentic CalB.

In many cases, an elevation of protein secretion mediated by such genetic or cellular engineering was not realized in high-cell density cultivation (Dresler et al., 2006a). To achieve a high-cell density and hence high concentrations of active CalBs, fed-batch fermentations of the recombinant *E. coli* BL21 star (DE3) strain harboring plasmid pET-26b(+)-P-CalB (Fig. 3A) or pET-26b(+)-P-D5-CalB (Fig. 3B) were carried out by using the pH-stat strategy. Both strains were grown in

the same pattern before IPTG induction. However, IPTG induction did not influence the growth of the recombinant cells overproducing P-D5-CalB, whereas it significantly inhibited the growth of the control strain overexpressing P-CalB. As expected, intracellular and extracellular D5-CalBs were expressed gradually or sharply after IPTG induction and their expression was visualized by SDS-PAGE analysis (Fig. 3C). Eventually, the fed-batch culture of the BL21 star (DE3) harboring pET-26b(+)-P-D5-CalB resulted in 95.6 g/L of the maximum dry cell weight, 223 U/ml of intracellular lipase activity and 65.4 U/ml of extracellular activity in the culture broth. These values were 1.4-, 5.0- and 8.1-fold higher than the corresponding values of the CalB alone (Table S3), indicating that the 5 aspartate tag system triggers both intracellular and extracellular expression of CalB even in the high-cell density fermentation. When the activities were converted to titers using the specific activity of D5-CalB, the extracellular titer of D5-CalB was determined to be 1.9 g/L. The activity and titer of CalB secreted in the culture broth of recombinant *E. coli* were the highest values ever reported (Table S4). Meanwhile, pathogenic *E. coli* strains are known to release some particles of outer membrane into the culture medium during high-cell density culture, which may be able to entrap the secreted proteins (Bielaszewska et al., 2013; Kesty et al., 2004). Considering the high expression of functional CalB and no information

about the membrane release in the BL21 star (DE3) strain, CalB expressed in the medium fraction seemed not to be trapped in any organelles including outer membrane vesicles.

Biochemical properties of recombinant CalBs

It is doubtful that the amino acid tagging can change the enzymatic characteristics of the authentic CalB. To assess the effects of the five aspartate tag on biochemical properties of CalBs, recombinant CalB and D5-CalB fused with the His-tag at their C-termini were collected from the culture broth after the fed-batch fermentation. After purification by the His-tag system and removal of the His-tag, the same protein concentration of the purified CalB and D5-CalB, and a commercially available CalB were subjected to determination of kinetic constants, optimal pH and temperature and thermal stability. As summarized in Table S5, D5-CalB possessed a 80% higher substrate affinity (K_m) than, and a similar rate constant (k_{cat}) to the commercial CalB, indicating that the purified D5-CalB and CalB showed 1.7 and 1.3 times higher k_{cat}/K_m value than the commercial CalB, respectively. Although tagging with five aspartates did not affect the optimal reaction pH and temperature, D5-CalB exhibited a narrow activity range on temperature (Fig. S3). For thermal stability, both D5-CalB and the standard CalB maintained similar lipase activity over 15 day

incubation at 4°C and 24 hours at 30°C (Fig. S4). In general, the five aspartate tag improved somewhat the reaction efficiency of CalB and also hardly altered biochemical properties of D5-CalB.

Structural analysis of D5-CalB

An alteration of N-terminal charge distributions of CalB by fusion of the five aspartate tag increased both intracellular and extracellular expression of CalBs without considerable changes of enzymatic properties. To gain a further insight into the structural organization of the extracellular D5-CalB, the crystal structure of D5-CalB was solved at 2.9 Å resolution with a good map quality (Table S2 and Fig. S5) and compared it with the structure of the authentic CalB (PDB code 1LBS). The N-terminal fusion tag (five aspartates) of D5-CalB was disordered in all four monomers in the asymmetric unit and four monomers of D5-CalB in the asymmetric unit were almost identical to each other. When the monomer A was compared with the other monomers, the r.m.s. deviations averaged over the other monomers (chains B–D): 0.3 Å for 286 C α atom pairs. When the monomer A of the D5-CalB model was overlapped with the monomer A of the CalB, the r.m.s. deviations were 0.4 Å for 303 C α atoms, suggesting that all monomer structures of the D5-CalB of interest were similar to those of the authentic CalB. The

quaternary structure of D5-CalB, in contrast, was changed dramatically compared with the authentic CalB. A previous study strongly suggested that CalB forms a dimer-based oligomer in crystal (Uppenberg et al., 1995). Notably, D5-CalB also showed dimer-based packing in crystal but in a completely different two-fold symmetry (Fig. 4A). When $\alpha 10$ helices are colored in green to highlight the relative orientations of CalB and D5-CalB, two subunits of D5-CalB form a dimer by facing parallel $\alpha 10$ helices ($\alpha 10$ and $\alpha 10'$ from each subunit), whereas anti-parallel $\alpha 10$ helices for the authentic CalB.

To evaluate the effect of interfering the dimeric interactions of D5-CalB, five interacting amino acids at the dimer interface were mutated to arginine such as L169R, V174R, V246R, P285R, and A308R. Leu169 and Val174 make a hydrophobic core with the neighboring residue (Ala308) of the other monomer at the dimer interface (Fig. 4B). Another hydrophobic core consists of Val246 and Pro285 (Fig. 4C). Thus, it was expected that the mutation of the five interacting amino acids would destabilize this hydrophobic core and disrupt the dimerization of D5-CalB. The specific activities of the intracellular D5-CalB mutants were retained or slightly decreased relative to that of D5-CalB (Fig. 5A), confirming that the mutations of D5-CalB did not affect its active site and intracellular expression level. Meanwhile, all of

the mutations reduced the secretion of D5-CalBs and especially, the V246R mutant showed a 13 times lower specific activity in the culture medium than D5-CalB. Considering these differences of intracellular and extracellular activity changes, it could be assured that the interfacial residues observed in the dimerization interface contribute to form the different dimeric structure of D5-CalB which would facilitate the secretion of D5-CalB into the culture medium.

Roles of general secretion pathway in CalB secretion

E. coli is known to secrete proteins through the general secretion pathway (GSP) (Pugsley, 1993a), in which the secretory proteins were unveiled to be encoded by two divergent operons of *gspCDEFGHIJKLMO* and *gspAB* from *E. coli* K12 (Blattner et al., 1997) but their actions on exoprotein secretion have not been revealed clearly (Francetic and Pugsley, 1996; Pugsley and Francetic, 1998). It was hypothesized that the *gsp* genes encoding a putative secretin would be a factor specifically affecting transport efficiency of the D5-CalB across the outer membrane. A *gspDE*-deficient background strain (designated here as Δ *gspDE*) lacking a part of the 15 *gsp* genes and its transformants overexpressing P-CalB or P-D5-CalB were constructed. The overall fermentation profiles of the strains Δ *gspDE*/P-CalB and Δ *gspDE*/P-D5-CalB were similar to those of P-CalB and P-D5-CalB,

respectively, except for a reduced extracellular secretion level of D5-CalB (Fig. S6). Both cytoplasmic and periplasmic expression of CalB and D5-CalB were not affected by the *gspDE* deletion (Fig. 5B). The destruction of a part of the GSP secreton resulted in a 31% decreased extracellular level of D5-CalB and did not prevent the secretion of the authentic CalB significantly. This result indicated that a transport efficiency enhancement of D5-CalB was partially ascribed to the specific recognition of the quaternary structure by the GSP components, which coincides with the secretion of elastase or extotoxin A in recombinant *E. coli* (Braun et al., 1996; Voulhoux et al., 2000).

Conclusions

As an example for the production of foreign proteins in *E. coli*, efforts to increase CalB production have focused on solubilization strategies in the cytoplasmic space or merely targeting this enzyme to the periplasmic space (Blank et al., 2006; Liu et al., 2006). However, these approaches are still limited by an inherent low expression yield. To solve this problem, CalB was targeted to the culture medium and improved its transport efficiency across the both inner and outer membranes using the poly amino acid tag systems along with the pelB signal sequence. Among several amino acid tags with different types and lengths, the five-aspartate tag fused at the N-terminal of CalB gave a remarkable improvement of protein secretion. As shown in a proposed mechanism (Fig. 6), the high density of negative charge in the N-terminus induces more translocation of D5-CalB from the cytoplasm to the periplasm and modifies its quaternary structure in the periplasm. The GSP machinery takes up the dimer form of D5-CalB easier than the authentic CalB structure, and hence a high amount of active recombinant CalB with the same enzymatic properties was obtained. The polyanionic amino acid tags also provide an efficient way for protein purification by anion-exchange chromatography as demonstrated previously (Lee et al., 2009). In conclusion, our approach

successfully improved extracellular production of CalB hardly expressed in *E. coli*.

References

- Anderson EM, Larsson KM, Kirk O. 1998. One biocatalyst–many applications: The use of *Candida antarctica* B-lipase in organic synthesis. *Biocatal Biotransfor* 16(3):181-204.
- Bielaszewska M, Ruter C, Kunsmann L, Greune L, Bauwens A, Zhang WL, Kuczus T, Kim KS, Mellmann A, Schmidt MA and others. 2013. Enterohemorrhagic *Escherichia coli* hemolysin employs outer membrane vesicles to target mitochondria and cause endothelial and epithelial apoptosis. *Plos Pathogens* 9(12).
- Blank K, Morfill J, Gump H, Gaub HE. 2006. Functional expression of *Candida antarctica* lipase B in *Escherichia coli*. *J Biotechnol* 125(4):474-483.
- Blattner FR, Plunkett G, 3rd, Bloch CA, Perna NT, Burland V, Riley M, Collado-Vides J, Glasner JD, Rode CK, Mayhew GF and others. 1997. The complete genome sequence of *Escherichia coli* K-12. *Science* 277(5331):1453-1462.
- Braun P, Tommassen J, Filloux A. 1996. Role of the propeptide in folding and secretion of elastase of *Pseudomonas aeruginosa*. *Mol Microbiol* 19(2):297-306.

- Choi JH, Lee SY. 2004. Secretory and extracellular production of recombinant proteins using *Escherichia coli*. *Appl Microbiol Biotechnol* 64(5):625-635.
- Datsenko KA, Wanner BL. 2000. One-step inactivation of chromosomal genes in *Escherichia coli* K-12 using PCR products. *Proc Natl Acad Sci USA* 97(12):6640-6645.
- Dresler K, van den Heuvel J, Muller RJ, Deckwer WD. 2006. Production of a recombinant polyester-cleaving hydrolase from *Thermobifida fusca* in *Escherichia coli*. *Bioprocess Biosyst Eng* 29(3):169-183.
- Emsley P, Cowtan K. 2004. Coot: model-building tools for molecular graphics. *Acta Crystallogr D Biol Crystallogr* 60(Pt 12 Pt 1):2126-2132.
- Francetic O, Pugsley AP. 1996. The cryptic general secretory pathway (gsp) operon of *Escherichia coli* K-12 encodes functional proteins. *J Bacteriol* 178(12):3544-3549.
- Jung HJ, Kim SK, Min WK, Lee SS, Park K, Park YC, Seo J-H. 2011. Polycationic amino acid tags enhance soluble expression of *Candida antarctica* lipase B in recombinant *Escherichia coli*. *Bioprocess Biosyst Eng* 34(7):833-839.

- Kesty NC, Mason KM, Reedy M, Miller SE, Kuehn MJ. 2004. Enterotoxigenic *Escherichia coli* vesicles target toxin delivery into mammalian cells. *Embo Journal* 23(23):4538-4549.
- Kweon DH, Kim SG, Han NS, Lee JH, Chung KM, Seo JH. 2005. Immobilization of *Bacillus macerans* cyclodextrin glycosyltransferase fused with poly-lysine using cation exchanger. *Enzyme Microb Tech* 36(4):571-578.
- Le Loir Y, Gruss A, Ehrlich SD, Langella P. 1998. A nine-residue synthetic propeptide enhances secretion efficiency of heterologous proteins in *Lactococcus lactis*. *J Bacteriol* 180(7):1895-1903.
- Lee DH, Kim SG, Kweon DH, Seo JH. 2009. Folding machineries displayed on a cation-exchanger for the concerted refolding of cysteine- or proline-rich proteins. *BMC Biotechnol* 9:27.
- Li P, Beckwith J, Inouye H. 1988. Alteration of the amino terminus of the mature sequence of a periplasmic protein can severely affect protein export in *Escherichia coli*. *Proc Natl Acad Sci USA* 85(20):7685-7689.
- Liang FC, Bageshwar UK, Musser SM. 2012. Position-dependent effects of polylysine on Sec protein transport. *J Biol Chem* 287(16):12703-12714.

- Liu D, Schmid RD, Rusnak M. 2006. Functional expression of *Candida antarctica* lipase B in the *Escherichia coli* cytoplasm--a screening system for a frequently used biocatalyst. *Appl Microbiol Biotechnol* 72(5):1024-1032.
- MacIntyre S, Eschbach ML, Mutschler B. 1990. Export incompatibility of N-terminal basic residues in a mature polypeptide of *Escherichia coli* can be alleviated by optimising the signal peptide. *Mol Gen Genet* 221(3):466-474.
- McCoy AJ, Grosse-Kunstleve RW, Storoni LC, Read RJ. 2005. Likelihood-enhanced fast translation functions. *Acta Crystallogr D Biol Crystallogr* 61(Pt 4):458-464.
- Mergulhao FJ, Summers DK, Monteiro GA. 2005. Recombinant protein secretion in *Escherichia coli*. *Biotechnol Adv* 23(3):177-202.
- Murshudov GN, Vagin AA, Dodson EJ. 1997. Refinement of macromolecular structures by the maximum-likelihood method. *Acta Crystallogr D Biol Crystallogr* 53(Pt 3):240-255.
- Neu HC, Heppel LA. 1965. The release of enzymes from *Escherichia coli* by osmotic shock and during the formation of spheroplasts. *J Biol Chem* 240(9):3685-3692.
- Otwinowski Z, Minor W. 1997. Processing of X-ray diffraction data

collected in oscillation mode. *Method Enzymol* 276:307-326.

Park YC, Kim SJ, Choi JH, Lee WH, Park KM, Kawamukai M, Ryu YW, Seo JH. 2005. Batch and fed-batch production of coenzyme Q₁₀ in recombinant *Escherichia coli* containing the decaprenyl diphosphate synthase gene from *Gluconobacter suboxydans*. *Appl Microbiol Biotechnol* 67(2):192-196.

Pugsley AP. 1993. The complete general secretory pathway in gram-negative bacteria. *Microbiol Rev* 57(1):50-108.

Pugsley AP, Francetic O. 1998. Protein secretion in *Escherichia coli* K-12: dead or alive? *Cell Mol Life Sci* 54(4):347-352.

Sandkvist M. 2001. Biology of type II secretion. *Mol Microbiol* 40(2):271-283.

Sorensen HP, Mortensen KK. 2005. Advanced genetic strategies for recombinant protein expression in *Escherichia coli*. *J Biotechnol* 115(2):113-128.

Tomassen J, Leunissen J, van Damme-Jongsten M, Overduin P. 1985. Failure of *E. coli* K-12 to transport PhoE-LacZ hybrid proteins out of the cytoplasm. *EMBO J* 4(4):1041-1047.

Uppenberg J, Oehrner N, Norin M, Hult K, Kleywegt GJ, Patkar S,

Waagen V, Anthonsen T, Jones TA. 1995. Crystallographic and molecular-modeling studies of lipase B from *Candida antarctica* reveal a stereospecificity pocket for secondary alcohols. *Biochemistry* 34(51):16838-16851.

Voulhoux R, Taupiac MP, Czjzek M, Beaumelle B, Filloux A. 2000. Influence of deletions within domain II of exotoxin A on its extracellular secretion from *Pseudomonas aeruginosa*. *J Bacteriol* 182(14):4051-4058.

Figure legends

Figure 1. Effects of polyanionic and polyhydrophilic fusion tags on functional expression of recombinant CalBs. (A) Schematic diagram of the structures of recombinant CalB expression cassettes. Symbols: *T7* promoter (*T7*), *lac* operator (*lacO*), ribosomal binding site (RBS), translational stop codon (stop) and genes coding for the signal sequence of pectate lyase B from *Erwinia carotovora* (*pelB*), *Candida antarctica* lipase B (*calB*), 1-9 aspartates (D1-D9), 5 glutamates (E5), 5 asparagines (N5), 5 glutamines (Q5), and 5 lysines (K5). (B and C) Specific activities of recombinant CalBs with different amino acid tags. The specific lipase activities of crude CalBs collected after 18 h IPTG induction were measured in triplicate using *p*-nitrophenyl butyrate and normalized to dry cell mass.

Figure 2. Effects of the five-aspartate tag on expression and localization of recombinant CalBs. Batch production of P-CalB (A) and P-D5-CalB (B) were conducted in triplicate using 20 g/L glucose at 200 rpm and a culture temperature was shifted from 37°C to 20°C after 0.2 mM IPTG induction.

Figure 3. Fed-batch production of P-CalB (A) and P-D5-CalB (B) in

recombinant *E. coli* stains. (A and B) After depletion of 20 g/L initial glucose, a high-concentrated glucose solution was fed into the bioreactor. At a target dry cell mass of 50 g/L, IPTG was added at a final concentration of 0.2 mM and temperature was shifted to 20°C. (C) Protein samples of the fed-batch cultivations after 13 h IPTG induction were analyzed by SDS-PAGE. Intracellular protein samples were prepared from the cells diluted at 10 OD₆₀₀. Extracellular protein sample was obtained from the supernatant of culture broth without any treatment. The arrow points the protein band of recombinant CalBs.

Figure. 4. Crystal structure of D5-CalB. (A) Stereo ribbon diagrams of the dimers of CalB and D5-CalB. Two monomers of CalB and D5-CalB are colored differently (salmon and light blue, respectively). Polyethylene glycol molecules bound in the middle of D5-CalB are shown as a stick model (colored in magenta). To compare relative positions of CalB and D5-CalB monomers, residues Pro293-Ala312 of CalB and D5-CalB are colored in green, respectively. All figures were produced using *PyMOL* (<http://www.pymol.org>). (B and C) Molecular interactions in the dimer interface of D5-CalB shown in detail. Two monomers are colored as in (A). Residues mutated in this study are shown in stick models.

Figure 5. Effects of lipase dimerization (A) and the general secretion pathway (B) on expression and localization of recombinant D5-CalB. (A) Five mutants of D5-CalB (L169R, V174R, V246R, P285R, and A308R) were designed to disrupt an interaction between two monomers of D5-CalB at the dimer interface. (B) *E. coli* BL21 star (DE3) strain and *gspDE*-deficient background strain ($\Delta gspDE$) were transformed with a plasmid encoding either the authentic P-CalB or P-D5-CalB. Protein samples prepared in triplicate after 19-20 h IPTG induction in batch cultures.

Figure 6. A model for extracellular secretion of P-CalB (A) and P-D5-CalB (B) in *E. coli*. The PelB signal sequence directs the polypeptide of P-CalB (A) and P-D5-CalB (B) to the SecB secretion machinery and is cleaved off by a specific inner membrane protease in the event of protein transport (1). In the periplasm, the negative charge in the 5 aspartate tag induces the conformational change of the quaternary structure of D5-CalB with the same tertiary structure as the authentic CalB. This structural change enhances an export efficiency of D5-CalB across the outer membrane via the main terminal branch of the general secretory pathway (GSP) (2).

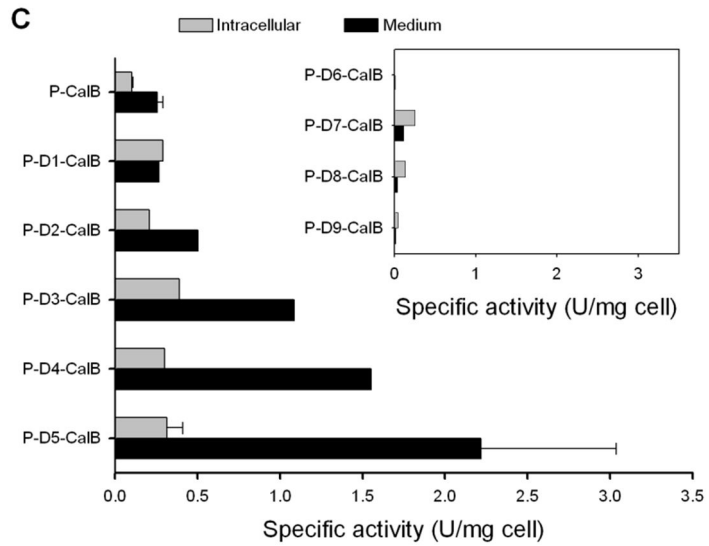
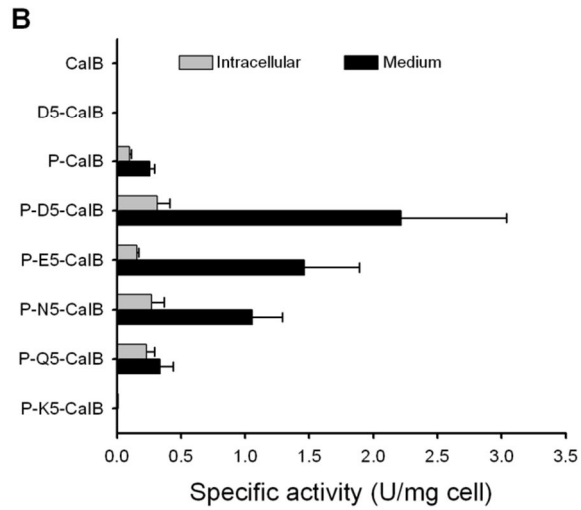
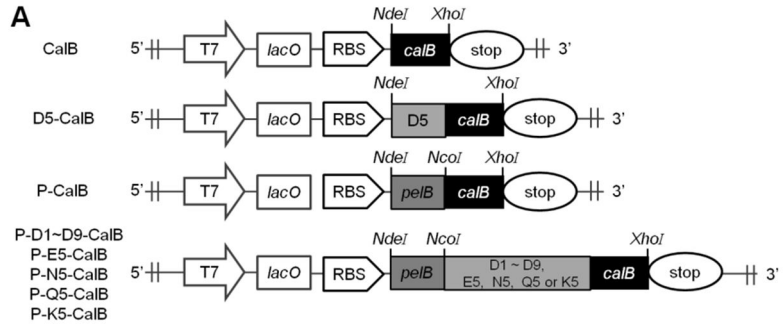


Figure 1

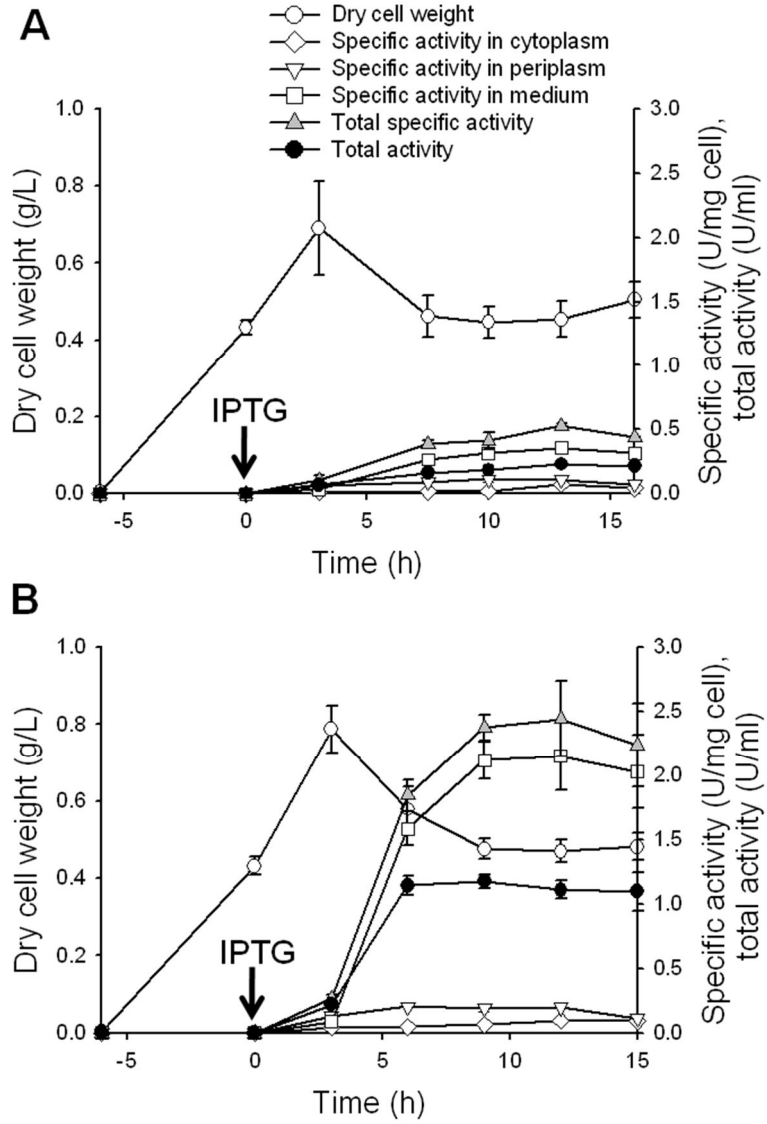


Figure 2

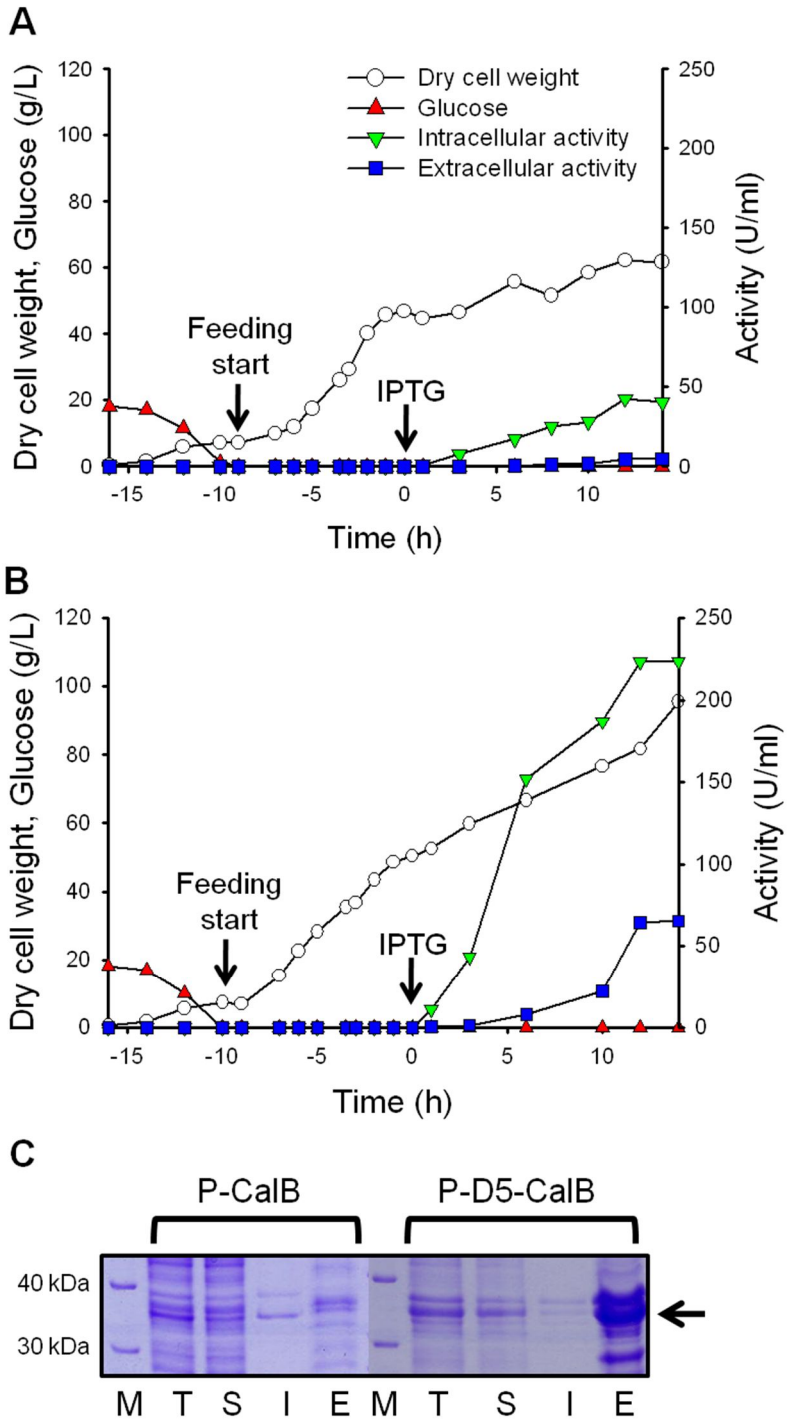
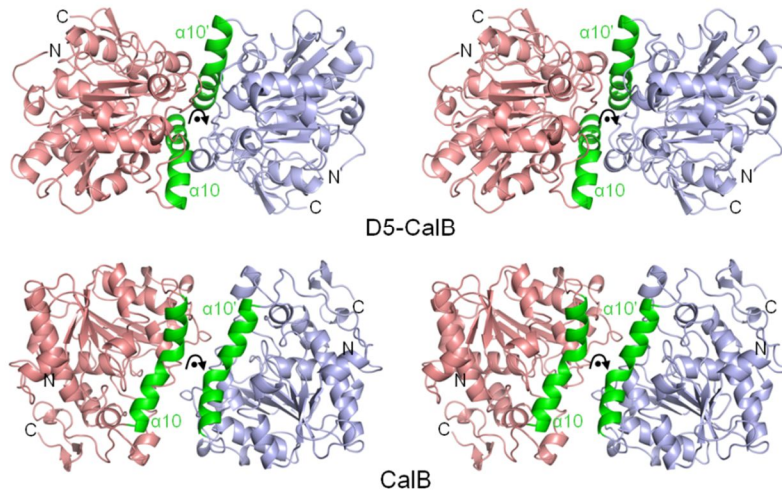
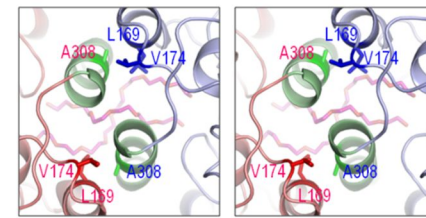


Figure 3

A



B



C

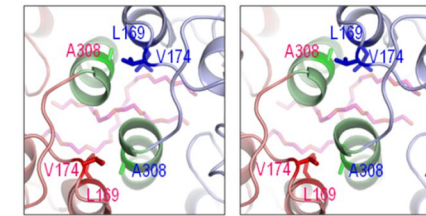


Figure 4

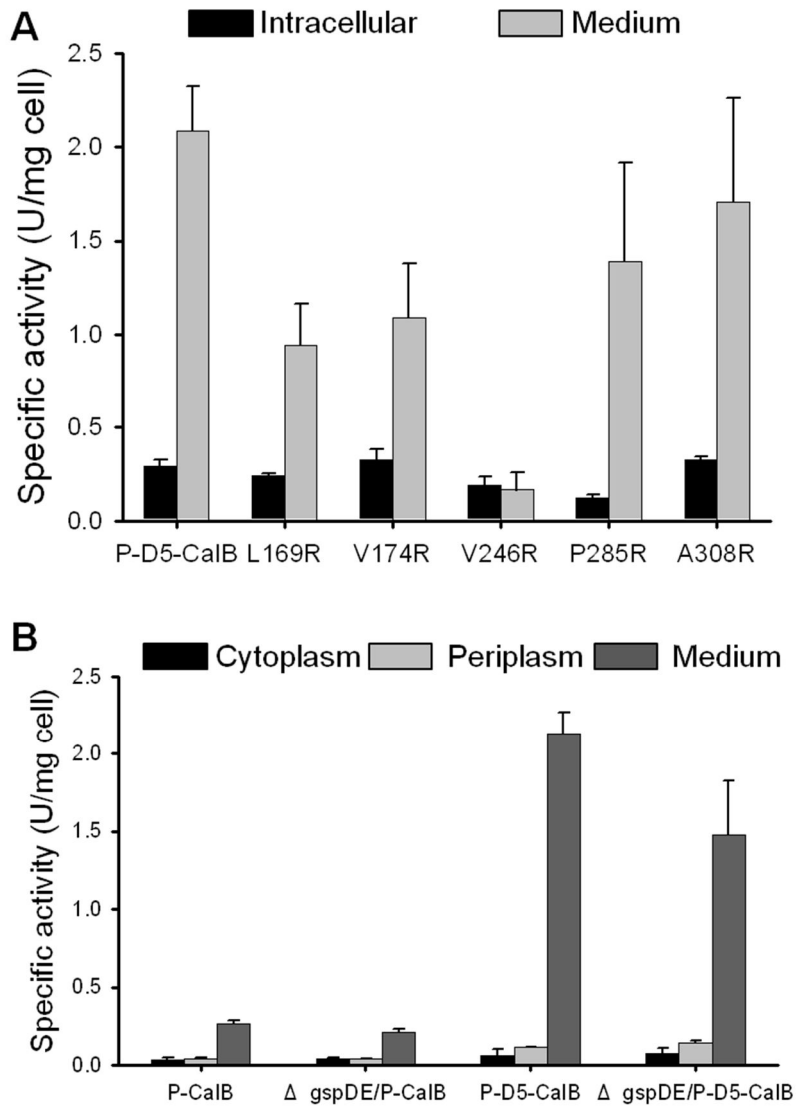


Figure 5

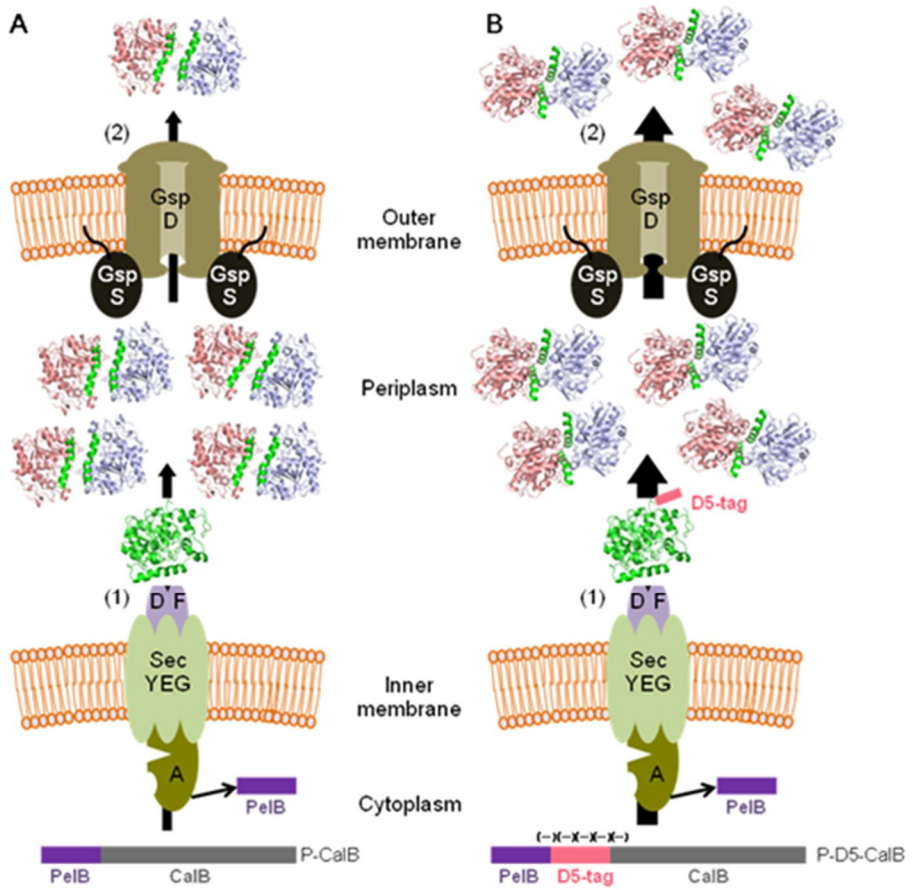
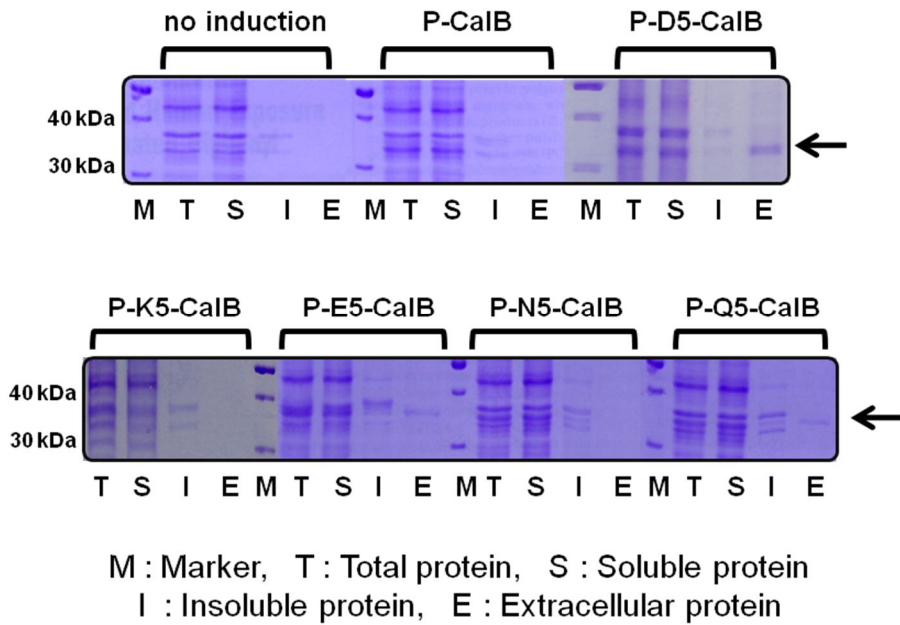
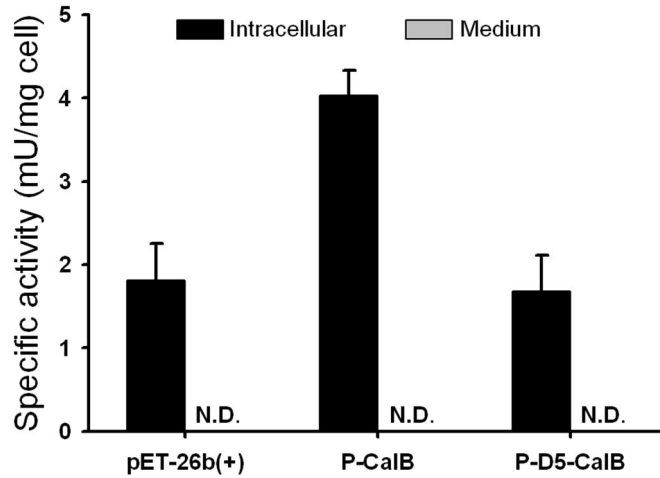


Figure 6

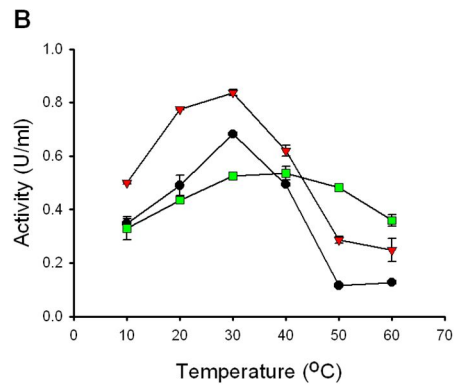
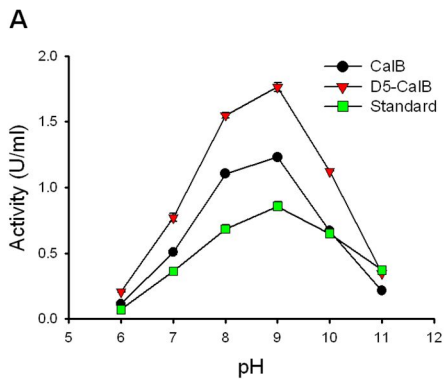
Supporting Information



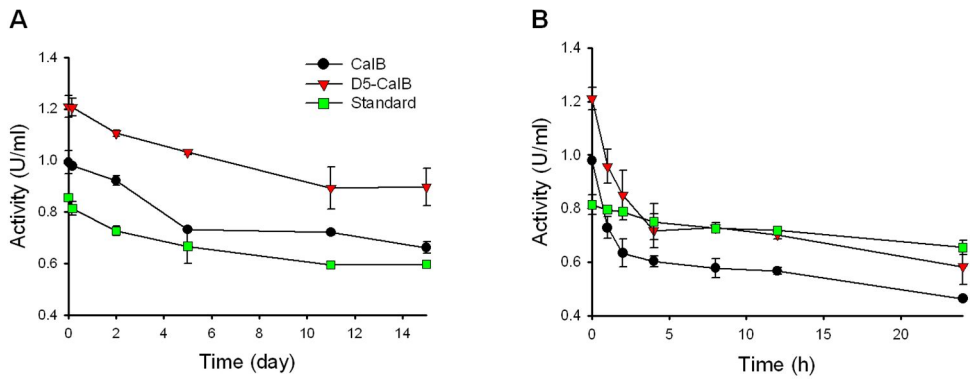
Supplementary Figure 1. SDS-PAGE analysis of recombinant CalBs fused with the various N-terminal tags. After 18 h induction, the cells were harvested, disrupted and fractionated into total (T), soluble (S), insoluble (I) and extracellular (E) protein fractions. M indicates the protein size marker and the arrow points the protein band of recombinant CalBs.



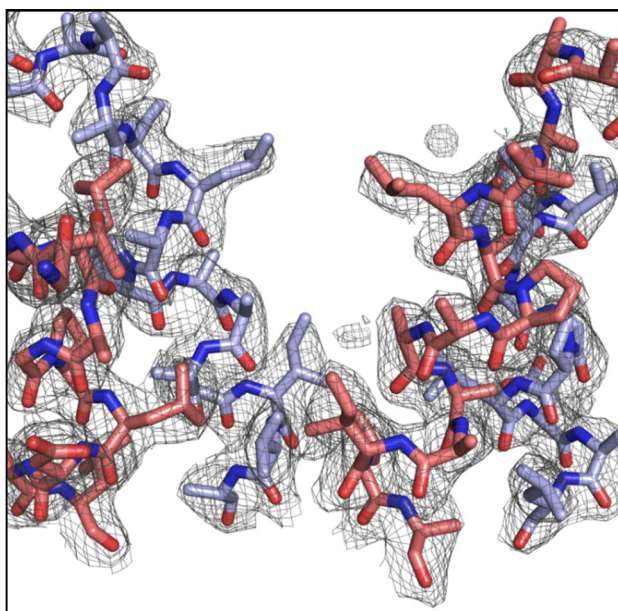
Supplementary Figure 2. Specific activities of alkaline phosphatase (PhoA). The crude cell extracts of BL21 star (DE3) expressing pET-26b(+), P-CalB and P-D5-CalB were prepared after 18 h IPTG induction. The specific activities of PhoA in the crude extracts were measured in triplicate using *p*-nitrophenyl phosphate and normalized to dry cell mass. N.D., not detected.



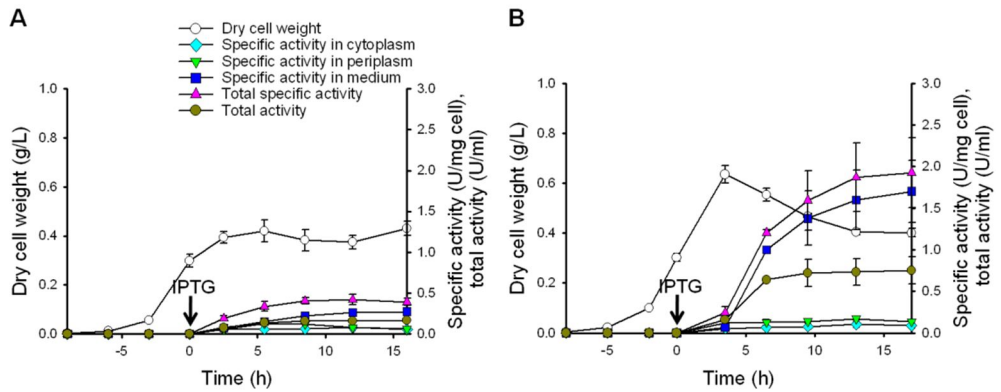
Supplementary Figure 3. Effects of pH (A) and temperature (B) on lipase activity of standard, and recombinant CalBs produced in this study.



Supplementary Figure 4. Thermal stability of recombinant CalBs at 4°C (A) and 30°C (B). Standard and purified CalBs were incubated in 50 mM Tris-HCl buffer (pH 9.0).



Supplementary Figure 5. 2Fo-Fc electron density map around the dimer-interface of D5-CalB. Residues are shown in sticks. Two monomers of D5-CalB are colored differently (salmon and light blue, respectively). The 2Fo-Fc electron density map is contoured at 1.3σ .



Supplementary Figure 6. Batch fermentations of recombinant *E. coli*. BL21 star (DE3) Δ gspDE expressing P-CalB (A) or P-D5-CalB (B). The recombinant cells were grown using 20 g/L glucose at 37°C and 230 rpm. After 0.2 mM IPTG induction (arrow), temperature and agitation speed were shifted to 20°C and 200 rpm, respectively. The culture was repeated in triplicate at the same conditions.

Supplementary Table 1. List of DNA oligomers used in this study. The italicized sequences indicate the recognition sites of the corresponding restriction enzymes. [F] and [R] mean the forward and reverse primers, respectively

Name	Sequence (5' → 3')	Restriction enzyme	Amplified gene
CalB[F]	GGAATTCC <i>CATATG</i> CTACCTTCCGGTTCGGAC	<i>NdeI</i>	CalB
P-CalB[F]	CATGCC <i>ATGGCC</i> CTACCTTCCGGTTCGGAC	<i>NcoI</i>	P-CalB
P-D1-CalB[F]	CATGCC <i>ATGGCC</i> GATCTACCTTCCGGTTCGGAC	<i>NcoI</i>	P-D1-CalB
P-D2-CalB[F]	CATGCC <i>ATGGCC</i> GATGATCTACCTTCCGGTTCGGAC	<i>NcoI</i>	P-D2-CalB
P-D3-CalB[F]	CATGCC <i>ATGGCC</i> GATGATGATCTACCTTCCGGTTCGGAC	<i>NcoI</i>	P-D3-CalB
P-D4-CalB[F]	CATGCC <i>ATGGCC</i> GATGATGATGATCTACCTTCCGGTTCGGAC	<i>NcoI</i>	P-D4-CalB
D5-CalB[F]	GGAATTCC <i>CATATG</i> GGATGATGATGATGATCTACCTTCCGGTTCGGAC	<i>NdeI</i>	D5-CalB
P-D5-CalB[F]	CATGCC <i>ATGGCC</i> GATGATGATGATGATCTACCTTCCGGTTCGGAC	<i>NcoI</i>	P-D5-CalB
P-D6-CalB[F]	CATGCC <i>ATGGCC</i> GATGATGATGATGATGATCTACCTTCCGGTTCGGAC	<i>NcoI</i>	P-D6-CalB
P-D7-CalB[F]	CATGCC <i>ATGGCC</i> GATGATGATGATGATGATGATCTACCTTCCGGTTCGGAC	<i>NcoI</i>	P-D7-CalB
P-D8-CalB[F]	CATGCC <i>ATGGCC</i> GATGATGATGATGATGATGATGATCTACCTTCCGGTTCGGAC	<i>NcoI</i>	P-D8-CalB
P-D9-CalB[F]	CATGCC <i>ATGGCC</i> GATGATGATGATGATGATGATGATGATGATCTACCTTCCGGTTCGGAC	<i>NcoI</i>	P-D9-CalB
P-K5-CalB[F]	CATGCC <i>ATGGCC</i> AAAAAAAAAAAAAAAAAACTACCTTCCGGTTCGGAC	<i>NcoI</i>	P-K5-CalB
P-E5-CalB[F]	CATGCC <i>ATGGCC</i> GAAGAAGAAGAAGAACTACCTTCCGGTTCGGAC	<i>NcoI</i>	P-E5-CalB
P-N5-CalB[F]	CATGCC <i>ATGGCC</i> ACAACAACAACAACCTACCTTCCGGTTCGGAC	<i>NcoI</i>	P-N5-CalB
P-Q5-CalB[F]	CATGCC <i>ATGGCC</i> CAGCAGCAGCAGCAGCTACCTTCCGGTTCGGAC	<i>NcoI</i>	P-Q5-CalB

(be continued)

Supplementary Table 2. Statistics for data collection and refinement

Data set	D5-CalB
<i>A. Data collection statistics</i>	
X-ray source	PLS BL-5C
X-ray wavelength (Å)	0.97951
Space group	P6 ₅
a (Å)	123.66
b (Å)	123.66
c (Å)	191.85
Resolution range (Å)	20–2.9
Total / unique reflections	329,662 / 36,843
Completeness (%)	100 (100) ^a
Average $I/\sigma(I)$	50.3 (20.2) ^a
R_{merge}^b (%)	9.3 (17.7) ^a
<i>B. Model refinement statistics</i>	
$R_{\text{work}} / R_{\text{free}}^c$ (%)	23.2 / 26.6
Number / average B -factor (Å ²)	
Protein nonhydrogen	4 × 2,324 / 37.0
Water oxygen atoms	364 / 37.5
Ligand molecules	4 × PEG / 48.0
R.m.s. deviations from ideal geometry	
Bond lengths (Å)	0.007
Bond angles (°)	1.06

(be continued)

Data set	D5-CalB
Protein-geometry analysis	
Ramachandran favored (%)	95.1 (1198/1260)
Ramachandran allowed (%)	4.9 (62/1260)
Ramachandran outliers (%)	0.0 (0/1260)

^aValues in parentheses refer to the highest resolution shell (2.95–2.90 Å).

^b $R_{\text{merge}} = \frac{\sum_{hkl} \sum_i |I_i(hkl) - \langle I(hkl) \rangle|}{\sum_{hkl} \sum_i I_i(hkl)_i}$, where $I(hkl)$ is the intensity of reflection hkl , \sum_{hkl} is the sum over all reflections, and \sum_i is the sum over i measurements of reflection hkl .

^c $R = \frac{\sum_{hkl} (|F_{\text{obs}}| - |F_{\text{calc}}|)}{\sum_{hkl} |F_{\text{obs}}|}$, where R_{free} was calculated for a randomly chosen 10% of reflections, which were not used for structure refinement and R_{work} was calculated for the remaining.

Supplementary Table 3. Kinetic parameters of batch and fed-batch fermentations

Target CalB	Batch			Fed-batch		
	Dry cell weight (g/L)	Specific activity in periplasm (U/mg cell)	Specific activity in medium (U/mg cell)	Dry cell weight (g/L)	Intracellular activity (U/ml)	Extracellular activity (U/ml)
P-CalB	0.69 ± 0.10	0.11 ± 0.001	0.36 ± 0.02	62.3	42.7	4.70
P-D5-CalB	0.79 ± 0.05	0.21 ± 0.003	2.2 ± 0.2	95.6	223	65.4

Supplementary Table 4. Production of recombinant CalBs in recombinant *E. coli* and fungal strains

Strain	System	Localization	Amount of CalB (g/L)		Activity (U/ml)	Reference
			Batch fermentation	Fed-batch fermentation		
<i>E. coli</i>	Mutagenesis	Intracellular	0.0033	-		1
<i>E. coli</i> Origami 2 (DE3)	Polycationic amino acid tags	Intracellular	0.0078	-		2
<i>E. coli</i> Origami B	Coexpression of chaperones	Intracellular	0.040	-		3
<i>E. coli</i> Rosetta (DE3)	PelB signal sequence	Periplasm	0.0052	-		4
<i>P. pastoris</i> SMD1168H	α -factor signal sequence	Medium	0.0445	-		4
<i>P. pastoris</i> SMD1168	Fusion with cellulose-binding module	Medium	0.025	-		5
		Medium	-	1.5		6
<i>P. pastoris</i>	Codon optimization	Medium	0.155	3.0	6100 ^a	7
<i>S. cerevisiae</i> BJ3505	α -factor signal sequence	Medium	-	-	40 ^a	8
<i>A. oryzae</i> niaD300	Integration of <i>calB</i> gene	Medium	-	-	0.35 ^b	9
<i>E. coli</i> BL21 star (DE3)	PelB signal sequence + 5 aspartate tag	Medium	0.031	1.9	65 ^b	This study

CalB activity was determined by using tributyrin^a or *p*-NPB^b as a substrate.

Supplementary Table 5. Kinetic parameters of standard CalB, and purified CalB and D5-CalB

Lipase	Specific activity (U/mg protein)	K_m ($\mu\text{M} \times 10^3$)	k_{cat} ($\text{min}^{-1} \times 10^3$)	k_{cat}/K_m ($\text{min}^{-1} \mu\text{M}^{-1}$)
Standard	20.0 ± 0.6	17.2 ± 3.3	30.5 ± 6.1	1.78 ± 0.01
CalB ^a	25.5 ± 0.2	6.04 ± 0.15	14.4 ± 0.5	2.39 ± 0.08
D5-CalB ^a	34.4 ± 0.5	9.69 ± 1.36	28.8 ± 5.1	2.95 ± 0.13

^a The purified CalB and D5-CalB were obtained in the medium fractions for the P-CalB and P-D5-CalB constructs fused with the His-tag system, respectively.

Supplementary References

1. Jung S, Park S. 2008. Improving the expression yield of *Candida antarctica* lipase B in *Escherichia coli* by mutagenesis. *Biotechnol Lett* 30(4):717-722.
2. Jung HJ, Kim SK, Min WK, Lee SS, Park K, Park YC, Seo JH. 2011. Polycationic amino acid tags enhance soluble expression of *Candida antarctica* lipase B in recombinant *Escherichia coli*. *Bioprocess Biosyst Eng* 34(7):833-839.
3. Liu D, Schmid RD, Rusnak M. 2006. Functional expression of *Candida antarctica* lipase B in the *Escherichia coli* cytoplasm--a screening system for a frequently used biocatalyst. *Appl Microbiol Biotechnol* 72(5):1024-1032.
4. Larsen MW, Bornscheuer UT, Hult K. 2008. Expression of *Candida antarctica* lipase B in *Pichia pastoris* and various *Escherichia coli* systems. *Protein Expr Purif* 62(1):90-97.
5. Rotticci-Mulder JC, Gustavsson M, Holmquist M, Hult K, Martinelle M. 2001. Expression in *Pichia pastoris* of *Candida antarctica* lipase B and lipase B fused to a cellulose-binding domain. *Protein Expr Purif* 21(3):386-392.
6. Jahic M, Gustavsson M, Jansen AK, Martinelle M, Enfors SO. 2003.

Analysis and control of proteolysis of a fusion protein in *Pichia pastoris* fed-batch processes. J Biotechnol 102(1):45-53.

7. Yang JK, Liu LY, Dai JH, Li Q. 2013. de novo design and synthesis of *Candida antarctica* lipase B gene and alpha-factor leads to high-level expression in *Pichia pastoris*. 8(1):e53939.

8. Zhang N, Suen WC, Windsor W, Xiao L, Madison V, Zaks A. 2003. Improving tolerance of *Candida antarctica* lipase B towards irreversible thermal inactivation through directed evolution. Protein Eng 16(8):599-605.

9. Tamalampudi S, Talukder MM, Hama S, Tanino T, Suzuki Y, Kondo A, Fukuda H. 2007. Development of recombinant *Aspergillus oryzae* whole-cell biocatalyst expressing lipase-encoding gene from *Candida antarctica*. Appl Microbiol Biotechnol 75(2):387-395.

Appendix 3

**Application of repeated aspartate tags to
improving extracellular production of *Escherichia
coli* L-asparaginase isozyme II**

Highlights

- L-asparaginase isozyme II (AnsB) from *E. coli* is a therapeutic agent against acute lymphoblastic leukemia.
- Repeated aspartate tags were devised to express AnsB extracellularly in *E. coli*.
- A five-aspartate tag was optimal for extracellular production of AnsB.
- 40.8 U/ml of AnsB was obtained in a batch fermentation.
- AnsB was secreted into medium via the *E. coli* general secretion pathway.

Abstract

Asparaginase isozyme II from *Escherichia coli* is a popular enzyme that has been used as a therapeutic agent against acute lymphoblastic leukemia. Here, fusion tag systems consisting of the pelB signal sequence and various lengths of repeated aspartate tags were devised to highly express and to release active asparaginase isozyme II extracellularly in *Escherichia coli*. Among several constructs, recombinant asparaginase isozyme II fused with the pelB signal sequence and five aspartate tag was secreted efficiently into culture medium at 34.6 U/mg cell of specific activity. By batch fermentation, recombinant *Escherichia coli* produced 40.8 U/ml asparaginase isozyme II in the medium. In addition, deletion of the *gspDE* gene reduced extracellular production of asparaginase isozyme II, indicating that secretion of recombinant asparaginase isozyme II was partially ascribed to the recognition by the general secretion machinery. This tag system composed of the pelB signal peptide and repeated aspartates can be applied to extracellular production of other recombinant proteins.

Keywords: L-asparaginase isozyme II; *Escherichia coli*; extracellular production; repeated aspartate tag; pelB signal sequence; general secretion pathway

1. Introduction

Asparaginase isozyme II (AnsB) from *Escherichia coli* (*E. coli*) is a prokaryotic protein studied over 50 years as a therapeutic agent against acute lymphoblastic leukemia (ALL) (Mashburn and Wriston, 1964). In combination with other agents, AnsB is also used in the treatment of Hodgkin's disease, acute myelocytic leukemia, acute myelomonocytic leukemia, chronic lymphocytic leukemia, lymphosarcoma, reticulosarcoma and melanosarcoma (Stecher et al., 1999). Studies have shown that only AnsB from *E. coli* is very effective in inhibiting tumors, while other bacterial asparaginases were either less active or completely inactive (Broome, 1965).

The *E. coli* AnsB enzyme naturally forms a homo-tetramer structure composed of two dimers of intimate dimers containing all the structural elements and functional groups, and the active enzyme is always a tetramer (Swain et al., 1993). Several research efforts have been made to express AnsB actively in *E. coli*. Medium optimization was undertaken to improve production of AnsB from wild type *E. coli* ATCC 11303, but this approach is still limited by an inherent low expression yield (Kenari et al., 2011). Among the *trc*, *tac* and *T7* promoter systems, the highest specific activity and expression level of recombinant AnsBs were obtained when the strong *T7* promoter was

adopted (Harms et al., 1991; Khushoo et al., 2005; Khushoo et al., 2004). A previous study showed that medium composition and induction strategy significantly influenced extracellular production of recombinant AnsB, and induction of the late log phase cells in TB medium was optimal for secretion of recombinant AnsB (Khushoo et al., 2004). Among various signal sequences including native AnsB signal sequence, *Bacillus* endoxylanase leader sequence and the pelB leader sequence, expression of recombinant AnsB fused to pelB leader resulted in maximum production in culture medium. Interestingly, recombinant AnsB was produced extracellularly up to 75% of total AnsB proteins by unknown mechanism when it was combined with the pelB signal sequence (Khushoo et al., 2005). While pelB leader sequence was also adopted to maximize AnsB secretion according to the previous studies. an efficient AnsB expression system in minimal medium was sought to construct because minimal medium is more beneficial than complex medium (TB medium) in terms of cost and tight control (Luo et al., 2014; Paliy and Gunasekera, 2007).

In most cases, extracellular production of target proteins in culture medium has several advantages over intracellular production: simplified downstream processing, enhanced biological activity, and higher protein stability and solubility (Cornelis, 2000; Makrides, 1996).

For the extracellular expression of target proteins in *E. coli*, two prerequisites are required: maintenance of their soluble and active forms, and their delivery to the extracellular space by penetrating cytoplasmic and outer membranes. For soluble expression of target proteins, many solubility-enhancing fusion partners have been devised: glutathione S-transferase (GST), maltose binding protein (MBP), thioredoxin (Trx), ubiquitin (Ub), N-utilization substance (NusA) and small ubiquitin-modifier (SUMO) (Esposito and Chatterjee, 2006; Waugh, 2005). To increase the active protein expression and secretion efficiency, combination of a signal sequence with the solubility-enhancing fusion partner is worthy to be considered. However, the fusion partners consisting of 76 (Ub) to 495 (NusA) amino acids are too big to go through the membrane structure and play their roles in the cytoplasmic space. Thus, other fusion partners should be developed to possess a small size and act in both cytoplasmic and periplasmic spaces.

Extracellular proteins commonly have highly negative charge in the first five amino acid residues (MacIntyre et al., 1990), whereas AnsB has only one at position +18. In our previous report, recombinant *Candida antarctica* lipase B (CalB) with the N-terminal 5-aspartate tag dramatically increased both expression and secretion of CalB with the aid of the pelB signal sequence in recombinant *E. coli* (Kim et al.,

2014). These facts suggest that an adequate alteration of the N-terminal end of AnsB by fusion of anion amino acids could improve soluble expression and transport efficiency across the membranes as done for recombinant CalB. In this study, extracellular expression of AnsB was designed by its connection with the pelB signal sequence and a series of aspartate tag, of which strategy was verified in a simple batch culture. Moreover, the general secretion pathway (GSP) of *E. coli* was modulated, and it was found that extracellular production of AnsB was partially ascribed to the recognition by the GSP components.

2. Materials and Methods

2.1. Bacterial strains and plasmids

E. coli TOP10 and BL21 star (DE3) (Invitrogen, Grand Island, NY, USA) strains were used for genetic manipulation and protein production, respectively. The AnsB gene and its recombinant genes were cloned behind the *T7* promoter in derivatives of plasmid pET-26b(+) (EMD Millipore, Darmstadt, Germany) and their transcription was induced by adding isopropyl- β -D-thiogalactopyranoside (IPTG). The chromosomal DNA of *E. coli* K-12 was used as the source of the AnsB gene. A *gspDE*-deficient background strain (designated here as Δ *gspDE*) lacking a part of the fifteen *gsp* genes was previously constructed (Kim et al., 2014).

2.2. Genetic manipulation

The AnsB genes were amplified by the polymerase chain reaction (PCR) using the chromosomal DNA of *E. coli* K-12 as a template. PCR DNA primers used for AnsB amplification were designed to be specific for the 5'- or 3'-end of the AnsB gene, and contain recognition sites of DNA digestion enzymes as shown in Table 1. To amplify the AnsB genes, DNA primers were formulated with a forward oligomer and a

reverse oligomer of AnsB[R]. For example, AnsB[F] or D5-AnsB[F] and AnsB[R] were used to express the gene coding for the authentic AnsB without any tags and native signal sequence or recombinant AnsB with the N-terminal 5-aspartate tag, respectively. To combine each recombinant AnsB gene with the gene coding for the N-terminal pelB leader sequence in plasmid pET-26B(+), the forward primers were designed to remove the transcriptional initiation codon (ATG) of the AnsB gene. The AnsB gene was then located behind the leader sequence in frame. After the gene amplification, all PCR products were cut with appropriate restriction enzymes (Table 1) and ligated with plasmid pET-26b(+) digested with the same enzymes. The nucleotide sequences of the recombinant AnsB genes were verified by DNA sequencing. Names of plasmids, recombinant AnsB gene products and schematic structures are shown in Fig. 1.

2.3. Culture condition

The recombinant *E. coli* BL21 star (DE3) cells harboring each AnsB expression vector were pre-cultured in LB medium (5 g/L yeast extract and 10 g/L bacto-trypton) at 37°C and 230 rpm for 12 h. After harvesting the cells, the cell pellets were used for inoculation. A batch culture using a 500 ml-scale baffled flask (Nalgene, Rochester, NY, USA) was carried out at 37°C and 230 rpm in 100 ml of a defined

medium (pH 6.8) containing (per liter) 20 g glucose, 4 g $(\text{NH}_4)_2\text{HPO}_4$, 13.5 g KH_2PO_4 , 1.7 g citric acid, 1.4 g $\text{MgSO}_4 \cdot 7\text{H}_2\text{O}$ and 10 ml trace metal solution. The trace metal solution was composed of per liter of 5 mol HCl, 10 g $\text{FeSO}_4 \cdot 7\text{H}_2\text{O}$, 2.25 g $\text{ZnSO}_4 \cdot 7\text{H}_2\text{O}$, 1 g $\text{CuSO}_4 \cdot 5\text{H}_2\text{O}$, 0.5 g $\text{MnSO}_4 \cdot 4\text{H}_2\text{O}$, 0.23 g $\text{Na}_2\text{B}_4\text{O}_7 \cdot 10\text{H}_2\text{O}$, 2 g CaCl_2 , 0.1 g $(\text{NH}_4)_6\text{Mo}_7\text{O}_{24}$. At the logarithmic phase of growth (optical density at 600 nm (OD_{600}) \approx 0.8-1.2), protein expression was induced by adding IPTG at a final concentration of 0.2 mM. The induced cells were cultivated at 20°C and 200 rpm for additional 24 h.

2.4. Protein fractionation

To collect the AnsBs secreted from the recombinant cells, the culture broth was centrifuged at 15,000 rpm for 10 min and its supernatant was named as the medium fraction. To obtain the intracellular protein fractions, the collected culture broth was concentrated or diluted to adjust its OD_{600} to be 10. This broth was centrifuged at 13,000 rpm and 4°C for 10 min. The cell pellets were suspended in 50 mM Tris-Cl buffer (pH 9.0) and disrupted by an ultrasonic machine (Cole-Parmer, USA) on ice. The total, soluble and insoluble fractions of intracellular proteins were prepared as described in the previous report (Jung et al., 2011). Briefly, after centrifugation of the cell lysate at 12,000 rpm and 4°C for 30 min, the supernatant and pellets were collected individually

and named as the soluble and insoluble protein fractions, respectively. The cell lysate containing both soluble and insoluble proteins was also regarded as the total protein fraction.

2.5. AnsB assays

To visualize recombinant AnsBs, the protein samples were fractionated by sodium dodecyl sulfate–polyacrylamide gel electrophoresis (SDS-PAGE) with 12% acrylamide. Protein bands on SDS-PAGE gels were stained with Coomassie brilliant blue R-250 and quantitatively analyzed by a densitometer (TotalLab 1.01, Nonlinear Dynamics Ltd.).

To determine AnsB activity, the reaction mixture was composed of 140 μ l of 0.1 M potassium phosphate buffer (pH 7.0), 50 μ l of 40 mM L-asparagine and 10 μ l of the crude enzyme solution, and preheated at 37°C for 5 min. The reaction was terminated by addition of 50 μ l of 15% (w/w) trichloroacetic acid, followed by centrifugation at 13,000 rpm for 2 min. 70 μ l of the supernatant was transferred into a 96-well microplate and mixed with 130 μ l of the Nessler's reagent for 10 min at room temperature. The absorbance change at 500 nm of wavelength was monitored by a 96-well microplate reader (Molecular Devices, Sunnyvale, CA, USA). Specific AnsB activity was calculated by the division of AnsB activity by dry cell weight.

2.6. Quantitative real-time PCR

Total cellular RNAs from the *E. coli* BL21 star (DE3) strains were isolated using the RNeasy Protect Bacteria Mini Kit in accordance with the manufacturer's protocol (Qiagen). Quantitative real-time PCRs were performed in a final volume of 20 μ l of SYBR Premix Ex Taq (Takara) containing cDNA synthesized with the AccuPower RT PreMix system for reverse transcription-PCR (Bioneer). Real-time PCRs were performed in triplicate using the iCycler iQ real-time detection system (Bio-Rad) with two specific PCR primers (Table 1). The primers include a housekeeping gene, *gapC*, used for an internal reference for normalization.

3. Results

3.1. Design of AnsB expression systems with N-terminal repeated aspartates

Based on our hypothesis that polyanionic amino acids locating at the N-terminal end of AnsB may facilitate their extracellular expression, various protein expression systems were designed to possess different length of repeated aspartate molecules. To express and secrete recombinant AnsB in *E. coli*, the 5'-end of the AnsB gene without its own translational initiation codon and signal sequence was combined with the genes coding for the pelB signal sequence and 3, 4, 5 or 6 aspartates in a row. By addition of the repeated aspartates, isoelectric points of recombinant AnsBs decrease from pH 5.44 (no aspartate) to 4.79 (6 aspartates). As controls, the AnsB gene and AnsB with N-terminal 5 aspartates (D5-AnsB) without the pelB signal sequence were inserted into plasmid pET-26b(+). Schematic diagrams for the AnsB expression cassettes in pET-26b(+) plasmid derivatives and their names are displayed in Fig. 1.

3.2. Effects of N-terminal repeated aspartates on AnsB expression

To investigate the effect of the aspartate tags on AnsB expression,

recombinant *E. coli* BL21 star (DE3) strains overexpressing each recombinant AnsB gene were cultured batchwise and crude AnsB enzymes present in the intracellular and extracellular fractions were subjected to asparaginase activity (Fig. 2) and SDS-PAGE (Fig. 3) analyses. The fusion of the *pelB* signal sequence improved both intracellular and extracellular asparaginase activities by more than 70%, relative to the control of the authentic AnsB. Among a series of repeated amino acids consisting of 3-6 aspartates, the four and five aspartates facilitated the secretion of AnsB and hence P-D5-AnsB showed a 1.9 times higher specific activity in the culture medium than P-AnsB. Even though the repeated aspartates did not affect intracellular accumulation of active asparaginase, they elevated a total expression level of AnsB by 51% and hence the best extracellular asparaginase activity (40.8 U/ml) was obtained by a simple batch fermentation of recombinant *E. coli* expressing P-D5-AnsB (Table 2). As well as the enzyme activity assay, SDS-PAGE analysis also showed efficient secretion of recombinant AnsB in the culture medium (Fig. 3). Protein band of the secreted AnsB for the case of P-D5-AnsB (Lane E) was much thicker than that for P-AnsB. It was located at a slightly higher position in the gel than the theoretical molecular weight (35 kDa) because the amino acid tag still remained at the N-terminus and the *pelB* signal sequence was cut off by a signal peptidase, which was

verified by the N-terminal amino acid sequencing of recombinant AnsBs present in the intracellular and extracellular spaces. Although protein band of the secreted AnsB for the case of P-D3-AnsB was also thicker than that for P-AnsB, specific activities of P-AnsB and P-D3-AnsB in the culture medium were almost identical. It was postulated that attachment of tags to N-terminal end of AnsB might alter the protein activity as previously reported (Feng et al., 2013; Kim et al., 2014) and hence result in similar specific activity in medium.

3.3. Time-course expression of recombinant AnsB and D5-AnsB

Recombinant AnsBs were targeted to the periplasm via the SecB-dependant pathway, which is one of the type II secretion systems in *E. coli*. AnsB export via this pathway was initiated by the N-terminal pelB signal (Mergulhao et al., 2005) and moreover the five-repeated aspartate tag played a role of protein transport through the outer membrane. To investigate the role of the five-repeated aspartate tag, batch cultures of the recombinant *E. coli* strain overexpressing P-AnsB or P-D5-AnsB were carried out and intracellular and extracellular asparaginase activities of recombinant AnsBs collected over time were analyzed. As shown in Fig. 4, the growth patterns of the two recombinant *E. coli* strains were almost identical. For asparaginase localization, the specific asparaginase activity of D5-AnsB (a processed

form of P-D5-AnsB) in the culture medium (37.2 ± 2.7 U/mg cell) was about 2.0 times higher than 18.3 ± 2.7 U/mg cell of AnsB (a processed form of P-AnsB) in the broth whereas the five-repeated aspartate tag did not affect intracellular accumulation of active asparaginase of which specific activity was around 24 U/mg cell. Although the relative amount of both extracellular AnsB and D5-AnsB increased over time, D5-AnsB had a much higher tendency of extracellular secretion than AnsB. These results indicated that the recombinant D5-AnsB in the periplasm has higher efficiency of transport across the outer membrane than the authentic AnsB.

3.4. Effects of partial disruption of general secretion pathway on recombinant AnsB secretion

In most Gram-negative bacteria, the SecB-dependent pathway which allows proteins to cross the inner membrane is extended by terminal branches of the general secretion pathway (GSP) that permit extracellular secretion (Pugsley, 1993b). It has been previously shown that the GSP machinery specifically exported the dimer form of D5-CalB (Kim et al., 2014). However, a previous study reported that the *gsp* genes are transcriptionally silent in the *E. coli* K-12 strain (Francetic et al., 2000). To confirm the expression of the *gsp* genes, the transcriptional level of *gspD* was investigated in BL21 star (DE3) and a

gspDE-deficient BL21 star (DE3) strain (Δ *gspDE*) using quantitative reverse transcription real-time PCR (Fig. 5A). The mRNA level of the *gspD* gene in BL21 star (DE3) strain was 43.7-fold higher than that of the Δ *gspDE*, indicating that the *gspD* gene was expressed in BL21 star (DE3) under fermentation condition performed in this study. It was hypothesized that the *gsp* genes encoding a putative secreton would be a factor specifically affecting transport efficiency of the D5-AnsB across the outer membrane as observed for D5-CalB. Based on this hypothesis, expression vectors of pET-26b(+)-P-AnsB and pET-26b(+)-P-D5-AnsB were transformed to Δ *gspDE* (Kim et al., 2014) lacking a part of the 15 *gsp* genes coding for all components of the GSP secreton. To assess the effects of destruction of a part of the GSP secreton on recombinant AnsBs expression, batch fermentations of the Δ *gspDE*/P-AnsB and Δ *gspDE*/P-D5-AnsB strains were performed and the crude proteins were subjected to AnsB activity assay (Fig. 5B). Intracellular levels of AnsB and D5-AnsB were not influenced by the *gspDE* deletion, and the destruction of *gspDE* resulted in 56% and 15% reduced extracellular specific activities of AnsB and D5-AnsB, respectively. These results indicated that the transport efficiency enhancement of D5-AnsB was partially ascribed to the specific recognition by the GSP components, and a large fraction of D5-AnsB might be transported across the outer membrane by presently unknown

mechanisms (Ni and Chen, 2009).

4. Discussion

An extracellular secretion strategy is beneficial for mass production of target proteins, reduction of metabolic burden on the host cells, prevention of intracellular proteolytic degradation, and easy separation and purification without a cell disruption process. Even though Gram positive bacteria and fungi are preferable for commercial production of various proteins, a work-horse of *E. coli* is also attractive as a host microorganism. Development of various signal peptides and modulation of periplasmic machineries have improved extracellular secretion of target proteins considerably, but of which titers are still lower than those expressed in other bacterial and fungal systems in many cases (Mergulhao et al., 2005; Ni and Chen, 2009) because of its inherent problems. Meanwhile, the enhancement of target protein solubility for reduction of its inactive inclusion bodies has been somewhat achieved by connecting highly soluble and cytoplasmic fusion partners with coexpression of chaperones and foldases (Esposito and Chatterjee, 2006; Waugh, 2005). However, an application of current solubility-enhancing strategies is limited to cytoplasmic protein expression since the fusion partners are probably too big to penetrate the cytoplasmic membrane and may hinder the attachment of signal peptides onto the cytoplasmic membrane (Riordan et al., 2008; Sorg et

al., 2006).

In the previous study, novel N-terminal tag systems with only 1-9 repeated anionic amino acids was developed to increase soluble expression or extracellular secretion of *C. antarctica* lipase B (CalB) by the pelB signal sequence (Kim et al., 2014). Especially, the 5-aspartate tag substantially increased an extracellular expression level of recombinant CalB. AnsB is an *E. coli* periplasmic enzyme with a molecular weight of 35 kDa and forms a homo-tetrameric structure composed of closely packed dimmers (Swain et al., 1993) like CalB. Therefore, 3-6 aspartate tags were applied to increasing extracellular secretion of AnsB. It was reported that recombinant AnsB fused with the pelB signal sequence was produced in the medium at about 5 g/L by an unknown mechanism (Khushoo et al., 2005). Introduction of the pelB signal sequence increased extracellular expression of AnsB by a 2 fold, relative to the expression of AnsB only (Fig. 2). In addition, the pelB signal sequence triggered intracellular expression of recombinant AnsBs, that accords with the general concept of reduced metabolic burden by extracellular protein expression. When five aspartates were inserted between the pelB signal sequence and AnsB, the total expression and extracellular secretion levels of AnsB further increased as the same as the case of CalB. Interestingly, expression patterns of

recombinant AnsBs were quite different in each case. As shown in Fig. 4, intracellular expression profiles of both P-AnsB and P-D5-AnsB were similar. Consistent with the other studies, the extracellular expression level of P-D5-AnsB increased considerably after the intracellular expression reached a certain level (Dresler et al., 2006b; Shin and Chen, 2008). Considering these phenomena, it was suggested that *E. coli* has a maximum intracellular space for protein accumulation and saturation of this space might be a prerequisite to efficiently secrete P-D5-AnsB in the medium. This hypothesis confirmed by the observation showing that the destruction of *gspDE* resulted in lower extracellular activities of recombinant AnsBs without affecting intracellular activities of it (Fig. 5B).

Although the *E. coli* K-12 strain contains the *gsp* genes that are homologous to those encoding other secretions, the *gsp* genes are transcriptionally silent under standard laboratory conditions (Francetic and Pugsley, 1996). However, it was observed that endogenous expression levels of the *gsp* genes in the BL21 star (DE3) strain are sufficient to transfer AnsB into culture medium. Actually, more than half of AnsB (56%) were exported to the medium by the GSP machinery.

In the periplasmic space, proteins adopts tertiary and even quaternary

structures in order to be recognized by the GSP secreton (Sandkvist, 2001). Attachment of the N-terminal five aspartate tag might induce a quaternary structure change of AnsB and affect the transport efficiency of AnsB across the outer membrane (Kim et al., 2014). The five aspartates decreased the portion of extracellular AnsB exported by the GSP components from 56% to 15%. This result indicated that a large fraction of D5-AnsB might be transported across the outer membrane by other mechanisms. In conclusion, it was clearly shown that simple fusion of aspartate could be applied to increasing total expression and extracellular secretion levels of *E. coli* AnsB up to 40.8 U/ml in fermentation medium. This pelB-anion amino acid tag-based expression system for AnsB can be extended to production of other proteins translocated to the periplasmic space by the pelB signal sequence and adopting a dimer-based oligomer as the same as recombinant AnsBs.

References

- [1] Mashburn LT, Wriston JC. Tumor inhibitory effect of L-asparaginase from *Escherichia coli*. Arch Biochem Biophys 1964;105:450-2.
- [2] Stecher AL, Morgantetti de deus P, Polikarpov I, Abrahao-Neto J. Stability of L-asparaginase: an enzyme used in leukemia treatment. Pharm Acta Helv 1999;74:1-9.
- [3] Broome JD. Antilymphoma activity of L-asparaginase *in vivo*: clearance rates of enzyme preparations from guinea pig serum and yeast in relation to their effect on tumor growth. J Natl Cancer Inst 1965;35:967-74.
- [4] Swain AL, Jaskolski M, Housset D, Rao JK, Wlodawer A. Crystal structure of *Escherichia coli* L-asparaginase, an enzyme used in cancer therapy. Proc Natl Acad Sci USA 1993;90:1474-8.
- [5] Kenari SLD, Alemzadeh I, Maghsodi V. Production of L-asparaginase from *Escherichia coli* ATCC 11303: Optimization by response surface methodology. Food Bioprod Process 2011;89:315-21.
- [6] Khushoo A, Pal Y, Mukherjee KJ. Optimization of extracellular

production of recombinant asparaginase in *Escherichia coli* in shake-flask and bioreactor. *Appl Microbiol Biotechnol* 2005;68:189-97.

[7] Harms E, Wehner A, Jennings MP, Pugh KJ, Beacham IR, Rohm KH. Construction of expression systems for *Escherichia coli* asparaginase II and two-step purification of the recombinant enzyme from periplasmic extracts. *Protein Expres Purif* 1991;2:144-50.

[8] Khushoo A, Pal Y, Singh BN, Mukherjee KJ. Extracellular expression and single step purification of recombinant *Escherichia coli* L-asparaginase II. *Protein Expres Purif* 2004;38:29-36.

[9] Luo YE, Mu TZ, Fan DD. Preparation of a low-cost minimal medium for engineered *Escherichia coli* with high yield of human-like collagen II. *Pak J Pharm Sci* 2014;27:663-9.

[10] Paliy O, Gunasekera T. Growth of *E. coli* BL21 in minimal media with different gluconeogenic carbon sources and salt contents. *Appl Microbiol Biotechnol* 2007;73:1169-72.

[11] Cornelis P. Expressing genes in different *Escherichia coli* compartments. *Curr Opin Biotechnol* 2000;11:450-4.

[12] Makrides S. Strategies for achieving high-level expression of genes in *Escherichia coli*. *Microbiol Rev* 1996;60:512-38.

- [13] Waugh DS. Making the most of affinity tags. Trends Biotechnol 2005;23:316-20.
- [14] Esposito D, Chatterjee DK. Enhancement of soluble protein expression through the use of fusion tags. Curr Opin Biotechnol 2006;17:353-8.
- [15] MacIntyre S, Eschbach ML, Mutschler B. Export incompatibility of N-terminal basic residues in a mature polypeptide of *Escherichia coli* can be alleviated by optimising the signal peptide. Mol Gen Genet 1990;221:466-74.
- [16] Kim S-K, Park Y-C, Lee HH, Jeon ST, Min W-K, Seo J-H. Simple amino acid tags improve both expression and secretion of *Candida antarctica* lipase B in recombinant *Escherichia coli*. Biotechnol Bioeng 2015;112:346-55.
- [17] Jung H-J, Kim S-K, Min W-K, Lee S-S, Park K, Park Y-C, et al. Polycationic amino acid tags enhance soluble expression of *Candida antarctica* lipase B in recombinant *Escherichia coli*. Bioproc Biosyst Eng 2011;34:833-9.
- [18] Feng S, Gong YY, Adilijiang G, Deng HT. Effects of the Fc-III tag on activity and stability of green fluorescent protein and human muscle creatine kinase. Protein Sci 2013;22:1008-15.

- [19] Mergulhao FJ, Summers DK, Monteiro GA. Recombinant protein secretion in *Escherichia coli*. *Biotechnol Advan* 2005;23:177-202.
- [20] Pugsley AP. The complete general secretory pathway in gram-negative bacteria. *Microbiol Rev* 1993;57:50-108.
- [21] Francetic O, Belin D, Badaut C, Pugsley AP. Expression of the endogenous type II secretion pathway in *Escherichia coli* leads to chitinase secretion. *Embo J* 2000;19:6697-703.
- [22] Ni Y, Chen R. Extracellular recombinant protein production from *Escherichia coli*. *Biotechnol Lett* 2009;31:1661-70.
- [23] Sorg JA, Blaylock B, Schneewind O. Secretion signal recognition by YscN, the *Yersinia* type III secretion ATPase. *Proc Natl Acad Sci USA* 2006;103:16490-5.
- [24] Riordan KE, Sorg JA, Berube BJ, Schneewind O. Impassable YscP substrates and their impact on the *Yersinia enterocolitica* type III secretion pathway. *J Bacteriol* 2008;190:6204-16.
- [25] Dresler K, van den Heuvel J, Muller RJ, Deckwer WD. Production of a recombinant polyester-cleaving hydrolase from *Thermobifida fusca* in *Escherichia coli*. *Bioproc Biosyst Eng* 2006;29:169-83.
- [26] Shin HD, Chen RR. Extracellular recombinant protein production

from an *Escherichia coli lpp* deletion mutant. *Biotechnol Bioeng* 2008;101:1288-96.

[27] Francetic O, Pugsley AP. The cryptic general secretory pathway (gsp) operon of *Escherichia coli* K-12 encodes functional proteins. *J Bacteriol* 1996;178:3544-9.

[28] Sandkvist M. Biology of type II secretion. *Mol Microbiol* 2001;40:271-83.

Figure legends

Fig. 1. Schematic diagram of the structures of recombinant AnsB expression cassettes in plasmid pET-26b(+) derivatives. The abbreviation and symbols are denoted as follows: T7, *T7* promoter; *lacO*, *lac* operator; RBS, ribosomal binding site; *pelB*, signal sequence of pectate lyase B from *Erwinia carotovora*; *ansB*, *E. coli* L-asparaginase isozyme II; stop, translational stop codon; D5, 5 aspartates; D3-D6, 3-6 aspartates.

Fig. 2. Specific activities of recombinant AnsBs in the intracellular fraction and culture medium. After 24 h of IPTG induction, the recombinant *E. coli* cells were collected, harvested and disrupted. The intracellular fraction containing both cytoplasmic and periplasmic proteins, and culture medium were subjected to assay of asparaginase activity, which were measured in triplicate and normalized to dry cell mass.

Fig. 3. SDS-PAGE analysis of recombinant AnsBs fused with the polyanionic tag consisting of 3, 4, 5 or 6 aspartates at the N-terminus of AnsB. After 24 h induction, the cells were harvested, disrupted and fractionated into total (T), soluble (S), insoluble (I) and extracellular (E)

protein fractions. M indicates the protein size marker and the arrow points the protein band of recombinant AnsBs.

Fig. 4. Production of recombinant AnsBs in batch fermentation of recombinant *E. coli* strains. Batch production of P-AnsB (A) and P-D5-AnsB (B) were conducted in triplicate using 20 g/L glucose at 200 rpm and a culture temperature was shifted from 37°C to 20°C after IPTG induction.

Fig. 5. Role of general secretion pathway in AnsB secretion. (A) The relative mRNA levels of *gspD* determined by quantitative real-time PCR analysis. Details for preparation of total cellular RNA and real-time PCR are given in materials and methods, and the mRNA levels of *gspD* were normalized to the *gapC* mRNA level. (B) Effects of the *gspDE* gene deletion on expression and localization of P-AnsB and P-D5-AnsB. Protein samples of AnsBs were prepared after 24 h of IPTG induction. *E. coli* BL21 star (DE3) strain and *gspDE*-deficient strain (Δ *gspDE*) were used as the host strains. The experiments were conducted in triplicate.

Table 1. List of DNA oligomers used in this study. The italicized sequences indicate the recognition sites of the corresponding restriction enzymes. [F] and [R] mean the forward and reverse primers, respectively

Name	Sequence (5' → 3')	Restriction enzyme	Amplified gene
AnsB[F]	GGAATTCC <i>ATATGTT</i> TACCCAATATCACCATTTTAGCAACC	<i>NdeI</i>	AnsB
P-AnsB[F]	CATGCC <i>ATGGCCTT</i> TACCCAATATCACCATTTTAGCAACC	<i>NcoI</i>	P-AnsB
P-D3-AnsB[F]	CATGCC <i>ATGGCCGATGATGATTT</i> TACCCAATATCACCATTTTAGCAACC	<i>NcoI</i>	P-D3-AnsB
P-D4-AnsB[F]	CATGCC <i>ATGGCCGATGATGATGATTT</i> TACCCAATATCACCATTTTAGCAACC	<i>NcoI</i>	P-D4-AnsB
D5-AnsB[F]	GGAATTCC <i>ATATGGATGATGATGATGATTT</i> TACCCAATATCACCATTTTAGCAA CC	<i>NdeI</i>	D5-AnsB
P-D5-AnsB[F]	CATGCC <i>ATGGCCGATGATGATGATGATTT</i> TACCCAATATCACCATTTTAGCAAC C	<i>NcoI</i>	P-D5-AnsB
P-D6-AnsB[F]	CATGCC <i>ATGGCCGATGATGATGATGATGATTT</i> TACCCAATATCACCATTTTAGC AACC	<i>NcoI</i>	P-D6-AnsB
AnsB[R]	CCGCTCGAGATTAGTACTGATTGAAGATCTGCTGGAT	<i>XhoI</i>	^a
gspD_RTPCR[F]	ATGAAAGGACTCAATAAAAATCACCTGCTGC	-	GspD
gspD_RTPCR[R]	TCACCGTGACGATGGCGCAG	-	
gapC_RTPCR[F]	ATGAGTAAAGTTGGTATTAACGGTTTTGGTGC	-	GapC
gapC_RTPCR[R]	TCAGAGTTTAGCGAATTTTTTCGAGGGTG	-	

^a In all cases of AnsB variants, AnsB[R] was used as the reverse primer.

Table 2. Production of AnsBs in *E. coli*

Strain	System	Activity ^a (U/ml)		Reference
		Intracellular	Extracellular	
<i>E. coli</i> ATCC11303		1.03		(Kenari et al., 2011)
<i>E. coli</i> BL21 (DE3)	<i>T7</i> promoter	3.9		(Harms et al., 1991)
<i>E. coli</i> BLR (DE3)	pelB signal sequence	8.2	22.5	(Khushoo et al., 2005)
<i>E. coli</i> BL21 star (DE3)	pelB signal sequence + 5 aspartate tag	19.2	40.8	This study

^a AnsB activity was determined by using L-asparagine as a substrate.

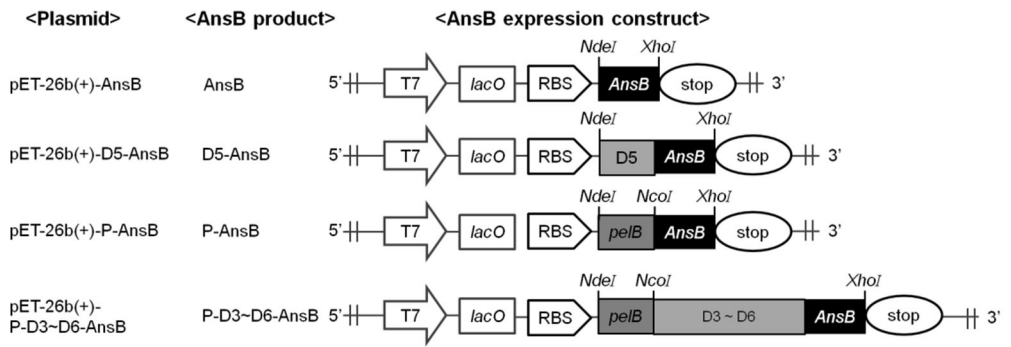


Figure 1

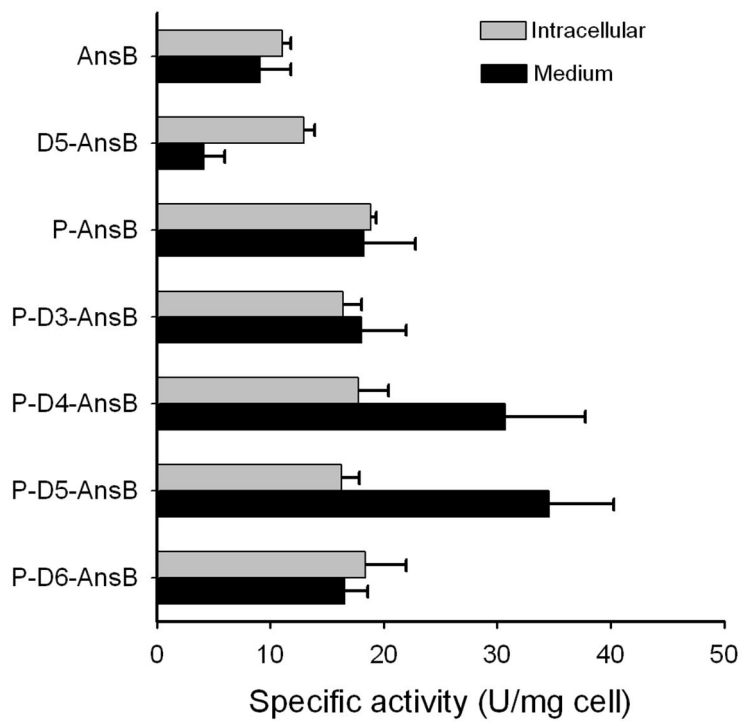


Figure 2

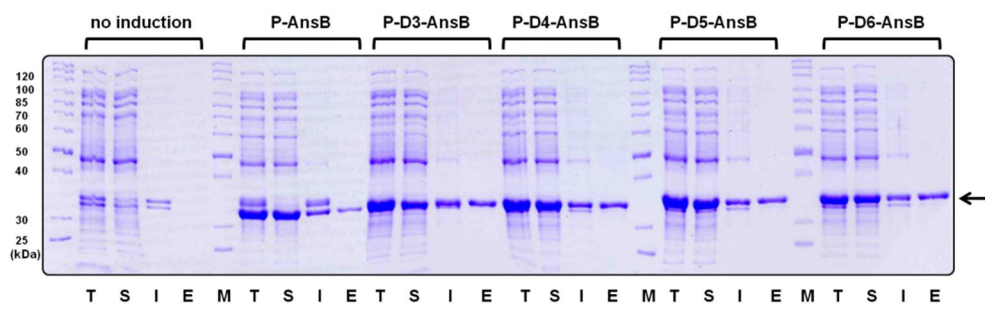


Figure 3

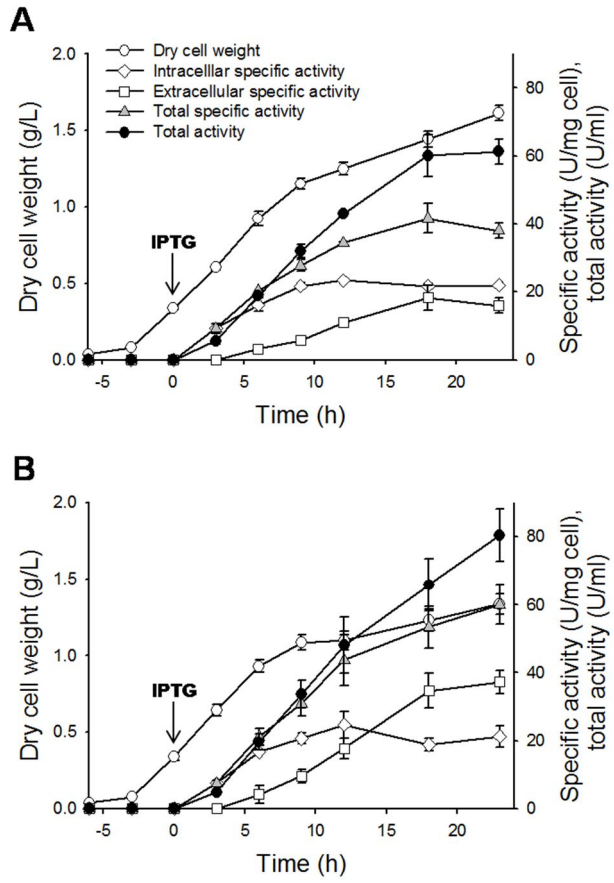


Figure 4

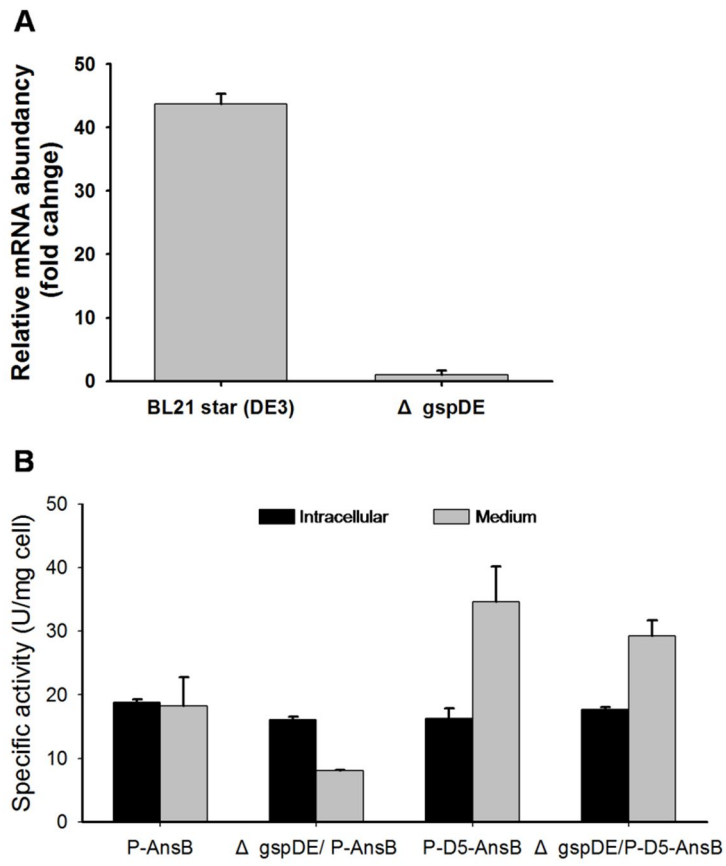


Figure 5

국문 초록

미생물을 이용한 목질계 바이오매스로부터의 바이오 연료 및 바이오 화학소재 생산은 바이오매스 당화물에 존재하는 발효저해제들에 의해 저해 받아 생산성이 크게 감소한다. 본 연구에서는 이러한 문제점을 극복하고자 폴리아민의 일종인 스퍼미딘(spermidine)을 *Saccharomyces cerevisiae* (이하 효모로 지칭) 배양액에 첨가하여 발효저해제들에 대한 내성을 증가시켰다. 또한 배지내 스퍼미딘 첨가 없이 자체적으로 스퍼미딘을 과량 축적하여 발효저해제들에 대한 내성이 증대된 재조합 효모를 구축하고자 하였다. 구체적으로는 스퍼미딘 생합성에 직접적으로 관련된 *SPE1*, *SPE2*, *SPE3* 유전자들을 과발현하였다. 또한 되먹임저해(feedback inhibition)에 관련된 유전자인 *OAZ1*과 스퍼미딘의 세포외 배출을 매개하는 단백질을 암호화하는 유전자인 *TPO1*을 추가적으로 과쇄하였다. 이렇게 유전자가 조작된 재조합 효모 균주 중에서 *OAZ1*, *TPO1* 유전자 과쇄와 *SPE3* 유전자 과발현이 조합된 균주의 경우 야생형 효모보다 171% 높은 1.1 mg spermidine/g cell의 세포내 스퍼미딘 농도를 나타냈으며, 푸란 유도체들을 포함하는 배지와 초산을 포함하는 배지에서 각각 60%와 33% 감소된 유도기(lag-phase)를 나타냈다. 이

처럼 재조합 효모의 내성이 고농도의 스퍼미딘에 의해 증가되었으나, 지나치게 높은 농도의 스퍼미딘은 대사과부하(metabolic burden)를 유도하여 오히려 내성을 감소시키는 현상을 관찰하였다. 따라서 내성이 증가된 재조합 효모 균주를 구축하기 위해서는 세포내 스퍼미딘 농도와 더불어 대사과부하 현상을 최소화시켜야 함을 보여주었다. 또한 퓨린 생합성과 세포벽, 크로마틴 안정성에 관련된 유전자들이 푸르푸랄(furfural)에 대한 내성 증가에 관여함을 증명하였다.

이렇게 구축된 고농도의 스퍼미딘과 내성을 동시에 갖는 재조합 효모 균주를 이용하여 반복 회분 발효(repeated-batch fermentation)와 발효저해제들을 포함하는 포도당과 자일로스의 혼합당 배지에서 에탄올 생산성을 증가시키고자 하였다. 먼저, 포도당을 탄소원으로 이용한 16번의 반복 회분 발효에서 고농도의 스퍼미딘을 갖는 재조합 효모는 야생형 효모보다 높은 생존능력과 에탄올 생산성을 유지하였다. 또한 고농도의 스퍼미딘 농도를 갖는 재조합 효모 균주에 자일로스 대사 관련유전자인 *XYL1*, *XYL2*, *XYL3*를 도입하여 자일로스 대사를 가능하게 하였다. 이렇게 구축된 균주는 고농도의 퓨란 유도체를 포함하는 인공 당화물과 고농도의 초산을 포함하는 인공 당화물

에서 각각 46%와 38% 향상된 에탄올 생산성을 나타냈다. 본 연구에서 구축된 재조합 효모 균주들은 에탄올 생산 이외에도 섬유소계 바이오매스로부터 다양한 바이오연료와 바이오 화학 소재를 효율적으로 생산하는데 이용될 수 있을 것으로 기대된다.

스퍼미딘은 피부노화 억제, 모발성장 촉진, 2형 당뇨병 치료, 과일의 저장기간 증대 등에 대한 기능이 검증되었다. 따라서 GRAS 미생물로서 안전하다고 알려진 효모를 이용한 스퍼미딘 생산 시스템의 구축은 경제적 잠재성이 클 것으로 사료된다. 스퍼미딘 생산량을 증대시키기 위해 스퍼미딘 생합성에 관련된 *SPE1*, *SPE2*, *SPE3* 유전자들이 과발현되고 되먹임저해에 관련된 유전자인 *OAZ1*이 과쇄된 재조합 효모를 이용하였다. 이 균주에 추가적으로 스퍼미딘의 세포외 배출을 매개하는 단백질을 암호화하는 유전자인 *TPO1*을 과발현하여 세포내의 스퍼미딘을 배지 중으로 배출하도록 하였다. 스퍼미딘 생산의 경우 자일로스로부터의 생산 수율이 4.0 mg spermidine/g glucose로, 포도당으로부터의 생산 수율보다 3.1배 높게 나타났다. 포도당 제한적인 유가식배양에서 SR8 OS123/pTPO1 균주는 최종적으로 37.4 g/L의 자일로스를 소모하여 224 mg/L의 스퍼미딘을 2.2

mg spermidine/g sugars의 수율로 생산하였다.

주요어: 바이오연료, 스퍼미딘, 발효저해제, 되먹임저해, 폴리
아민 이송 단백질, 자일로스, 반복 회분 발효

학번: 2009-21235